9-11-2013 12:00 AM

Development and Applications of a Novel Intermittent Solids Feeder for Pyrolysis Reactors

Federico M. Berruti
The University of Western Ontario

Supervisor
Dr. Cedric L. Briens
The University of Western Ontario

Graduate Program in Chemical and Biochemical Engineering
A thesis submitted in partial fulfillment of the requirements for the degree in Doctor of Philosophy

DEVELOPMENT AND APPLICATIONS OF A NOVEL INTERMITTENT SOLIDS FEEDER FOR PYROLYSIS REACTORS

(Thesis format: Integrated-Article)

by

Federico M. Berruti

Graduate Program in Engineering Science
Department of Chemical & Biochemical Engineering

A thesis submitted in partial fulfillment
of the requirements for the degree of
Doctor of Philosophy

The School of Graduate and Postdoctoral Studies
The University of Western Ontario
London, Ontario, Canada
July 2013

Abstract

This PhD research addresses the challenge of feeding biomass residues into fluidized bed reactors for pyrolysis, through the development of a novel intermittent solid slug feeder, both for laboratory-scale and large-scale reactors. The new feeder can successfully handle biomass residues that are either too cohesive or thermally sensitive for traditional feeders.

To optimize the novel feeder performance, a model for the pulsating solids flow was developed from experimental data collected with ideal slugs, as well as real biomass flow. The model was validated using both a laboratory-scale (< 10 kg/hr) and large-scale feeder (> 250 kg/hr). Several important variables were identified. They include the material flow properties, the pulse gas pressure and volume, and the feeding tube length and material. The goals of this study were to (a) characterize the fundamental dynamic behavior of the biomass slugs in the feeder, (b) maximize the solid-to-gas feeding ratio, and thus minimize energy consumption and cost, (c) minimize the accumulation of “straggler” biomass material in the feeding tube between pulses, and thus prevent biomass heating in the feeding tube, which can induce plugging, and (d) develop and validate a predictive model for the slug velocity at any location in the feeding tube, which can be applied to feeder design for any biomass feedstock.

An advantage of the new large-scale feeder technology is that it can handle larger biomass particles than traditional feeder technologies. An issue with large particles is that they require relatively long drying, which must be optimized. A model was

therefore developed for drying, which takes shrinkage, and internal and external mass transfer limitations into account.

The thesis is supplemented with additional work based on the application of the novel feeder for pyrolysis studies with various biomass residues. The feeder technology made it possible to perform the first ever pyrolysis studies, in industrially-relevant equipment, on pure meat and bone meal residue, and on unmodified and undiluted Kraft lignin. Appendices include a business case-study of the implementation of the technologies developed in this thesis on large-scale pyrolysis and an additional pyrolysis study on *tucumã* seeds, which utilized the novel feeder.

Keywords

Feeder, feed rate, injection, powder, pulsations, slugs, cohesive, temperature-sensitive, granules, feedstock, biomass, agricultural residue, forestry residue, pyrolysis, gasification, fluidized bed, oil, bio-oil, bio-char, biochar, dried distiller's grains, meat and bone meal residues, optimization.

Co-Authorship Statement

Chapters 1 through 6, and Appendix I and II, encompass research studies which have been published or submitted to peer-refereed journals. Individual contributions of all authors for each publication are summarized below.

CHAPTER 1

This chapter incorporates sections of the two following published papers:

Article Title	**Novel Fluid Bed Pilot Plant for the Production of Bio-oil from Biomass through Fast Pyrolysis.**
Authors	F.M. Berruti, K. Lenkiewicz, R. Xu, R.J. Bedmutha, S. Nova, F. Berruti, C. Briens
Current Status	Published in *Récents Progrès en Génie des Procédés*, Numéro 94 – 2007, ISBN 2-910239-68-3, Ed. SFGP, Paris, France.
F.M. Berruti and K. Lenkiewicz conducted the literature review, the reactor assembly, the experimental work, the data analysis and F.M. Berruti wrote the manuscript. R. Xu and R.J. Bedmutha performed supplemental experimental work and some chemical analysis. The experimental work was supervised by S. Nova. C. Briens and F. Berruti jointly supervised, reviewed and revised several drafts of the work.	

Article Title	**Biomass residue fast pyrolysis: the future outlook**
Authors	F.M. Berruti
Current Status	Published in the *Canadian Biomass Magazine,* 2013 (http://www.canadianbiomassmagazine.ca/content/view/3954/133/)
F.M. Berruti conducted the literature review and wrote the manuscript.	

CHAPTER 2

Article Title	**Preliminary Design and Optimization of an Intermittent Slug Injection System for Sawdust Biomass Pyrolysis**
Authors	F.M. Berruti, L. Ferrante, F. Berruti, C. Briens
Current Status	Published in the *International Journal of Chemical Reactor Engineering*, Volume 7, 2009, A84.
F.M. Berruti conducted the literature review, the feeder design and manufacturing, the experimental work, the data analysis and wrote the manuscript. L. Ferrante supervised the experimental work and data analysis. C. Briens and F. Berruti jointly supervised, reviewed and revised several drafts of the work.	

CHAPTER 3

Article Title	**Novel intermittent solid slug feeder for fast pyrolysis reactors: fundamentals and modelling**
Authors	F.M. Berruti, C. Briens
Current Status	Published in *Powder Technology* 247, 2013, 95-105.
F.M. Berruti performed the literature review, equipment design and assembly, experimental work, data analysis, modelling and wrote the manuscript. C. Briens supervised, reviewed and revised several drafts of the work.	

CHAPTER 4

Article Title	**Novel intermittent solid slug feeder for fast pyrolysis reactors: Scale-up, alternate geometries, and feeder design procedure**
Authors	F.M. Berruti, C. Briens
Current Status	Currently Unpublished Work.
F.M. Berruti performed the literature review, equipment design and assembly, experimental work, data analysis, modelling and wrote the manuscript. C. Briens supervised, reviewed and revised several drafts of the work.	

CHAPTER 5

Article Title	**Model for convective drying of carrots for pyrolysis**
Authors	F.M. Berruti, M. Klaas, C. Briens, F. Berruti
Current Status	Published in the *Journal of Food Engineering*, 92, 2009, 196-201.
F.M. Berruti and M. Klaas performed the literature review, apparatus assembly, experimental work and data analysis. F.M. Berruti completed the modelling and data analysis and wrote the manuscript. C. Briens and F. Berruti jointly supervised, reviewed and revised several drafts of the work.	

CHAPTER 6

Article Title	**Pyrolysis of cohesive meat and bone meal in a bubbling fluidized bed with an intermittent solid slug feeder**
Authors	F.M. Berruti, L. Ferrante, C. Briens, F. Berruti
Current Status	Published in the *Journal of Analytical and Applied Pyrolysis*, 94, 2012, 153-162.
F.M. Berruti performed the literature review, apparatus and reactor assembly and modifications, experimental work and data analysis and wrote the manuscript. L. Ferrante supervised the experimental work and a portion of the data analysis (GC-MS). C. Briens and F. Berruti jointly supervised, reviewed and revised several drafts of the work.	

APPENDIX I

Article Title	**Green-Tech: Bio-Fuels High Growth Strategy (Case and Teaching Note)**
Authors	F.M. Berruti, Heng-Yih (Gordon) Liu
Current Status	Published by *Ivey Publishing* (9B11M123 and 8B11M123), 2012
F.M. Berruti and Heng-Yih (Gordon) Liu jointly wrote the case and teaching note.	

APPENDIX II

Article Title	**Fast pyrolysis of Amazon tucumã (Astrocaryum aculeatum) seeds in a bubbling fluidized bed reactor**
Authors	C. Lira, F.M. Berruti, P. Palmisano, F. Berruti, C. Briens, A.A.B. Pécora
Current Status	Published in the *Journal of Analytical and Applied Pyrolysis*, 99, 2013, 23-31.
C. Lira, F.M. Berruti, and P. Palmisano performed the experimental work and data analysis. C. Lira conducted the literature review and wrote the manuscript draft. F.M. Berruti supervised the work and completed the data analysis, edited, finalized and submitted the manuscript, and was in charge of taking the manuscript through the peer review process. C. Briens and F. Berruti jointly supervised, reviewed and revised several drafts of the work. A.A.B. Pécora revised the manuscript first draft.	

APPENDIX III

Article Title	**Kraft Lignin Pyrolysis in a Fluidized Bed Reactor**
Authors	P. Palmisano, F.M. Berruti, V. Lago, F. Berruti, C. Briens
Current Status	Published at TCBiomass 2011, Chicago, Illinois, USA
P. Palmisano, F.M. Berruti and V. Lago performed the experimental work and data analysis. C. Briens and F. Berruti jointly supervised, reviewed and revised several drafts of the work. P. Palmisano prepared and presented the work at TCBiomass in Chicago, IL, USA.	

Acknowledgments

Firstly, I would like to extend my deepest appreciation and gratitude to my brilliant supervisor, Dr. Cedric Briens. Cedric has always been outstanding in his role as my supervisor, providing continuous encouragement, constructive criticism, technical skill, guidance, trust and understanding throughout my doctoral studies. What is even better is that from great "supervisor", Cedric is now also my friend, mentor and colleague, who I hope to continue to have the privilege to work with in the future.

I also wish to extend my gratitude to my great colleagues and friends at ICFAR who I have worked with along the way, especially Dr. Lorenzo Ferrante, Dr. Ran Xu, Dr. Pietro Palmisano, Martin Huard, Claudio Lira, Matthew Klaas, Craig Mara, and Rob Taylor. I greatly appreciate their suggestions, help, work and conversations at various stages of my thesis, and most importantly, their friendship.

My gratitude is also extended to the Ontario Centres of Excellence (OCE), the Natural Sciences and Engineering Research Council of Canada (NSERC) Vanier Canada Graduate Scholarship program, the great team at Agri-Therm Ltd. who I have loved working with, and Western University for the financial support of the research program. I gratefully acknowledge the Faculty of Engineering at Western University for the financial support in the forms of Western Engineering Scholarships (WES) and Graduate Thesis Research Awards (GTRA).

I would also like to acknowledge the University Machine Services (UMS), Information Technology Service (ITS), Electronics Shop and Engineering Financial Store (EFS).

Moreover, the valuable time, advice and assistance from Clayton Cook, Souheil Afara, Brian Dennis, and Eugen Porter is greatly appreciated.

Last, but certainly not least, I would like to thank my parents, Franco and Alessandra Berruti, my close friend, Valter Feyles, and my partner, Meg Atkinson, for their incredible love, patience, guidance and support for me to have my opportunities and achieve my goals.

I am very close to my parents, in particular to my mother, Alessandra. Her love, energy and thoughtful nurturing have made me the happy and confident person I am today, and I will continue to cherish her love and inspiring ideas and advice throughout my life.

I have also had the amazing privilege of working alongside my father, Dr. Franco Berruti, for various projects over these great years. It goes without saying that his energy, vision, sincerity, creativity, curiosity and honour is appreciated by everyone who experiences it, and I will continue to learn an immeasurable amount from him.

Dedications

For my outstanding, supportive and unconditionally-loving parents, Franco and Alessandra Berruti, and for my great supporter and friend, Valter Feyles, without whom none of this would be remotely possible.

For my incredible, supportive, loving and understanding partner, Meg Atkinson, who inspires me to be my curious self and to love every moment of this life.

In memory of my grandfathers, Cornelio Berruti and Agostino Gianetto.

To my whole family and all my close friends.

Table of Contents

List of Tables

List of Figures

Key Abbreviations

ICFAR – Institute for Chemicals and Fuels from Alternative Resources

DDG – Dried Distillers' Grains

MBM – Meat & Bone Meal

HHV – Higher Heating Value

LHV – Lower Heating Value

MPT – Mobile Pyrolysis Technology

LPT – Laboratory-Scale Pyrolysis Technology

BFB – Bubbling Fluidized Bed

CFB – Circulating Fluidized Bed

Chapter 1

1 Chapter 1: Introduction[1]

1.1 Introduction & Background

The declining reserves of fossil fuels and fossil-fuel-related environmental issues, especially greenhouse gas (CO_2, CH_4) emissions, have posed a great threat and challenge to the sustainability of the world economy, the global environment and hence the quality of life of human beings [1]. The depleting resources and fluctuating prices of petroleum have intensified the search for alternative resources for both energy and chemical production. Forest and agricultural resources have traditionally been viewed as the source for traditional products such as timber/pulp/paper, combustion or food, whereas the emerging "green" bio-economy of Canada targets new processes for their conversion into renewable fuels and other value-added products. This can be accomplished by developing advanced bio-refining technologies to convert biomass, and particularly, residues or selected energy crops grown on marginal lands (rather than food competition), into various valuable products, including bio-energy, bio-fuels, and

[1] Parts and versions of this chapter have been published in the following:

Berruti, F.M., Lenkiewicz, K., et al. (2007). Novel Fluid Bed Pilot Plant for the Production of Bio-oil from Biomass through Fast Pyrolysis. *Récents Progrès en Génie des Procédés*, *Numéro 94*. ISBN 2-910239-68-3, Ed. SFGP, Paris, France.

Berruti, F.M. (2013). Biomass Residue Fast Pyrolysis: the Future Outlook. *Canadian Biomass*, February 12, 2013: http://www.canadianbiomassmagazine.ca/content/view/3954/133/.

bio-based chemicals and materials, as outlined in the Roadmap for Canadian Forest Biorefineries [2].

It is estimated that the share of global power generation from biomass power has reached about 10% in 2011 [3]. **Fig. 1-1** [3] illustrates the contribution of biomass and renewables to the world primary energy demand [4]. Although this percentage is in the same order of magnitude as the other conventional sources such as oil, nuclear and natural gas, its application and use is relatively limited to biomass combustion for personal use[2] and more recently to new developments in bio-ethanol and biodiesel production. However, as a result of increasing awareness of environmental impacts of conventional energy technologies and new environmental legislation being passed in many industrialized countries, researchers now project that the overall percentage of global energy demand derived from biomass renewable sources worldwide could increase to nearly 16% by 2035 [4].

[2] Wood, charcoal, leaves, agricultural residue, animal/human residues, and urban residues

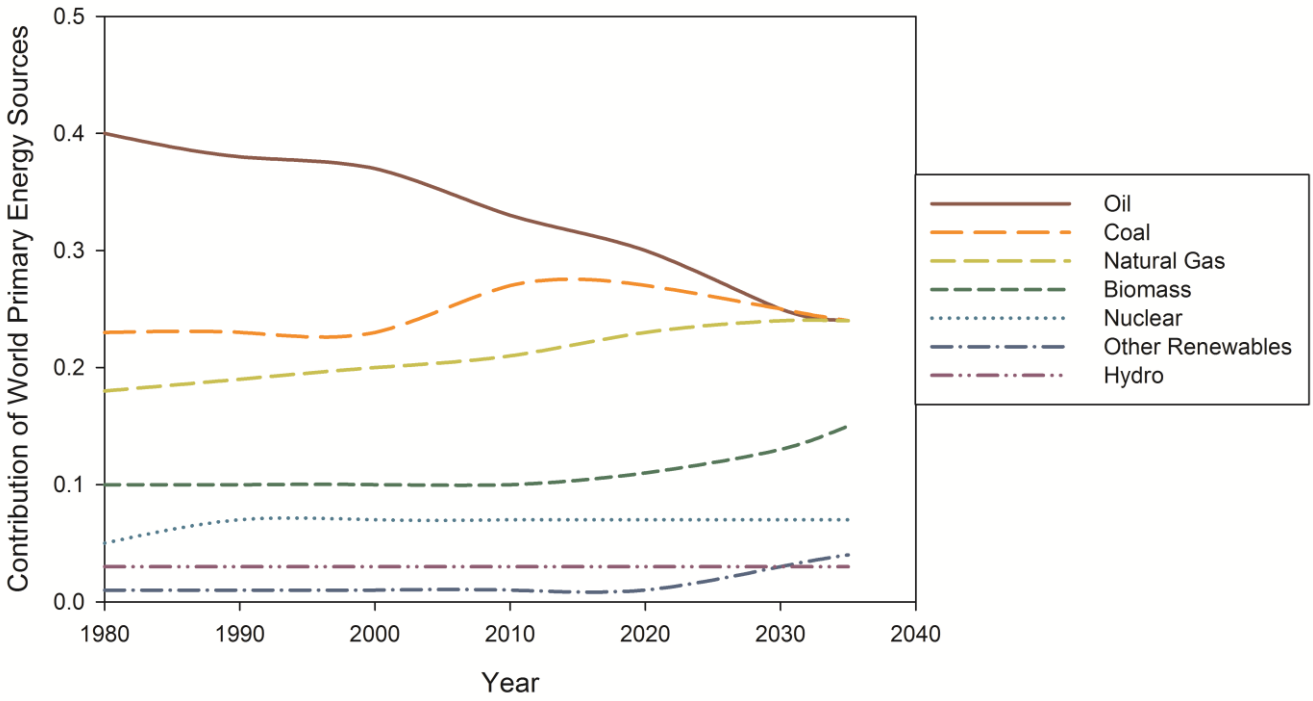

Figure 1-1: Contribution of World Primary Energy Sources

1.2 Introduction to Biomass Pyrolysis

Biomass is a composite material made up of oxygen-containing organic components (cellulose, hemicellulose, lignin, organic extractives) and of inorganic minerals. It is a renewable and carbon dioxide neutral source of energy, essentially a form of stored solar energy captured through the process of photosynthesis by green plants. The green plants obtain their carbon by fixing the atmospheric carbon dioxide during photosynthesis. Traditionally, the term "biomass" also includes animal materials, sludges, some sorted municipal residues, and biosolids from wastewater treatment plants. Unprocessed biomass is not well suited for direct energy production. Typically, the moisture content of the biomass varies between 50 and 60 wt% and passive drying can reduce this to 30 wt%. Active silo drying can reduce the moisture content further to 12-15 wt% [5]. The high moisture content and the low energy density of the raw biomass (one tenth of that of conventional liquid fuels) make it an uneconomical source of energy. Nevertheless, biomass can be converted through fast pyrolysis into a transportable liquid known as bio-oil with an energy density five times higher than that of the biomass.

Pyrolysis is the thermochemical cracking of organic macromolecules in the absence of oxygen. Historically, the term pyrolysis was applied to the slow carbonization of carbon containing materials, such as wood, for charcoal production. Nowadays, pyrolysis is being used to convert biomass to liquid (bio-oil), solid (bio-char) and gas products. The aim of these products is to create added commercial value, including chemicals,

petrochemicals and fuels, through the control of heating rates, reaction temperature and residence times [6]. **Fig. 1-2** illustrates the process of pyrolysis and some potential product utilization.

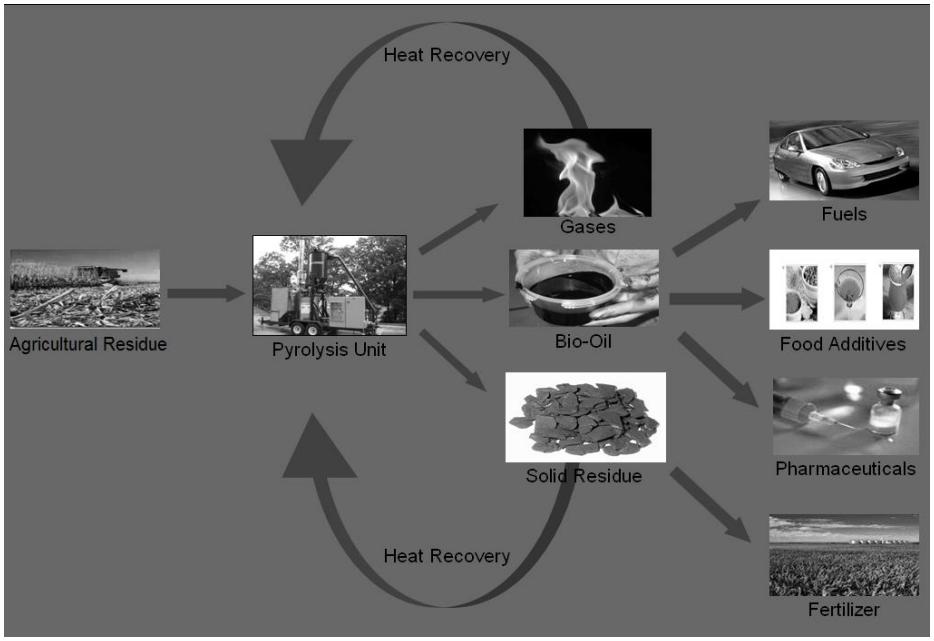

Figure 1-2: Pyrolysis Process Chart

1.3 Environmental Benefits of Pyrolysis

The conversion of agricultural, food, biofuel and forestry residues into value-added products via pyrolysis presents many advantages:

1. It prevents these residues from being landfilled with potential environmental hazards such as surface and groundwater pollution, biohazards, foul odours, and methane, which is a highly damaging greenhouse gas produced by the anaerobic degradation of biomass.

2. It prevents direct combustion in open-air of the residues by users, and, consequently, pollution or particulate controls.

3. It produces renewable and sustainable alternatives to depleting fossil fuels.

4. Biomass fuels produce virtually no sulfur emissions, and help mitigate acid rain. Emissions of NO_x are typically much lower as well. Additionally, the utilization of biomass is carbon-neutral (or even carbon-negative with the carbon sequestration within the bio-char produced, if it is returned to the earth for soil amendment purposes). The plants or crops from which biomass fuels are derived feed on carbon dioxide as they grow. As such, their use as a fuel does not add to the existing levels of carbon in the atmosphere.

1.4 Types of Pyrolysis

Conventional pyrolysis (also known as slow pyrolysis) is defined as the thermal cracking of organic-based materials in the absence of oxygen at slow heating rates (0.1-10 °C/s). Solid char is the main product, with properties that are typically used for combustion (charcoal) rather than soil amendment.

Fast pyrolysis is a high-temperature process (400 – 550 °C) in which biomass is rapidly heated (10-200 °C/s) and decomposed to form vapours, aerosols, gases and char. Bio-oil is collected by rapid quench and condensation of the vapours and by coalescence of aerosols. Fast pyrolysis processes can produce 50- 85 wt% of liquid bio-oil, 15-25 wt% of solid char and 10-20 wt% of non-condensable gases, depending upon the feedstock used and the operating conditions. No residue is produced: bio-oil is the main desirable product while the char co-product can be handled and has properties that could be attractive for soil amendment (high surface area, water retention, greenhouse gas absorption) or further conversion to activated carbon, while the gases can be recycled back into the process as fuel [7].

Flash pyrolysis is the term used to characterize a thermal-cracking process at a very high heating rate (>1000°C/s) and a very short vapour residence time to minimize secondary cracking and keep the liquid yields high. Particle sizes utilized must be very small to mitigate internal heat transfer limitations. This type of pyrolysis can typically only be achieved in fast fluidized beds, circulating fluidized beds, and in downer reactors, which are also scalable technologies [8].

Table 1-1 summarizes the types of pyrolysis and typical reactor configurations used for the processes [8].

Table 1-1: Types of Pyrolysis [8]

	Conventional Pyrolysis	Fast Pyrolysis	Flash Pyrolysis
Operating Conditions			
Heating Rate (°C/s)	0.1-10	10-200	>1000
Particle Size (mm)	5-50	<1	<0.2
Vapour Residence Time (s)	450-550	0.5-10	<0.5
Product Yields (wt%)			
Liquid	~30	60-75	~80
Char	~35	15-25	~15
Gas	~35	15	~5
Reactor Configurations	Fixed Bed, Vacuum Reactors	Ablative, Auger, Fluidized Bed, Circulating Fluidized Bed Reactors	Fluidized Bed, Circulating Fluidized Bed, Downer Reactors

1.5 Bio-oil Product Overview

1.5.1 Description and Properties

Bio-oil is a dark brown complex homogeneous mixture containing hundreds of polar organic compounds (including oxygenated organic compounds) and water (20 – 25 wt %) [9]. Bio-oils are more attractive than the simple biomass due to their potential as fuels in internal combustion engines, furnaces, boilers and turbines as substitutes for fuel oil or diesel, either alone or as a suspension with other liquid fuels [10]. Also several organic compounds with added commercial value can be extracted from the bio-oil for food flavouring and pharmaceutical industries. Additional advantages and benefits of the bio-oil over the biomass is that it is easy to store and transport. In power generation systems, like turbines and engines, the gasification of bio-oil gives higher efficiencies as compared to those processes where direct gasification of the solid biomass is done [11].

Bio-oil can be made from a wide variety of forest and agricultural residue materials, including wood, sugar cane bagasse, rice hulls and straw, peanuts hulls, switchgrass, wheat straw, corn, tobacco stalks, coconut fibres, and many others [7]. Other organic byproducts of the poultry industry (chicken litter), of the pulp and paper industry (lignin, sludge), and of the ethanol manufacturing (dry distillers' grains) are also excellent feedstocks.

The physical properties and composition of the bio-oil depend on the type of feedstock and the operating conditions at which the pyrolysis reaction is carried out. Short vapour residence times and long solid residence times have been reported to give high yields of

liquid bio-oil (75 – 80 wt % on a dry feed basis). The particle size of the feedstock fed to the pyrolysis reactors also influences the yield of bio-oil. Small biomass particle sizes (< 2 mm) render higher yields of liquid bio-oil than big particles sizes (if they are not elutriated out of the reactor before they are fully converted) as they have a higher specific surface area, which increases their heating rate. Rapid cooling of the product vapours is also essential to stop the thermal cracking of the bio-oil into non-condensable gases, which would reduce the liquid yield [12]. Even when dry, bio-oil contains 45-50 wt% oxygen, which is the primary difference between bio-oil and hydrocarbon fuels. Among the many chemical species found in bio-oils, the most important are hydroxyaldehydes, hydroxyketones, sugars and dehydrosugars, carboxylic acids and phenolics [13]. On a volume basis, the lower heating value (LHV) of bio-oil is typically 17 to 30 MJ/kg, or approximately 50-75% of that of hydrocarbon oils, due to the oxygen and water content and the higher density (specific gravity of 1.2 as opposed to 0.94) [9]. Addition of water causes the separation of the bio-oil into two fractions: a viscous lignin-containing phenolic fraction that settles and a water-soluble fraction, rich in carbohydrate-derived compounds and acids, that floats [7, 13]. Bio-oils typically have a viscosity between 35-1000 cP at room temperature and therefore they can require some mild heating to pump easily [9]. Fractional condensation of the pyrolytic vapours provides a dry bio-oil that is much more attractive as a fuel because of its low acidity, low water content, and high heating value (> 30 MJ/kg) [59].

In addition to transforming a low-value residue into a potentially high-value energy source; the manufacture and use of bio-oil has the following features:

- It is CO_2 neutral, contains no sulfur and, when combusted, produces less than 50-percent of the NO_X produced by fossil fuels.
- It is combustible (with lower particulate emissions and fouling than direct biomass combustion).
- It contains 60-80% of the energy value of fossil fuels.
- It can process residues, eliminating impacts on food supply and pricing.
- Often, it is completely biodegradable (in the event of a spill or accident).
- It reduces the negative environmental impacts of burning biomass and agricultural residues.
- It destroys pathogens found in animal renderings and rotting plant biomass.
- It mitigates the impact of directing these residues to existing landfills.

However, bio-oil is subjected to aging when exposed to temperatures at or above room temperature for long periods of time. This deterioration is manifested in an increase in viscosity for 2-3 months, typically reaching a plateau after some time. The addition of ethanol or methanol improves the bio-oil properties and stability [7]. In addition, bio-oil can be of low or high pH, depending on the feedstock, and can be corrosive on common construction materials such as aluminum and copper [14]. Bio-oil can also contain some ash depending on the condensation and filtration system, which can cause corrosion and fouling of combustion equipment [15].

1.5.2 Bio-oil Applications and Upgrading

Crude Bio-oil has the potential for multiple applications ranging from a variety of combined heat and power options to the extraction of specialty chemicals and flavours.

1.5.2.1 Applications for Heat and Power Generation

Liquid bio-oil has a significantly higher energy density than biomass and can be easily transported and stored with existing infrastructure and technology. Significant work has been carried out on research and development for the application of bio-oil for the heat and power generation, including the design and study of specialized bio-oil burners at CANMET and at the Combustion Research Laboratory of The University of Toronto [16]. However, as discussed earlier, several bio-oil properties; including the oxygen content, water content, oil stability and aging, and ash content can make the conversion into heat and power significantly more challenging and ultimately limit the range of its applications. Extensive research in the areas of emulsification and blending [17–19], deoxygenation by catalytic vapour cracking [20] and hydrotreating [21], and aqueous phase fermentation and steam reforming [22] is currently being performed to facilitate the use of bio-oil to produce conventional fuel products in an economic manner.

[23–26] provide in-depth reviews of bio-oil upgrading, technologies, products, blending with biodiesel and challenges.

1.5.2.2 Chemicals and Materials

Pyrolysis bio-oil contains hundreds of components, some of which are attractive due to their higher value compared to fuels and energy products. As a result, the most

economically sound approach to developing products from bio-oils may be to extract valuable chemicals and material building blocks from the oil first, and to utilize the remaining bio-oil as a crude fuel, which can be upgraded and fractionated into conventional fuels, if required. Currently, there is much research and development focused on the extraction and production of the chemicals and products from bio-oil. A list of some products from bio-oil is shown in **Table 1-2** [8, 9].

Table 1-2: Products from Bio-oil

Fuels	Levoglucosan	Flavouring Agents/Guaiacols
Pesticides	Preservatives	Hydrogen
Pharmaceuticals	Rare Sugars	Adhesives/Resins
Acetic Acid	Colouring	Fire-Resistant Foams

Food flavouring agents [27] are commercially produced from wood pyrolysis products in many countries, with the key components being guaiacols [28]. Phenols contained in the bio-oil can also be used to replace fossil-fuel based phenols in the production of resins, adhesives and fire-resistant foams [29]. Due to its typical insecticidal, fungicidal and bactericidal characteristics, the bio-oil can also be used as a wood preservative [30] and as a pesticides [31].

1.6 Pyrolysis Reactor Technologies

All over the world researchers have been studying the pyrolysis of agricultural residues (straw, husks, corncobs, tea residues, sesame stalks, hazelnuts, sugarcane, sorghum, almond shells, rapeseeds, tobacco stalks and leaves, algae, cotton straw, sunflower bagasse, switch grass, woods and forestry residues, and many others) by utilizing a

variety of different reactor technologies (fluidized beds, ablative reactors, rotating cone reactors, vacuum reactors, and auger reactors) [32].

The heart of the fast pyrolysis process is the reactor, and considerable research and development has focused on different reactor technologies. During the past two decades, several different reactor designs have been studied and some processes have been proposed. Examples include the Agri-Therm mobile fluidized bed reactor, the AbriTech auger reactor, the Tech-Air process, the Ensyn circulating fluidized bed; the Waterloo Fast Pyrolysis fluid bed, from which the RTI and the Dynamotive processes have been derived; the BTG rotating cone; the Karlsruhe BTL2; the Georgia Tech entrained flow reactor; the NREL vortex ablative system; and the Pyrovac vacuum process [7]. Few of these processes have reached the commercial scale, and none of them is fully operational on a continuous basis. The only current commercially relevant application of bio-oil chemicals, from the aqueous phase, is that of wood flavours, browning agents and liquid smoke. Bridgwater, 1999 [11] published an excellent review that classifies the reactors into (1) bubbling fluidized beds, (2) circulating fluidized beds, (3) ablative (vortex and rotating blade) reactors, (4) rotating cone and vacuum reactors, and (5) auger reactors.

1.6.1 Fluidized Bed Reactor

These types of reactors utilize vessels containing a mass of heated particles, such as inert sand or catalyst particles, that are “fluidized” by passing inert gas or recycled product gas through the particle bed. Biomass residue particles are injected into or

above the hot sand bed by a solids feeder, such as a screw feeder or the intermittent solid slug feeder developed in this study.

1.6.1.1 Bubbling Fluidized Bed (BFB) Reactor

Bubbling fluidized bed reactors utilize fluidized bed reactors with gas passing through the reactor so that the solids fluidization is in the "bubbling" regime, i.e. the bed has fully expanded and is bubbling aggressively, but without reaching the turbulent flow regime. A schematic of a bubbling fluidized bed reactor process can be seen in **Fig. 1-3**. Industrially, this type of reactor was been used for pyrolysis by Dynamotive (400 kg/h) and RTI (20 kg/h) for stationary plants and by Agri-Therm Inc. (200 kg/h) as a modified bubbling fluidized bed for a mobile pyrolysis system [8]. After the shredded biomass enters the bed, it interacts with the hot and abrasive bubbling sand environment while reacting. Once the particles become small enough, they are blown out of the fluidized bed and captured in specially designed cyclones. For larger particle sizes, specially designed char segregation zones can be created in the reactor to segregate the char produced from the bed material and continuously remove it from the reactor with high purity [58]. In laboratory-scale reactors, hot filters can be used to retain the char particles in the bed until the end of the experiments [1]. Typically, the vapour residence time in bubbling fluidized bed reactors is between 0.2-5 s, depending on the reactor size [33].

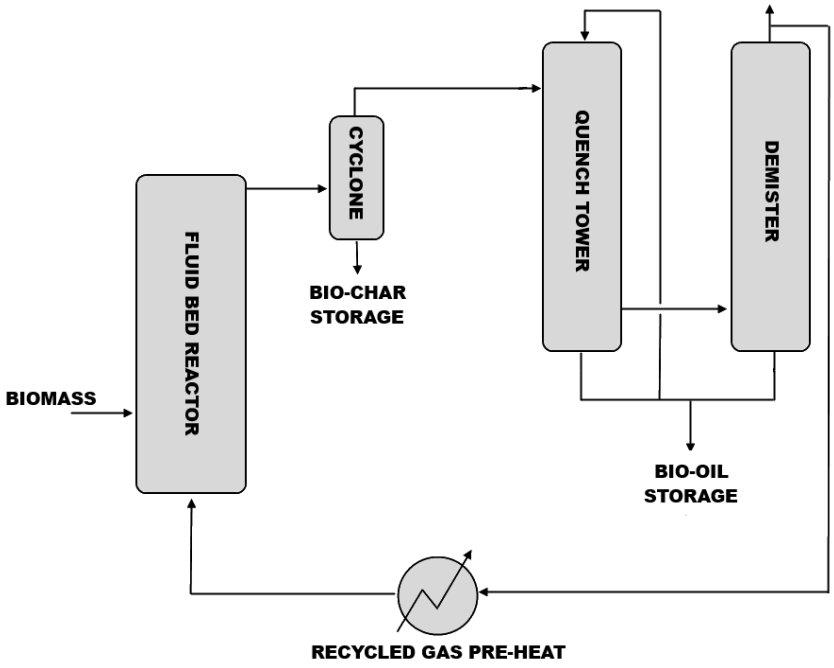

Figure 1-3: BFB Reactor Technology

Bubbling fluidized bed reactor capacities are dependent on surface heat transfer limitations (depending on reactor size) and also on the heat supply. Heat can be provided by direct heating of the sand through the reactor wall in small scale units or using heat exchangers [8].

Table 1-3 illustrates the advantages and challenges of the BFB reactor technology.

Table 1-3: Advantages and Drawbacks of the BFB

Advantages	Drawbacks
Good temperature control and mixing	Product dilution from fluidization gas
Easy to scale up	Condensation train & separation challenges
Well-established technology	Particle size restricted
Intense heat and mass transfer	Char contaminated with sand

1.6.1.2 Circulating Fluidized Bed (CFB) Reactor

Like BFB reactors, CFB reactors also have high heat transfer rates and short vapour residence times (0.5-1 s). In these reactors, the heat transfer medium is the bed of particles (sand, catalyst, etc.) which is circulated, using high flowrates of gas, from the reactor vessel into a burner. In the burner, the particles are exposed to oxygen and recycled product gas or solid reaction products are burned to heat the particles that are then circulated back to the reactor vessel (**Fig. 1-4**). As a result, the solid residence time is approximately the same as the vapour residence time, and the reactor operates at high superficial gas velocities (in transport conditions). As a result of these high flowrates, solids separation and bio-oil vapour condensation can become more challenging. CFB reactors can be either upflow (more traditionally) or downflow (i.e. downers, used for plug flow control of short residence times).

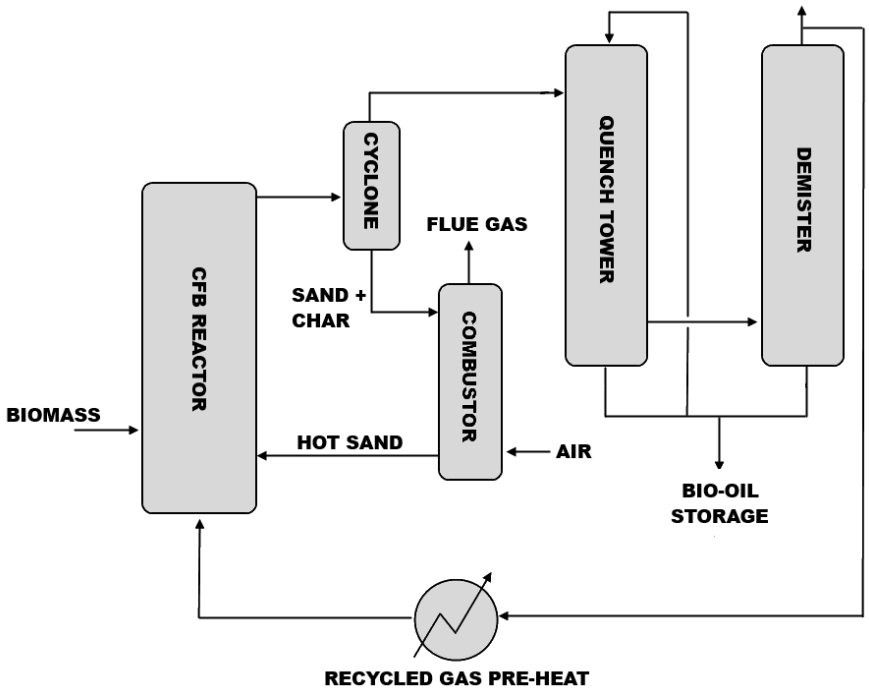

Figure 1-4: Circulating Fluidized Bed Reactor Technology

Table 1-4 illustrates the advantages and challenges of the CFB reactor technology.

Table 1-4: Advantages and Drawbacks of the CFB

Advantages	Drawbacks
Well-established technology	Challenging to operate/condensation/separation
Very large processing capacity	Smaller biomass particles required
Controllable residence time	High gas flow and product dilution
High heating rate	Char attrition, Char contains some sand
Good heat and mass transfer	High separation and quenching requirements

1.6.2 Ablative Reactor

Ablative pyrolysis processes involve the contact between the biomass residue and a hot reaction surface, which also performs mechanical ablation of the biomass surface and removes the char layers formed. Ablation eliminates intra-particle heat transfer limitations in these processes, and therefore relatively large particles can be used (< 20 mm). However, heat transfer limitations are often present in delivering the heat required to the reaction surface. **Fig. 1-5** illustrates the Ablative reactor process, and **Table 1-5** summarizes the advantages and drawbacks of this system.

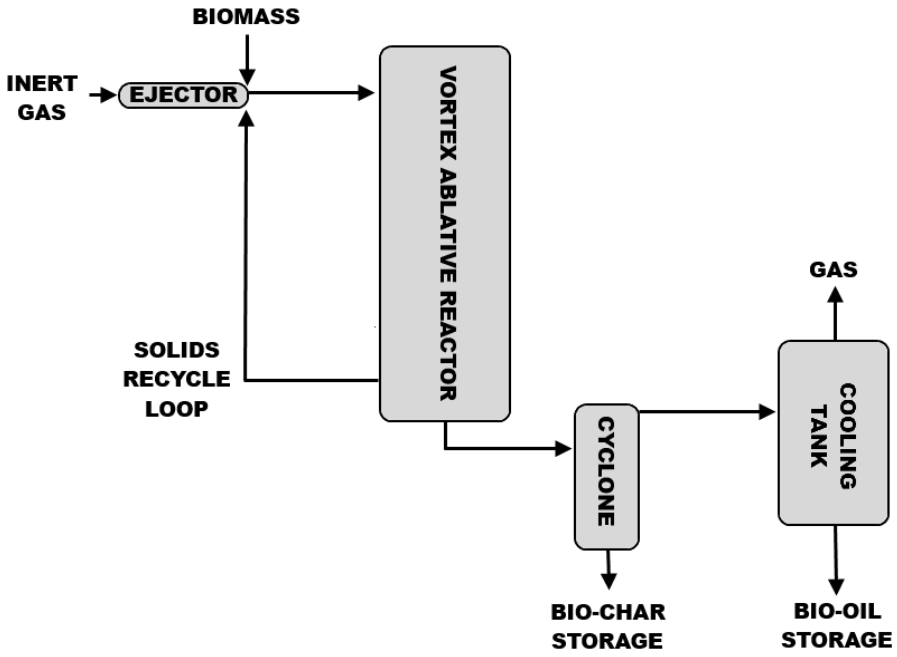

Figure 1-5: Ablative Reactor Technology

Table 1-5: Advantages and Drawbacks of the Ablative Reactor

Advantages	Drawbacks
Large particle sizes can be used	Reaction rates limited by heat transfer to the reactor
Inert gas is not required	Process is surface area controlled, high cost to scale up
System is more intensive	
Good heat transfer	

1.6.3 Rotating Cone Reactor

Developed by a joint collaboration between the University of Twente and BTG (120 kg/h) [34], the rotating cone reactor involves the introduction of biomass residue particles and heat carrier particles (sand or catalyst) at the bottom of a rotating cone, where the solids are mixed and forced against the hot rotating surface for reaction. The solid are then forced upwards and out by the rotating cone (residence time can be controlled by rotation speed). Upon exiting the cone, the vapours are diverted to a condensation train while the solids are combusted in a fluidized bed (generating the heat for the process). **Fig. 1-6** [34] illustrates the Rotating Cone reactor technology, and **Table 1-6** summarizes the advantages and drawbacks of this system.

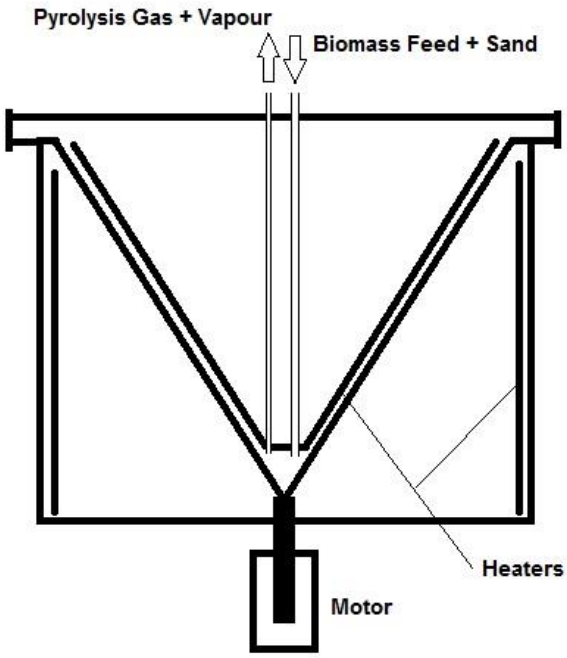

Figure 1-6: Rotating Cone Reactor Technology [34]

Table 1-6: Advantages and Drawbacks of the Rotating Cone Reactor

Advantages	**Drawbacks**
Centrifugal forces moves heated sand and biomass, no carrier gas needed	Complex process
	Difficult to scale up
Easy quenching	High capital costs
	Small particle size needed

1.6.4 Vacuum Reactor

Vacuum pyrolysis is performed at a total pressure of about 15 kPa, with the biomass material moving in a hot (~450 °C) agitation device. The biomass particles are exposed to a long residence time to fully react (due to the low heat transfer rate); while the organic vapour residence time is very short due to being under vacuum. **Fig. 1-7** illustrates the vacuum pyrolysis technology and **Table 1-7** summarizes the advantages and drawbacks of this system. This technology was developed at the Université Laval and commercialized by Pyrovac [8].

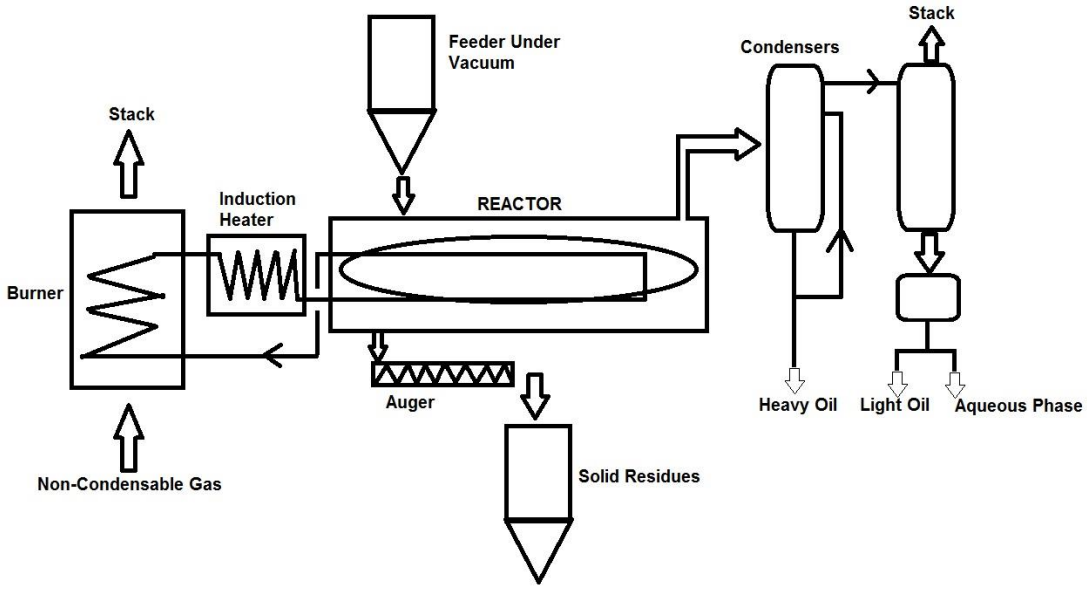

Figure 1-7: Vacuum Reactor Technology

Table 1-7: Advantages and Drawbacks of the Vacuum Reactor

Advantages	Drawbacks
Feed particle size flexibility	Low bio-oil yield, Increased pyrolytic water generation
Fewer aerosols formed (easier quenching)	Low heating efficiency
Bio-oil free of char	Absorption of liquid effluents in the liquid ring compressor pump
No additional carrier gas/product dilution	High capital cost, maintenance cost and high sealing/gasket requirements

1.6.5 Auger Reactor

Auger pyrolysis reactors (**Fig. 1-8**) were developed in the 1940s in Germany (Lurgi-Ruhrgas process) and refined at Mississippi State University (1 kg/h). They have been commercialized by various parties including Renewable Oil International (ROI, 200 kg/h), and ABRI-TECH Inc. (1 tonne/day) [8]. A hot auger is used to react and drive the biomass residue for a given residence time. The vapours are then diverted to a condensation train and the char produced is forced out the outlet of the auger into a char storage system. In large-scale auger reactor, recycled heat carrier particles (such as metal balls) are used to ensure good heat distribution across the diameter of the auger. **Table 1-8** summarizes the advantages and drawbacks of this system.

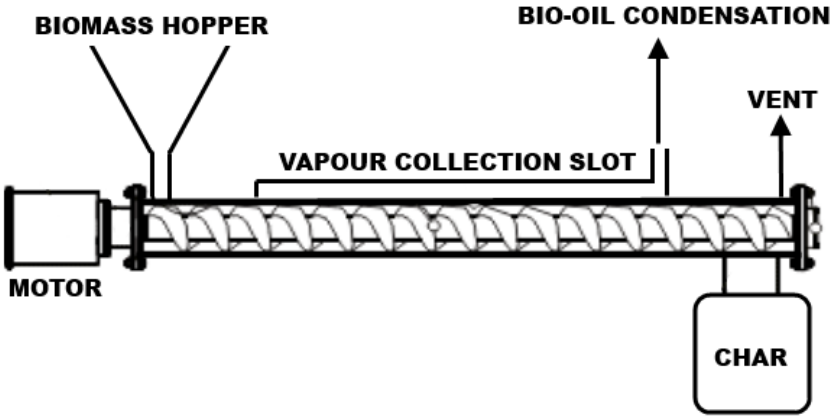

Figure 1-8: Auger Reactor Technology

Table 1-8: Advantages and Drawbacks of the Auger Reactor

Advantages	Drawbacks
Low pyrolysis temperature (400^{o}C)	Plugging risk
Compact design	Low bio-oil yield
No carrier gas/dilution	Moving parts in the hot zone
	Heat transfer limitations at large scale

1.7 Pyrolysis Reactor Selection Criteria

Scott et al. [35] analyzed several reactors for fast biomass pyrolysis and concluded that none of the reactor concepts fully satisfies all requirements in their present state of development. Based on their analysis, they indicated that the bio-oil quenching requirements should be minimized using the smallest possible gas to biomass feed ratio, and that the pyrolysis reactor should operate at the minimum possible temperature. They also concluded that a biomass conversion process, especially one producing liquid fuels, would be most useful if it were a simple process, not capital intensive, and that it could be operated efficiently on a small scale, while being scalable to larger sizes as well. Such a plant would not necessarily be suited as a centralized conversion plant, attempting to service a large area, as raw material shipping costs would make the economics prohibitive. On the contrary, an economical plant would have to be sited where the raw material could be easily supplied at a reasonable or at no cost – with raw materials that have a "negative" value and minimum transportation requirements. The liquid product could then be used or modified on site, or more readily and economically transported to a central upgrading facility than the raw biomass [36].

Table 1-9 illustrates the valuation of the different reactor technologies, given these considerations. The Bubbling Fluidized Bed reactor technology and Auger reactor are shown to be the most promising overall. However, the Auger reactor technology was eventually rejected due to the following limitations: the bio-oil yields are lower due to a slower pyrolysis reaction (secondary cracking), the moving parts are a long-term operation risk, and there are potential heat transfer challenges limitations at larger

scale. As a result, the fluidized bed was selected at the Institute for Chemicals and Fuels from Alternative Resources (ICFAR) as the reactor of choice for laboratory-scale testing of different biomass feedstock, as it could also be scaled and give representative results of a potentially large-scale economic process. In addition, these considerations inspired the development of a joint venture between ICFAR at Western University and private investors, leading to the creation of a spin-off company (Agri-Therm Inc.). Agri-Therm (www.agri-therm.com) is dedicated to developing, manufacturing and marketing portable (mobile) pyrolysis plants for the production of bio-oil and bio-products from biomass, specifically agricultural residues, residues and transition crops. The technology is based on an innovative fluidized bed reactor technology that addresses the unique issues associated with agricultural residues. Appendix I is a published business case study (and teaching note) based on the Agri-Therm Inc. mobile pyrolysis system. The case outlines the technical and business challenges and potential solutions for operating a small-business enterprise within the renewable energy industry.

An updated list of global competitors and research groups, with descriptions of their respective technologies for fast pyrolysis and upgrading, can be found in [23].

Table 1-9: Reactor Selection Criteria

Reactor Type	Simple	Capital Expense	Low Temperature	Low Gas/Solid Ratio	Operating Expense	Easy Scale-up
BFB	**Very Good**	**Excellent**	**Very Good**	**Good**	**Very Good**	**Excellent**
CFB	Fair	Good	Very Good	Poor	Fair	Very Good
Ablative	Fair	Very Good	Very Good	Excellent	Good	Very Poor
Rotating Cone	Fair	Good	Very Good	Very Good	Fair	Poor
Vacuum	Fair	Excellent	Excellent	Excellent	Poor	Good
Auger	Very Good	Excellent	Very Good	Excellent	Good	Poor

1.8 The Future Outlook of Biomass Fast Pyrolysis [38]

Pyrolysis has yet to break through into business success and, in fact, has had its fair share of failures so far. Many companies have come and gone, and there are always articles about the next greatest pyrolysis breakthrough in someone's garage, but few enjoy commercial success. The fact of the matter is that technical development is challenging; it took the oil industry over 100 years to become a standardized and fully successful enterprise world-wide (with many improvements and optimizations still happening today) and pyrolysis is trying to develop in a much shorter time-frame while competing with existing fuels, chemicals and government policies. In addition, bio-oil is not a quality raw crude: it has typically high water and oxygen content (more challenging for upgrading to conventional fuels), is unstable and can phase separate and age with time, and tends to be highly corrosive, viscous and contains some heavy tars. Suffice it to say, there are still some significant technical challenges in this "blue-ocean" new market.

In order to maximize current market opportunities and to optimize pyrolysis technology for the most promising of markets, pyrolysis companies should focus product development and testing programs around the two largest biomass contributors: wood and corn residues. The International Energy Agency (IEA) estimates the annual worldwide biomass contribution from wood to be 1.4 billion bone dry tonnes (BDt), over two times the next closest contributor, corn [3]. Corn residues are also an important feedstock due to their fibrous nature, making them a perfect proxy for other fibrous

feedstocks such as sugar cane, rice and grains. Canada could particularly benefit by this strategy of development, as these feedstocks are in abundant accessible supply. In addition, Canada also has [continuously expanding] advanced infrastructure in place for low-cost biomass and fuel exports.

Heat and electric power production as well as manufacturing of renewable fertilizers and soil amendments, with potential supportive government policies and programs, could be a first step to jump start the renewable bio-oil and bio-char markets, respectively. In fact, unlike direct biomass combustion, bio-oil has a very low ash content which is attractive for long-term combustion (fouling prevention). As a result of this characteristic, bio-oil is also a much better feedstock for gasification than raw biomass. Significant work has been carried out on research and development for the application of bio-oil for the heat and power generation, including the design and study of specialized bio-oil burners, engines and furnaces at CANMET [39] and the Combustion Research Laboratory, at The University of Toronto [16] and also significant testing and development for power generation from bio-oil in diesel engines, gas turbines and co-firing processes [10, 11]. However, once the markets for both bio-oil and bio-char become more established, higher-value uses will emerge for both of these products, such as specialty chemicals and materials production from bio-oil, upgrading and refining of bio-oil into conventional fuel products and upgrading of bio-char for handling, energy uses and safe soil amendment purposes.

In order to implement technologies to harness this available energy, one must also consider that labour and transportation are the dominant operating costs, and find an optimum operating model to minimize these costs [42]. Moreover, steady biomass availability is a challenge, being seasonal, geographically distributed and of different sizes. Stationary or centralized pyrolysis units (or wood-fired direct combustion for localized electricity production or gasification systems) require that all of the raw material biomass residue must be hauled in its raw form to the plant site, which significantly increases transportation costs and would likely limit an economic raw biomass transportation radius of under 200 km from the plant location [43]. However, one central plant could take advantage of economies of scale and could supply several energy users in distributed locations, while also reducing downside risk and increasing net returns [44]. Mobile pyrolysis plants would successfully reduce raw material and product transportation costs by a factor of 2 [43], but are subject to increased labour and set-up costs, depending on how often and how far the unit would need to move [44]. An additional business model of interest has been proposed by bioliq® in Karlsruhe, Germany, where pyrolysis is performed at distributed plants and the bio-oil and bio-char products are mixed together, forming a slurry, and shipped to a centralized plant for gasification to produce a high quality syngas [45]. Ultimately, however, the probability of success of both mobile and stationary pyrolysis business models will heavily depend on the steady availability of feedstock and on mitigating raw feedstock costs (if feedstocks with a “negative” value are used, the economics are much more favourable) and securing long-term raw material contracts, mean crude oil and natural

gas prices over time, and the ability to sell/move bio-oil and bio-char to the market easily (have direct bio-oil applications and an end user supply). In addition, improvements in pyrolysis technologies to further increase yields and process energy efficiency will also increase the probability of a successful business model.

Based on these considerations, one could attempt to design and finance a business that would design, manufacture and operate large-scale (>10 BDt/day) mobile pyrolysis systems, that would take advantage of both the minimized transportation costs of a mobile system, but the cost-effective nature of operating at a relatively large capacity, large enough to realize economies of scale, but small enough to be realistic about how much process-worthy biomass could be in one location (to be able to operate continuously for a period of time). Notwithstanding the potential sensitivity to the aforementioned variables that would be difficult to predict in the market, one could operate over 2,200 units of this kind to process the available wood and corn residue biomass in Canada alone. This ignores any market opportunities to sell units directly to self-consuming markets in China, India and Central & South America.

Finally, a critical recommendation for the pyrolysis industry is to team up. With government support and commitments from industry, a national consortium should be created that maximizes the "know-how" of every aspect of the production chain and connects the forestry and agricultural operators, pyrolysis experts (academic and business), market uptake, and business world. The epistemology of pyrolysis exists for all of these areas, but is fragmented – in order to push through and become a

commercial success and reality, these connections are absolutely necessary. Individuals or organizations with the following areas of expertise should be part of the consortium:

- Biomass residue sourcing, preparation, drying, densification and transportation.
- Biomass feeding technology to ensure successful continuous feeding of large varieties of biomass residues without the risk of plugging and down-time. Standard pyrolysis feeder technologies have been developed for sawdust and forestry residues, but have faced major difficulties when being adapted for processing feedstocks such as Kraft lignin, meat and bone meal residues, and dried distillers' grains [46].
- Pyrolysis reactor technology: reactor design and operation (both small and large scale; mobile and stationary).
- Bio-char characterization, handling, pelletization, transportation and utilization (soil and energy).
- Bio-oil characterization, fractionation, stabilization, handling, upgrading, transportation and utilization (oil & petrochemical companies).
- Business: management, financing, securing preliminary contracts and upgrading partnerships, and connecting the dots.

1.9 Reactor Feeding Technology

Fluidized bed technology has been demonstrated to have good potential as a reactor technology of choice for the production of pyrolysis oil and bio-char, via fast biomass pyrolysis [35]. In a fluidized bed pyrolysis process, raw biomass material particles must be conveyed or injected into the reactor, using the least energy intensive and most practical feeding system. Currently there are three main types of feeders being used in industry: dilute phase pneumatic transport feeders, dense phase pneumatic transport feeders, and screw/auger feeders. However, in the flash pyrolysis process, where the temperature of the reactor is high, typically between 450 and 550 °C, and where relatively high mass flow rates of raw biomass can be processed, these commonly used feeding systems tend to encounter some problems with some feedstocks [1, 46].

1.9.1 Dilute-Phase Pneumatic Feeders

Dilute-phase pneumatic transport feeders utilize a large amount of gas, which is typically recycled and cooled product gas, in order to suspend and convey particle materials in the feeding tube. This operation results in high energy consumption within the reactor and requires a larger, more sophisticated and much more expensive condensation train due to extensive product vapour dilution [46].

1.9.2 Screw/Auger Feeders

Screw/Auger feeding systems are quite common with many pyrolysis reactor systems, given the advantage of having very low gas consumption (if any). Similarly to dense-phase pneumatic feeders, the solids in the screw feeder are forced down the feeding tube relatively slowly, resulting in potential reaction and chemical changes in the

feedstock prior to entering the reactor body. This may result in plugging and down-time, particularly with temperature-sensitive feedstocks such as meat and bone meal residues, Kraft lignin or dried distiller's grains.

In addition, the screw/auger feeders are mechanical, with continuously moving parts, which results in a higher maintenance and downtime requirement over long-term operation.

With bubbling fluidized bed reactors, the screw feeder feeding port often needs to be above the fluidized bed level to prevent plugging and backflow (due to the pressure fluctuations in the fluidized bed). Since the biomass typically is less dense than the inert reactor heat transfer medium, the biomass will float on top of the hot fluid bed resulting in poorer mixing and heat transfer and increased secondary cracking, resulting in lower product yields [47].

1.9.3 Novel ICFAR Intermittent Solid Slug Feeder

To prevent plugging and help the raw biomass particles effectively penetrate and spread into the pyrolysis fluidized beds, one could inject the particles using intermittent slugs created by propelling loosely packed particles with gas pulses and transporting them along horizontal or inclined feeding pipes into the fluidized bed section of the reactor [48]; this combines the advantages of the low gas consumption of the screw feeders and the short residence time in high temperature zones of dilute phase feeders.

Among many other potential applications, intermittent solid slug feeders can be used to effectively inject biomass materials into fluidized bed reactors for pyrolysis. In particular,

these feeders can be used to convey biomass materials that are highly cohesive to prevent plugging or undesirable reaction in the feeding tube.

The design, modeling, optimization, scale-up procedure and applications of this type of feeder represent the core of this thesis.

1.9.4 Dense-Phase Pneumatic Feeders

An analogy to the ICFAR intermittent solid slug feeder technology is dense-phase pneumatic transport. However, if this type of feeder were used, it would also consume a large amount of gas to ensure a constant low velocity (above the particle saltation requirement). The flow of dense-phase solids naturally begins to form larger intermittent slugs or dunes (resulting in inconsistent solid loading delivery in the bed), with a thin-layer of stragglers across the entire pipe [49–57]. The straggler particles may begin to react in the hot feeding tube, which can result in plugging and down-time, particularly with temperature-sensitive feedstocks such as meat and bone meal residues, Kraft lignin or dried distiller's grains.

1.10 Thesis Objectives & Outline

The work in this thesis examines and reports on many aspects related to the novel ICFAR feeding technology, including:

- The preliminary design, testing and trial-and-error optimizations of the novel feeder technology (**Chapter 2**).
- Development and experimental validation of the fundamental model for the novel feeding technology (**Chapter 3**).
- Application of the predictive model to the development of alternate feeder geometries and scale-up procedures (**Chapter 4**). A full design procedure and optimization curves are proposed in this chapter.
- The new large-scale feeder technology allows for the feeding of large biomass particles that traditional feeder technologies cannot handle. An issue with large particles is that they require relatively long drying, which must be optimized. A model was therefore developed for the feed preparation and drying required for large-scale feeding and pyrolysis (**Chapter 5**).
- The implementation and application of the feeder for fast pyrolysis in laboratory-scale pyrolysis reaction for meat and bone meal residues (**Chapter 6**), *tucumã* seeds (**Appendix II**), and Kraft lignin (**Appendix III**). The new feeder technology made it possible to perform the first ever pyrolysis studies on pure meat and

bone meal residue and unmodified and undiluted Kraft lignin in industrially-relevant equipment.

- The general thesis impacts and conclusions (**Chapter 7**).

In addition, this thesis work also discusses general pyrolysis considerations and touches on the economics of the pyrolysis process from a technical (**Chapter 6 and Appendix II**) and business standpoint (**Section 1.8**). **Appendix I** is a published business case study (and teaching note) based on a mobile pyrolysis company called Agri-Therm Inc. The case outlines the technical and business challenges and potential solutions for operating a small-business enterprise within the renewable energy industry.

1.11 References

[1] F. M. Berruti, K. Lenkiewicz, R. Xu, R. J. Bedmutha, S. Nova, F. Berruti, and C. L. Briens, "Novel Fluid Bed Pilot Plant for the Production of bio-oil from Biomass through Fast Pyrolysis," *Récents Progrès en Génie des Procédés, Ed. SFGP, Paris, France, ISBN 2-910239-68-3*, no. 94, pp. 1–8, 2007.

[2] Canada, "Industry Canada - Towards a Technolology Roadmap for Canadian Forest Biorefineries," 2006.

[3] WEO, "The IEA World Energy Outlook 2011," 2011.

[4] H. Khatib, "IEA World Energy Outlook 2011—A comment," *Energy Policy*, vol. 48, pp. 737–743, Sep. 2012.

[5] A. Demirbas, "Effect of initial moisture content on the yields of oily products from pyrolysis of biomass," *Journal of Analytical and Applied Pyrolysis*, vol. 71, no. 2, pp. 803–815, Jun. 2004.

[6] A. V. Bridgewater, S. Czernik, and J. Piskorz, "Progress in Thermochemical Biomass Conversion," *Bridgewater A.V. Ed., Blackwell Science, London*, p. 977, 2001.

[7] D. Mohan, C. U. Pittman, and P. H. Steele, "Pyrolysis of Wood / Biomass for bio-oil : A Critical Review," no. 4, pp. 848–889, 2006.

[8] R. Xu, "Development of Advanced Technologies for Biomass Fast Pyrolysis (Doctoral Thesis)," Western University, 2010.

[9] S. Czernik and A. V Bridgewater, "Overview of Applications of Biomass Fast Pyrolysis Oil," no. 12, pp. 590–598, 2004.

[10] E. Pütün, "Biomass to Bio-oil via Fast Pyrolysis of Cotton Straw and Stalk AY SE," no. February 2001, pp. 275–285, 2002.

[11] A. V. Bridgwater, “Principles and practice of biomass fast pyrolysis processes for liquids,” *Journal of Analytical and Applied Pyrolysis*, vol. 51, no. 1–2, pp. 3–22, Jul. 1999.

[12] A. V. Bridgwater, “Renewable Fuels and Chemicals by Thermal Processing of Biomass,” *Chemical Engineering Journal*, vol. 91, no. 2–3, pp. 87–102, Mar. 2003.

[13] J. Piskorz, D. S. Scott, and D. Radlein, “Pyrolysis Oils from Biomass: Producing, Analyzing and Upgrading,” *ACS Washington*, pp. 167–175, 1988.

[14] H. Darmstadt, M. Garcia-Perez, A. Adnot, A. Chaala, D. Kretschmer, and C. Roy, “Corrosion of Metals by Bio-oil Obtained by Vacuum Pyrolysis of Softwood Bark Residues. An X-ray Photoelectron Spectroscopy and Auger Electron Spectroscopy Study,” *Energy & Fuels*, vol. 18, no. 5, pp. 1291–1301, Sep. 2004.

[15] Q. Zhang, J. Chang, T. Wang, and Y. Xu, “Review of biomass pyrolysis oil properties and upgrading research,” *Energy Conversion and Management*, vol. 48, no. 1, pp. 87–92, Jan. 2007.

[16] T. Tzanetakis, N. Farra, S. Moloodi, W. Lamont, A. McGrath, and M. J. Thomson, “Spray Combustion Characteristics and Gaseous Emissions of a Wood Derived Fast Pyrolysis Liquid-Ethanol Blend in a Pilot Stabilized Swirl Burner,” *Energy & Fuels*, vol. 24, no. 10, pp. 5331–5348, Oct. 2010.

[17] M. . Boucher, a Chaala, H. Pakdel, and C. Roy, “Bio-oils obtained by vacuum pyrolysis of softwood bark as a liquid fuel for gas turbines. Part II: Stability and ageing of bio-oil and its blends with methanol and a pyrolytic aqueous phase,” *Biomass and Bioenergy*, vol. 19, no. 5, pp. 351–361, Nov. 2000.

[18] M. . Boucher, a Chaala, and C. Roy, “Bio-oils obtained by vacuum pyrolysis of softwood bark as a liquid fuel for gas turbines. Part I: Properties of bio-oil and its blends with methanol and a pyrolytic aqueous phase,” *Biomass and Bioenergy*, vol. 19, no. 5, pp. 337–350, Nov. 2000.

[19] M. Ikura, M. Stanciulescu, and E. Hogan, “Emulsiÿcation of pyrolysis derived bio-oil in diesel fuel,” vol. 24, pp. 221–232, 2003.

[20] Adjaye, J.D., Bakhshi, N.N. "Production of hydrocarbons by catalytic upgrading of fast pyrolysis biooil," vol. 45, num. 3, pp. 185-202 (18), 1995.

[21] S. Czernik, R. Evans, and R. French, “Hydrogen from biomass-production by steam reforming of biomass pyrolysis oil☆,” *Catalysis Today*, vol. 129, no. 3–4, pp. 265–268, Dec. 2007.

[22] S. Czernik, R. French, C. Feik, and E. Chornet, “Biomass Thermoconversion Processes,” pp. 4209–4215, 2002.

[23] A. V Bridgwater, “Review of fast pyrolysis of biomass and product upgrading,” *Biomass and Bioenergy*, vol. 38, pp. 68–94, 2011.

[24] A. V Bridgwater, “Upgrading Biomass Fast Pyrolysis Liquids,” vol. 31, no. 2, pp. 261–268, 2012.

[25] A. Alcala and A. V. Bridgwater, “Upgrading fast pyrolysis liquids: Blends of biodiesel and pyrolysis oil,” *Fuel*, Mar. 2013.

[26] K. Jacobson, K. C. Maheria, and A. Kumar Dalai, “Bio-oil valorization: A review,” *Renewable and Sustainable Energy Reviews*, vol. 23, pp. 91–106, Jul. 2013.

[27] D. Radlein and J. Piskorz, “Production of Chemicals from Bio-oil, in Gasification and Pyrolysis of Biomass,” *A.V. Bridgwater, CPL. Press, Newbury, UK.*, pp. 307–315, 1997.

[28] R. Simon, B. de la Calle, S. Palme, D. Meier, and E. Anklam, “Composition and analysis of liquid smoke flavouring primary products,” *Journal of Separation Science*, vol. 28, no. 9–10, pp. 871–882, Jun. 2005.

[29] E. Athanassiadou, S. Tsiantzi, and P. Nakos, “Wood adhesives made with pyrolysis oils,” pp. 1–8.

[30] B. Freel and R. G. Graham, “Bio-oil Preservatives,” 2002.

[31] R. J. Bedmutha, “Pesticides from Fast Pyrolysis of Agricultural Residues,” The University of Western Ontario, 2008.

[32] A. V Bridgwater and G. V. C. Peacocke, “Fast pyrolysis processes for biomass,” vol. 4, 2000.

[33] C. L. Briens, J. Piskorz, and F. Berruti, “Biomass Valorization for Fuel and Chemicals Production - A Review,” *International Journal of Chemical Reactor Engineering2*, vol. 6, no. 2, 2008.

[34] B. M. Wagenaar, W. Prins, and W. P. M. V. Swaaij, “Pyrolysis of Biomass in the Rotating Cone Reactor: Modelling and Experimental Justification,” *Chemical Engineering Science*, vol. 49, no. 24B, pp. 5109–5126, 1994.

[35] D. S. Scott, P. Majerski, J. Piskorz, and D. Radlein, “A second look at fast pyrolysis of biomass—the RTI process,” *Journal of Analytical and Applied Pyrolysis*, vol. 51, no. 1–2, pp. 23–37, Jul. 1999.

[36] D. S. Scott and J. Piskorz, “The Continuous Flash Pyrolysis of Biomass,” *The Canadian Journal of Chemical Engineering*, vol. 62, no. 3, pp. 404–412, 1984.

[37] F. M. Berruti and H. Liu, “Green-Tech: Bio-Fuels High Growth Strategy,” *Ivey Publishing*, 2012.

[38] F. M. Berruti, “Biomass Residue Fast Pyrolysis: the Future Outlook,” *Canadian Biomass*, 2013. [Online]. Available: http://www.canadianbiomassmagazine.ca/content/view/3954/133/. [Accessed: 12-Feb-2013].

[39] F. Preto, I. Coyle, J. Wong, and F. Zhang, “Combustion of Pyrolysis Bio-oils ” in a Tunnel Furnace Canadian Fast Pyrolysis Developers.”

[40] D. Chiaramonti, A. Oasmaa, and Y. Solantausta, “Power generation using fast pyrolysis liquids from biomass,” *Renewable and Sustainable Energy Reviews*, vol. 11, no. 6, pp. 1056–1086, Aug. 2007.

[41] D. Wissmiller, “Pyrolysis oil combustion characteristics and exhaust emissions in a swirl-stabilized flame,” 2009.

[42] A. L. Brown, P. D. Brady, C. D. Mowry, and T. T. Borek, “An Economic Analysis of Mobile Pyrolysis for Northern New Mexico Forests,” no. December, 2011.

[43] P. C. Badger and P. Fransham, “Use of mobile fast pyrolysis plants to densify biomass and reduce biomass handling costs—A preliminary assessment,” *Biomass and Bioenergy*, vol. 30, no. 4, pp. 321–325, Apr. 2006.

[44] M. A. Palma, J. W. Richardson, and B. E. Roberson, “Economic Feasibility of a Mobile Fast Pyrolysis System for Sustainable Bio-crude Oil Production,” *International Food and Agribusiness Management Review*, vol. 14, no. 3, pp. 1–16, 2011.

[45] “Bioliq,” 2012. [Online]. Available: www.bioliq.de. [Accessed: 30-Nov-2012].

[46] F. M. Berruti, L. Ferrante, F. Berruti, and C. L. Briens, “Optimization of an Intermittent Slug Injection System for Sawdust Biomass Pyrolysis,” *International Journal of Chemical Reactor Engineering*, vol. 7, 2009.

[47] E. Cascarosa, I. Fonts, J. M. Mesa, J. L. Sánchez, and J. Arauzo, “Characterization of the liquid and solid products obtained from the oxidative pyrolysis of meat and bone meal in a pilot-scale fluidised bed plant,” *Fuel Processing Technology*, vol. 92, no. 10, pp. 1954–1962, Oct. 2011.

[48] M. O. Guedon, T. Baron, C. L. Briens, and T. M. Knowlton, “Intermittent injection of prepolymer in a pressurized fluidized bed,” *Powder Technology*, no. 78, pp. 25–32, 1994.

[49] S. S. Mallick, “University of Wollongong Thesis Collection Modelling of fluidised dense-phase pneumatic conveying of powders Soumya Suddha Mallick,” 2009.

[50] J. Li, C. Webb, S. S. Pandiella, G. M. Campbell, T. Dyakowski, a. Cowell, and D. McGlinchey, “Solids deposition in low-velocity slug flow pneumatic conveying,” *Chemical Engineering and Processing: Process Intensification*, vol. 44, no. 2, pp. 167–173, Feb. 2005.

[51] R. Pan and P. W. Wypych, “Pan & Wypych (1997) - Pressure Drop and Slug Velocity in Low-Velocity Pneumatic Conveying of Bulk Solids.pdf,” *Powder Technology*, vol. 94, pp. 123–132, 1997.

[52] M. Sakai and S. Koshizuka, “Large-scale discrete element modeling in pneumatic conveying,” *Chemical Engineering Science*, vol. 64, no. 3, pp. 533–539, Feb. 2009.

[53] J. Xiang and D. McGlinchey, “Numerical simulation of particle motion in dense phase pneumatic conveying,” *Granular Matter*, vol. 6, no. 2–3, pp. 167–172, Oct. 2004.

[54] T. Zhao and M. Takei, “Design of a Plug Formation Detector Based on the Capacitance Measurement Technique,” *Advanced Powder Technology*, vol. 19, no. 6, pp. 559–572, Nov. 2008.

[55] Y. Tsuji, T. Tanaka, and T. Ishida, “Lagrangian numerical simulation of plug flow of cohesionless particles in a horizontal pipe,” *Powder Technology*, vol. 71, no. 3, pp. 239–250, 1992.

[56] S. S. Mallick and P. W. Wypych, “An Investigation into Modeling of Solids Friction for Dense-Phase Pneumatic Conveying of Powders,” *Particulate Science and Technology*, vol. 28, no. 1, pp. 51–66, Jan. 2010.

[57] R. Pan, “Material properties and flow modes in pneumatic conveying,” pp. 157–163, 1999.

[58] Mara, Craig, "An Investigation of Biochar Removal Systems for Pyrolysis Reactors" (2012). University of Western Ontario: Master's Thesis.

[59] Tumbalam Gooty, Akhil, "Fractional Condensation of Bio-Oil Vapors" (2012). University of Western Ontario - Electronic Thesis and Dissertation Repository. Master’s Thesis - Paper 979. http://ir.lib.uwo.ca/etd/979

Chapter 2

2 Chapter 2: Preliminary Design and Optimization of a Lab-Scale Intermittent Solid Slug Feeder[3]

2.1 Introduction

Biomass is a composite material made up of oxygen-containing organic components (cellulose, hemicellulose, lignin, organic extractives) and of inorganic minerals. It is a renewable and carbon dioxide neutral source of energy, essentially a form of stored solar energy captured through the process of photosynthesis by green plants. Fresh biomass, however, is not suitable for producing energy directly. The high moisture content and low energy density of the raw biomass (one tenth of that of conventional liquid fuels) make it an uneconomical source of energy. However, after a certain extent of drying, biomass has been used as a combustion fuel for centuries. The convenience of handling, processing, upgrading and utilizing liquid fuels has also prompted the development of technologies to transform solid biomass into liquids. For example, biomass can be converted through fast pyrolysis into a versatile and transportable liquid known as bio-oil, with an energy density five to six times higher than that of the raw biomass. In addition, fast pyrolysis produces valuable bio-char and product gas [1].

---

[3] A version of this work has been published in the International Journal of Chemical Reactor Engineering:

Berruti, F.M., Ferrante, L., Briens, C., Berruti, F. (2009). Optimization of an Intermittent Solid Slug Injection System for Sawdust Biomass Pyrolysis. *International Journal of Chemical Reactor Engineering (IJCRE)*: Vol. 7: 1.

Bio-oil can be made from a wide variety of forest and agricultural waste materials, including wood, sugar cane bagasse, rice hulls and straw, peanuts hulls, switchgrass, wheat straw, corn, tobacco stalks, coconut fibres, and many other [2]. Other organic byproducts of the poultry industry (chicken litter), of the pulp and paper industry (sludge), and of the ethanol manufacturing (dry distillers' grains) are also excellent feedstocks [3].

Fluidized bed technology has been demonstrated to be excellent for fast biomass pyrolysis. In a fluidized bed pyrolysis process, raw biomass material particles must be conveyed or injected into the reactor, using the least energy intensive and most practical feeding system. Dilute phase pneumatic transport lines and screw feeders are currently being used by several pyrolysis processes and similar processes such as coal fluidized bed combustors and food delivery systems. However, in the flash pyrolysis process, where the temperature of the reactor is high and typically between 450 and 550 °C, and where relatively high mass flowrates of raw biomass can be processed, with high solid/gas ratios, these commonly used feeding systems tend to encounter some problems [3]. For example, the high temperature coupled with pressure fluctuations at the inlet into the reactor can often lead to severe plugging in both dilute phase pneumatic transport injectors as well as screw feeders, potentially causing significant damage to the equipment or down time in the operating process. In addition, many desirable feeds for pyrolysis tend to be very cohesive particulate solids which tend to plug the feeding lines.

To prevent plugging and help the raw biomass particles effectively penetrate and spread into the pyrolysis fluidized beds, one could inject the particles using intermittent slugs created by propelling loosely packed particles with gas pulses and transporting them along horizontal or inclined feeding pipes into the fluidized bed section of the reactor [4]. For biomass feeding, it is crucial to feed within the dense phase region of the reactor, as the biomass would otherwise remain floating on top of the fluidized bed due to its low density and its heating rate would drop, reducing the yield of higher value liquids [5]. For this reason, it is necessary to feed horizontally or at an angle, to enter the reactor on the side, and penetrate the fluidized bed, ideally reaching a zone of intense agitation where the heat transfer from bed to biomass particles will be at its highest. In addition, pulse feeding off-centre within the fluidized bed can enhance lateral mixing within the fluidized bed with the penetration of every pulse. The gas used to propel the slug must be oxygen-free to preserve the effectiveness of the pyrolysis process, and, therefore, inert gases or recycled gas products from the pyrolysis process should be used. The pulses of gas also serve the purpose of keeping the feeding tube cool and clear of condensing volatiles or backflow of sand. The very short residence time of the biomass in regions of the feeding tube near the hot reactor also helps prevent its thermal degradation. Although some feeders of this design have been shown to work very effectively [4], they have not been studied in detail or optimized for the pyrolysis process. In addition, the operating conditions required to obtain predictable and consistent mass flowrates and slugs of desirable characteristics need to be established.

The purpose of this work was to design, build and demonstrate the operation of a horizontal intermittent solid slug feeder for a laboratory scale pyrolysis reactor (approximately 1 g/s) and to optimize its operation, using sawdust as the feed material, by maximizing the solid-to-gas feed ratio. Fine sawdust is an extremely cohesive and difficult biomass to inject, but one that holds great potential as an important renewable feedstock for pyrolysis [1]. In addition, sawdust has a bulk density of less than 1000 kg/m^3, meaning that the only method to transport it pneumatically in dense phase is by plug flow, rather than by fluidized transport [6]. This is desirable in order to reduce gas consumption and improve energy efficiency. Once optimized, the feeder would be tested in a hot laboratory-scale pyrolysis reactor with various feedstocks.

2.2 Experimental Procedure

2.2.1 Equipment Description

The novel intermittent solid slug feeder designed for this work is illustrated in **Fig. 2-1**, as it would be installed in a pyrolysis pilot plant. **Fig. 2-2** illustrates the feeder on its own, as used for experimentation, by replacing the reactor with a cyclone for solids collection.

The feeder consisted of a pressurized vertical solids storage silo leading to a 19 mm pneumatic pinch valve. The silo had a 4 L volume (0.102 m inner diameter), with a cone angle of 70° from the horizontal. Within the silo, a rotating 'egg-beater' mixer prevented the bridging of solids. The instantaneous mass flow of gas flowing into the silo was determined using a 5.1 mm orifice meter and measuring the instantaneous pressure

drop (ΔP) across the orifice. The pinch valve was controlled by solenoid valves (S.V. 1A and 1B) connected to a relay timer (IMO iSmart Relay, 10 I/O AC). Solids exiting the pinch valve flowed into a 12.7 mm, 1 m long horizontal feeding tube through a ninety degree angle connection. The volume within such connection, between the end point of the pinch valve and the horizontal feeding tube is called 'slug chamber'. The volume and design of this chamber has material implications on the performance of the feeder and will be discussed later. However, for the purpose of the current study, a simple "T" fitting of constant diameter (12.7 mm) was utilized, with a vertical, 63.5 mm long section. In some experiments, a continuous air flow (measured using a 0.7mm sonic nozzle) was fed into the feeding tube. Also intermittent pulses of air were fed at a set pressure (P2) to propel the biomass slugs, delivered from an expandable control volume consisting of 3 canisters, each of 75 mL volume, separated by ball valves. The timing of the pulses was controlled by solenoid valves (S.V. 2 and S.V. 3) with the relay timer.

When the pinch valve opens and closes, solids fall into the 'slug chamber' forming a plug, which is then propelled by the pulsating gas into the reactor through the feeding tube. The solid mass flowrate was measured by separating the gas from the solids using a cyclone and collecting the solids into a container located on a digital mass balance connected to a computer. The entire apparatus was manufactured using clear PVC, to allow for visual inspection of the feeder operation and for characterization of the solids flow using lasers. To prevent electrostatic effects from disrupting the operation of the feeder, 0.1 wt% of Larostat powder was added to the feed sawdust. The sawdust used had a particle density of 800 kg/m^3 and a Sauter mean diameter of 247 μm.

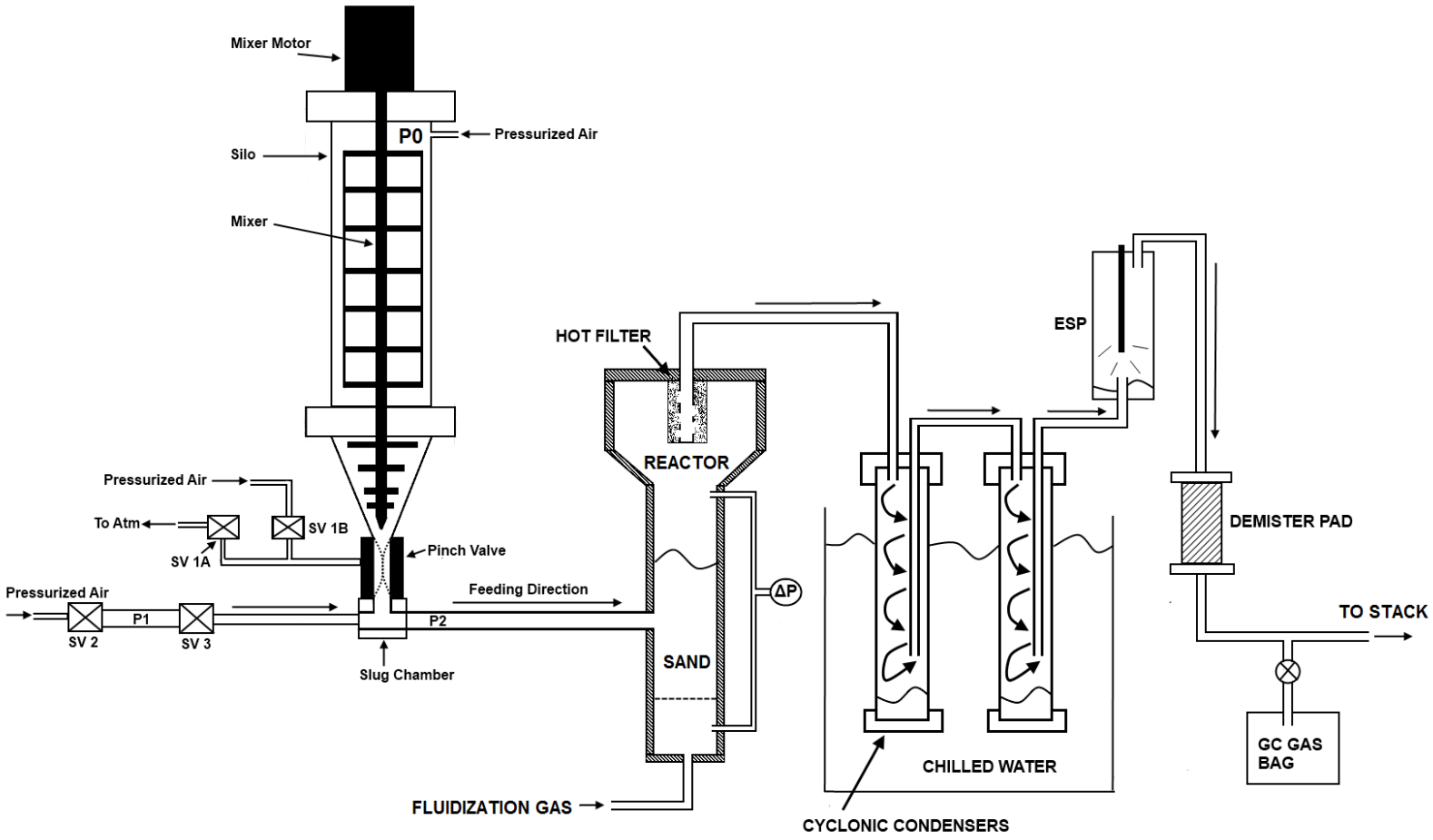

Figure 2-1: ICFAR Novel Feeder Installed on Full Reactor Setup

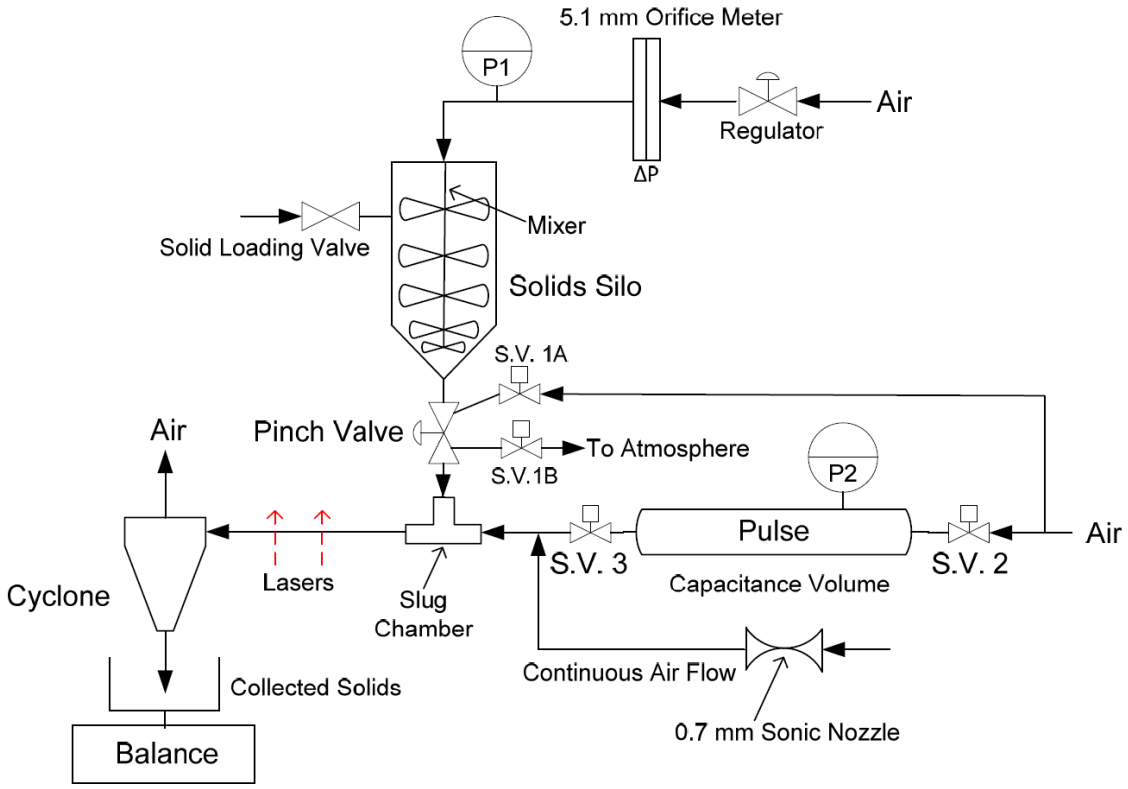

Figure 2-2: Intermittent Solid Slug Feeder Experimental Apparatus

2.2.2 Variable Definition

Several variables were considered that could potentially affect the performance and consistency of the intermittent solid slug feeder. They included:

- the silo pressure (affecting the air mass flowrate through the silo),
- the solids mixing rate within the silo,
- the pressure and volume of the injected pulses (i.e. the mass of each gas pulse),
- the continuous air mass flowrate,

- the open pinch-valve time interval, and
- the pinch-valve cycle length (i.e. injection frequency).

The goals of this initial study were:

a) to maximize the solid-to-gas ratio of mass flowrates (F_S/F_G), since the gas mass flux must be minimized to avoid wasting energy,

b) to define operating conditions required to inject consistent biomass mass flowrates of around 1 g/s into a laboratory scale pyrolysis reactors, and

c) to propose initial design criteria and a calibration procedure for intermittent solid slug feeders.

2.2.3 Procedure

To operate the feeder, one must first program the relay timer to open and close the pinch valve (controlled by solenoid valves S.V. 1A and 1B), the timing of each pulse (controlled by solenoid valves S.V. 2 and 3) at the desired operating conditions, and the cycle time. The capacitance (i.e. the canisters) can be recharged with gas within the pinch valve opening time, while the slug chamber is being recharged with solids, and the subsequent pulse time should be always kept as short as possible, with a small safety margin, to ensure that there is no excess dead time in which continuous gas flow would be unnecessarily injected into the reactor. For each experiment, the sawdust is funnelled into the silo through the loading valve, with the mixer already turned on to prevent compaction or bottlenecking of solids. Once the solids are loaded, the silo

pressure (P1), pulse pressure (P2), and the continuous flow pressure are set to the desired experimental conditions. A computer is used to acquire data from the digital mass balance to determine the instantaneous flowrate of injected sawdust, as well as data from the pressure transducers. Using the acquired data, one can determine the mass flowrates of injected solids, air through the silo, and continuous gas through the feeding tube. The gas mass flowrate injected due to the pulses can be determined from the pressure (P2) and the capacitance volume, using the ideal gas law and the pulse frequency. After a series of preliminary tests, it was determined that the silo mixing rate did not affect in any way the operation of the slug feeder, as long as it was high enough to prevent any bottlenecking of solid flow upstream of the pinch valve.

2.3 Results and Discussion

Initially, the effect of each of the injection process variables was decoupled to begin to understand the mechanism of efficient sawdust slug injection and to optimize each aspect of the feeder individually, before optimizing multiple interacting variables at once.

The first investigation was carried out to determine the optimum pressure and volume combination for the pulse injection (i.e. the mass of individual air pulses). The criteria for defining the optimum pressure was to generate a pulse strong enough to clear completely the feeding tube of the largest possible sawdust slug generated using the pinch valve. To perform this experiment, the pinch valve opening time (Δt_{open}) was set at 2 seconds, which is a long enough time to fill completely the slug chamber, and then the

pressure and volume of the air capacitance were changed until the lowest critical pressure value required to deliver the entire slug was found for every volume (1, 2 or 3 of the 75 mL canisters).

Fig. 2-3 shows the calculated critical air mass required to successfully propel the full sawdust slug for each volume, while maintaining a constant continuous air flow of 0.25 g/s. To determine the amount of air mass injected with every pulse, the mass of gas contained in the canister at atmospheric pressure (representing the pressure downstream of the feeding tube) was subtracted from the mass of gas contained in the canister at the full operating pressure, found using the ideal gas law. Regardless of the continuous flow, every test clearly showed that smaller volumes at higher pressures worked more effectively to convey the sawdust slugs, thus utilizing smaller masses of propelling gas, which in turn would assist in increasing the flowrate of solids to flowrate of gas ratio (F_S/F_G). In addition, given the mass required at each capacitance, it can be shown that using 1 canister requires 32% and 47% less energy than using 2 or 3 canisters, respectively, assuming isentropic compression. Therefore, the critical value of an intermittent solid slug feeder should be determined for any given geometry, by maximizing the pressure within safe limits and minimizing the capacitance volume to achieve a sufficient mass to deliver the biomass slugs.

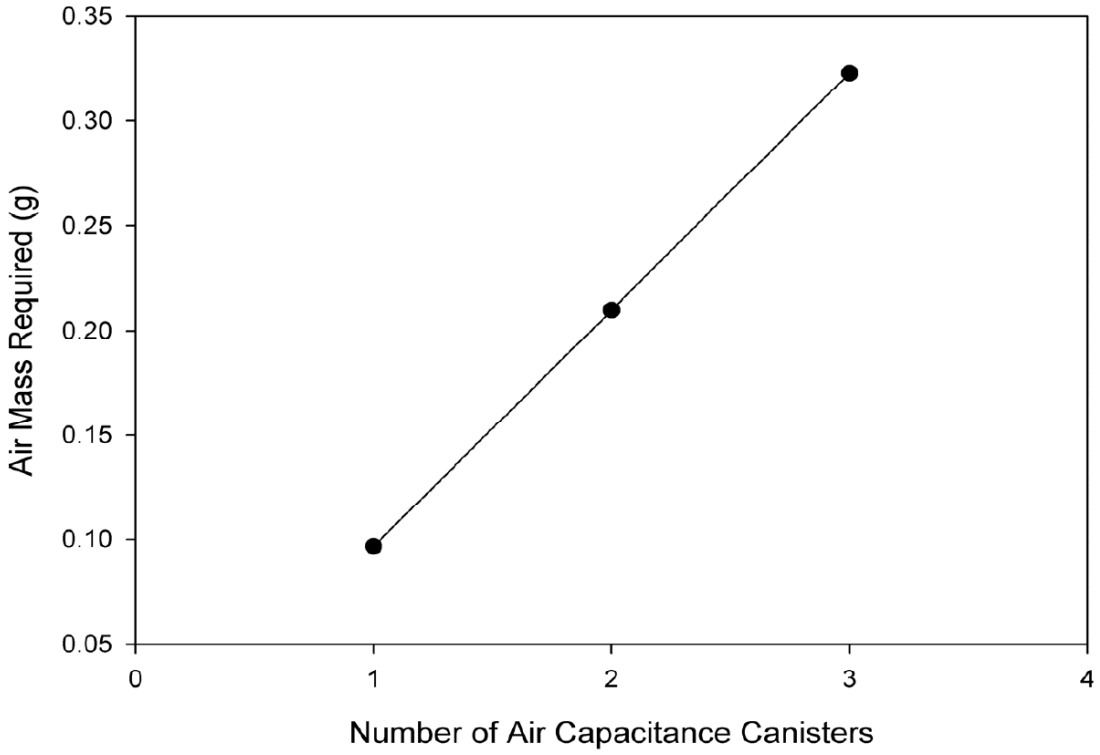

Figure 2-3: Calculated critical mass of air required to clear feeding tube vs. number of capacitance canisters at Δt_{open} = 2 s and continuous mass flowrate = 0.25 g/s

Next, the effect of the continuous air mass flowrate on the performance of the slug injection was investigated. It was found that at greater pinch valve opening times (Δt_{open}), the continuous air mass flowrate had a material effect, while at smaller opening times, the effect was virtually negligible. **Fig. 2-4** illustrates the effect of the continuous flow for the extremes of the range of pinch valve opening times tested. **Fig. 2-4** clearly shows that, for the shorter pinch valve opening time (0.5 s), the sawdust mass flowrate is consistent, constant, and independent of the continuous air flow, since the pulse flow alone is sufficient to entirely deliver the small sawdust slugs formed and clear completely the line. However, for the longer pinch valve opening time of 2 s, required to fill entirely the volume of the slug chamber, low continuous air flowrates are

insufficient for a complete delivery of the sawdust slugs, due to their larger and irregular size and, likely, to slight solids compaction and plugging of the slug chamber resulting from the pinch valve being open for too long. However, as the continuous gas rate increases, it becomes large enough to clear all the contents of the slug chamber and the line; at high continuous flows, a plateau, is reached with sawdust mass flowrate values similar to those attained using the shorter, more ideal, pinch valve opening times (**Fig. 2-4**). This phenomenon is depicted in **Fig. 2-5**.

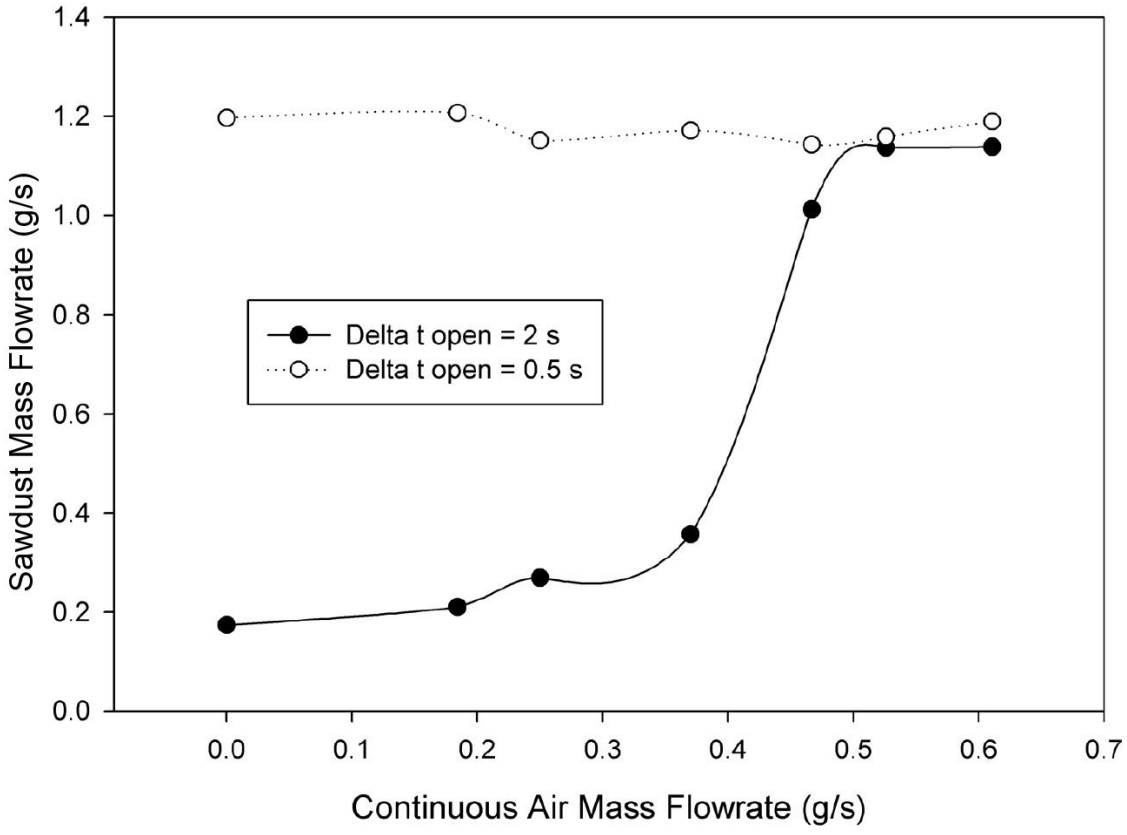

Figure 2-4: Effect of continuous air mass flowrate on sawdust mass flowrate

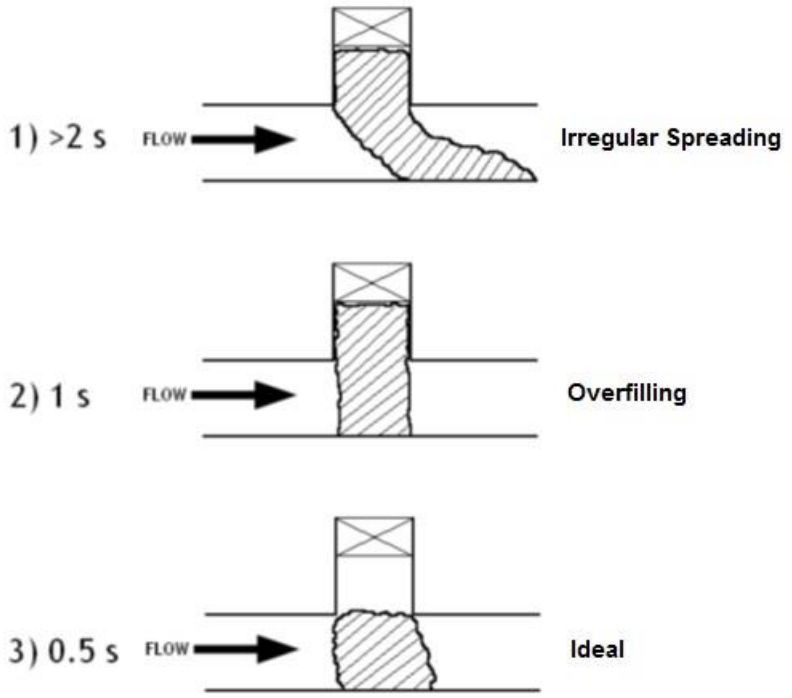

Figure 2-5: Slug chamber illustrations at different pinch valve Δt_{open} values

As a result of this, it can be established that the pinch valve opening time should be optimized to fill the slug chamber just enough to completely cover the feeding horizontal tube cross-section, forming a small plug (**Fig. 2-5**, case 3). Visual observations confirmed that the size of the optimal slug appear to be roughly corresponding to an equivalent diameter equal to twice that of the feeding tube (due to some spreading). Under the optimal conditions, the short opening time would prevent overfilling (cases 1 and 2) and, thus, the risks of possible bridging or plugging, which would require higher continuous gas flowrates to completely empty the feeding line. However, it is clear that the geometrical design of the slug chamber is also very important and that, therefore, different slug chamber geometries should be investigated to further optimize the solid

slug formation and ensure complete solids delivery with minimal continuous gas flowrates.

Finally, the intermittent slug feeder was tested in full operation within the functional pinch valve open time range (Δtopen) of 0.5 to 2s. Open times lower than 0.5 s were found to malfunction due to pinch valve mechanical limitations, and larger times were found to consistently plug due to the excessively large and irregular size of the slugs (similar to case 1, **Fig. 2-5**). **Fig. 2-6** illustrates the calculated maximum solid-to-gas mass flowrate ratio (F_S/F_G) obtained at 0.5, 1, and 2 second opening times. In all three cases, the maximum was found at zero continuous air flowrates and very minimal silo pressures. Although a concern could be that without continuous air flowrates, backflow into the feeding tube can occur (when injecting in a fluid bed), it is likely that at high pulse frequencies, the pulse itself can be enough to prevent backflow and plugging. Otherwise, very minimal continuous air flowrates should be used. The silo pressure was kept well below 0.2 psig (resulting in virtually negligible air flow), which is high enough to prevent any irregular flow resulting from a variation in the head of solids during the emptying of the silo. Based on the results of the study illustrated in **Fig. 2-3**, only one pulse canister volume was utilized at the highest safe pressure of 27 psig (15 psig was the experimentally identified critical value), to ensure easy feeding of the slugs. Under these optimized conditions, it was found that the maximum FS/FG, exceeding 9, was achieved with the shortest pinch valve open time of 0.5 s, creating consistent slugs of approximately 1.5 g each. Higher FS/FG values should be attainable if the feeder is operated at pulse pressures closer to the critical value. However, a margin of safety

should always be utilized during operation, in order to compensate for slight slug mass variations.

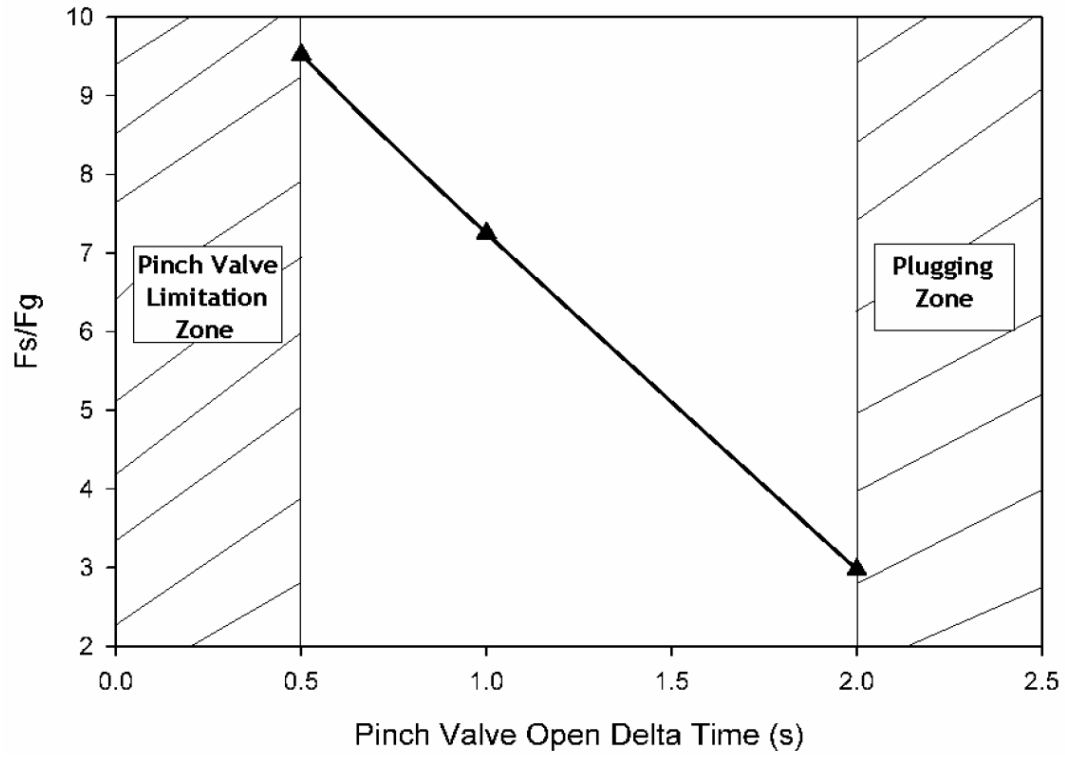

Figure 2-6: Calculated maximum Experimental Fs/Fg vs. Pinch Valve Δt_{open} values

The optimal operation (maximum F_S/F_G and consistent flow) of the specific sawdust slug feeder utilized in this study was achieved using the shortest possible pinch valve opening time of 0.5 s, thus producing small and regular slugs with an equivalent diameter equal to twice that of the slug chamber, which can be easily and completely propelled by gas pulses produced with the highest possible gas pulse pressure of 27 psig and the lowest canister volume (1 canister). Under these conditions, the sawdust feed rate can be easily and accurately controlled by adjusting the cycle time, or, effectively, either the time delay before opening the pinch valve and releasing solids into the

feeding tube after each pulse injection (preferably), or the time delay after closing the pinch valve before delivering the new gas pulse. However, it is obvious that longer cycle times would be undesirable as continuous carrier gas would be unnecessarily wasted. Therefore, when designing a new feeder, the geometrical scale of the slug chamber and of the feeding tube should be chosen to achieve the desired solids flowrates consisting of small and uniform slugs of a diameter equivalent to twice that of the slug chamber, typically also equal to that of the feeding tube, selecting a pinch valve opening time sufficient to deliver such size of slugs, and adjusting the time delays and the pulsation time to achieve the desired solids mass flowrate.

Following the optimization experiments, the feeder was introduced to the laboratory-scale pyrolysis reactor, and was utilized to successfully pyrolyze various feedstocks including sawdust, coffee husks, dried distiller's grains, hemp seeds, sugarcane bagasse, grape skins, chicken litter, apple pomace, rice straw, flax straw and even unaltered Kraft lignin, a notoriously difficult material to feed into pyrolysis reactors [7]. From these experiments, a sense of the wear of the feeding technology has also been developed, indicating that the only part of the assembly subject to wear is the pinch valve sleeve (made of pure gum rubber or other more durable materials such as polyurethane), which is sensitive over time to erosion. This sleeve can be easily and economically replaced as required.

2.4 Conclusions and Recommendations

A horizontal intermittent solid slug feeder, suitable to feed sawdust at a rate of approximately 1 g/s into a laboratory scale pyrolysis reactor, has been designed, built and operated successfully.

Several operating variables have been tested in order to optimize the performance of the feeder and the consistency of the feeding rate. They included the silo pressure, mixing rate, gas pulse pressure and volume, continuous gas mass flowrate, and the open pinch-valve time interval.

As a result of the experimental work described in this study, the operating conditions required to maximize the solid-to-gas ratio of mass flowrates have been identified as well as those required to inject constant and stable biomass mass flowrates. The results also provided some initial guidance relative to initial design and scale-up criteria for intermittent slug feeders, and demonstrated the effectiveness of the feeding technology in a hot laboratory-scale pyrolysis reactor.

2.5 Acknowledgements

The financial support for this research from the Natural Sciences and Engineering Research Council of Canada (NSERC) is gratefully acknowledged.

2.6 References

[1] Bridgewater, A.V., Czernik, S. Piskorz, J. (2001). Progress in Thermochemical Biomass Conversion. Bridgewater A.V. Ed.

[2] Mohan, D., Pittman, C.U. Jr., Steele, P.H. (2006). Energy & Fuels, 20, 848.

[3] Berruti, F. M., Lenkiewicz, K., Xu, R., Bedmutha, R. J., Nova, S., Berruti, F., Briens, C. (2007). Novel Fluid Bed Pilot Plant for the Production of Bio-oil from Biomass through Fast Pyrolysis. Récents Progrès en Génie des Procédés, Numéro 94. ISBN 2-910239-68-3, Ed. SFGP, Paris, France.

[4] Guedon, M.O., Baron, T., Briens, C.L., Knowlton, T.M. (1994). Intermittent injection of prepolymer in a pressurized fluidized bed. Powder Technology, 78 (1994), 25-32.

[5] F. M. Berruti, L. Ferrante, C. L. Briens, and F. Berruti, “Pyrolysis of cohesive meat and bone meal in a bubbling fluidized bed with an intermittent solid slug feeder,” Journal of Analytical and Applied Pyrolysis, vol. 94, pp. 153–162, Mar. 2012.

[6] Pan, R. (1999). Material properties and flow modes in pneumatic conveying. Powder Technology, 104 (1999), 157-163.

[7] P. Palmisano, F. M. Berruti, V. Lago, F. Berruti, and C. Briens, “Lignin Pyrolysis in a Fluidized Bed Reactor,” The International Conference on Thermochemical Biomass Conversion Science, Chicago, Illinois, USA, 2011.

Chapter 3

3 Chapter 3: Novel Intermittent Solid Slug Feeder for Fast Pyrolysis: Fundamentals and Modelling[4]

3.1 Introduction

Fluidized bed technology has been demonstrated to have good potential as a reactor technology for the production of pyrolysis oil and bio-char, via fast biomass pyrolysis [1]. In a fluidized bed pyrolysis process, raw biomass material particles must be conveyed and injected into the reactor using the least energy-intensive and most practical feeding system. Dilute phase pneumatic transport lines and screw feeders are currently being used by several pyrolysis processes. However, in the flash pyrolysis process, where the temperature of the reactor is high, typically between 450 and 550 °C, and where relatively high mass flow rates of raw biomass can be processed, these commonly used feeding systems tend to encounter some serious problems [2]. For example, the high temperature coupled with pressure fluctuations at the inlet into the reactor can often lead to severe plugging in screw feeders, potentially causing significant damage to the equipment or down time in the operating process [15]. This is especially the case for temperature-sensitive and cohesive biomass residues such as Kraft lignin and meat and bone meal residues [2–4]. Dilute phase pneumatic transport feeders consume a large amount of gas, which is typically recycled product gas, resulting in higher energy

[4] A version of this chapter has been published as follows:

Berruti, F.M., Briens, C. (2013). Novel Intermittent Solid Slug Feeder for Fast Pyrolysis: Fundamentals and Modeling. *Powder Technology*, 247, 95-105.

consumption and requiring a more sophisticated condensation train due to product vapour dilution. In addition, many industrial operators attempting to feed challenging biomass into reactors are forced to feed above the bed, which often results in poor mixing with the hot sand, as the biomass simply floats on top of the hot bed [5].

To prevent plugging and help the raw biomass particles effectively penetrate and spread into the pyrolysis fluidized beds, one could inject the particles using intermittent slugs created by propelling loosely packed particles with gas pulses and transporting them along horizontal or inclined feeding pipes into the fluidized bed section of the reactor [6]; this would combine the advantages of the low gas consumption of the screw feeders and the short residence time in high temperature zones of dilute phase feeders.

Among many other potential applications, intermittent solid slug feeders can be used to effectively inject biomass materials into fluidized bed reactors for pyrolysis. In particular, these feeders can be used to convey biomass materials that are highly cohesive to prevent plugging or undesirable reaction in the feeding tube. Although feeders of this design have been tested, roughly optimized through trial and error, and shown to work very effectively for pyrolysis applications [2, 7], fundamental results and a verified model are required for full optimization and, eventually, scale-up.

The objective of this study was to develop a predictive model for the solids flow induced by a gas pulse, by utilizing a sequential approach and validation with dedicated instrument data.

3.2 Materials and Methods

3.2.1 The ICFAR Intermittent Solid Slug Feeding Technology

The Institute for Chemicals and Fuels from Alternative Resources (ICFAR) intermittent solid slug feeder technology [7] designed for this work and illustrated in **Fig. 3-1** has been used extensively at ICFAR for bubbling bed pyrolysis reactor experiments for long operation and has also been scaled up [2]. The feeder for this work consisted of a slightly pressurized vertical solids storage silo (P_0 – kept between atmospheric pressure and 120 kPa) leading to a 19 mm diameter pneumatic pinch valve. The silo had a 4 L volume (0.102 m inner diameter), with a cone angle of 70° from the horizontal. Within the silo, a specially-designed rotating 'egg-beater' mixer prevented the bridging of solids. The instantaneous mass flow of gas flowing into the silo was determined by acquiring the Gas-Trak Sierra mass flowmeter signal responsible for delivering the nitrogen gas to the silo. The pinch valve was controlled by Granzow Inc. solenoid valves (SV_{1A} and SV_{1B} in **Fig. 3-1**, series 21EN) connected to a relay timer (IMO iSmart Relay, 10 I/O AC). Solids exiting the pinch valve flowed into a 15.3 mm (inner diameter), electrically-grounded clear PVC or carbon steel horizontal feeding tube through a ninety degree angle connection. Various feeding tube lengths were studied from 0.08 m to 1.145 m. The volume between the end point of the pinch valve and the start of the horizontal feeding tube is called "slug chamber". For the purpose of the current study, a simple "T" fitting of constant diameter (15.3 mm) has been utilized, with a vertical, 63.5 mm long section (measured from the base of the horizontal part of the "T" block). Intermittent pulses of nitrogen were fed at a set pressure (P_1 – usually above 240 kPa to

ensure the biomass can exit the longest feeding tubes tested) to propel the biomass slugs, delivered from a control volume consisting of an 80 mL steel canister (labeled as P_1 in the figure). The timing of the pulses was controlled by Granzow Inc. solenoid valves (SV_2 and SV_3 in **Fig. 3-1**, series 21EN) with the relay timer. When the pinch valve opens and closes, the biomass falls into the 'slug chamber' forming a plug, which is then propelled into the reactor through the feeding tube by a pulse of pressurized nitrogen gas (or recycled product gas) from the canister. The pressures in the silo (P_0), capacitance volume (P_1), and feeding tube (P_2), were measured by an Omega PX181 series semiconductor pressure transducer at 2 kHz. The pressure transducer is reported to have a response time of less than 2 ms, with a best-fit straight line accuracy measurement of 0.3%.

The entire apparatus was manufactured using clear PVC to allow for visual inspection of the feeder operation and for characterization (position and velocity) of the solids flow with red lasers and a photo-resistor apparatus, which gave a continuous signal, recorded at 10 kHz by a National Instruments NI USB-6008 data acquisition card and NI LabVIEW software. As the slug passed through the laser, the photoresistor outputted a signal peak due to the change in light intensity, the start of which was interpreted as the point at which the bulk of the slug passed in front of the laser. The response time of the photoresistor apparatus was experimentally measured to be less than 2 ms, and thus the potential experimental error on the slug position (also considering the pressure transducer response time), knowing the maximum slug velocity, was calculated to be less than 2.5 % of the total tube length, in all cases.

The solid mass flow rate was measured by separating the fed biomass in a cyclone (operated successfully under unsteady conditions) with the solids outlet leading to a digital scale, which continuously outputs the instantaneous mass data to a computer at 8.4 Hz. The fines losses in the cyclone over long feeding runs were found to be immaterial compared to the bulk feeding rate for both feedstocks. For visual observations, a CASIO HS EX-FS10 Exilim High-Speed camera was used at 410 frames per second.

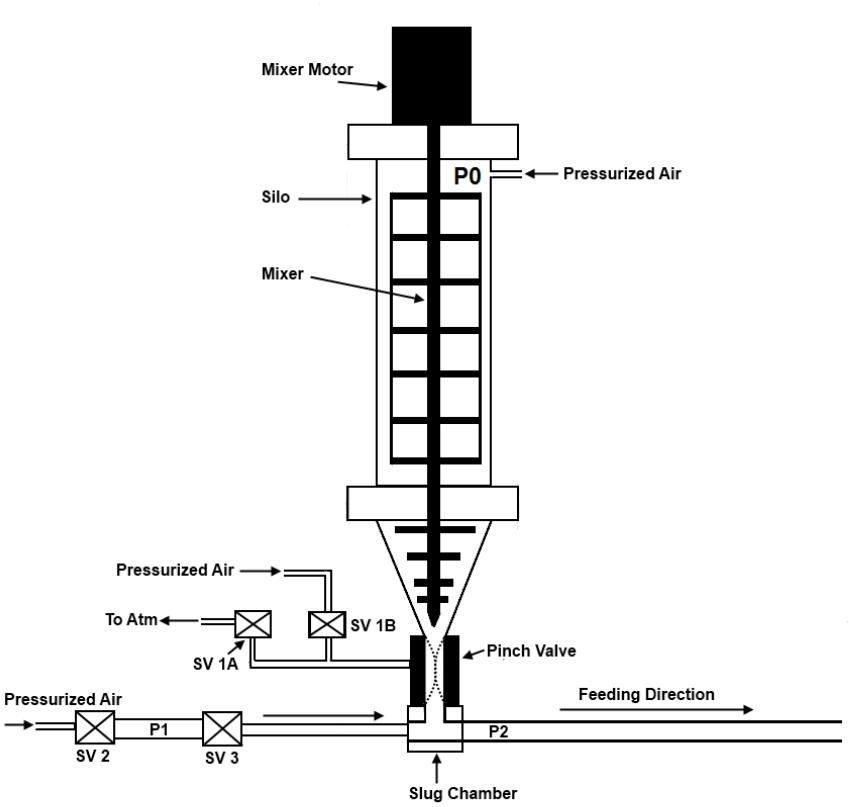

Figure 3-1: ICFAR Intermittent Solid Slug Feeder Schematic

3.2.2 Materials and Feedstocks

Table 3-1 illustrates some of the critical physical properties of the feedstocks utilized in this study.

Dried Distillers' Grain (DDG) was the primary feedstock for testing and modelling, but meat and bone meal residues (MBM) were also tested for model validation. These biomass feedstocks were selected as much work has been done to attempt to process these feedstocks into value-added products via pyrolysis, but they also possess very challenging flow characteristics and properties that are very different from each other (particle size, cohesivity, temperature sensitivity, density) [2]. As a result, creating a predictive model that can successfully model these challenging feedstocks is the basis to model any biomass of interest.

The dried distillers' grain (DDG) feedstock used in this study was obtained from GreenField Ethanol in Chatham, Ontario, Canada. 0.5 wt% of Larostat powder was added to the DDG to mitigate electrostatic effects in the feeder over time.

The meat and bone meal residue (MBM) used in this study was supplied by Thorndale Farm Supplies, a meat renderer and producer located in Thorndale, Ontario, Canada. More details and specifications than indicated in **Table 3-1** on the MBM can be found in [2].

The ball projectile (used as an ideal slug), purchased from McMaster-Carr, was made of wear-resistant nylon and had an outer diameter of 15.875 mm. In order to fit the ball tightly into the 15.3 mm inner diameter feeding tube and prevent rolling, one

circumference of the ball was sanded down by hand smoothly to create a virtually leak-proof seal in the feeding tube, while still allowing the projectile to slide freely. WD40 lubricant as coated on the ball prior to each run to ensure smooth sliding and low friction.

The projectile ball was selected as a theoretically ideal slug, as the gas leakage was prevented. The DDG and MBM represent challenging biomass feedstocks. According to [8], the Hausner ratio can be used as a good metric to predict flow type and material cohesiveness, and both the DDG and MBM have a relatively high Hausner ratio, which would indicate passable flow for the DDG and poor flow for the MBM. Indeed the MBM avalanching flow indicator characteristics from the Mercury Scientific Revolution Powder Analyzer, performed at 0.3 RPM for 150 avalanche data points and averaged over 3 replicates, also demonstrate that MBM has a relatively higher cohesion and poorer bulk flow characteristics than DDG, as all metrics chosen from literature and illustrated in **Table 3-1** have higher values for MBM than DDG [9]. The feeding challenge for DDG pyrolysis lies in the prevention of "straggler" biomass in the feeding tube, i.e. particles left behind the moving slug, since if the DDG pre-maturely begins to react in the feeding tube its physical characteristics change dramatically, resulting in a foam-type blockage [11, 12].

Table 3-1: Feedstock Properties

Property	Units/Reference	DDG	MBM	BALL
Sauter mean diameter	µm	577	25.14	15290
Bulk density	kg/m^3	503	467	1229
Particle density	kg/m^3	915	778	1229
Hausner ratio	-	1.26	>1.35	1
Revolution Powder Analyzer:				
Avalanche time	s	4.06	6.03	-
Avalanche median	s	4.29	6.50	-
Avalanche energy	kJ/kg	19.8	27.8	-
Energy std. deviation	kJ/kg	16.1	24.4	-
Avalanche angle	°	56.6	72.4	-
Rest angle	°	44.4	50.3	-
Flow Characterization:				
Flow Type	[8, 10]	Passable	Poor	Excellent

3.3 Fundamental Operation Results and Discussion

3.3.1 Feeder Operating Conditions and Feeding Rate

In chapter 2, the successful operation and preliminary optimization of the ICFAR intermittent solid slug feeder was demonstrated. In this study, the same pinch-valve opening time of 0.5 s was selected since it provided uniform slugs that fill the slug chamber well, resulting in regular feeding rates (15 trials were performed at each condition with a variance less than 4.8% from the average). A cycle time of 2.4 s was used as an appropriate delay for the pinch-valve to open and close and for the gas pulse to completely clear the feeding tube before the next cycle. **Fig. 3-2** and **3-3** illustrate the cumulative mass fed vs. time for DDG and MBM, respectively. The linear R^2 value of regression was 0.9998 and 0.9948 for DDG and MBM, respectively, demonstrating

relatively regular feeding for both feedstocks but higher regularity with DDG than MBM due to their lower cohesivity and higher overall flowability.

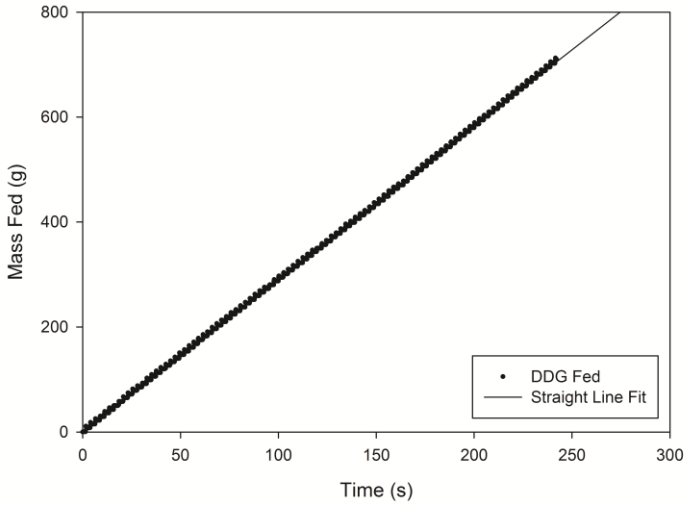

Figure 3-2: DDG Feeding Rate

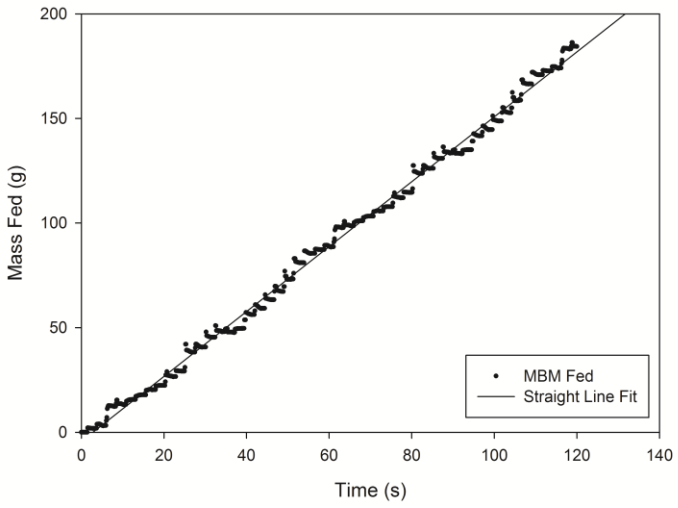

Figure 3-3: MBM Feeding Rate

3.3.2 Flowrate-of-Solids to Flowrate-of-Gas Ratio

As established in [7], an important metric to establish the energy efficiency of the feeder implemented is the solids to gas flowrate ratio (F_s/F_g). **Fig. 3-4** and **3-5** illustrate the F_s/F_g obtained at different pulse pressures using DDG and MBM, respectively. The DDG can reach a higher F_s/F_g than MBM, as the slugs formed by the DDG in the slug chamber are larger (more flow during the 0.5 s opening time of the pinch valve) and slightly spread down the tube (due to lower cohesivity and higher flowability), while the MBM slugs have a higher internal angle of friction and remain as a packet, simply filling the cross section of the feeding tube. Therefore the mass of feedstock fed per pulse (if successfully cleared from the feeding tube) is higher for DDG than MBM. Below a 240 kPa pulse pressure, with the 80 mL capacitance volume used, the pulse may not be able to propel the biomass from the slug chamber out of the feeding tube, depending on the length of the feeding tube. The F_s/F_g curve can easily be developed for any feed material when examining the energy implications and designing the appropriate feeder operating conditions for a given process.

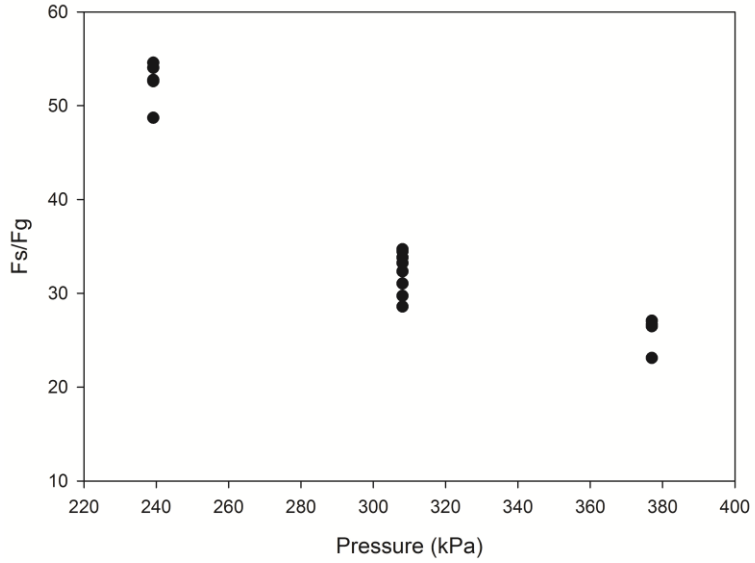

Figure 3-4: DDG Solids-to-Gas Flowrate Ratio vs. Pulse Pressure

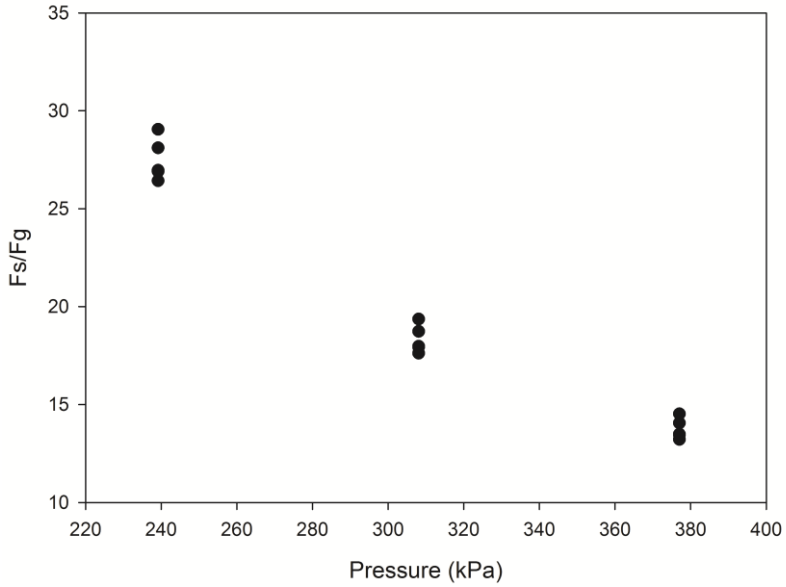

Figure 3-5: MBM Solids-to-Gas Flowrate Ratio vs. Pulse Pressure

3.3.3 Effect of Pulse Pressure on Feeding Rate

As demonstrated in Chapter 2, as long as the silo pressure (P_0) is balanced properly with the reactor back-pressure (with the mixer operating conditions working well enough to prevent bottlenecking in the feeder silo), the pinch-valve opening time is set properly such that the biomass essentially just fills the feeding tube cross section (without over-filling), and the pulse pressure is high enough to propel the biomass slug out of the feeding tube of a given length without straggler accumulation, then the effect of pulse pressure on the feeding rate was found to be effectively negligible. **Fig. 3-6** illustrates this point for DDG, with a mixer RPM of 127.5 (high) for both a clear PVC and smooth carbon steel feeding tube.

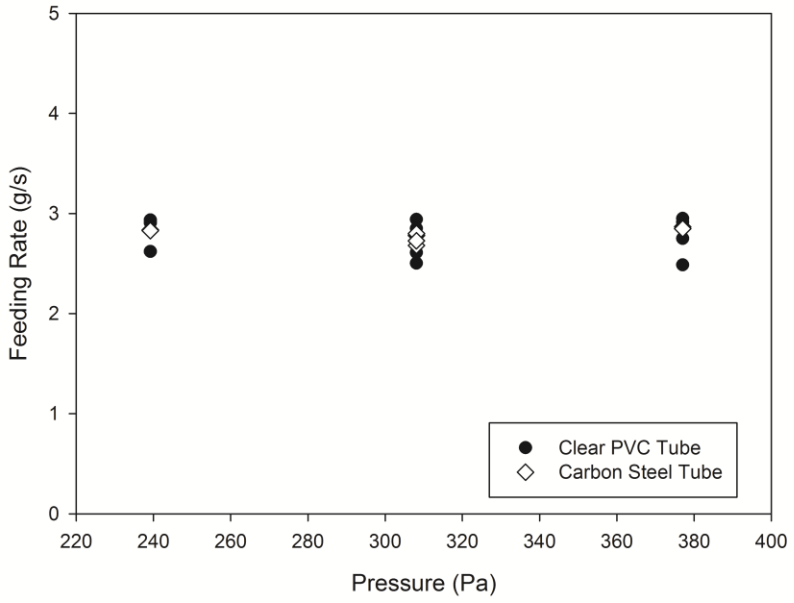

Figure 3-6: Effect of Pulse Pressure on DDG Feeding Rate

3.3.4 Effect of Mixer RPM on Feeding Rate

As described earlier, the mixer RPM in the silo needs only to have the breaking energy to avoid bottlenecking and bridging within the silo, above which the RPM will not have a material effect on the feeding rate. The feeding rate is controlled by the pinch-valve opening time and flowrate out of the silo orifice. Some types of biomass feedstocks (such as very light lignins or low-density group C powders) experience high aeration (and slow de-aeration) with a high mixing rate, which results in a negative impact on the ability of the feedstock to the flow out of the silo orifice [13]. In general, tests can be performed to ensure that the mixer is fast enough to avoid bottlenecks and bridging with a safety margin, but not much faster. **Fig. 3-7** illustrates this concept for DDG at a constant pulse pressure of 308 kPa, for both clear PVC and carbon steel feeding tubes. For both DDG and MBM this mentioned aeration effect does not occur, and therefore a mixer RPM of 40-60 is recommended. Electrostatic effects could explain the slightly increased variation in data for the clear PVC tube compared to the carbon steel tube.

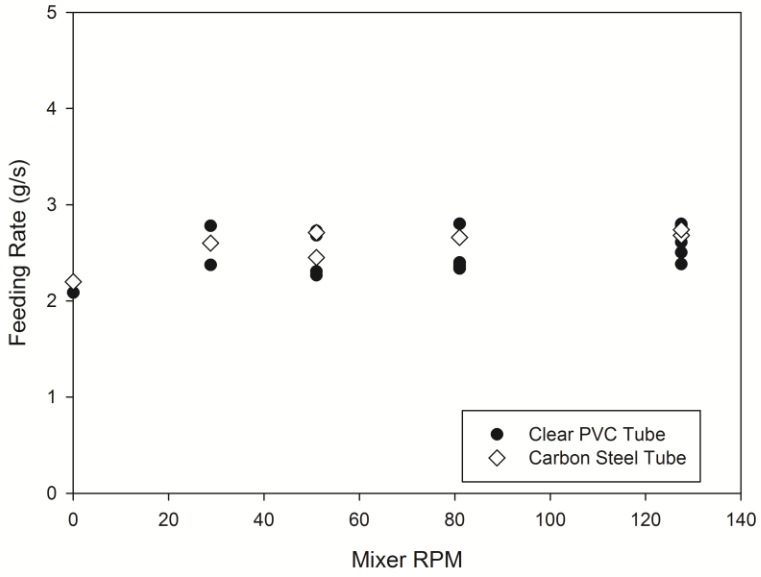

Figure 3-7: Effet of Mixer RPM on DDG Feeding Rate. P = 308 kPa.

3.3.5 Effect of Pulse Pressure on Straggler Accumulation

Straggler prevention is of critical importance for pyrolysis feeder to prevent pre-cooking, plugging and downtime [2, 7]. Experiments were performed to determine the effect of key feeder operating variables on the accumulation of stragglers, by performing individual pulses and then weighing the amount of biomass particles remaining in the longest feeding tube tested (1.145 m). No significant effect was observed by changing the tube material or silo mixer RPM. **Fig. 3-8** illustrates the effect of pulse pressure on the accumulation of DDG stragglers in the feeding tube between pulses. The amount of straggler DDG material found in the tube at lower pulse pressures was significantly higher and more erratic (likely due to electrostatic effects and small differences in biomass slug shape and packing). At 240 kPa, the straggler mass represented nearly 40% of the initial slug mass – indicating that the pulse pressure was not high enough to

prevent tailing stragglers to clear the length of tube, due to a loss in pulse energy. Therefore, if a lower pressure is desired for operation on a unit, one must select a shorter feeding tube, which also has the disadvantage of conducting heat from the reactor down the shorter tube potentially reaching the slug chamber. This must be avoided to prevent biomass immediately coming from the silo from changing in physical properties or reacting.

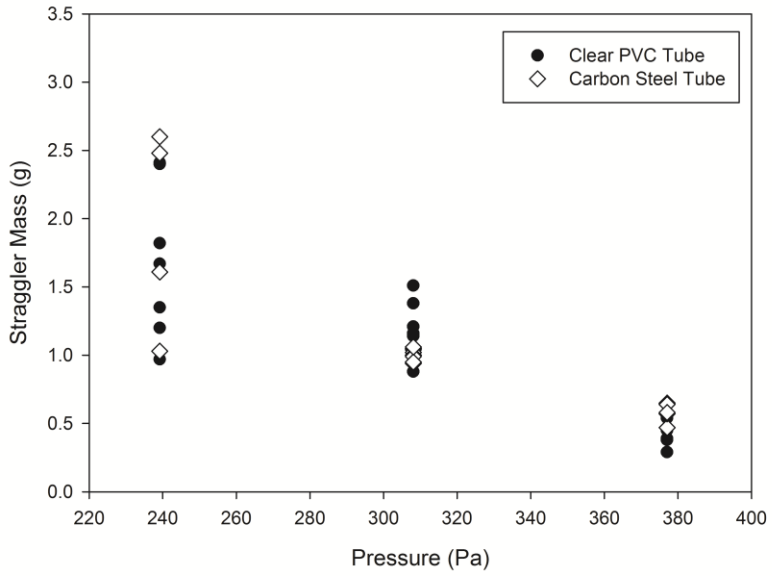

Figure 3-8: Effect of Pulse Pressure on DDG Straggler Accumulation. L = 1.12 m, ID = 0.0127 m.

3.3.6 Effect of Pulse Pressure on Slug Spreading during Motion

By using a high-speed camera described in the methods section, the moving DDG plugs were examined while in motion. The length of the slugs was determined by having background markers in the image and knowing that the high speed camera was recording at 410 frames per second (taking an average slug speed and determining an

approximate length of the passing slug). The DDG was selected for this study as its larger particle size and lower cohesivity would result in more dynamic spreading than with MBM or other challenging pyrolysis biomass feedstocks. Preliminary high-speed camera tests with MBM showed undetectable spreading due to its higher cohesivity. Unlike in low-velocity dense-phase pneumatic conveying, where feedstock exhibits a "two-layer" model type motion due to the significant wall shear effects compared to the suspended particles [14], the feeder pulse flow appears to nearly fully suspend the biomass slug at high velocity, lowering the effect of wall friction and spreading. **Fig. 3-9** illustrates the spreading of the biomass slug of DDG at different points along the feeding tube at different pulse pressures. At the highest pulse pressure tested of 377 kPa, the bulk of DDG slug spread from an initial length of 60 mm to just over 100 mm, over a distance of 1.2 m.

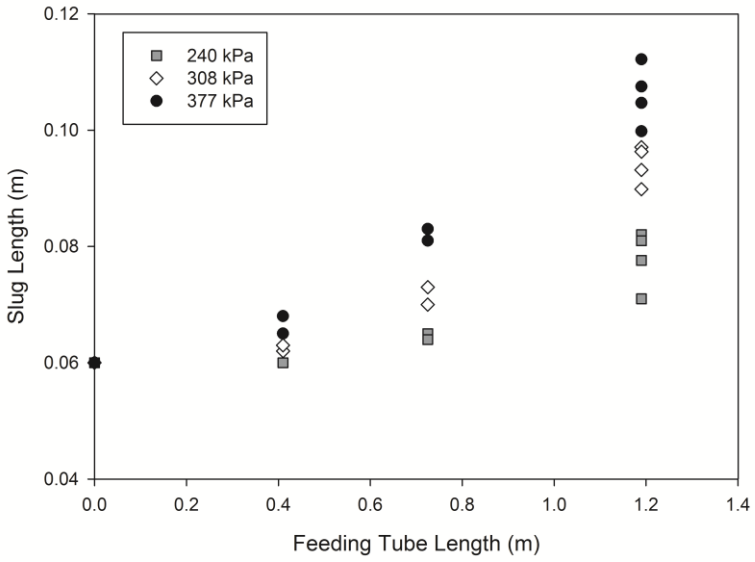

Figure 3-9: Effect of Pressure on DDG Slug Length Spreading

3.4 Feeder Modelling Results & Discussion

3.4.1 Modelling Approach and Objectives

With the fundamental physical understanding of the feeder operation and flow characterization, the next step was to develop a model that connects all of the findings and allows for the development of a practical predictive model for successful feeder design, considering energy implications and process economics.

To summarize, the goals of the feeder model are to (a) ensure the complete flow of the slug out of the feeding tube, thus eliminating the issues caused by stragglers, (b) predict the maximum feeding tube length allowable for a particular feedstock and given operating conditions, (c) predict the position of the slug at any given time after the pulse, and thus its velocity, (d) predict the key feeder operation results based on input data (of the biomass feedstock characteristics and operating conditions) that are simple to obtain through quick measurements or experiments.

The following step-by-step approach was taken to model the feeder flow from when the biomass slug enters the slug chamber until it exits the feeding tube, as illustrated in **Fig. 3-10**:

1. Calibrate pressure measurements, flow coefficients and model flows using a 0.125” (3.175 mm) orifice at the end of the feeding tube (no slug or projectile within feeding tube) and obtain model confirmation of the calculated orifice gas flow coefficient by fitting the measured (P_1 and P_2) and predicted pressures, and ensuring a good pulse gas mass balance closure. The flow coefficient for

solenoid valve SV_3 was thus determined and used in all following experiments. SV_3 was assumed to open instantaneously.

2. Calibrate pressure measurements, flow coefficients and model flows using a nylon projectile ball, selected as an 'ideal' slug. The nylon ball was static, and held in place by a metal cage (negligible pressure drop measured) at the end of the feeding tube. The gas flow coefficient past the ball was obtained by fitting the measured (P_1 and P_2) and predicted pressures, and ensuring a good pulse gas mass balance closure. The SV_3 flow coefficient was confirmed from step 1, and used for all following experiments.

3.

    a. Experiments were performed by front loading the nylon projectile ball ('ideal' slug) in the feeding tube and sending one pulse of gas (at various pressures) to eject the ball. The measured pressures (P_1 and P_2) were matched with the predicted model pressures (while ensuring a good mass balance closure) in order to predict volume change in the feeding tube and, thus, the ball movement. The ball movement was then compared to the measured position, which had been obtained by using red lasers along the feeding tube (which had given the ball position vs. time), as a third confirmation.

    b. A **predictive model** for the biomass slug movement in the large-scale feeder was then validated. The slugs were assumed to have a constant

cross sectional area, equal to that of the feeding tube. For each type of feed particles, the model outputs:

- slug position vs. time
- slug velocity
- maximum tube length

The predictive model requires the following input data:

- feeding tube inner diameter (D)
- initial pulse pressure (P_1)
- downstream pressure (P_2)
- capacitance volume (V_1)
- slug mass (m_s)
- the orifice size and average flow coefficient for open solenoid valve SV_3 (obtained in step 1)
- empirical scale-independent friction factor (φ_s) and critical pressure (ΔP_c) of the slug solids on the clear PVC tube material, determined from laboratory-feeder experiments (described in the following sections)

4. Same as step 3, but for a DDG slug rather than the ball.

5. Once the predictive model was created and tested for the ball and DDG, it was further validated with MBM.

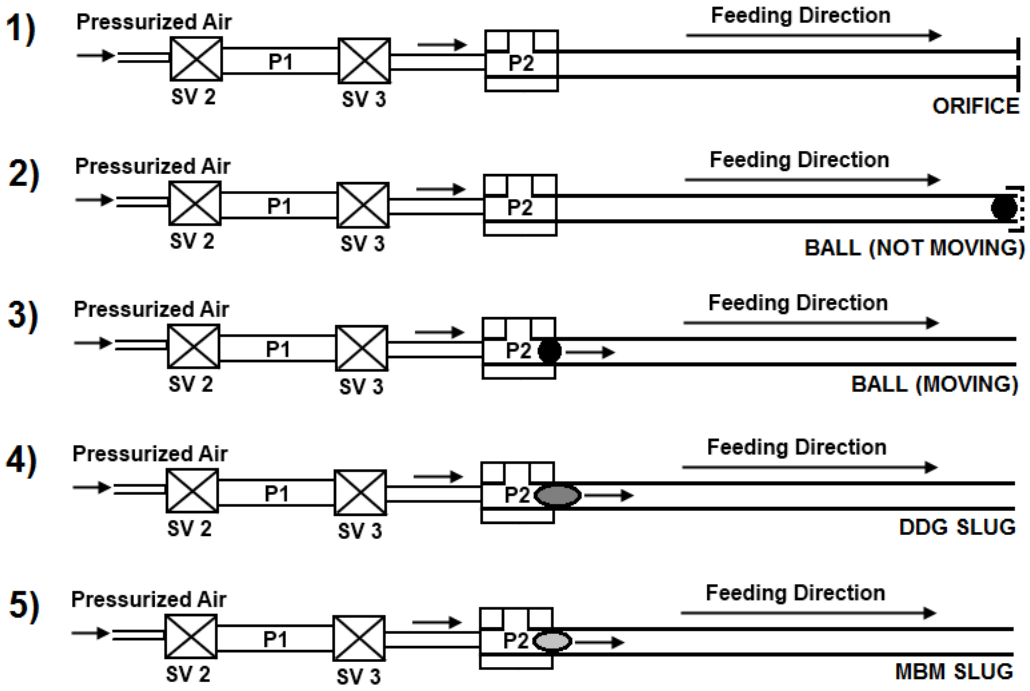

Figure 3-10: Step-Wise Modelling Approach

3.4.2 Model Equations

To model the pulse gas flow leaving the capacitance volume one must consider the flow through the orifice and whether the flow is sonic or sub-sonic.

For sonic gas flow, the following isentropic expression is used to calculate the mass flowrate ($\dot{m}$):

$$\dot{m} = C_V A_{OR} P_{UP} \sqrt{k \frac{M}{RT} \left(\frac{2}{k+1}\right)^{\frac{k+1}{k-1}}} = \alpha C_V P_{UP}$$

Equation 1

where C_V is the gas flow coefficient through the orifice (assumed instantaneously open for solenoid valves), A_{OR} is the cross sectional area of the orifice (m^2), P_{UP} is the upstream absolute pressure (Pa), k is the C_p/C_v for the gas (1.4 for air), M is the gas molecular weight (0.029 g/mol for air), R is the universal gas constant (8.314 m^3 Pa K^{-1} mol^{-1}), and T is the ambient temperature (298 K).

For isentropic sub-sonic gas flow, the following expression is used to calculate the mass flowrate:

$$\dot{m} = C_V A_{OR} Y \sqrt{\left(\frac{2M}{RT}\right) P_{UP}(P_{UP} - P_{DOWN})} = \beta C_V \sqrt{P_{UP}(P_{UP} - P_{DOWN})}$$

Equation 2

where

$$Y = \sqrt{\left(\frac{P_{DOWN}}{P_{UP}}\right)^{\frac{2}{k}} \left(\frac{k}{k-1}\right) \left[\frac{1 - \left(\frac{P_{DOWN}}{P_{UP}}\right)^{\left(\frac{k-1}{k}\right)}}{1 - \left(\frac{P_{DOWN}}{P_{UP}}\right)}\right]}$$

Equation 3

and P_{DOWN} is the absolute pressure downstream of the orifice (Pa).

To determine an approximation of the upstream pressure P_{UP} corresponding to the transition point between sonic and sub-sonic flow, one can set the equations equal to each other:

$$\alpha C_V P_{UP} = \beta C_V \sqrt{P_{UP}(P_{UP} - P_{DOWN})}$$

Equation 4

Simplifying **Eqn. 4** results in the following conclusions:

If $\left(\frac{P_{DOWN}}{P_{UP}}\right) < \left[1 - \left(\frac{\alpha}{\beta}\right)^2\right]$ then the gas flow is sonic, otherwise it is sub-sonic.

Assuming isothermal flow, one can perform mass balances on the capacitance canister (V_1) and also on the feeder system volume (V_2, which changes as the slug moves through the feeding tube) in order to predict the changing pressures (P_1 for the canister and P_2 for the feeding tube). To create a fully predictive model, the unknowns are $\dot{m}_{12}$, P_1, P_2, and V_2. The initial values for P_1, P_2 and V_2 are known, however (starting boundary condition as an input).

$\dot{m}_{12}$ can be calculated as a function of the known C_{V1} (SV_3 gas flow coefficient) as described with **Eqns. 1** and **2**, once P_1 and P_2 are calculated.

For the flow out of the pressurized canister, the ideal gas law gives:

$$dP_1 = -\dot{m}_{12} \frac{RTdt}{V_1 M}$$

Equation 5

where $\dot{m}_{12}$ represents the gas mass flowrate from the canister to the feeding tube, V_1 is the volume of the canister, R is the universal gas constant, M is the molecular weight of air and T is the gas temperature (ambient).

For P_2, V_2 changes as the slug moves down the feeding tube, using the ideal gas law:

$$P_2 dV_2 + V_2 dP_2 = \frac{(\dot{m}_{12} - \dot{m}_{20})RTdt}{M}$$

$$dP_2 = \frac{(\dot{m}_{12} - \dot{m}_{20})RTdt}{MV_{2avg}} - \frac{P_{2avg}dV_2}{V_{2avg}}$$

Equation 6

where $\dot{m}_{20}$ represents the flow of gas from the feeding tube out to the atmosphere. P_{2avg} and V_{2avg} are determined numerically as the model code operates sequentially.

The fourth equation required is a force balance across the slug described as

$$(P_2 - P_0)A = m\frac{du}{dt}$$

Equation 7

where P_0 is the atmospheric pressure, A is the cross sectional area of the slug (assumed to be equal to the cross sectional area of the feeding tube for simplification), m is the slug mass, and u is the slug velocity, which can also be defined by the following:

$$u = \frac{dV_2}{Adt}$$

Equation 8

By differentiating this equation and substituting it into **Eqn. 7**, the following expression is found:

$$\frac{d^2V_2}{dt^2} = \frac{(P_2 - P_0)A^2}{m}$$

Equation 9

Finally, this expression can be used in the sequential model code to determine the change in V_2. A solids friction term (λ_S) was added that can be found empirically and is described in section 3.4.7:

$$dV_{2(i+1)} = dV_{2(i)} + \frac{(P_2 - P_0)A^2dt^2}{m_s} - \lambda_s dt^2$$

Equation 10

3.4.3 Modelling Pulse Gas Flow through Orifice

A 3.175 mm orifice was placed at the outlet end of the feeding tube as a threaded cap and a pulse of gas was performed and modelled. The SV_3 flow coefficient (C_{V1}) was determined in these experiments using the model (by fitting the measured pressures and predicted pressure and reducing the error by adjusting C_{V1}). The solenoid valve had an orifice size of 9.7×10^{-5} m^2 and was assumed to open instantaneously. The pulse mass balance closure was ensured to be within 98% in all experiments. The average C_{V1} was

found to be 0.165, with a very low standard deviation of 0.18% of the mean, as shown in **Table 3-2**.

Table 3-2: Solenoid Valve Flow Coefficient

Experiment	Pressure (kPa)	Cv_1
1	240	0.164527
2	240	0.164511
3	240	0.165142
4	308	0.164988
5	308	0.164985
6	308	0.165231
7	377	0.165270
8	377	0.165265
9	377	0.165221
	Mean Average:	0.165016
	Standard Deviation:	0.000302

By fitting the experimental measured pressures with the predicted pressures, the 3.175 mm orifice flow coefficient (at the end of the feeding tube) was also matched with the theoretical flow coefficient value of 0.857, which had been determined by steady state testing of the orifice alone with another orifice plate. Therefore the model performance was validated and the flow coefficients were determined. **Fig. 3-11** illustrates the fit between the model curves (solving for C_{V1} and matching the theoretical orifice flow coefficient) for a pulse at 240 kPa through the orifice; this shows that both the model equations and the measuring instruments were adequate for further study.

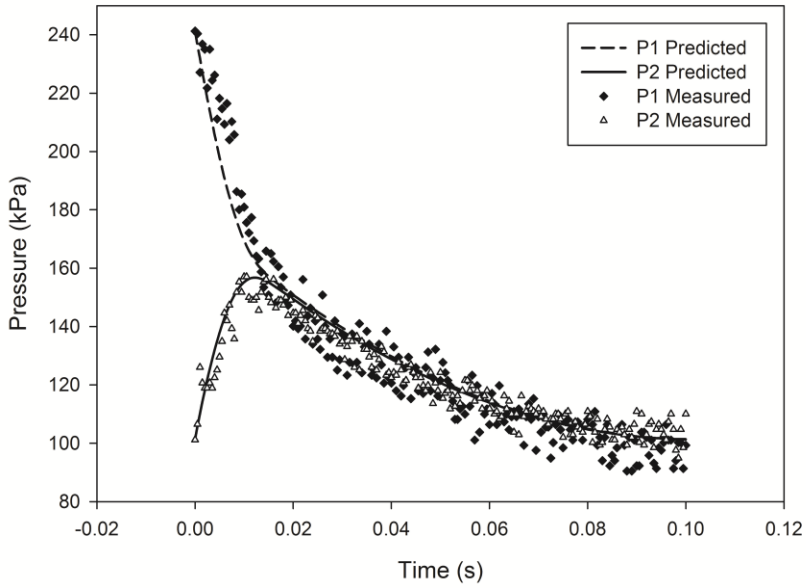

Figure 3-11: Measured and Predicted Pressure Curves for Orifice Pulse Flow

3.4.4 Modelling the Static Solid Ball

The ideal slug (selected as a modified nylon ball) was held in a thimble cage (with negligible pressure drop) at the end of the feeding tube and a gas pulse was injected and modelled. The SV_3 valve was assumed to open instantaneously and its flow coefficient was matched with that from the orifice tests (0.165). The flow coefficient of the ball (C_{V2}) was found to be 15.75 on average, with a 0.0231% standard deviation, as illustrated in **Table 3-3**.

Table 3-3: Static Ball Flow Coefficient

Experiment	Pressure (kPa)	Cv_2
1	240	15.75727
2	240	15.75728
3	308	15.75430
4	308	15.75428
5	377	15.74921
6	377	15.74928
	Mean Average:	15.7536
	Standard Deviation:	0.003632

Fig. 3-12 illustrates an example of the good fit generated by the model when compared to the experimental pressure results of a pulse at 308 kPa, which solves for the flow coefficient of the ball by fitting the measured vs. predicted pressures and also minimizing the mass balance closure error (99.89% closure in this case). Thus, the model was further confirmed and validated with a slug type object in the feeding tube.

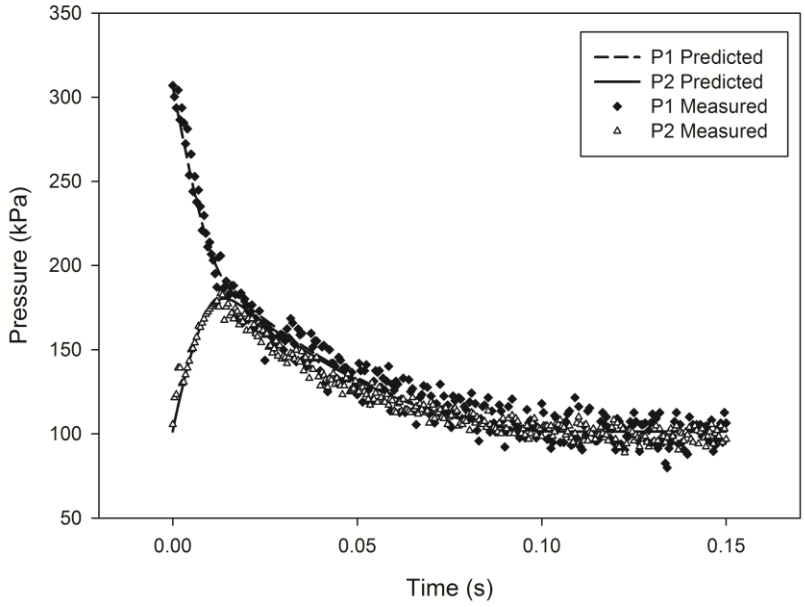

Figure 3-12: Measured and Predicted Pressure Curves for Static Ball Pulse Flow

3.4.5 Modelling the Dynamic Solid Ball Projectile

At this point the model had been validated and tested with stationary objects. The next step was to test it with an ideal projectile, i.e. a modified nylon ball with very low gas leakage. The ball was front-loaded in the feeder and pushed back to the slug chamber. The pulse was used to send the ball as a projectile out of the feeder. A red laser coupled with a photoresistor was used to detect when the ball exits the tube, using different tube lengths, to determine the position vs. time profile for the ball. Using the unsteady state C_{V1} value for SV_3 of 0.165, the model was used to fit the experimental pressures with the model pressures, and minimize the mass balance error, by changing the gas flow coefficient past the moving ball (C_{V2}). C_{V2} was found to be zero, meaning the ball travels at the speed of the gas allowing negligible gas leakage. Therefore, the ball can be used as a benchmark for an ideal slug projectile. **Fig. 3-13** shows that the predicted pressures fit the measured pressures very well, from the start time until the time that the ball exits the feeding tube (in this example a 377 kPa pulse was used, forcing the ball out of the 1.145 m feeding tube) – the predicted pressures fit with a sum of squares error of 3.3 and a mass balance closure of 98.72%. Lasers were used to also demonstrate that the small shoulder seen in the P_2 pressure rise is the point at which the ball actually begins to move (the pressure builds and the static friction is overcome at that point).

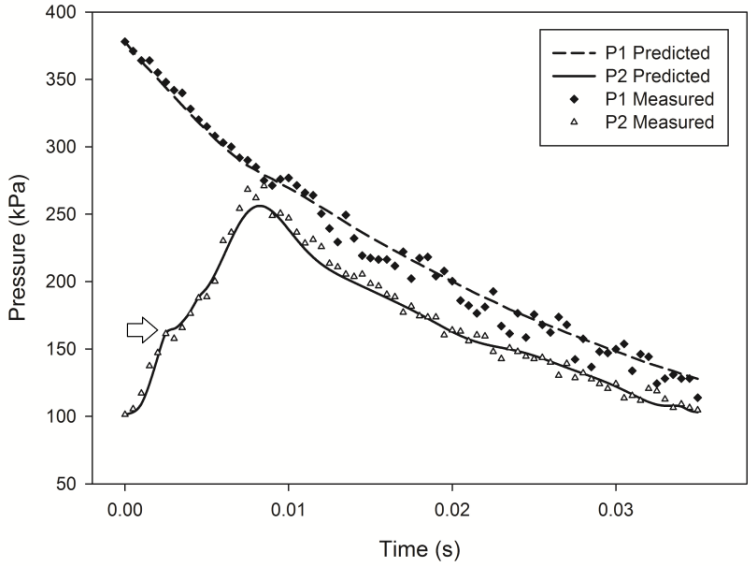

Figure 3-13: Measured and Predicted Pressure Curves for Dynamic Ball Projectile Pulse Flow

The model calculates the flow from the pressure canister to the feeding tube system. As a result, the volume change (due to the projectile ball moving) with respect to time can be calculated using the ideal gas law and thermodynamics, described in section 3.4.2. By knowing the volume change from the model (based on the measured pressures), and the actual volume of the feeder tube line, one can convert the volume to a distance travelled, plot the theoretical position of the ball vs. time from the model and compare it to the positional information from the lasers. **Fig. 3-14** shows that the model fits the laser data very well with the introduction of the friction factor in **Eqn. 10** (justified and described further in section 3.4.7) – some minor scatter in the replicates can be due to how fast the ball is moving compared to the laser detection response time. The ball was forced to hit a target to hover in the air for a millisecond so that the laser could detect the interruption of the signal due to the presence of the ball. The model position

prediction also considers the initial inertia before the ball begins to move based on the laser data (which is also identified from the shoulder in the P_2 pressure rise, indicated by the arrow in **Fig. 3-13**).

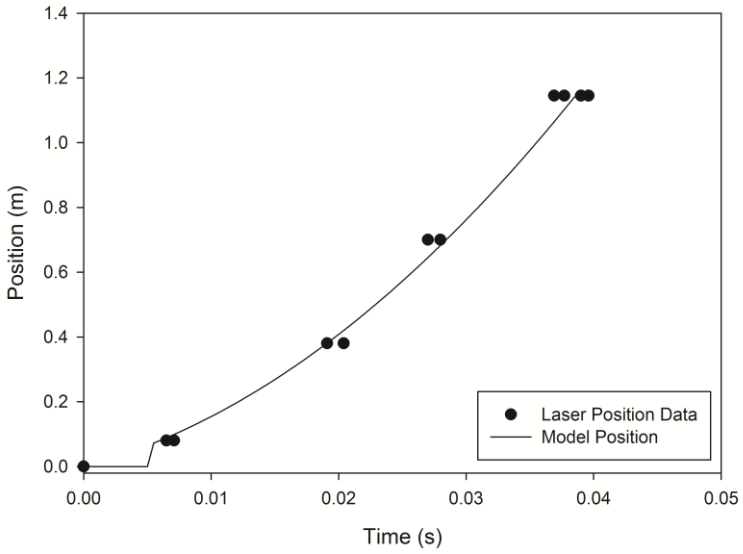

Figure 3-14: Predicted and Measured Dynamic Ball Position vs. Time

3.4.6 Modelling Dynamic Dried Distillers' Grain Slug

After modelling the ideal nylon ball projectile, the model aim was shifted to realistic biomass feedstocks for modelling, which are typical of many other potential feedstocks. The visual observations of the moving DDG slugs indicated that the particles stayed together quite well, as also shown in section 3.3.6. Once the particles left the feeding tube they spread apart significantly (which may be attractive from a mixing and reaction perspective), as expected, since the feeder action could be compared to a cylindrical bore (no choke) shotgun shell, however without the extra wadding to help keep the

pellets together and separate from the powder charge and prevent excessive lateral spreading after exiting the barrel.

Fig. 3-15 illustrates the predicted and measured pressures of a 377 kPa pulse forcing a DDG slug out of the 1.145 m feeding tube. The average C_{V1} of 0.165 was used to model the SV_3 released pulse gas flow. The difference between the predicted and measured pressures was minimized, while also minimizing the mass balance closure error for the capacitance volume, while changing C_{V2}. The best fit was found at C_{V2} = 0, demonstrating that the DDG slug, at this operating condition, did not allow significant gas leakage and travelled in a well packed manner similar to the nylon ball projectile out of the feeding tube. The shoulder on the P_2 pressure rise was observed at a lower pressure than for the nylon ball, however, indicating that the DDG would begin moving at a lower pressure and therefore has lower overall solids friction than the ball. This is due to the fact that the ball was designed to prevent gas leakage and therefore has a tight fit within the feeding tube.

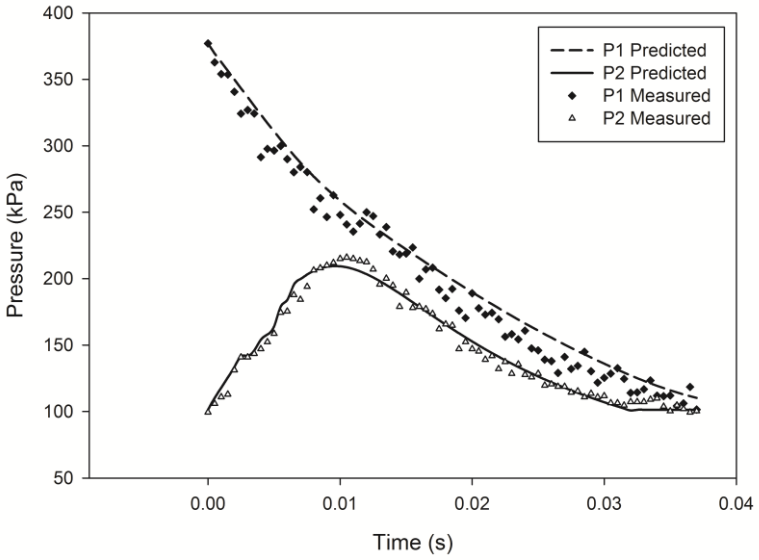

Figure 3-15: Measured and Predicted Pressure Curves for Dynamic DDG Slug Pulse Flow

Similarly to the dynamic nylon ball, we can also now calculate the volume change in the feeder tube to find the position with respect to time of the DDG, and compare it with the information from the laser and photoresistor system, to verify the model fully. The model calculates the flow from the pressure canister to the feeding tube system. **Fig. 3-16** illustrates the modelled position vs. the laser data position for the same run as above at 377 kPa. The model fits the laser data very well with the introduction of the friction factor in **Eqn. 10** (described further in section 3.4.7) and thus verifies the model's ability to characterize the solids flow. The position prediction also considers the initial inertia before the DDG begins to move based on the laser data (which is also identified as the shoulder in the P_2 pressure rise).

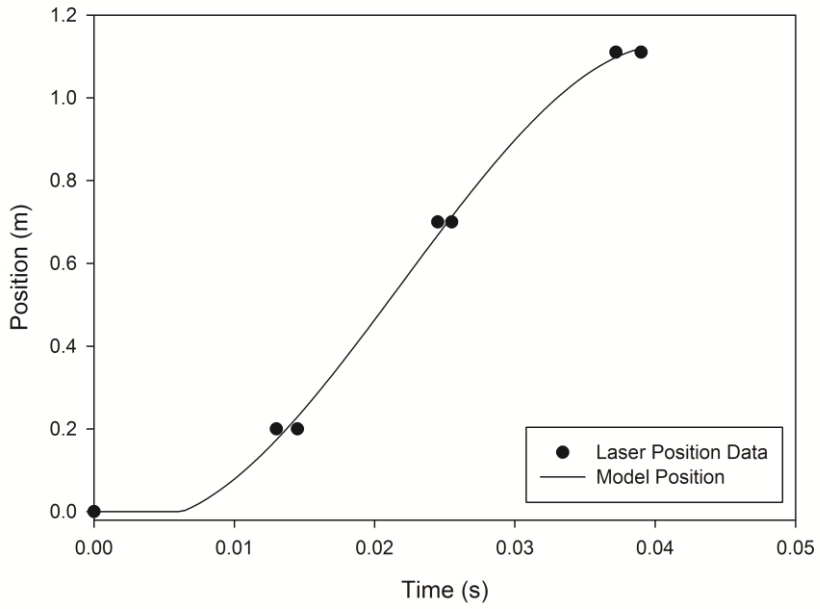

Figure 3-16: Predicted and Measured Dynamic DDG Slug Position vs. Time

3.4.7 Friction Factor and the Fully Predictive Model

To create a fully predictive model, the unknowns are $\dot{m}_{12}$, P1, P2, and V2. The initial values for P1, P2 and V2 are known, however. The other required input variables for the fully predictive model are the SV_3 orifice area, C_{V1} (SV_3 flow coefficient), the critical shoulder pressure required to move the slug (described below), the mass of the slug (m), and the cross sectional area of the tube (A). Sections 4.5 and 4.6 illustrate the model's ability to determine the flow coefficients by matching the predicted and measured pressures, ensuring a good mass balance closure and then verifying the successful model further by examining the predicted position vs. time of the slug (based on the measured pressures) compared to the laser data. For a fully predictive model, one must be able to solve for all of the variables without having the measured pressures depart from their initial values.

As discussed in sections 3.4.5 and 3.4.6, in order to match the predicted slug position with the measured position from the laser data, a simple friction factor had to be considered as shown in **Eqn. 10**. Since the friction factor would be a measure of the solids friction against the tube wall and also against each other, a relationship between the friction factor and the shoulder pressure (the pressure at which the slug begins moving after the P_2 pressure increase), was evaluated. By adjusting the friction factors, relative to the slug mass, the trend shown in **Fig. 3-17** was established. **Fig. 3-18** illustrates the fact that the shoulder pressure observed for the different slugs is constant and does not change with pulse pressure. As a result, with more experimentation, a complete index could be built for the friction factors for different materials simply by adjusting for the different mass of the slug and for the observed shoulder pressure, also to reduce the error margin and scatter for the friction factor. Eventually, with further work, a relationship between the feeder friction factor and specific and easy to measure particle characteristics (such as certain avalanching or dynamic shear cell measurements) could be found.

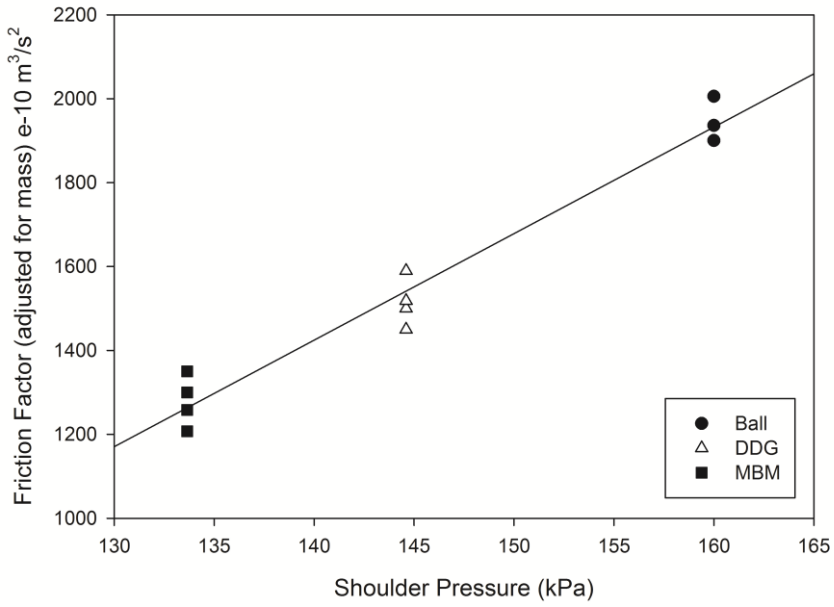

Figure 3-17: Friction Factor vs. Shoulder Critical Pressure Index for Feedstocks

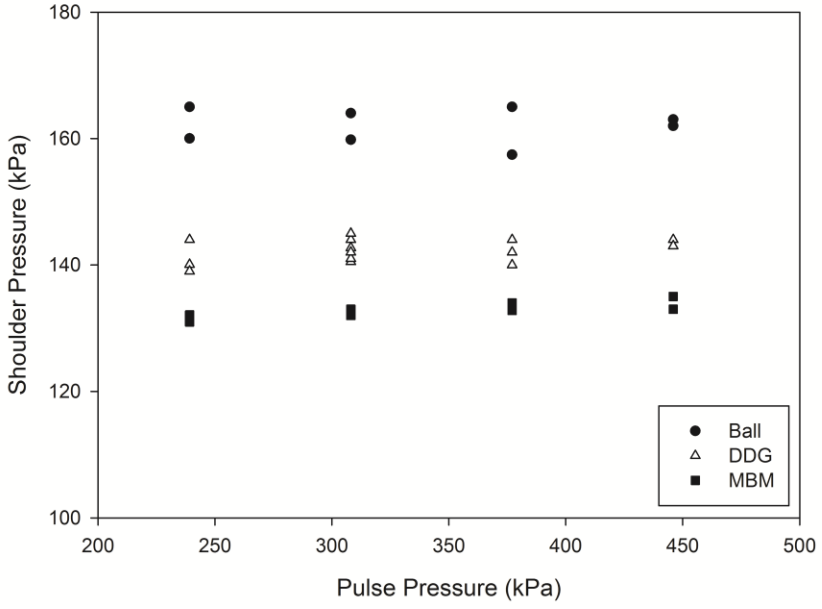

Figure 3-18: Shoulder Critical Pressure vs. Pulse Pressure for Feedstocks

Figs. 3-19, **3-20** and **3-21** illustrate position vs. time curves obtained with the fully predictive model for the nylon ball, DDG, and MBM at different pulse pressures, all with

a capacitance volume of 80 mL. The curves plateau at the theoretical maximum tube length allowable before the rapid energy loss of propulsion gas, leading to spreading and particle settling (stragglers). In addition, the slopes of the curves illustrate a difference in the velocity of the slugs, with lower slopes indicating lower energy, straggler formation and non-ideal flow. Since the ball has a high friction factor, all of the curves have significantly different slopes in **Fig. 3-19**; whereas, at high enough pressures, the model shows that DDG and MBM all have similar slopes (**Figs. 3-20** and **3-21**). MBM seems to demonstrate the best slug flow characteristics in the feeder tube due to its low friction factor but high internal cohesivity, allowing the slugs to stick together better during flow, preventing gas leakage, spreading and, most importantly, straggler formation. By examining the curves, it appears that for DDG (with the current capacitance volume), the best operating condition would be to operate at 377 kPa (as above that pressure the slope does not increase significantly and the energy efficiency of the feeder would decrease), with a feeding tube length shorter than 1.1 m by a good safety margin. While for MBM (with the current capacitance volume), the best operating condition would be to operate around 308 kPa (as above that pressure the slope does not increase significantly and the energy efficiency of the feeder would decrease), with a feeding tube length shorter than 0.8 m by a good safety margin.

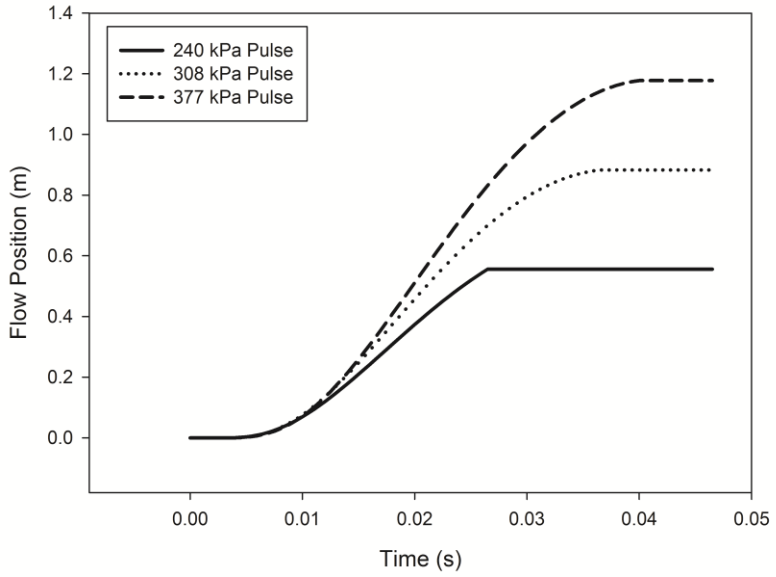

Figure 3-19: Predictive Model - Ball Position vs. Time at Different Pulse Pressures

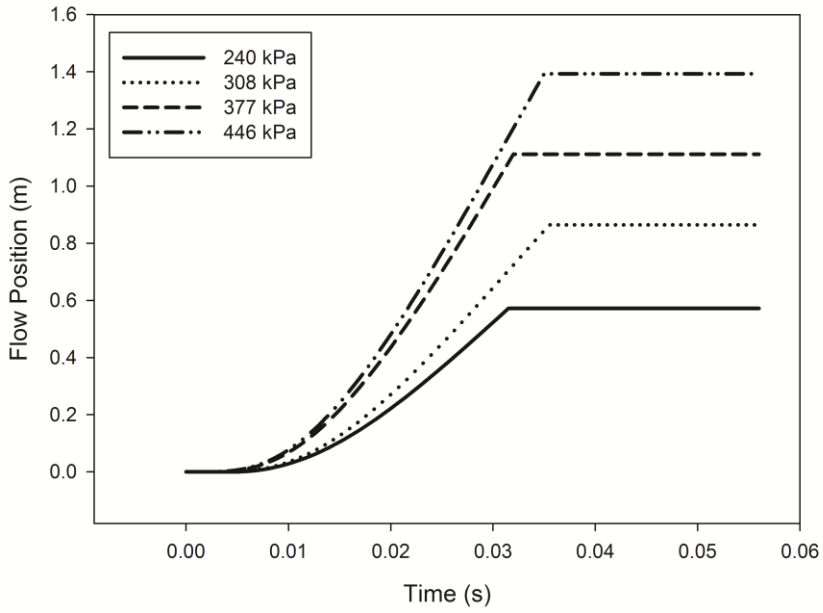

Figure 3-20: Predictive Model - DDG Slug Position vs. Time at Different Pulse Pressures

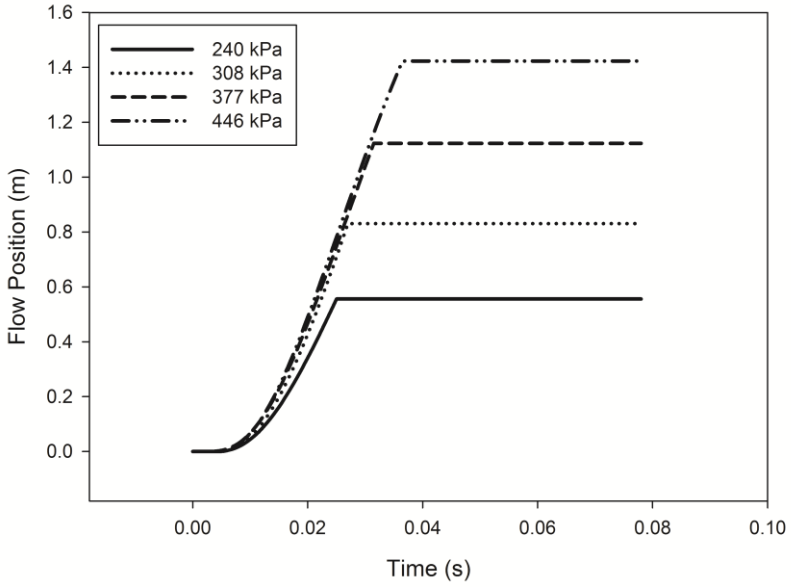

Figure 3-21: Predictive Model - MBM Slug Position vs. Time at Different Pulse Pressures

3.4.8 Model Utilization and Design Criteria

As shown in section 3.4.7, the fully predictive model can successfully be used to estimate the biomass slug flow at different operating conditions. Therefore, one could utilize the model as a design tool to develop a feeder for a given material and application, while being able to balance physical constraints (required feeding tube lengths for example) with capital and energy costs. For example, one could compare difference capacitance volume vessel sizes for energy and construction efficiency for given materials and feeding tube lengths. **Fig. 3-22** illustrates the feeding of MBM with either a larger capacitance tank at lower pressure (0.0001031 m^3 at 240 kPa) or a smaller capacitance tank at higher pressure (0.00008 m^3 at 308 kPa), such that the tanks will contain the same number of moles. As demonstrated by the model by the higher

slope and longer feeding tube maximum length, and also shown in [7], higher pressures and smaller volumes are better for conveying materials due to higher pulse energy (even in the case of significantly fewer moles). However, as part of one's design, gas compression energy and costs should also be considered.

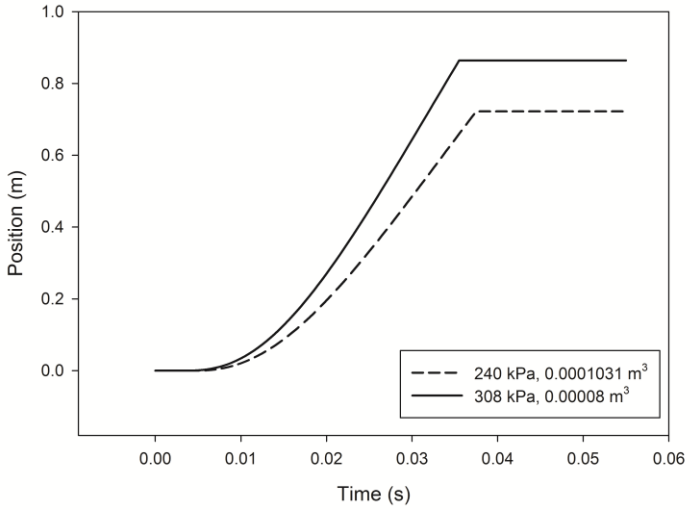

Figure 3-22: Predictive Model - DDG Position vs. Time at Different Capacitance Volumes with Equal Gas Moles

3.5 Conclusions

The ICFAR intermittent solid slug feeder has been developed to feed temperature-sensitive, cohesive, and challenging residual biomass feedstocks into fluidized bed pyrolysis reactors. In this study, the high-velocity slug flow fundamentals in the feeder have been observed and characterized. In addition, a predictive model for the feeder operation was successfully developed by utilizing a sequential approach with validation from dedicated experimental data, using DDG, MBM and an 'ideal' nylon ball slug. The predictive model can be used as a design tool to develop an effective feeder for a given

material and application, while being able to balance physical constraints with capital and energy costs. Further work will be performed to validate the model for larger scale ICFAR feeders and to explore alternate feeder design geometries for further operation and efficiency optimization.

3.6 Acknowledgements

The Authors wish to express their gratitude to the Natural Sciences and Engineering Research Council of Canada (NSERC), the NSERC Vanier Canada Graduate Scholarship program, Agri-Therm Inc. and Western University for the financial support of this research program.

3.7 Notation

Symbol	Units	Definition
A_{OR}	m^2	Orifice cross-sectional area
A	m^2	Cross-sectional area of tube/slug
C_V	--	Flow coefficient
C_{V1}	--	Flow Coefficient of SV_3
DDG	--	Dried Distillers' Grain
ICFAR	--	Institute for Chemicals and Fuels from Alternative Resources
k	--	C_p/C_v of the gas
$\dot{m}$	kg/s	Mass flowrate
m	kg	Mass of slug
M	kg/mol	Molecular weight
MBM	--	Meat and Bone Meal
P	Pa	Gas pressure
R	$Pa*m^3/mol*K$	Universal gas constant
SV_3	--	Solenoid Valve 3 (controls pulse)
T	K	Temperature
u	m/s	Velocity of slug
V	m^3	Volume
Y	--	Constant (defined in Eqn. 3)
λ_s	m^3/s^2	Empirical friction factor

References

[1] F. M. Berruti, K. Lenkiewicz, R. Xu, R. J. Bedmutha, S. Nova, F. Berruti, and C. L. Briens, "Novel Fluid Bed Pilot Plant for the Production of Bio-oil from Biomass through Fast Pyrolysis," *Récents Progrès en Génie des Procédés, Ed. SFGP, Paris, France, ISBN 2-910239-68-3*, no. 94, pp. 1–8, 2007.

[2] F. M. Berruti, L. Ferrante, C. L. Briens, and F. Berruti, "Pyrolysis of cohesive meat and bone meal in a bubbling fluidized bed with an intermittent solid slug feeder," *Journal of Analytical and Applied Pyrolysis*, vol. 94, pp. 153–162, Mar. 2012.

[3] R. A. Garcia, R. A. Flores, and C. E. Mazenko, "Factors contributing to the poor bulk behavior of meat and bone meal and methods for improving these behaviors.," *Bioresource Technology*, vol. 98, no. 15, pp. 2852–2858, Nov. 2007.

[4] P. Palmisano, F. M. Berruti, V. Lago, F. Berruti, and C. Briens, "Lignin Pyrolysis in a Fluidized Bed Reactor," *The International Conference on Thermochemical Biomass Conversion Science, Chicago, Illinois, USA*, 2011.

[5] E. Cascarosa, I. Fonts, J. M. Mesa, J. L. Sánchez, and J. Arauzo, "Characterization of the liquid and solid products obtained from the oxidative pyrolysis of meat and bone meal in a pilot-scale fluidised bed plant," *Fuel Processing Technology*, vol. 92, no. 10, pp. 1954–1962, Oct. 2011.

[6] M. O. Guedon, T. Baron, C. L. Briens, and T. M. Knowlton, "Intermittent injection of prepolymer in a pressurized fluidized bed," *Powder Technology*, no. 78, pp. 25–32, 1994.

[7] F. M. Berruti, L. Ferrante, F. Berruti, and C. L. Briens, "Optimization of an Intermittent Slug Injection System for Sawdust Biomass Pyrolysis," *International Journal of Chemical Reactor Engineering*, vol. 7, 2009.

[8] R. B. Shah, M. a Tawakkul, and M. a Khan, "Comparative evaluation of flow for pharmaceutical powders and granules.," *Aaps Pharmscitech*, vol. 9, no. 1, pp. 250–258, Jan. 2008.

[9] B. C. Hancock, K. E. Vukovinsky, B. Brolley, I. Grimsey, D. Hedden, A. Olsofsky, and R. a Doherty, “Development of a robust procedure for assessing powder flow using a commercial avalanche testing instrument.,” *Journal of Pharmaceutical and Biomedical Analysis*, vol. 35, no. 5, pp. 979–990, Sep. 2004.

[10] R. Bhadra, K. Muthukumarappan, and K. A. Rosentrater, “Flowability Properties of Commercial Distillers Dried Grains with Solubles (DDGS),” *Cereal Chemistry*, vol. 86, no. 2, pp. 170–180, 2009.

[11] G. Eriksson, “Residues from Biochemical Production of Transport Biofuels in Northern Europe,” Thesis from Luleå University of Technology, Sweden, 2009.

[12] D. Geldart, N. Harnby, and A. C. Wong, “Fluidization of cohesive solids,” *Powder Technology*, no. 37, pp. 25–37, 1984.

[13] R. Freeman, “The Importance of Air Content on The Rhealogy of Powders,” *Particulate Systems Analysis, Harrogate, UK*, pp. 1–5, 2003.

[14] S. S. Mallick and P. W. Wypych, “Modeling Solids Friction for Dense-Phase Pneumatic Conveying of Powders,” *Particulate Science and Technology*, vol. 27, no. 5, pp. 444–455, Sep. 2009.

[15] J. Dai, H. Cui, J.R. Grace, “Biomass feeding for thermochemical reactors,” Progress in Energy and Combustion Science, 38, pp. 716-736, 2012.

Chapter 4

4 Chapter 4: Novel Intermittent Solid Slug Feeder for Fast Pyrolysis Reactors: Application of Predictive Model for Scale-Up, Alternate Geometries, and Optimized Feeder Design Procedure

4.1 Introduction

Fluidized bed technology has been demonstrated to have good potential as a reactor technology for the production of pyrolysis oil and bio-char, via fast biomass pyrolysis [1]. In a fluidized bed pyrolysis process, raw biomass material particles must be conveyed and injected into the reactor using the least energy-intensive and most practical feeding system. Dilute phase pneumatic transport lines and screw feeders are currently used by several pyrolysis processes. However, in the flash pyrolysis process, where the temperature of the reactor is high, typically between 450 and 550 °C, and where relatively high mass flow rates of raw biomass must be processed, these commonly used feeding systems tend to encounter some serious problems [2, 17]. For example, the high reactor temperature coupled with pressure fluctuations at the inlet into the reactor can often lead to severe plugging in screw feeders, potentially causing significant damage to the equipment or down time in the operating process. This is especially the case for temperature-sensitive and cohesive biomass residues such as Kraft lignin and meat and bone meal residues [2–4]. Dilute phase pneumatic transport feeders consume a large amount of gas, which is typically recycled product gas, resulting in higher energy consumption and requiring a more sophisticated condensation train due to product vapour dilution. In addition, many industrial operators attempting to feed challenging

biomass into reactors with conventional feeders are usually forced to feed above the bed, without the good fluidized bed penetration that can be achieved with the pulse feeder. This very often results in poor mixing with hot sand and thus a negatively affected reaction, as the biomass simply trickles out of the feeding tube and floats on top of the hot bed [5]. This prevents the rapid heat transfer from the sand bed to the biomass particles, which is essential to achieve the fast pyrolysis conditions that have been shown to maximize both the yield and quality of pyrolytic liquids [6].

To prevent plugging and help the raw biomass particles effectively penetrate and spread into the pyrolysis fluidized beds, one can inject the particles using intermittent slugs created by propelling loosely packed particles with gas pulses and transporting them along horizontal or inclined feeding pipes into the fluidized bed section of the reactor [7]; this combines the advantages of the low gas consumption of the screw feeders and the short residence time in high temperature zones of dilute phase feeders. It also injects the biomass in the central, well-mixed region of the fluidized bed, maximizing heat transfer to the biomass particles.

Among many other potential applications, intermittent solid slug feeders can be used to effectively inject biomass materials into fluidized bed reactors for pyrolysis. In particular, these feeders can be used to convey biomass materials that are highly cohesive and/or heat sensitive to prevent plugging or undesirable reaction in the feeding tube. Although laboratory-scale feeders of this design have been studied and modelled [8] (Chapter 3), and shown to work very effectively for pyrolysis applications [2], [9] (Chapter 6,

Appendix II and III), the model created requires validation on a large-scale and an optimized design procedure should be developed for the implementation of this technology in industrial facilities.

Dried Distillers' Grain (DDG) was the primary feedstock used in this work for testing and modelling, but meat and bone meal residues (MBM) were also tested for model validation. These biomass feedstocks were selected as they possess very challenging flow characteristics, and properties that are very different from each other (particle size, cohesivity, temperature sensitivity, density) [2]. As a result, a model that can successfully predict the pulse feeding of these challenging feedstocks will likely work for any biomass of interest.

This study had three objectives:

1. Use the previously developed predictive model [8], to design a large-scale feeder for two different types of biomass feedstocks using the same, simple feeder slug chamber used in the previous study [8], and test this feeder.

2. The main goal of this study was to apply the predictive model to create a comprehensive design procedure that can be utilized to develop an effective feeder for any material and application, while being able to balance physical constraints with capital and energy costs.

3. The model suggested that the standard "T" slug chamber previously used was not optimal. An alternate slug chamber design, which is able to provide the

optimal slug mass predicted by the model, was successfully tested at the laboratory scale.

4.2 Materials and Methods

4.2.1 The ICFAR Intermittent Solid Slug Feeding Technology

The Institute for Chemicals and Fuels from Alternative Resources (ICFAR) intermittent solid slug feeder technology [9] designed for this work and illustrated in **Fig. 4-1** (figure applies for both laboratory and large-scale) has been used extensively at ICFAR for bubbling bed pyrolysis reactor experiments for long operation and has also been scaled up [2]. It should be noted that in practice a neutral gas (such as N_2 or recycled product gas), instead of air, would be used to inject biomass materials into pyrolysis reactors (since absence of oxygen is required for the reaction).

4.2.1.1 The Laboratory-Scale ICFAR Intermittent Solid Slug Feeder

The laboratory-scale feeder for this work consisted of a slightly pressurized vertical solids storage silo, with a pressure P_0 kept between atmospheric pressure and 120 kPa, leading to a 19 mm diameter pneumatic pinch valve. The silo had a 4 L volume, with a cone angle of 70° from the horizontal. Within the silo, a specially-designed rotating 'egg-beater' mixer prevented solids bridging. The instantaneous mass flow of gas flowing into the silo was determined by acquiring the Gas-Trak Sierra mass flowmeter signal on the nitrogen line to the silo. The pinch valve was controlled by Granzow Inc. solenoid valves (SV_{1A} and SV_{1B} in **Fig. 4-1**, series 21EN) connected to a relay timer (IMO iSmart Relay, 10 I/O DC). Solids exiting the pinch valve flowed into a 15.3 mm i.d., electrically-grounded

clear PVC or carbon steel horizontal feeding tube through a 90^{o} angle connection. The feeding tube length was varied from 0.08 to 1.145 m, as the optimum length for this feeder size would very likely fall within this range for biomass feedstocks.

The volume between the end point of the pinch valve and the start of the horizontal feeding tube is called "slug chamber" (see **Fig. 4-2**). Three slug chamber designs were tested in the current study. The first was a simple "T" fitting of constant diameter (15.3 mm), with a vertical, 63.5 mm long section (measured from the base of the horizontal part of the "T" block). The second slug chamber (#2 in **Fig. 4-2**) is a short angled slug chamber of equivalent volume to the "T", with a smooth and constant diameter (15.3 mm). The angled section was on a 45° angle and was 50 mm long. The third slug chamber (#3 in **Fig. 4-2**) is a long angled slug chamber of constant diameter (15.3 mm), which can be used to increase the slug size further while still ensuring a good tube cross-sectional area biomass fill. The angled section was also on a 45° angle and was 178 mm long.

Intermittent pulses of nitrogen at a set pressure were used to propel the biomass slugs, delivered from a control volume consisting of an 80 mL steel canister. The timing of the pulses was controlled with a relay timer activating Granzow Inc. solenoid valves (SV_2 and SV_3 in **Fig. 4-1**, series 21EN). When the pinch valve opens, the biomass falls into the 'slug chamber' forming a plug, the pinch valve closes and the biomass plug is then propelled through the feeding tube into the reactor by a pulse of pressurized gas from the canister. The pressures in the silo (P_0), capacitance volume (P_1), and feeding tube (P_2),

were measured at 2 kHz by Omega PX181 series semiconductor pressure transducers connected to a data acquisition system (National Instruments NI USB-6008 data acquisition card and NI LabVIEW software).

The entire apparatus was manufactured using clear PVC to allow for visual inspection of the feeder operation and for characterization of the solids flow with red lasers and a photo-resistor apparatus, which gave a signal that was recorded at 10 kHz by a National Instruments NI USB-6008 data acquisition card and NI LabVIEW software. Passage of the slug through the laser beam was detected from the associated change in photoresistor signal. The response time of the photoresistor apparatus was experimentally measured to be less than 2 ms, and thus the maximum experimental error on the slug position, was estimated from the maximum slug velocity to be less than 2.5 % of the total tube length, in all cases.

The solid mass flow rate was measured by separating the fed biomass in a cyclone with the collected solids flowing to a MY WEIGH i601 digital scale, which continuously output the instantaneous mass data to a computer at 8.4 Hz. The fines losses were insignificant relative to the mass feeding rate due to the very high cyclone efficiency at these operating conditions.

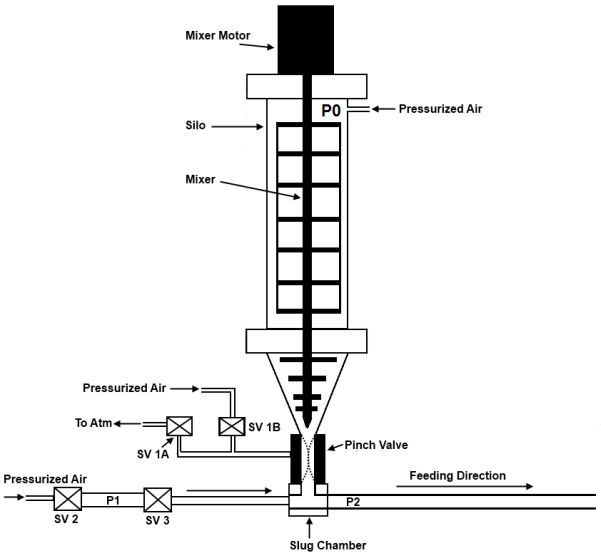

Figure 4-1: ICFAR Intermittent Solid Slug Feeder Schematic (laboratory-scale and large-scale)

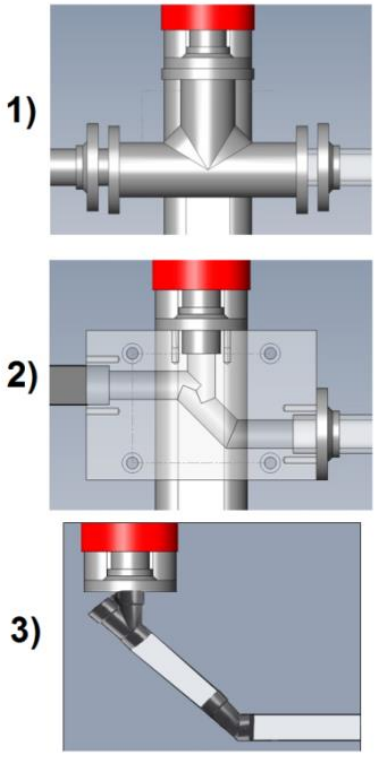

Figure 4-2: ICFAR Intermittent Solid Slug Feeder Slug Chamber Designs

4.2.1.2 The Large-Scale ICFAR Intermittent Solid Slug Feeder

The large-scale ICFAR intermittent solid slug feeder can also be described by **Fig. 4-1**. The feeding tube was manufactured from clear PVC and has an internal diameter of 51.13 mm. The feeding tube was typically utilized at a length of 0.8 m, but can be replaced by any tube length at the slug chamber flange. The large feeder has only one slug chamber option, composed of carbon steel, which is "T"-shaped. The top of the T (flowing from the silo) has an inner diameter of 78 mm and gradually throttles in shape to the 51.13 mm inner diameter of the horizontal feeding tube. The length from the base of the "T" to the bottom of the 78 mm inner diameter pinch valve (3" Red Valve Type A-Full Port, 0.3 m long) was 0.381 m. A 36 L non-agitated or mixed silo is utilized above the pinch valve (attached by a flange) to load the solids for continuous feeding. The silo has a 0.254 m diameter at the top and remains cylindrical for 0.5 m, followed by a gradual restriction to 0.1 m over a 0.38 m length.

The pulse (SV_3) is controlled by a GC Valves brass body 25.4 mm NPT normally closed solenoid valve (S201GF02C5FG9) with a full-size 25.4 mm orifice. The solenoid valves controlling the inlet of the capacitance tank (SV_2) and the outlet of the pinch valve (SV_{1A}) were brass body 12.7 mm NPT normally closed GC Valves (S201GF02V5DG4). The solenoid valve controlling the inlet of the pinch valve (SV_{1B}) was a brass body 12.7 mm NPT normally open GC Valves (S202GF02V5DG4). A 120 V, 4 channel IMO iSmart relay (10 I/O AC) was utilized to program the solenoid valves, and thus the feeder operation and cycle time.

The capacitance tank was an 18 L (0.254 m diameter and 0.355 m in length) carbon steel pressure-rated vessel. The solids feeding rate was determined by capturing the biomass in a specially designed bin sitting on a MY WEIGH HD150 digital scale, outputting the mass to the computer at 8.4 Hz. The same pressure and laser measurement setup was used for the large-scale feeder as the small-scale feeder described in **4.2.1.1**.

4.2.2 Materials and Feedstocks

Table 4-1 illustrates some of the critical physical properties of the feedstocks utilized in this study.

The dried distillers' grain (DDG) feedstock used in this study was obtained from GreenField Ethanol in Chatham, Ontario, Canada. 0.5 wt% of Larostat powder was added to the DDG to mitigate electrostatic effects.

The meat and bone meal residue (MBM) used in this study was supplied by Thorndale Farm Supplies, a meat renderer and producer located in Thorndale, Ontario, Canada. More details and specifications than indicated in Table 1 on the MBM can be found in [2].

DDG and MBM represent challenging biomass feedstocks. According to [10], the Hausner ratio can be used as a good metric to predict flow type and material cohesion, and both the DDG and MBM have a relatively high Hausner ratio, which would indicate passable flow for the DDG and poor flow for the MBM. Indeed the MBM avalanching flow indicator characteristics from the Mercury Scientific Revolution Powder Analyzer, performed at 0.3 RPM for 150 avalanche data points and averaged over 3 replicates,

also demonstrate that MBM has a relatively higher cohesion and poorer bulk flow characteristics than DDG, as all metrics chosen from literature and illustrated in **Table 4-1** have higher values for MBM than DDG [11]. The feeding challenge for DDG pyrolysis lies in the prevention of "straggler" biomass in the feeding tube, i.e. particles left behind the moving slug, since, if the DDG pre-maturely begins to react in the feeding tube, its physical characteristics change dramatically, resulting in a foam-type blockage [11, 12].

Table 4-1: Feedstock Properties

Property	Units/Reference	DDG	MBM
Sauter mean diameter	µm	577	25.14
Bulk density	kg/m^3	503	467
Particle density	kg/m^3	915	778
Hausner ratio	-	1.26	>1.35
Revolution Powder Analyzer:			
Avalanche time	s	4.06	6.03
Avalanche median	s	4.29	6.50
Avalanche energy	kJ/kg	19.77	27.80
Energy std. deviation	kJ/kg	16.10	24.40
Avalanche angle	°	56.6	72.4
Rest angle	°	44.4	50.3
Flow Characterization:			
Flow Type	[8, 10]	Passable	Poor

4.3 Results and Discussion

4.3.1 Maximum Solid Flowrate for the Large-Scale Feeder

The maximum solid flowrate that can be delivered by the large-scale feeder is the maximum solids flowrate that can be delivered to, and fill, the slug chamber (volumetric limitation). As shown in Chapter 2, the pinch valve should be opened just long enough to fill the T-shaped slug chamber, without overfilling.

After several iterations of the relay program, the maximum feeding rate of the large-scale feeder was determined to be 254 kg/h of DDG and 228 kg/h of MBM. The difference in feeding rate was largely due to the difference in bulk density between the biomass products, as the feeder is effectively a volumetric feeder.

The optimum feeding program had a 1.8 s cycle time where the pinch valve would open for 0.3 s allowing the biomass to fill the cross-sectional area of feeding tube completely, without the slug chamber overfilling as described in [15]. The capacitance volume was pressurized with air for a period of 1.2 s, which was found to be enough time to reach the desired pressure, set by the upstream pressure regulator, for the given capacitance volume and the inlet tube and regulator sizes. After the capacitance was filled, a 0.1 s safety margin was allowed before the gas pulse would occur, with SV_3 staying open for a total of 0.4 s to ensure that the slug had exited the feeding tube and all of the air had exited the capacitance. Following the closure of SV_3, a 0.1 s safety margin was allowed before the cycle restart.

The same large-scale feeder has also been demonstrated to also be able to feed large (roughly 1 cm^3) wood chips by Agri-Therm Inc. [6], [16].

Fig. 4-3 illustrates the regularity of the feeding rate for both DDG and MBM.

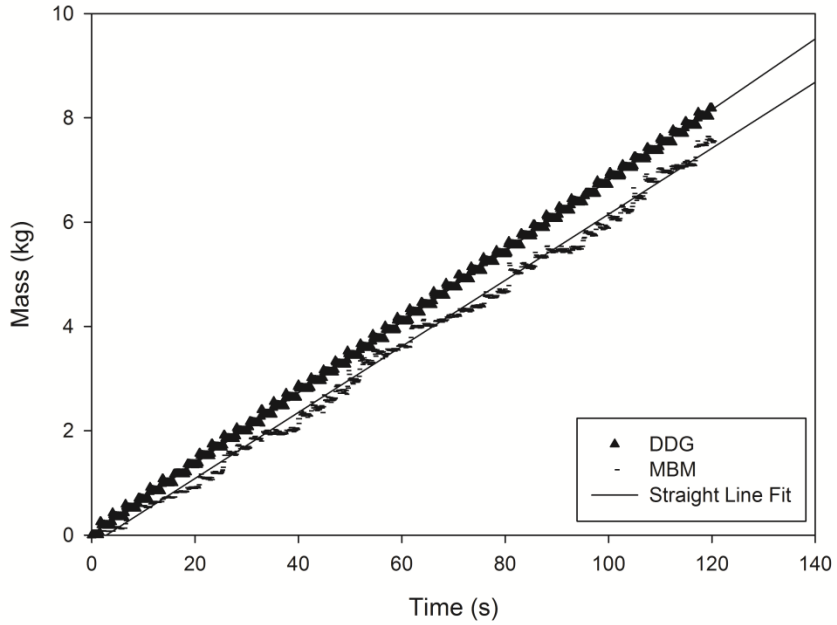

Figure 4-3: Maximum Achievable DDG and MBM Feeding Rate on Large-Scale Feeder (1.8 s cycle time and 155 kPa air pulse pressure)

4.3.2 Modelling Approach and Objectives

The fundamental physical understanding of the feeder operation, flow characterization, and modelling were developed in [8] (Chapter 3) for the laboratory-scale feeder. The next step was to validate the predictive model for the large-scale feeder.

To summarize, the goals of the feeder model are to:

a) Ensure the complete flow of the slug out of the feeding tube, thus eliminating the plugging and downtime issues that can be caused by straggler accumulation

b) Predict the maximum feeding tube length allowable for a particular feedstock and given operating conditions

c) Predict the position of the slug at any given time after the pulse, and thus its velocity

d) Predict and report the key feeder operation results based on biomass feedstock characteristics that can be obtained through quick experiments

The following step-by-step approach was taken to develop and validate the predictive model of the large-scale feeder, from when the biomass enters the slug chamber until it exits the feeding tube, as shown in **Fig. 4-4**:

1) Preliminary experiments were conducted to calibrate the equipment:

    - Pressure transducers were calibrated
    - The flow coefficient (C_V) of the fully open solenoid valve SV_3 was determined using a 0.0127 m orifice (with a flow coefficient of 1.718 that was determined from steady-state experiments) at the end of the 0.05113 m inner-diameter feeding tube of the large-scale feeder.

2) Experiments were conducted in the laboratory-scale feeder to determine the scale independent solids friction factor φ_s and also the critical pressure (ΔP_c)

(observed as a shoulder in the P_2 pressure rise) required to move the slug [8], that characterizes the interaction of a given solids feedstock with a given tube wall material (as defined in **Eqn. 19**, in section **4.3.3.2**).

3) A **predictive model** for the biomass slug movement in the large-scale feeder was then validated. The biomass slugs (a) DDG and b) MBM) were assumed to have a constant cross sectional area, equal to that of the feeding tube. For each type of feed particles, the model outputs:

    - slug position vs. time
    - slug velocity
    - maximum tube length

The predictive model requires the following input criteria:

- feeding tube inner diameter (D)
- initial pulse pressure (P_1)
- downstream pressure (P_2)
- capacitance volume (V_1)
- slug mass (m_s)
- the orifice size and average flow coefficient for open solenoid valve SV_3 (obtained in step 1)

- empirical scale-independent friction factor (φ_s) and critical pressure (ΔP_c) of the slug solids on the clear PVC tube material, determined from laboratory-feeder experiments (obtained in step 2)

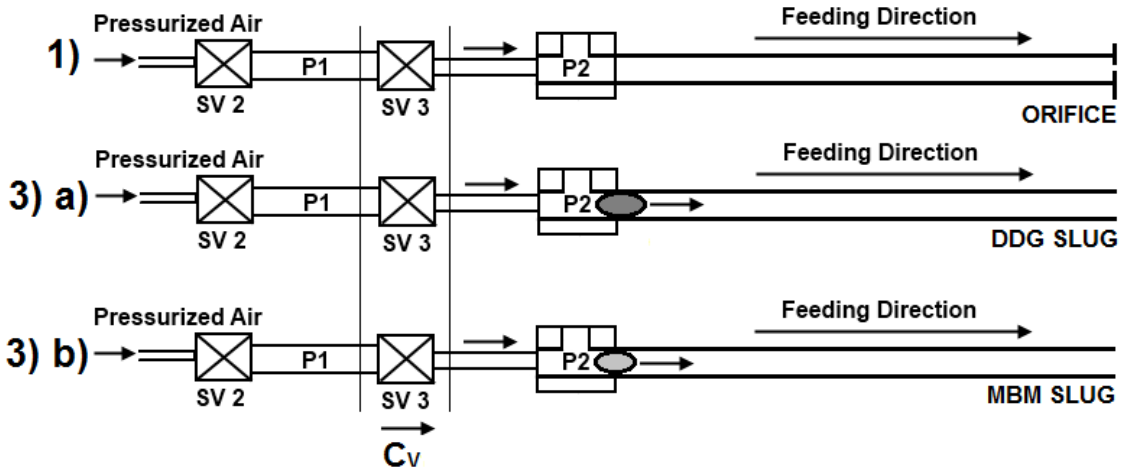

Figure 4-4: Modelling Approach Schematic

4.3.3 Predictive Model

4.3.3.1 Fundamental Equations

To model the pulse gas flow leaving the capacitance volume one must consider the flow through the fully open solenoid valve orifice SV_3 and whether the flow is sonic or sub-sonic.

For sonic gas flow, the following expression is used to calculate the mass flowrate ($\dot{m}$):

$$\dot{m} = C_V A_{OR} P_{UP} \sqrt{k \frac{M}{RT} \left(\frac{2}{k+1}\right)^{\frac{k+1}{k-1}}} = \alpha C_V P_{UP}$$

Equation 1

where C_V is the gas flow coefficient for the valve SV_3, which was assumed to open instantaneously, A_{OR} is the cross-sectional area of the valve orifice (m^3), P_{UP} is the upstream absolute pressure (Pa), k is the heat capacity ratio (C_p/C_v) for the gas (1.4 for air), M is the gas molecular weight (0.029 g/mol for air), R is the universal gas constant (8.314 m^3 Pa K^{-1} mol^{-1}), and T is the ambient temperature (298 K).

For sub-sonic gas flow, the following expression is used to calculate the mass flowrate:

$$\dot{m} = C_V A_{OR} Y \sqrt{\left(\frac{2M}{RT}\right) P_{UP}(P_{UP} - P_{DOWN})} = \beta C_V \sqrt{P_{UP}(P_{UP} - P_{DOWN})}$$

Equation 2

where:

$$Y = \sqrt{\left(\frac{P_{DOWN}}{P_{UP}}\right)^{\frac{2}{k}} \left(\frac{k}{k-1}\right) \left[\frac{1 - \left(\frac{P_{DOWN}}{P_{UP}}\right)^{\left(\frac{k-1}{k}\right)}}{1 - \left(\frac{P_{DOWN}}{P_{UP}}\right)}\right]}$$

Equation 3

and P_{DOWN} is the absolute pressure downstream of the orifice (Pa).

To determine an approximation of the upstream pressure P_{UP} corresponding to the transition point between sonic and sub-sonic flow, one can set the equations equal to each other:

$$\alpha C_V P_{UP} = \beta C_V \sqrt{P_{UP}(P_{UP} - P_{DOWN})}$$

Equation 4

Simplifying **Eqn. 4** results in the following conclusions:

If $\left(\frac{P_{DOWN}}{P_{UP}}\right) < \left[1 - \left(\frac{\alpha}{\beta}\right)^2\right]$ then the gas flow is sonic, otherwise it is sub-sonic.

Assuming isothermal conditions, one can perform mass balances on the capacitance canister (V_1) and also on the feeder system volume (V_2, which changes as the slug moves through the feeding tube) in order to predict the changing pressures (P_1 for the canister and P_2 for the feeding tube). To create a fully predictive model, the unknowns are $\dot{m}_{12}$, P_1, P_2, and V_2 while the initial values for P_1, P_2 and V_2 are known.

$\dot{m}_{12}$ can be calculated as a function of the known C_V (SV_3 gas flow coefficient) as described with **Eqns. 1** and **2**, once P_1 and P_2 are calculated.

For the flow out of the pressurized canister, the ideal gas law gives:

$$dP_1 = -\dot{m}_{12} \frac{RTdt}{V_1 M}$$

Equation 5

where $\dot{m}_{12}$ represents the gas mass flowrate from the canister to the feeding tube, V_1 is the volume of the canister, R is the universal gas constant, M is the molecular weight of air and T is the gas temperature (ambient).

For P_2, V_2 changes as the slug moves down the feeding tube. Therefore, using the ideal gas law:

$$P_2 dV_2 + V_2 dP_2 = \frac{(\dot{m}_{12} - \dot{m}_{20})RTdt}{M}$$

$$dP_2 = \frac{(\dot{m}_{12} - \dot{m}_{20})RTdt}{MV_{2avg}} - \frac{P_{2avg} dV_2}{V_{2avg}}$$

Equation 6

where $\dot{m}_{20}$ represents the flow of gas from the feeding tube out to the atmosphere. P_{2avg} and V_{2avg} are determined numerically as the model code operates sequentially.

The fourth equation required is a force balance across the slug described as

$$(P_2 - P_0)A = m_s \frac{du}{dt}$$

Equation 7

where P_0 is the atmospheric pressure, A is the cross sectional area of the slug (assumed to be equal to the cross sectional area of the feeding tube for simplification), m_s is the slug mass, and u is the slug velocity, which can also be defined by the following:

$$u = \frac{dV_2}{Adt}$$

Equation 8

By differentiating this equation and substituting it into **Eqn. 7**, the following expression is found:

$$\frac{d^2V_2}{dt^2} = \frac{(P_2 - P_0)A^2}{m_s}$$

Equation 9

Finally, this expression can be used in the sequential model code to determine the change in V_2. A solids friction term (λ_s) was added that can be found empirically and is described in [8]:

$$dV_{2(i+1)} = dV_{2(i)} + \frac{(P_2 - P_0)A^2dt^2}{m_s} - \lambda_s dt^2$$

Equation 10

4.3.3.2 Scale-Up Model Equations to Determine the Solids Friction Factor

In order to scale-up the feeder model, the effect of changes in the feeding tube inner diameter (D) and the mass of the slug (m_s) on the critical pressure to move the slug (ΔP_c) relative to the downstream pressure, and on the friction factor (λ_s) is required, as these parameters are inputs in the predicted model.

Experimentally, both the small-scale and large-scale feeding systems tested had smooth clear PVC feeding tubes, and therefore the effect of the feeding tube material is neglected for this analysis. It is expected that the effect of the difference between a smooth clear PVC feeding tube and a smooth stainless steel or carbon-steel tube would

be fairly minimal on the feeder performance, unless electrostatic effects are not controlled. If a significantly rougher feeding tube is to be used, quick experiments should then be performed to re-calibrate the friction factor and critical pressure, apply the scaling rules and validate them experimentally.

λ_s is defined as:

$$\lambda_s = \frac{F\ A_s}{m_s}$$

Equation 11

where F is the friction force acting on the slug, and A_s is the slug cross-sectional area (i.e. the cross-sectional area of the feeding tube). Thus it can be shown that:

$$\frac{\lambda_{s2}}{\lambda_{s1}} = \left(\frac{F_2}{F_1}\right)\left(\frac{D_2}{D_1}\right)^2\left(\frac{m_{s1}}{m_{s2}}\right)$$

Equation 12

The friction force (F) can also be expressed as a function of the critical pressure multiplied by the cross sectional area of the tube (A), in order to make the slug move, and is also proportional to the area of contact of the slug with the pipe wall. Therefore, the following expressions can be written:

$$\frac{F_2}{F_1} = \left(\frac{\Delta P_{c2}}{\Delta P_{c1}}\right)\left(\frac{A_2}{A_1}\right) = \left(\frac{\Delta P_{c2}}{\Delta P_{c1}}\right)\left(\frac{D_2}{D_1}\right)^2$$

Equation 13

$$F \propto D\, L_s$$

Equation 14

where L_s is the slug length, which can be written as

$$L_s = \frac{4\, m_s}{D^2\, \pi\, \rho_b}$$

Equation 15

where $\rho_b$is the bulk density of the biomass slug, which is assumed to be constant and not change.

By substituting **Eqn. 15** into **Eqn. 14**, the following expression is found:

$$\frac{F_2}{F_1} = \left(\frac{m_{s2}}{m_{s1}}\right)\left(\frac{D_1}{D_2}\right)$$

Equation 16

By substituting **Eqn. 16** into **Eqn. 13**, one can isolate the critical pressure scale-up equation:

$$\frac{\Delta P_{c2}}{\Delta P_{c1}} = \left(\frac{m_{s2}}{m_{s1}}\right)\left(\frac{D_1}{D_2}\right)^3$$

Equation 17

By substituting **Eqn. 16** into **Eqn. 12**, one can determine the friction factor scale-up equation, which is independent of the slug mass:

$$\frac{\lambda_{s2}}{\lambda_{s1}} = \left(\frac{D_2}{D_1}\right)$$

Equation 18

We can then introduce the scale independent solids friction factor φ_s, that characterizes the interaction of a given solids feedstock with a given tube wall material:

$$\varphi_S = \frac{\lambda_S}{D}$$

Equation 19

4.3.4 Determination of the Empirical Model Parameters

4.3.4.1 Flow Coefficient for Solenoid Valve SV_3

The flow coefficient (C_V) of the valve SV_3 was obtained by performing gas pulse experiments (with no solids) with a 0.0127 m orifice at the tip of the feeding tube (with known flow coefficient of 1.718). By fitting the predicted pressures to the measured pressures (P_1 and P_2), as shown in **Fig. 4-5**, and ensuring a good pulse gas mass balance closure, the SV_3 flow coefficient (C_V) was found.

By repeating the experiment at different pressure conditions, the average flow coefficient for solenoid valve SV_3 was determined to be 0.50 and used in all following experiments. It was verified that SV_3 could therefore be assumed to open instantaneously. These preliminary experiments also verified that the total feeding tube line volume was as assumed.

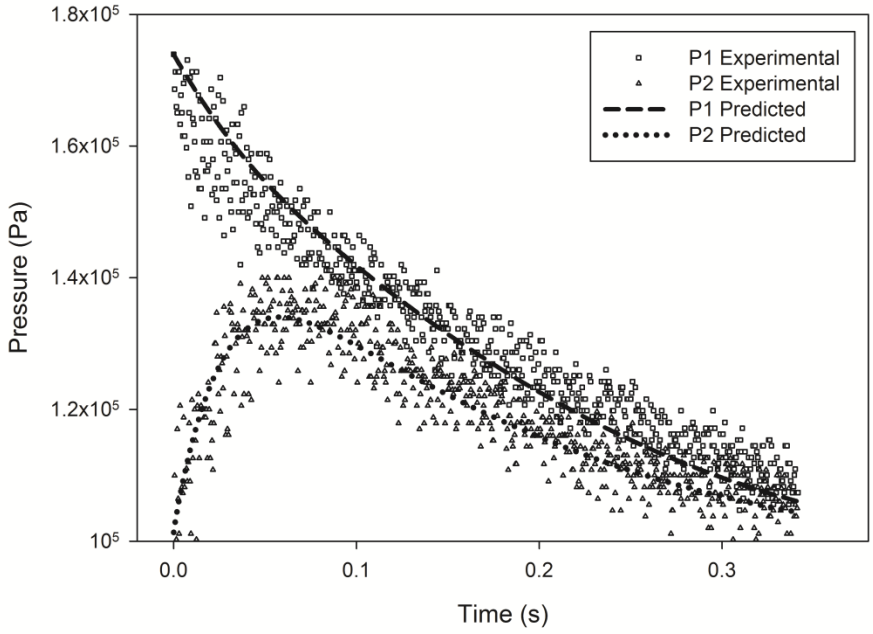

Figure 4-5: Pressure matching to find SV_3 flow coefficient for Large-Scale Feeder (knowing feeding tube tip orifice flow coefficient of 1.718 and no solids flow)

4.3.4.2 Scale-independent friction factor (ϕ_s) and Critical Pressure (ΔP_c) for DDG and MBM

As illustrated in [8] in more detail, laboratory-scale experiments were performed with DDG and MBM slugs at different conditions. In order to match the predicted slug position with the measured position from the laser data (and also ensure pressure matching and mass balance closure), a simple friction factor (λ_S) had to be considered, as shown in **Eqn. 10**. The average friction factor for DDG on the laboratory-scale feeder (0.0152 m i.d.) was found to be 0.58 m^3/s^2, and thus the scale-independent friction factor (φ_s) was 37.96 m^2/s^2 for DDG. The average friction factor for MBM on the laboratory-scale feeder (0.0152 m i.d.) was found to be 0.84 m^3/s^2, and thus the scale-independent friction factor (φ_s) was 54.80 m^2/s^2 for MBM.

By examining the P_2 pressure signals for DDG and MBM slugs, a shoulder was observed in the pressure rise (illustrated in **Fig. 4-6** for DDG) which was validated using lasers to correspond to the time that the slugs would overcome the static friction on the tube wall material and begin to move, and thus was an important input parameter for the model. As expected, the critical pressure was found not to change at different operating conditions or pulse pressures. Section 3.3.2 describes the procedure used to scale-up the critical pressures found on laboratory-scale feeder. In situations where the shoulder pressure cannot be observed during the laboratory-scale tests due to instrument noise, the critical pressure can also be approximated by using **Eqn. 10** and knowing the friction factor (setting the change in volume equal to zero and solving for P_2), as previously illustrated in [8] in the friction factor index that relates the friction factor to the shoulder pressure linearly. Future work on further building the friction factor index for more biomass feedstocks and validating the direct relationship between the friction factor and the critical pressure will be performed.

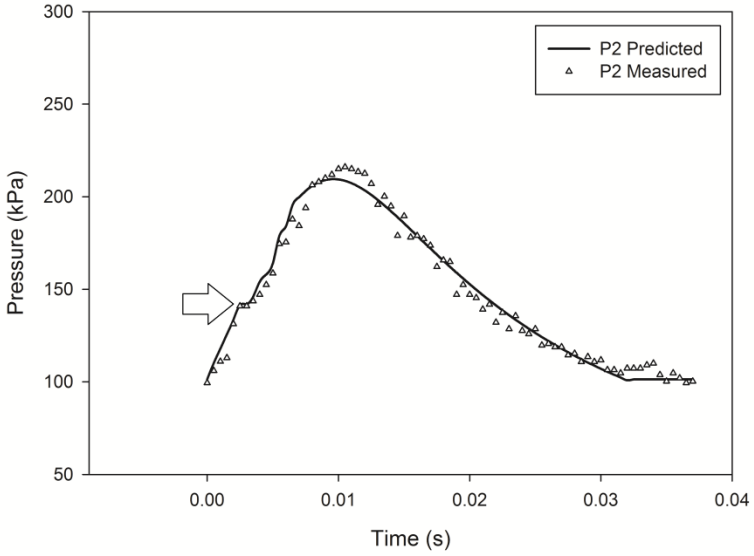

Figure 4-6: Critical Pressure (shoulder) in Pulse Pressure Signal for DDG Slug

4.3.5 Validation of Model on Large-Scale Feeder with DDG and MBM

Fig. 4-7 illustrates an example of the predicted and experimental pressure matching found for a pulse of one 0.150 kg DDG slug at 210 kPa. The scale-up equations were used to adjust the critical pressure value and friction factor for the larger feeder, based on the laboratory-scale experimental values found in [8]. The pulse SV_3 flow coefficient of 0.5 described previously was utilized and the solenoid valve was assumed to open instantaneously. Similarly to [8], the flow coefficient through the slugs was found to be zero, meaning that for the duration of the feeding tube pulse, there is a negligible leakage of gas past the slug at these high velocities. The scale-independent solids friction factor, φ_s, was 37.96 m^2/s^2 for the DDG. The predicted pressures matched the experimental pressures well, with a mass balance closure greater than 96.5% in all cases.

Fig. 4-8 illustrates the predicted position versus time results using the predictive model for DDG slugs at different pulse pressures. The points on the graph are the experimental values measured using the laser detection system, demonstrating the good fit between the model predictions and the experimental results.

The meat and bone meal residues were highly cohesive, as shown by the higher friction factor (**φ_s** = 54.80 m^2/s^2). **Figs. 4-9** and **4-10** demonstrate the validation of the predictive model for the meat and bone meal.

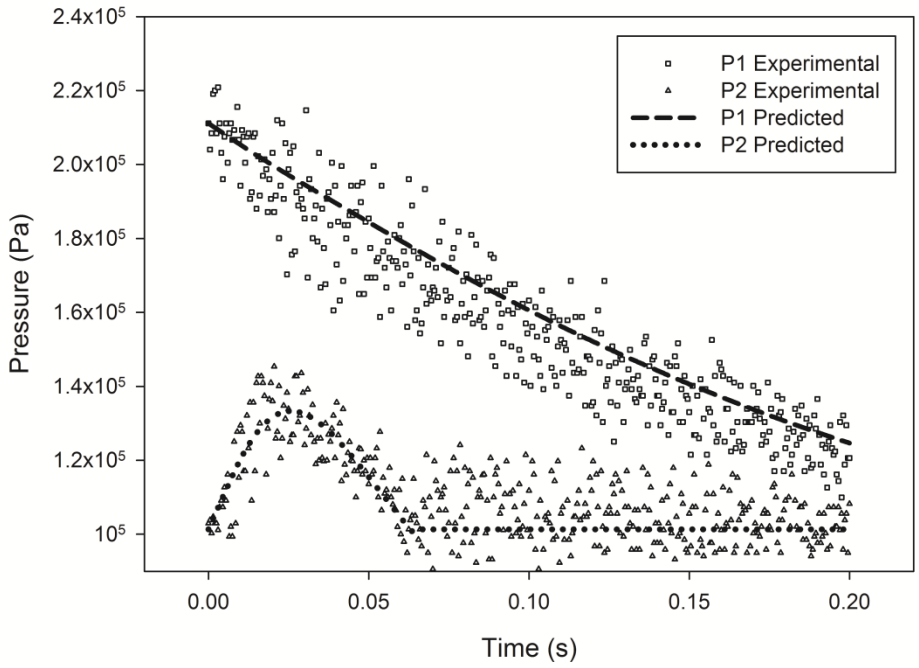

Figure 4-7: Predicted and Experimental Pressures of DDG Slug on Large-Scale Feeder (m_s = 0.150 kg, P_1 = 210 kPa, P_C = 130 kPa)

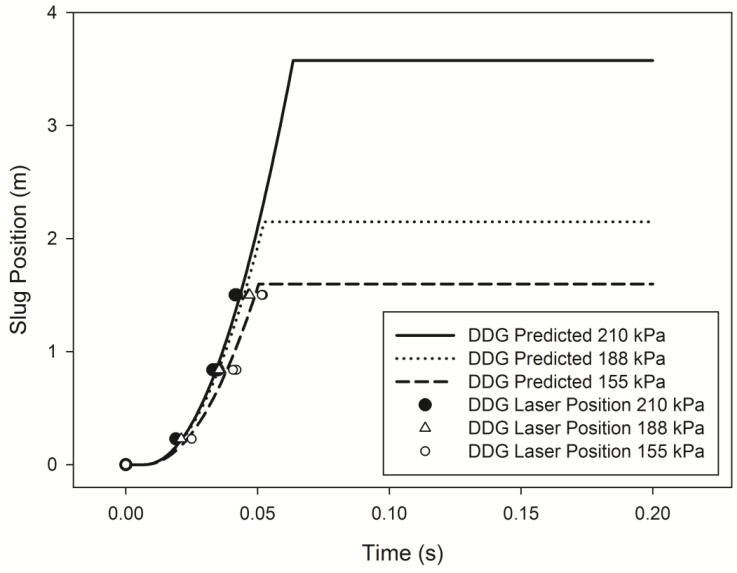

Figure 4-8: Large-Scale Feeder DDG Predictive Model (m_s = 0.150 kg, P_C = 130 kPa)

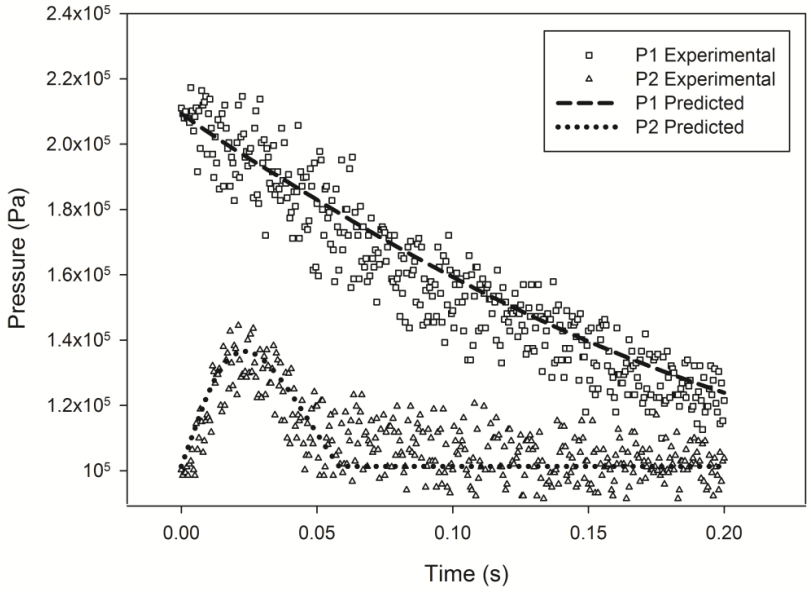

Figure 4-9: Predicted and Experimental Pressures of MBM Slug on Large-Scale Feeder (m_s = 0.130 kg, P_1 = 210 kPa, P_C = 122 kPa)

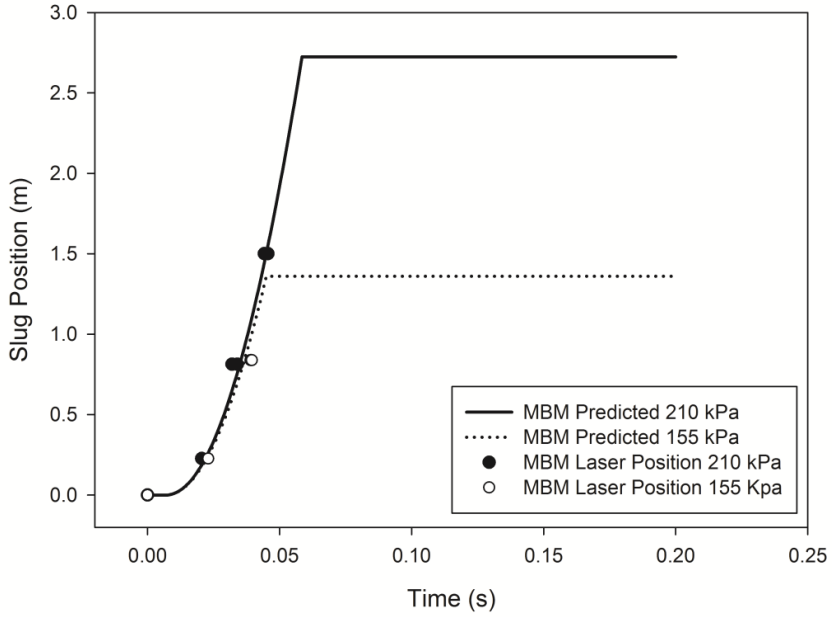

Figure 4-10: Large-Scale Feeder MBM Predictive Model (m_s = 0.130 kg, P_C = 122 kPa)

4.3.6 Slug Chamber Geometry Design Improvements & Design Procedure

By using the developed predictive model, one can input design parameters and compare the efficiency (mass of solids to mass of pulse gas ratio, m_s/m_g) of the feeder for different slug sizes (m_s). **Fig. 4-11** illustrates the laboratory-scale m_s/m_g vs. m_s curves for DDG, assuming a 1 m feeding tube length (L) and different typical compression pressures generated by industrial equipment (different levels of capital costs). The slug mass ranges utilized started at the minimum slug mass required to fill the cross-sectional area of the feeding tube (knowing the angle of repose of the DDG to be 44.4° and modelling the 3D slug shape, 1.2 g) and the maximum slug mass being the mass required to reach the critical length of the solids (18.8 g). The critical length of the solids

is equal to the inner diameter multiplied by the tangent of the angle of internal friction of the solids (α). Above this length, the slug of solids will be unable to move through the tube regardless of the force applied to it.

Centrifugal blowers can generate up to 136 kPa of pressure, Roots-type blowers can generate up to 205 kPa of pressure, and typical reciprocating-type compressors can typically generate 722 kPa or more (in our laboratory experiments throttled down to 377 kPa for safety precautions with clear PVC). In the case of the laboratory-scale feeder, the predictive model found that 136 kPa (centrifugal blower) was not capable of delivering the slug over the full 1 m feeding tube length, while all the other pressures worked. The higher pulse pressure utilized (and the higher the gas kinetic energy), the higher the m_s/m_g curves and peaks. The vertical grey lines represent the improvement from switching from the original "T" or small-angled slug chambers (generating slugs of about 6 g) to a specially designed slug chamber that could generating slugs of about 9.5 g. At the reciprocating compressor pulse pressure of 722 kPa, the m_s/m_g improved by a factor of 1.52 from the 6 g slug to the 9.5 g slug.

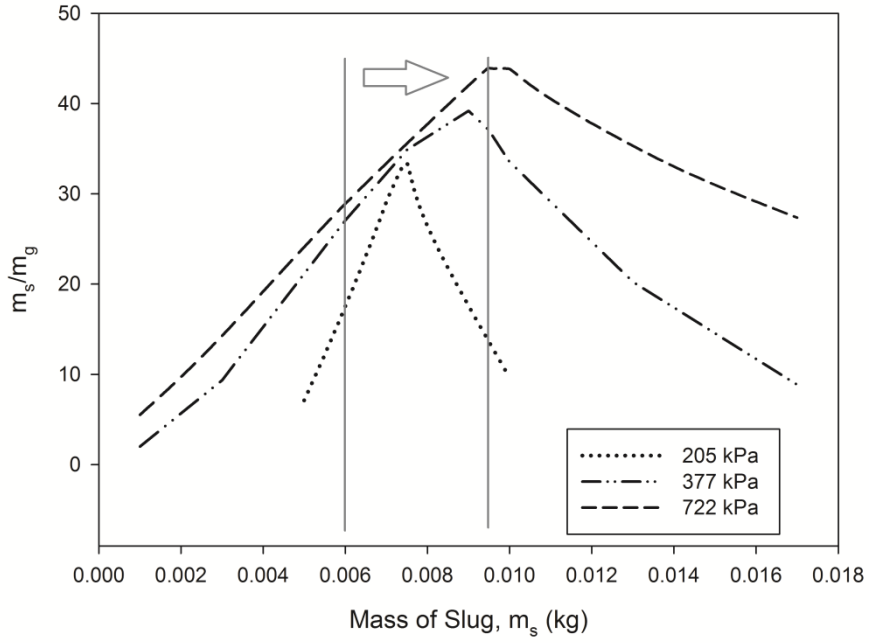

Figure 4-11: Predicted Laboratory-Scale Feeder m_s/m_g vs. m_s Performance Curves from Predictive Model (L = 1 m, D = 0.0153 m)

Therefore, in order to improve the performance of the feeder, one must be able to control the size of the slugs that are formed to be able to design the feeder to operate in the "sweet-spot" range where the ratio of solids-to-gas required to inject the slug is maximized. The upper end of the slug size is dictated by the critical length of the solids for the given tube size, which can be calculated by measuring the angle of internal friction of the solid materials. For DDG (used as the example in this section), the angle of internal friction was found to be 85.7°, which results in a laboratory-scale feeding tube critical length of 0.203 m. Knowing the bulk density of the solids from **Table 4-1**, the maximum critical slug mass was found to be 18.8 g for DDG.

As a result of the model predictions indicating the improvement potential of increasing the slug size, two new angled slug chambers were designed (#2 and #3 in **Fig. 4-2**) that could allow the solids to accumulate down the tube into a larger slug mass, with the aim to reach the 9.5 g size indicated in **Fig. 4-11**.

Fig. 4-12 illustrates the model results using the real experimental pressures obtained from testing for a DDG slug pulse (308 kPa) using the "T"-shaped slug chamber and the angled slug chamber (#1 and #2 slug chambers in **Fig. 4-2**, both were of the same volume). Therefore, no negative impact of using an angled slug chamber compared to the traditional "T"-shaped slug chamber was observed on the laboratory-scale feeder. The difference in the curves based on the area below the curve was found to be 0.64%.

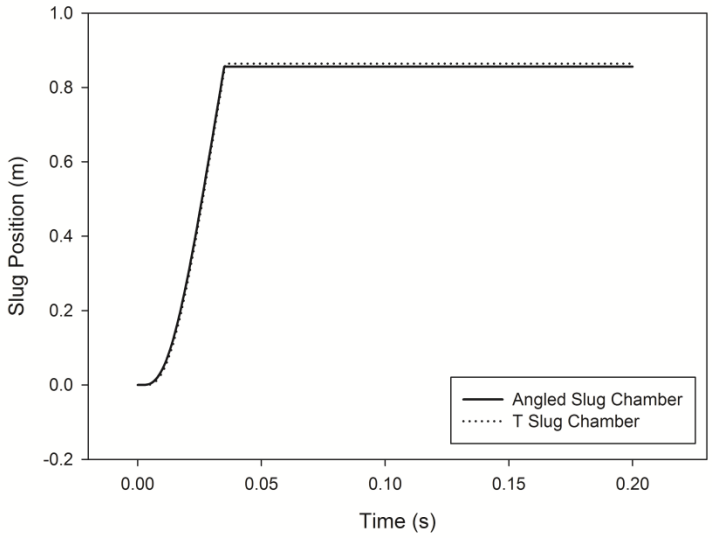

Figure 4-12: Predictive Model Difference between equivalent volume "T" and Angled Slug Chambers (6 g DDG slug and 308 kPa air pulse)

Therefore, by using a longer or shorter angled slug chamber, and while adjusting the pinch-valve opening time, one can control the slug size and mass for optimization purposes. As an experiment, the slug chamber design #3 in **Fig. 4-2** was designed to be significantly longer (178 mm compared to 50 mm) than the equivalent volume angled slug chamber, resulting in larger slugs (approximately 9.5 g compared to 6 g per slug), while keeping the overall cycle time the same. **Fig. 4-13** illustrates the increased feeding rate of DDG due to the longer angled slug chamber on the laboratory-scale feeder, compared to the "T" slug chamber and short-angled slug chamber (both equivalent). As a result, this long-angled slug chamber was able to achieve the optimized operation described in **Fig. 4-11**.

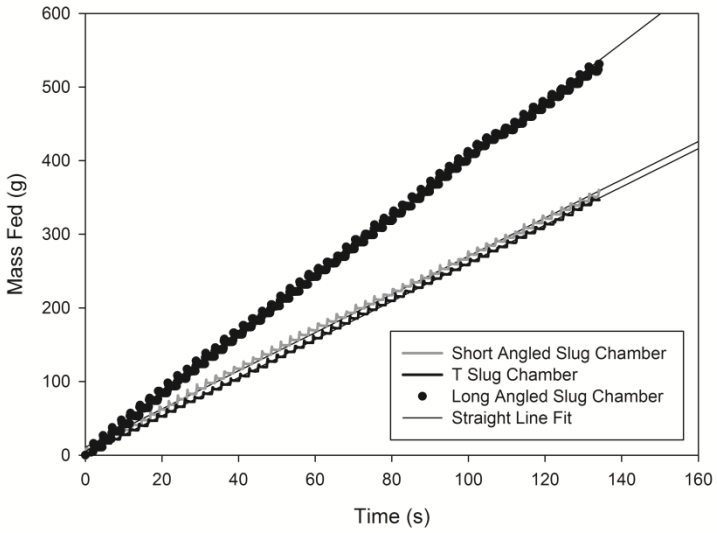

Figure 4-13: DDG Feeding Rates with Different Slug Chamber Designs (optimized 2.4 s cycle time)

This theory can thus also be applied to any biomass and any scale feeder, allowing for an optimized feeder design procedure. **Fig. 4-14** and **4-15** illustrate the predictive feeder performance curves for the same conditions as **Fig. 4-11** (1 m tube length at different pulse gas pressures depending on the standard industrial equipment selected), but for a 0.0267 m inner diameter feeder scale and for the large-scale (0.05113 m inner diameter feeder). As the feeder tube size increases, the maximum m_s/m_g obtained increases, due to the larger pressure contact area per unit mass of the slugs, relative to the surface contact area and friction. With the large-scale feeder (0.05113 m inner diameter) an m_s/m_g of over 100 was obtained at a slug mass around 0.26 kg. As a general rule, however, it is best to give a safety margin for the predictive model and operate the feeders to the left side of the peaks.

In all cases, it can be seen that above 250 kPa, the improvements in maximum m_s/m_g obtained are quite marginal, and therefore significant capital cost savings can be realized by utilizing medium compression systems such as a Roots-type blower. It also shows that large-scale feeders are more efficient than small-scale feeders.

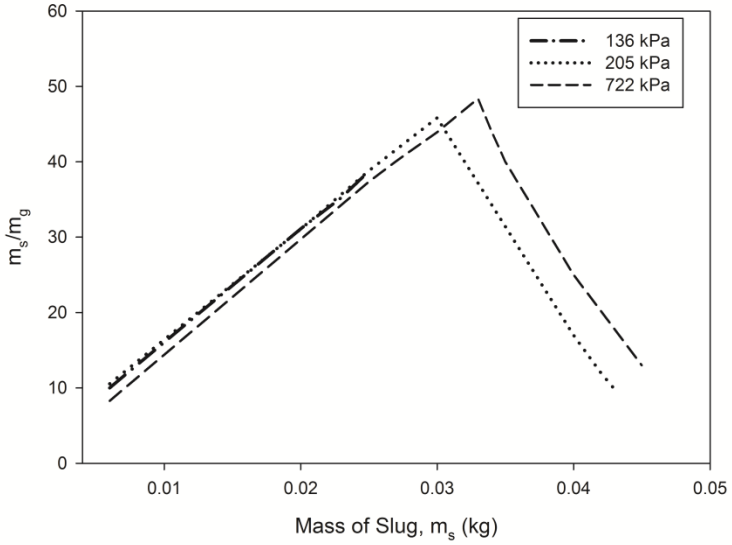

Figure 4-14: Predicted Medium-Sized Theoretical Feeder ms/mg vs. ms Performance Curves from Predictive Model (L = 1 m, D = 0.0267 m)

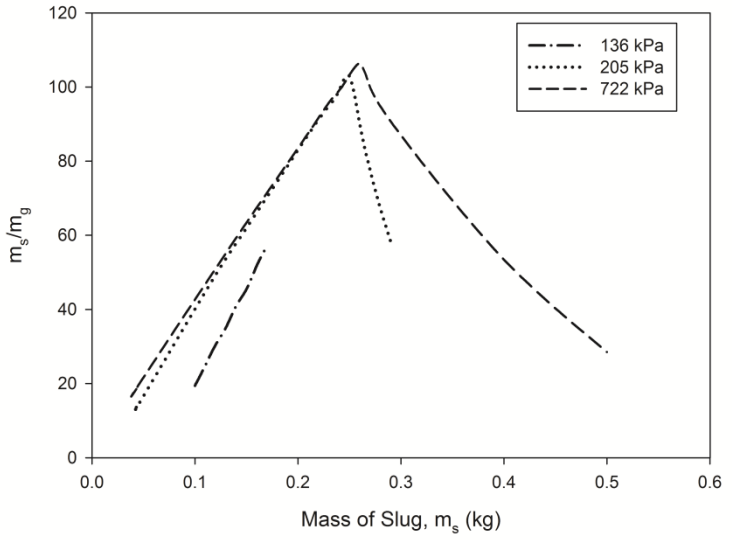

Figure 4-15: Predicted Large-Scale Feeder ms/mg vs. ms Performance Curves from Predictive Model (L = 1 m, D = 0.05113 m)

4.3.7 Additional Feeder Design Considerations

Thus far, using the predictive model, it has been shown that one can create various feeder performance curves of m_s/m_g versus the slug mass (m_s), for any given set of the following fixed parameters: feeding tube length (L), feeder inner diameter (D), material critical pressure for motion P_c (relative to the downstream or bed pressure), material friction factor (λ_s), and selected capacitance pressure (P_{UP}), which in turn sets the size of the capacitance volume (V_1). The bulk density, angle of repose and angle of internal friction are required to set the operation boundaries, used to determine the minimum slug size to fill the cross-sectional area of the feeding tube perfectly and also to ensure that the slug remains below the critical length.

The final element to consider is whether to utilize one large feeder at a given cycle time to meet the feeding rate requirement, or whether to utilize an array of smaller feeders. The feeder performance (maximum m_s/m_g obtained) has been shown to improve with feeder size, suggesting that one should utilize the largest feeder possible to meet the feeding rate requirement. However, from a mixing and reaction perspective, several feeders operating out of phase may be advantageous. Operating out of phase also could allow one to moderate the reactor pressure fluctuations resulting from the formation of product gas and vapours from the feeder pulse gas, which in turn could lead to improved fluidized bed stability and fewer vapour-loading related challenges in the condensation train. Further work on the effects of this type of feeding system on the reactor stability and on the condensation train is recommended.

4.4 Conclusions

The ICFAR intermittent solid slug feeder has been demonstrated to successfully feed temperature-sensitive, cohesive, and challenging residue feedstocks into fluidized bed pyrolysis reactors. In this study, the previously developed predictive feeder model has been validated with a significantly scaled-up feeder (from <20 kg/h to 250 kg/h). In addition, the application of the predictive model as a design tool has been described, allowing a user to develop an effective feeder for any given material and application, while being able to balance physical constraints with capital and energy efficiencies. Further work on the effects of the feeder on the fluidized bed reactor stability and on the condensation train is recommended.

4.5 Acknowledgements

The Authors wish to express their gratitude to the Natural Sciences and Engineering Research Council of Canada (NSERC), the NSERC Vanier Canada Graduate Scholarship program, Agri-Therm Inc. and Western University for the financial support of this research program.

4.6 Notation

Symbol	Units	Definition
A_{OR}	m^3	Orifice cross-sectional area
A	m^2	Cross-sectional area of tube/slug
C_V	--	Flow coefficient for Solenoid Valve 3 (SV_3)
D	m	Inner diameter of feeding tube
DDG	--	Dried Distillers' Grain
F	N	Friction force on slug
ICFAR	--	Institute for Chemicals and Fuels from Alternative Resources
k	--	C_p/C_v of the gas
L	m	Feeding tube length
L_s	m	Length of slug
M	kg/mol	Molecular weight
MBM	--	Meat and Bone Meal
$\dot{m}$	kg/s	Mass flowrate
m_s	kg	Mass of slug
P	Pa	Gas pressure
P_c	Pa	Critical pressure (absolute)
ΔP_c	Pa	Critical pressure difference to move slug
R	$Pa*m^3/mol*K$	Universal gas constant
SV_3	--	Solenoid Valve 3 (controls pulse)
T	K	Temperature
u	m/s	Velocity of slug
V	m^3	Volume
Y	--	Constant (defined in Eqn. 3)
λ_s	m^3/s^2	Empirical friction factor
φ_s	m^2/s^2	Scale-independent friction factor

4.7 References

[1] F. M. Berruti, K. Lenkiewicz, R. Xu, R. J. Bedmutha, S. Nova, F. Berruti, and C. L. Briens, "Novel Fluid Bed Pilot Plant for the Production of Bio-oil from Biomass through Fast Pyrolysis," *Récents Progrès en Génie des Procédés, Ed. SFGP, Paris, France, ISBN 2-910239-68-3*, no. 94, pp. 1–8, 2007.

[2] F. M. Berruti, L. Ferrante, C. L. Briens, and F. Berruti, "Pyrolysis of cohesive meat and bone meal in a bubbling fluidized bed with an intermittent solid slug feeder," *Journal of Analytical and Applied Pyrolysis*, vol. 94, pp. 153–162, Mar. 2012.

[3] R. A. Garcia, R. A. Flores, and C. E. Mazenko, "Factors contributing to the poor bulk behavior of meat and bone meal and methods for improving these behaviors.," *Bioresource Technology*, vol. 98, no. 15, pp. 2852–2858, Nov. 2007.

[4] P. Palmisano, F. M. Berruti, V. Lago, F. Berruti, and C. Briens, "Lignin Pyrolysis in a Fluidized Bed Reactor," *The International Conference on Thermochemical Biomass Conversion Science, Chicago, Illinois, USA*, 2011.

[5] E. Cascarosa, I. Fonts, J. M. Mesa, J. L. Sánchez, and J. Arauzo, "Characterization of the liquid and solid products obtained from the oxidative pyrolysis of meat and bone meal in a pilot-scale fluidised bed plant," *Fuel Processing Technology*, vol. 92, no. 10, pp. 1954–1962, Oct. 2011.

[6] D. Meier, B. Van De Beld, A. V Bridgwater, D. C. Elliott, A. Oasmaa, and F. Preto, "State-of-the-art of fast pyrolysis in IEA bioenergy member countries," vol. 20, pp. 619–641, 2013.

[7] M. O. Guedon, T. Baron, C. L. Briens, and T. M. Knowlton, "Intermittent injection of prepolymer in a pressurized fluidized bed," *Powder Technology*, no. 78, pp. 25–32, 1994.

[8] F. M. Berruti and C. L. Briens, "Novel intermittent solid slug feeder for fast pyrolysis reactors: fundamentals and modelling," *Powder Technology*, vol. Submitted, 2013.

[9] F. M. Berruti, L. Ferrante, F. Berruti, and C. L. Briens, “Optimization of an Intermittent Slug Injection System for Sawdust Biomass Pyrolysis,” *International Journal of Chemical Reactor Engineering*, vol. 7, 2009.

[10] R. B. Shah, M. a Tawakkul, and M. a Khan, “Comparative evaluation of flow for pharmaceutical powders and granules.,” *Aaps Pharmscitech*, vol. 9, no. 1, pp. 250–258, Jan. 2008.

[11] B. C. Hancock, K. E. Vukovinsky, B. Brolley, I. Grimsey, D. Hedden, A. Olsofsky, and R. a Doherty, “Development of a robust procedure for assessing powder flow using a commercial avalanche testing instrument.,” *Journal of Pharmaceutical and Biomedical Analysis*, vol. 35, no. 5, pp. 979–990, Sep. 2004.

[12] R. Bhadra, K. Muthukumarappan, and K. A. Rosentrater, “Flowability Properties of Commercial Distillers Dried Grains with Solubles (DDGS),” *Cereal Chemistry*, vol. 86, no. 2, pp. 170–180, 2009.

[13] G. Eriksson, “Residues from Biochemical Production of Transport Biofuels in Northern Europe,” Luleå University of Technology, Sweden, 2009.

[14] D. Geldart, N. Harnby, and A. C. Wong, “Fluidization of cohesive solids,” *Powder Technology*, no. 37, pp. 25–37, 1984.

[15] F. M. Berruti, L. Ferrante, F. Berruti, and C. Briens, “Optimization of an Intermittent Slug Injection System for Sawdust Biomass Pyrolysis,” *International Journal of Chemical Reactor Engineering*, vol. 7, 2009.

[16] “Agri-Therm Inc.,” 2013. [Online]. Available: www.agri-therm.com. [Accessed: 29-Jun-2013].

[17] J. Dai, H. Cui, J.R. Grace, “Biomass feeding for thermochemical reactors,” Progress in Energy and Combustion Science, 38, pp. 716-736, 2012.

Chapter 5

5 Chapter 5: Feed Preparation and Model for Convective Drying of Carrots for Pyrolysis[5]

5.1 Introduction

Biomass is a composite material made up of oxygen-containing organic components (cellulose, hemicellulose, lignin, organic extractives) and of inorganic minerals. It is a renewable and carbon dioxide neutral source of energy, essentially a form of stored solar energy captured through the process of photosynthesis by green plants. Fresh biomass, however, is not suitable for producing energy directly. The high moisture content and low energy density of the raw biomass (one-tenth of that of conventional liquid fuels) make it an uneconomical source of energy. However, after a certain extent of drying, biomass has been used as a combustion fuel for centuries. The convenience of handling, processing and utilizing liquid fuels has also prompted the development of technologies to transform solid biomass into liquids. For example, biomass can be converted through fast pyrolysis into a versatile and transportable liquid known as bio-oil, with an energy density five to six times higher than that of the raw biomass. In addition, fast pyrolysis produces valuable biochar and biogas [1].

---

[5] A version of this work has been published in the Journal of Food Engineering:

Berruti, F.M. Klaas, M., Briens, C., Berruti, F. (2009). Model for convective drying of carrots for pyrolysis, *Journal of Food Engineering* 92, 196-201, doi:10.1016/j.jfoodeng.2008.10.036

As introduced in Chapter 4, the novel ICFAR large-scale intermittent solid feeder is capable of handling and feeding large biomass particles (such as wood chips) into fluidized bed pyrolysis reactors. Feeding larger particles has the advantage of realizing significant savings due to lower grinding costs, and also simplified particle recovery equipment within the reactor. In addition, fine particle contamination of the bio-oil in the condensation train would be reduced. However, feeding larger particles also result in two challenges:

1) Heat transfer and rate limitations within the larger particle can result in lower bio-oil yields [1, 2].

2) The larger feed particles need to be dried for improved pyrolysis results and energy efficiency [3]. The drying of large particles is challenging due to mass and heat transfer limitations.

In order to process biomass using flash pyrolysis without wasting excessive energy, the moisture of the raw material needs to be minimized. Typically, the moisture content of the raw biomass varies between 50 and 60 wt%, and passive drying can reduce it to 30 wt%. Active or direct drying methods can reduce the moisture content further to 12–15 wt% [4]. Overall, the economics of the drying process, either due to energy consumption or required time, make biomass a difficult energy source to exploit. Consequently, it is very important to identify the best and most efficient technology to dry a given biomass material, by understanding the drying mechanism and characteristics of the material, prior to its liquefaction via fast pyrolysis.

Bio-oil can be made from a wide variety of forest and agricultural waste materials, including wood, sugar cane bagasse, rice hulls and straw, peanuts hulls, switchgrass, wheat straw, corn, tobacco stalks, coconut fibres and many others [5]. Other organic byproducts of the poultry industry (chicken litter), of the pulp and paper industry (lignin and sludge) and of the ethanol manufacturing (dry distillers' grains) are also excellent feedstocks [6, 7].

The carrot is a widely available vegetable, able to grow in most agricultural areas around the world. Due to its high vitamin and fibre content, the carrot is a common source for human nutrition and is grown and farmed extensively for this purpose. In 2006, the net world production of edible carrots, as a final product, was an estimated 27 million metric tons [8]. A final production of this magnitude, therefore, also produces an immense amount of carrot waste, mostly consisting of carrots that do not meet grocery or processing specifications and hence discarded. These carrots, through an economical drying and pyrolysis process, could produce a significant amount of bio-oil, which could be used for producing fuel, flavouring agents, or valuable chemicals.

This chapter will focus on the convective drying characteristics of carrots (unaltered, peeled or blanched), leading to the modelling and prediction of moisture diffusivity in varying temperature and dry air velocity conditions. The final goal of this work consists in creating a stable drying model, which can be effectively used to model and eventually optimize the drying of carrot residues. This model could then be further extended to apply to other types of biomass that display similar drying characteristics and

mechanisms. An additional reason for the selection of carrots for this study is that, in contrast to materials such as wood, the diffusivity of water through carrots, as with other types of organic residues, changes as the carrots dry.

5.2 Mathematical Modelling

Doymaz (2004) [9] investigated the convective air-drying characteristics of thin-layer carrots, and studied the effects of air temperature, air flowrate and sample thickness on the drying kinetics of carrots cubes. In addition, two mathematical models, the Page model and the Henderson and Pabis model [10], were used to predict the effective diffusivity of the carrot drying process [9]. However, both of these models suffer from two serious limitations:

- They do not take into account the external mass transfer limitation and can, therefore, only be applied to conditions where the drying gas velocity is very high. Such conditions are typically impractical and uneconomical.

- They assumed negligible shrinkage in the drying process, which was a point of contention in the work by Zielinska and Markowski [11]. These authors studied the drying behaviour of carrots dried in a spout-fluidized bed dryer. Although Zielinska and Markowski [11] observed similar trends to Doymaz [9] with respect to the effect of temperature and air flowrate on the carrot drying rates, they found slightly different values for their effective diffusivities. They argued that if shrinkage is taken into consideration, since it is typically very significant, the

diffusion path is shorter and the diffusion coefficient should be lower than that calculated when shrinkage is neglected.

Several other investigations reported in the literature dealing with the drying of foods products also suffered from the above limitations and did not consider shrinkage or external mass transfer limitations, such as convective drying of pumpkin slices [12], moisture diffusivity in pears [13], drying characteristics of hull-less pumpkin seeds (14), and convective hot air-drying of blanched yam slices (15).

Mulet [16-18] proposed three models of varying complexity to describe carrot drying using hot air. In these experiments, peeled 1 cm carrot cubes were exposed to different drying temperatures at air flowrates above 6000 kg/m_2 h, which they had found to be high enough to make the internal resistance much more important than the external resistance. The temperature throughout the carrot particle was also assumed to be uniform and was measured with a thin thermocouple. The conclusion of the experiments was that neglecting shrinkage would produce an underestimation of the test particle moisture content and that the most complex model, taking into account internal and external limitations, shrinkage and heat transfer produced a reasonable approximation for the drying of small cubic carrot particles at high air flowrates.

In addition, Bialobrzewski et al. [19] proposed a new drying model which takes internal and external limitations and nonhomogenous shrinkage of carrot cube samples into consideration. Although the model can be reasonably applied to describe the moisture content, temperature and deformation of drying carrot samples in a spouted drier, it is

also a very complicated solution, requiring software for finite element analysis and COMSOL MULTIPHYSICS software.

As a result of these limitations and complexity, a simpler, yet accurate model should be developed to take into account external and internal mass transfer limitations, as well as the considerable shrinkage experienced by the biomass material during drying, allowing for a simple and reliable evaluation of the effective moisture diffusivity within a drying biomass material. This model should also be able to predict the drying of carrots samples at lower air flowrates, more realistic for practical energy efficiency purposes when used as an upstream preparation process before fast pyrolysis. In addition, the model should be able to predict the drying of carrot samples that are not peeled and perfectly geometric, but rather realistic sample slices that could be easily prepared prior to an industrial drying process.

In a drying process, diffusion is the mechanism for the transport of moisture from the inside of an object to its surface, which is then followed by the mass transfer of the moisture via evaporation to the environment surrounding the object. There are many methods used to calculate drying diffusion, the most common being the solution of Fick's second law for a sphere, assuming that the moisture transport is primarily by diffusion with no external mass transfer limitation, that shrinkage is negligible, and that the diffusivity does not change with time and space [20].

$$\mathrm{MR} = \frac{m - m_\mathrm{e}}{m_0 - m_\mathrm{e}} = \frac{6}{\pi^2} \sum \frac{1}{n^2} \exp\left(-\frac{\pi^2 n^2 D_\mathrm{eff} t}{r^2}\right)$$

Equation 5.1

where m, m_0 and m_e are the instantaneous, initial and equilibrium moisture contents on a dry basis, respectively, r is the volume equivalent radius, t is the time and D_{eff} is the effective diffusivity (m^2/s). The equilibrium moisture content (m_e) was determined by performing a very long experimental run and finding the dry basis at which the carrot sample could not be dried further within the operating conditions. The assumption that the sample is a sphere can be roughly applied in the case of small cylindrical samples as well, using the volume equivalent radius in the equation, since the moisture is basically lost in all directions of the cylinder rather than just along the axis. However, the carrot samples do experience significant shrinkage; therefore, to take this into account, it was necessary to consider the effect of changing radius on the calculated diffusivity.

One of the models considered in this work is the Henderson and Pabis model [9], which is simply the first term of the general series expansion of Fick's second law, since the subsequent terms were found to be negligible [10].

$$\mathrm{MR} = \frac{m - m_e}{m_0 - m_e} = \frac{6}{\pi^2} \exp\left(-\frac{\pi^2 D_{\mathrm{eff}} t}{r^2}\right)$$

Equation 5.2

Since the values of m_e are very small compared to m or m_0, Eq. (5.2) can be simplified to:

$$\mathrm{MR} = \frac{m}{m_0} = k \exp(-ct)$$

Equation 5.3

where $k = \frac{6}{\pi^2}$ and $c = \frac{\pi^2 * D_{eff}}{r^2}$.

Therefore, by plotting $\ln(m/m_0)$ vs t, and given that k is known, it is possible to calculate the effective diffusivity (D_{eff}). However, this model does not allow for consideration of external mass transfer limitations, and can only be used to compare experimental values obtained to experiments performed in the literature.

In order to investigate and model the more practical case of a significant external mass transfer limitation, the following equation derived for the surface evaporation in a plane sheet was used as a good approximation for a thin-sliced cylindrical carrot sample [20].

$$\frac{C - C_2}{C_0 - C_2} = 1 - \sum_{n=1}^{\infty} \frac{2L \cos(\beta_n x/L) \exp(-\beta_n^2 Dt/l^2)}{(\beta_n^2 + L^2 + L)\cos\beta_n}$$

Equation 5.4

where D is the diffusivity, x is between negative l and positive l (i.e. l is half the thickness of the plane sheet), L = lα/D, where α is a computational parameter defined as

$$-D\frac{\delta C}{\delta x} = \alpha(C_0 - C_s)$$

Equation 5.5

The β_n values are the positive roots of $\beta\tan\beta = L$, C is the concentration at any given location x in the profile, C_0 is the concentration required to maintain equilibrium with the surrounding atmosphere, C_2 is the initial uniform concentration and C_S is the actual concentration just within the sheet. It should be noted that if an entire carrot is to be dried, Eq. (5.4) should be altered to the surface evaporation of a finite cylinder, since this equation would better represent the physics of the sample. In this case, a plane sheet was used, as a thin-sliced carrot cylinder behaves more similarly to a plane sheet than a finite cylinder.

In order to use this equation, a computational model was created in MS Excel, using the solver operation and a programmed Visual Basic module to reduce the square of the errors between the measured evolution of the volume-averaged moisture to that predicted by the model, by changing the diffusivity (D), the mass transfer coefficient (k_y), or both simultaneously. Eq. (5.4) was integrated over the drying body in order to determine volume-averaged moisture content over the entire solid. Once solved, the model was stabilized by using the assumption that the diffusivity is affected by temperature, but should be independent of air speed, and that the mass transfer coefficient was the opposite. The mass transfer coefficient was correlated using a power law with respect to the air speed, in order to predict its value at the higher air speeds, whereas the value of the diffusivity was fixed for the changing air speeds at the same temperature. In addition, several constraints were added to the minimization solver calculation to increase the stability of the model. For example, it was assumed that the mass transfer coefficient (k_y) must always be greater than zero and a minimum diffusion

value was inserted as a constraint, solved from the following equation for the diffusion from a slab in the absence of external mass transfer limitation [20].

$$\frac{C - C_2}{C_0 - C_2} = \frac{8}{\pi^2}\left(e^{-Dt\pi^2/4b^2} + \frac{1}{9}e^{-9Dt\pi^2/4b^2} + \frac{1}{25}e^{-25Dt\pi^2/4b^2} + \ldots\right)$$

Equation 5.6

where D is the diffusivity, t is time and b is half the thickness of the carrot sample. C_0 is the initial concentration of solute throughout the slab, C is the concentration at any given time, t and C_2 is the concentration at infinite time.

In order to take shrinkage into account in this model, a new modification to the mass transfer flux equations is postulated in this paper, to then be tested experimentally, to obtain a reasonable approximation of the effect of shrinkage on the drying process.

The flux of water within a slab can be described as

$$F = -D\frac{dX}{dx}$$

Equation 5.7

where F is the flux, D is the diffusivity, X is mass of water per mass of dry solid and x is the position coordinate within the slab. Substituting a dimensionless value y, defined as x/l gives

$$F = -D\frac{dX}{dy}l$$

Equation 5.8

where l is half the thickness of the slab at any time (t). An assumption can be made that the relative reference position of dry material (η) within the slab will remain the same through the drying process, giving

$$y = \frac{x}{l} = \eta = \frac{x_0}{l_0}$$

Equation 5.9

where x_0 and l_0 are the initial position and initial thickness of the slab, respectively. In order to describe the idea that, as the carrot material dries, it becomes denser, decreasing the diffusivity, it can be assumed that the product of the diffusivity at any given time (t) by the thickness at that time (t), is constant, giving

$$Dl = D_{\text{eff}}l_0$$

Equation 5.10

where D_{eff} is the diffusivity at t = 0.

By substituting Eqs. (5.9) and (5.10) into Eq. (5.8), a much simplified equation is proposed (Eq. (5.11)), which will be investigated in this chapter to prove that it gives a

reasonable and accurate evaluation of the effective diffusivity within a carrot slab, while taking shrinkage into account.

$$F = -D_{\text{eff}} \frac{dX}{d\eta} l_0$$

Equation 5.11

5.3 Materials and Methods

In order to investigate the process of diffusion of moisture through carrot samples, drying experiments have been performed in a Plexiglas® tunnel dryer. The dryer consisted of a hollow rectangular prism tunnel (25.6 x 12.7 cm) equipped with a controlled air supply and with a removable hatch opening to insert or remove the carrots. Upstream of the tunnel an electric air heater was used to heat up part of the air before entering the tunnel. A bypass pipe, equipped with a ball valve, was used to control the downstream temperature by adjusting the air flowrates through the heated pipes and the non-heated bypass section. Upstream of the heater, a calibrated 7/32" sonic nozzle allowed for the control of the air flowrate into the tunnel, using a pressure regulator and an accurate pressure transducer.

Carrots purchased from a local grocery store and stored in a refrigerator at 4°C were used in the experiments. At the start of each experiment the carrots were cut into three cylinders (three pieces from each carrot) having a diameter of 2.2 cm and a height of 1.3 cm, resulting in a volume equivalent diameter of 2.11 cm. Next, for each experiment, one of the cylinders was blanched in 100°C water for 5 min, immediately cooled in 10°C

water and then patted dry with a paper towel. One cylinder was peeled using a kitchen knife, and a third was left unaltered. The three samples were then placed in respective rotating gear holders and the air flow was turned on and adjusted to the desired flowrate and temperature. Three air temperatures of 21, 42, and 56°C were used for different runs. The change in mass, due to the drying, was measured on a balance at regular 20 min time intervals at the beginning of the run, and then at longer intervals (hours to several hours) later on in the run, to obtain the final equilibrium moisture content values. The carrot cylinders were deemed dry and at their equilibrium moisture level when the moisture content reached an asymptotic value corresponding to 8% (w/w) from an initial value of 88% (w/w). The dry carrot samples were then stored in plastic containers in a refrigerator at 4°C.

5.4 Results and Discussion

Drying experiments were performed at 0.5, 0.625, 0.75 and 0.95 m/s, at 21, 42 and 56°C, for blanched, peeled and unaltered carrot samples. After performing the set of runs, the moisture ratio (m/m_0) was plotted against time, allowing for the derivative to be calculated to determine the drying rate plots at all conditions using Matlab r2007a. **Figs. 5-1** and **5-2** illustrate examples of the variation of the moisture ratio with time for the unaltered carrot samples.

In general, all plots show a decrease in moisture ratio with increases in air velocity and temperature, which shows that there is a significant external mass transfer limitation.

This means that the model from Henderson and Pabis [10] would be inaccurate and not applicable to this case.

Fig. 5-3 illustrates the drying rate vs. time of peeled, unaltered and blanched samples at 21°C and at an air speed of 0.5 m/s. The fastest drying rate occurs in the case of the peeled sample, while the blanched and unaltered carrot samples follow similar rates. However, after about 1000 min, the peeled and unaltered samples plateau at approximately the same drying rate, while the blanched sample falls to a lower drying rate. A similar trend is observed in all other rate experiments. In **Fig. 5-4** the results show clearly that the higher air speeds result in higher drying rates. **Fig. 5-5** illustrates the drying rate vs. time for an unaltered carrot sample at an air speed of 0.95 m/s and at different air temperatures. Apart from the fact that the fastest drying rate is observed for the test at 42°C at the beginning of the run, it appears that, overall, the higher the temperature, the higher the drying rate: this phenomenon cannot be explained by changes in the external mass transfer coefficient and, therefore, it must be caused by changes in the diffusivity of water through the carrots. This suggests that internal and external mass transfer limitations are both significant.

To investigate more thoroughly the characteristics of the drying process, the drying rate is plotted against solid moisture content in **Fig. 5-6**.

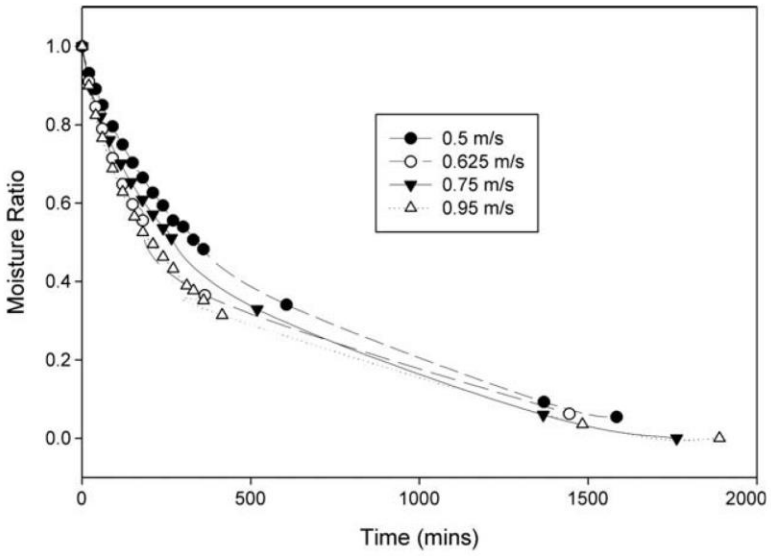

Figure 5-1: Variation of moisture ratio of unaltered carrot cylinders drying under different air speeds at 21°C

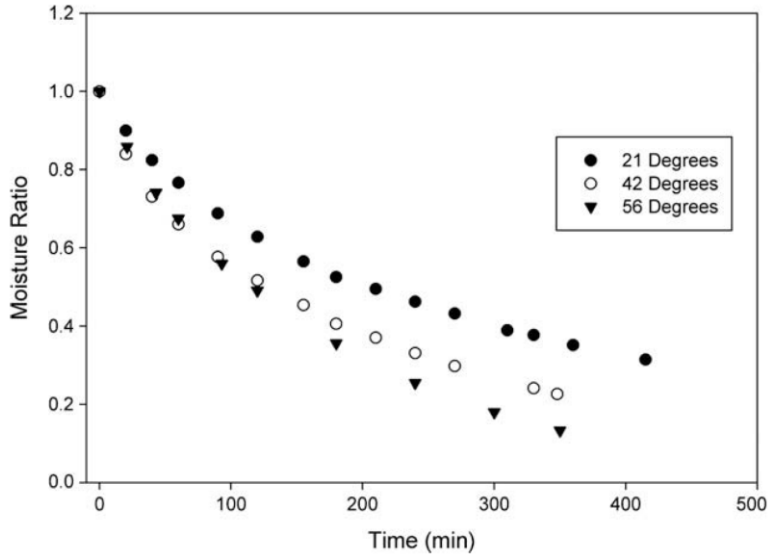

Figure 5-2: Variation of moisture ratio of unaltered carrot cylinders drying under different temperatures at 0.95 m/s

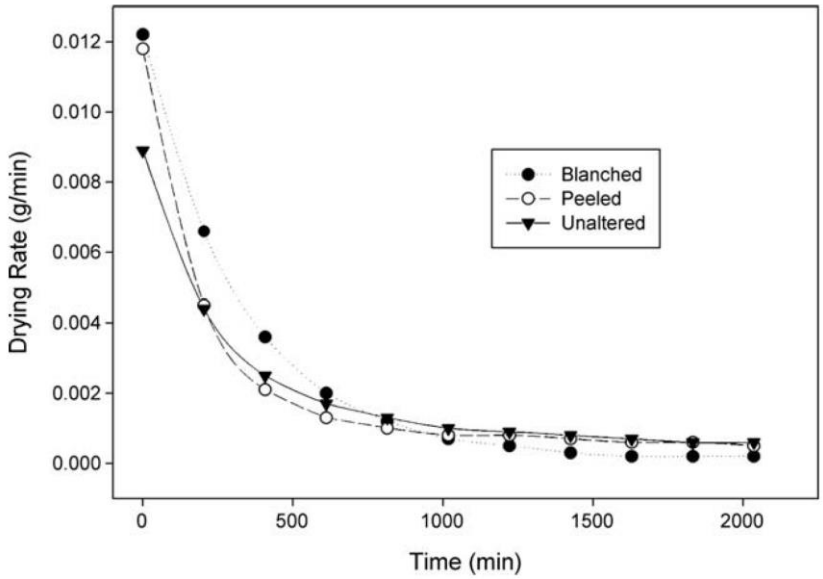

Figure 5-3: Variation of drying rate of carrot cylinders for different carrot preparations at 21°C and 0.5 m/s

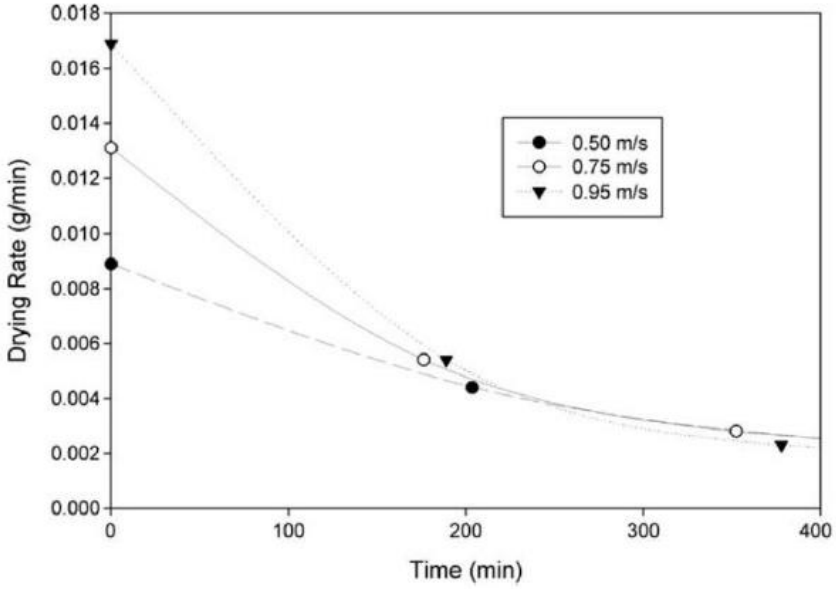

Figure 5-4: Variation of drying rate of carrot cylinders for unaltered carrots at different air speeds at 21°C

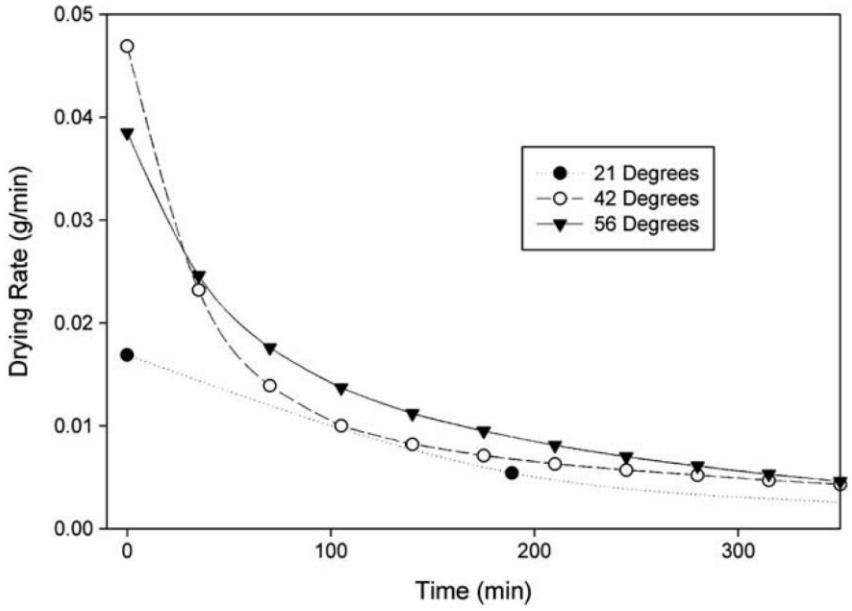

Figure 5-5: Variation of drying rate of carrot cylinders for unaltered carrots at different temperatures and 0.95 m/s

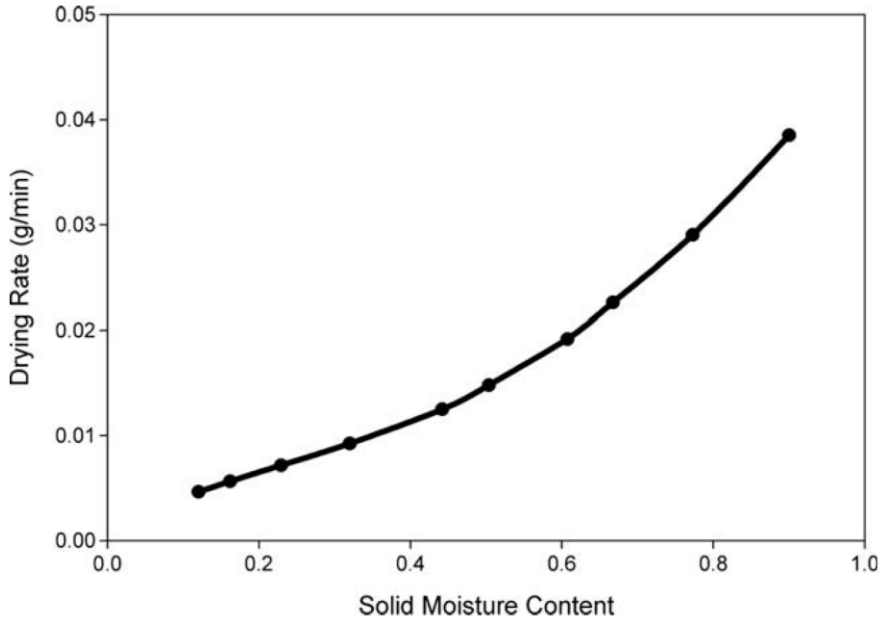

Figure 5-6: Drying rate vs. solid moisture content at 56°C and 0.95 m/s.

It can be seen in **Fig. 5-6** that the drying is always in the falling rate period and that there is no constant drying rate period for the drying of carrot samples. This confirms that internal mass transfer resistance is significant.

Although the Henderson and Pabis model (Eq. 5.3) cannot take external mass transfer limitations into consideration, it was used to determine the effective diffusivity (D_{eff}) of the moisture through the carrot samples, for reference purposes. Solving for D_{eff}, the natural logarithm of the moisture ratio is plotted against time and fitted with a linear relation.

From Eq. (5.3) the slopes of the natural logarithm lines formed are equal to:

$$\frac{\pi^2 * D_{\text{eff}}}{r^2}$$

Equation 5.12

and, consequently, D_{eff} can be easily be calculated. The R^2 values of the plots for all runs are above 0.970. **Table 5-1** illustrates the calculated initial values for effective diffusivity of all performed experiments. The values found for the blanched carrot diffusivities are reasonably consistent with those found by Doymaz [9] and Zielinska and Markowski [11].

Table 5-1: Summary of calculated initial effective diffusivities for all experiments using the Henderson and Pabis model

Temperature (°C)	Air speed (m/s)	Unaltered diffusivity (10^{-9} m^2/s)	Peeled diffusivity (10^{-9} m^2/s)	Blanched diffusivity (10^{-9} m^2/s)
21	0.5	0.316	0.324	0.448
21	0.625	0.346	0.311	0.548
21	0.75	0.372	0.387	0.709
21	0.95	0.397	0.409	0.512
42	0.95	0.790	1.079	1.519
56	0.95	1.046	1.363	1.285

In order to take external mass transfer limitations into consideration, as well as the significant shrinkage which occurs in the carrot samples, a model other than the Henderson–Pabis model must be used. The Crank model for the surface evaporation of a plane sheet (Eq. 5.4), described in the introduction, is used to create a computational model for the unaltered carrot samples. Using this model, the square of the errors of the differences in concentration found at any given time (t) are minimized using the MS Excel solver and a programmed Visual Basic module, by changing the diffusivity (D) and mass transfer coefficient (k_y). **Table 5-2** illustrates the results.

Table 5-2: Summary of results provided by the Crank computational model

Temperature °C	Air speed (m/s)	k_y (mol/m^{2}s)	Diffusivity (10^{-9} m^2/s)	Error^2
21	0.5	0.000798	0.558	0.0384
21	0.625	0.000888	0.558	0.00730
21	0.75	0.00879	0.558	0.0132
21	0.95	0.01406	0.652	0.00532
42	0.95	0.01588	1.401	0.00315
56	0.95	0.01588	2.312	0.0375

The effect of temperature on diffusivity values can be described using the Arrhenius relationship,

$$D = D_0 \exp\left(-\frac{E_a}{\mathrm{RT}}\right)$$

Equation 5.13

where D_0 is the constant diffusivity basis (m^2/s), E_a is the activation energy (kJ/mol), T is the air temperature (K) and R is the universal gas constant (kJ/mol K). The plot of the Arrhenius relationships using the data in **Table 5-2**, having taken the average diffusivity for the values at 21°C, is illustrated in **Fig. 5-7**. The relation has an R^2 value of 0.99999 indicating a very close fit of the experimental data using the Arrhenius relationship. From the slope of the line described in Eq. 5.12, the activation energy, E_a, was calculated to be 31.76 kJ/mol, which is very close to other drying activation energies for various foods found in the literature [9]. Due to the close fit of the relationship between diffusivity and temperature, diffusivity values in the Crank computational model were fixed at constant temperatures to further stabilize the model, as long as all other physical constraints were met (see Eq. 5.6).

The Crank computational model was able to effectively and accurately predict the mass transfer coefficients (k_y) and diffusivities for all unaltered carrot sample experiments, with all error squared values being below 4%. Given the low errors, it can be assumed that the simplification proposed to the general mass transfer equations (Eq. 5.11) gave a very reasonable approximation for the consideration of shrinkage in the Crank computational model. Overall, the trend of increasing mass transfer coefficient with

increasing air speed, and increasing diffusivity with increasing temperature is confirmed by the Crank computational model.

It is interesting to note that the k_y values obtained from the Crank model were always considerably smaller than the k_y values obtained from the Frossling correlation [21]. Although the models did not provide the same k_y values, the values obtained from both methods deviated less as air speed was increased. This infers that the models may converge to similar k_y values at higher air speed and also infers that either the Crank model or the Frossling correlation may not be suitable for low air superficial velocity situations.

5.5 Conclusion

The effects of air temperature and air flowrate on the drying of blanched, peeled or unaltered carrot cylinder samples in a drying tunnel were successfully investigated and modelled. A new and simple model, based on the Crank computational model, has been proposed that effectively allows the shrinkage and internal and external mass transfer limitations to be considered in order to give a very reasonable prediction of the diffusivity and mass transfer coefficient of biomass samples during drying. Overall it was found that the mass transfer coefficient increases with increasing air speed, and that diffusivity increases with temperature, as expected. The activation energy for moisture diffusion was found to be 31.76 kJ/ mol, which is comparable to values found in literature for the drying of various foods. The developed Crank computational model should be utilized further for the purpose of understanding the drying characteristics of

several types of biomass, potentially leading to the development of intense drying techniques for the biomass, which can then be employed upstream of pyrolysis reactors.

5.6 Acknowledgements

The authors wish to express their gratitude to Dr. Lauren Briens for her gracious assistance and permission to utilize and modify her lab equipment. A special thanks to William Brennan for the helpful discussions and assistance with the lab equipment.

The financial support for our research from the Natural Sciences and Engineering Research Council of Canada (NSERC) is gratefully acknowledged.

5.7 References

[1] Bridgwater, A.V., Czernik, S., Piskorz, J., 2001. Progress in Thermochemical Biomass Conversion. Bridgewater, A.V. (Ed).

[2] Alcala, A., Bridgwater, A.V. 2013. Review and upgrading fast pyrolysis liquids. Fuel. 10.1016/j.fuel.2013.02.058.

[3] Klaas, M. 2011. Investigating Potential Pathways to Optimize the Effectiveness of the Pyrolysis Process. The University of Western Ontario Thesis.

[4] Demirbas, A.J., 2004. Journal of Analytical and Applied Pyrolysis 71, 803.

[5] Mohan, D., Pittman Jr., C.U., Steele, P.H., 2006. Energy and Fuels 20, 848.

[6] Berruti, F.M., Lenkiewicz, K., Xu, R., Bedmutha, R.J., Nova, S., Berruti, F., Briens, C., 2007. Novel fluid bed pilot plant for the production of bio-oil from biomass through fast pyrolysis. Récents progrès en génie des procédés, numéro 94. ISBN 2–910239-68–3. Ed. SFGP, Paris, France.

[7] F. M. Berruti, L. Ferrante, C. L. Briens, and F. Berruti, "Pyrolysis of cohesive meat and bone meal in a bubbling fluidized bed with an intermittent solid slug feeder," Journal of Analytical and Applied Pyrolysis, vol. 94, pp. 153–162, Mar. 2012.

[8] Brunke, H., 2006. Commodity Profile: Carrots. Agricultural Issues Centre, University of California. Agricultural Marketing Resource Centre.

[9] Doymaz, I., 2004. Convective air-drying characteristics of thin-layer carrots. Journal of Food Engineering 61, 359–364.

[10] Henderson, S.M., Pabis, S., 1961. Grain drying theory I: temperature effect on drying coefficient. Journal of Agricultural Research Engineering 7, 85–89.

[11] Zielinska, M., Markowski, M., 2007. Drying behaviour of carrots dried in a spout fluidized bed dryer. Drying Technology 25, 261–270.

[12] Doymaz, I., 2007. The kinetics of forced convective air-drying of pumpkin slices. Journal of Food Engineering 79, 243–248.

[13] Guiné, R.P.F., 2006. Moisture diffusivity in pears: experimental determination and derivation of a mathematical prediction model. International Journal of Food Science and Technology 41, 1177–1181.

[14] Sacilik, K., 2007. Effect of drying methods on thin-layer drying characteristics of hull-less seed pumpkin. Journal of Food Engineering 79, 23–30.

[15] Sobulkola, O.P., Dairo, O.U., Odunewu, A.V., 2008. Convective hot air-drying of blanched yam slices. International Journal of Food Science and Technology 43, 1233–1238.

[16] Mulet, A., Berna, A., Rossello, C., 1989a. Drying of carrots I. Drying models. Drying Technology 7 (3), 537–557.

[17] Mulet, A., Berna, A., Rossello, C., Pinaga, F., 1989b. Drying of carrots II. Evaluation of drying models. Drying Technology 7 (4), 641–661.

[18] Mulet, A., 1994. Drying modelling of water diffusivity in carrots and potatoes. Journal of Food Engineering 22, 329–348.

[19] Bialobrzewski, I., Zielinska, M., Mujumdar, A.S., Markowski, M., 2008. Heat and mass transfer during drying of a bed of shrinking particles – simulation for carrot cubes dried in a spout-fluidized-bed drier. International Journal of Heat and Mass Transfer 51, 4704–4716.

[20] Crank, J., 1975. The Mathematics of Diffusion, second ed. Oxford University Press.

[21] Briens, L., Briens, C., 2008. Mass Transfer Operations: Course Notes. The University of Western Ontario (Chapter: 1–3, 7).

Chapter 6

6 Chapter 6: Pyrolysis of Cohesive Meat and Bone Meal Residues in a Laboratory-Scale Bubbling Fluidized Bed Reactor using an Intermittent Solid Slug Feeder[6]

6.1 Introduction

This chapter demonstrates the application of the ICFAR novel intermittent solid slug feeder for the conveying and first fast pyrolysis of meat and bone meal residues study in industrially relevant equipment.

The presence of bovine spongiform encephalopathy (BSE) in meat and bone meal (MBM) residues, which can cause the devastating 'Creutzfeldt-Jacob disease (vCJD)' in cattle and humans, has led to a complete ban of the use of MBM in animal feed and a need for safe disposal techniques for the millions of tonnes of MBM that are produced annually world-wide [1].

The prions that cause BSE pathogens can be destroyed by rapid combustion in incinerators at 850 °C for at least 2 s, or at 133 °C for 20 min under 3 bar of pressure [2]. In England and Belgium, many incineration plants are operated to destroy the pathogens in MBM, in cases where there is sufficient MBM supply to justify continuous operation, while in Canada and the United States, MBM is processed in cement kilns [3].

---

[6] A version of this work has been published in the Journal of Analytical and Applied Pyrolysis:

Berruti, F.M., Ferrante, L., Briens, C., Berruti, F. (2012). Pyrolysis of Cohesive Meat and Bone Meal in a Bubbling Fluidized Bed with an Intermittent Solid Slug Feeder. *Journal of Analytical and Applied Pyrolysis* 94, 153-162, doi:10.1016/j.jaap.2011.12.003

In Canada, landfill disposal is also an accepted means of disposal, according to the Canadian Food Inspection Agency (CFIA), but tight regulations and inspections are resulting in thermal combustion treatments becoming the prevalent method for safe disposal [1]. Although these high temperature techniques are functional, there are serious operational issues associated with (a) the feeding of cohesive and temperature sensitive MBM [2,4], (b) ash stickiness and agglomeration [1,2], (c) the need to co-process the MBM with other material such as peat [5] or coal [6] to ensure proper combustion, and (d) long-term equipment fouling due to the high MBM ash content (approximately 20–40 wt%). In addition, many incineration and cement kiln processes result in low-grade heat recovery from the combustion products, while also producing hazardous dioxins and furans at elevated temperatures [1]. As a result of these limitations, there is still an industrial need for improved safe-disposal methods that can lead to the generation of high-value products or chemicals and fuels with high-quality combustion potential that can be transported.

MBM has a calorific value of approximately 17–20 MJ/kg and contains a large amount of fats and organic compounds, making it an attractive material for energy recovery processes such as pyrolysis [1,7,8]. Pyrolysis is defined as the thermo-chemical decomposition of materials in the absence of oxygen, which can result in the production of a transportable and workable bio-oil liquid fuel, which is a source for specialty chemicals and pharmaceuticals, flavoring agents, fuel for combustion in turbines to generate electricity or an intermediate for subsequent conversion to synthesis gas, from which clean fuels and chemicals can be produced. Pyrolysis by-products include (i) a

solid called bio-char, which can be used as a fertilizer, fuel source, coke substitute for metallurgical applications, and as carbon-sequestering soil additive and adsorbent; and (ii) a combustible product gas, which can be recycled into the process to provide the energy required for the pyrolysis reactions. However, there is virtually no data available in the literature on fundamental MBM pyrolysis studies under continuous feeding operation [8], and, more specifically, no studies in a bubbling fluidized bed reactor, which is one of the most practical pyrolysis reactors due to its superior heat transfer and mixing capabilities (which help break apart the feedstock), scalability (most common industrial heavy-oil upgrading reactor), simplicity (no moving parts), relatively low capital, operating and energy expense, and relatively low temperature and gas/solid ratio [9].

Chaala and Roy [7] used a vacuum pyrolysis reactor system to convert MBM to valuable products. The experiment was performed at 500 °C (claimed to be the best pyrolysis condition) with a heating rate of 15°C/min and they produced a combustible product gas with a lower heating value (LHV) of 12.9 MJ/kg and a bio-oil with a high heating value (HHV) of 34.2 MJ/kg. They obtained product yields of 39 wt% solid bio-char, 9.4 wt% combustible gases and 48.7% wt% liquids (including both organic and aqueous phases, which represented 37.1% and 11.6% respectively). They also analyzed their char and found that it was quite rich in minerals. The small aqueous phase was rich in organics. However, in order to complete the experiments successfully, the authors had to operate the vacuum pyrolysis reactor as a batch process and to use pretreatment and pelletization of the MBM, due to the complications of feeding and operating a reactor

with such a fluffy, cohesive and temperature-sensitive feedstock [4]. The authors mentioned that in order to operate as a continuous feed reactor the MBM would require even further pre-treatment and hardening in the pelletization process. They performed no experiments in order to establish trends or optimize the product distribution and quality with respect to operating conditions. In addition, the fact that the biomass had to be pelletized not only introduced additional energy and capital cost requirements, but can also lead to heat transfer limitations during pyrolysis, which could adversely alter the product yields and quality. The authors indeed observed significant small and large agglomerates of char and solids in the reactor after the experiments, which confirm poor mixing and heat transfer limitations.

Ayllón et al. [2] also performed batch pyrolysis of MBM in a fixed bed reactor, and studied the effects of some operating conditions on the products, including the final pyrolysis temperature and heating rate. Once again the experiments were performed in batches due to the extreme challenges of feeding MBM continuously, but no pelletization was required in the fixed bed. 30 g samples of MBM were placed in a steel basket inside the reactor, and the authors described a way to try to minimize the temperature profiles across the small samples to have the reaction occur at a constant temperature. Inevitably, however, a temperature profile and heat transfer limitations would exist in a fixed bed hot environment, likely leading to char agglomeration with trapped unreacted MBM or char inside. Fast pyrolysis conditions, which are required to maximize the liquid yield and quality of liquid products, were not achieved [10]. In

addition, the sample size was quite small to predict performance in a commercial scale process.

Cascarosa et al. [11] performed a study on the auto-thermal pyrolysis of MBM at a larger pilot scale, feeding 18 kg/h of MBM above the surface of a fluidized bed. By operating auto-thermally and feeding above the bed, the authors risked that the MBM simply floats on top of the hot bed, resulting in poor mixing with the hot sand. This can, in turn, have significant effects on product quality and distribution, as heat transfer is hindered by the poor mixing and because the solid product can be entrained with the gases exiting the reactor, before complete reaction. Unfortunately, the experimental setup used for this study could not quantify the product yields and distributions and the process heat balances, so the study could not be used as a reference point for comparison to the laboratory scale results and optimizations in this work. However, it is valuable to note the evidence in their study that MBM could be processed at a larger scale effectively and that coupled with the process recommendations and optimizations in this work could be scaled-up for industrial production.

The objective of this work is to present the first comprehensive experimental study of the pyrolysis of MBM in a laboratory-scale bubbling fluidized bed reactor, utilizing the ICFAR novel intermittent solid slug feeder technology [12], now being commercialized by Agri-Therm Inc. (www.agri-therm.com), operating continuously and without co-processing of any kind. The aim of the study included the effect of temperature on product yields and quality; the determination of the optimal operating conditions from a

product quality and overall energy balance perspective; and the determination of heat of pyrolysis.

6.2 Materials and Methods

6.2.1 The Feedstock

The MBM used in this study was supplied by Thorndale Farm Supplies, a meat renderer and producer located in Thorndale, Ontario, Canada. The feedstock characteristics are illustrated in **Table 6-1**. The MBM moisture content was determined using a Mettler Toledo HB 43-S Halogen moisture analyzer, the proximate analysis was performed in a Lab-Heat ME 351 muffle furnace, by applying the ASTM E872 standard method, the Elemental Analysis was determined using a Thermo Electron Corporation CHNS-O Analyzer, the main component analysis was given by the supplier, and the heating values were determined using an IKA C 200 bomb calorimeter. The Hausner ratio (HR), shown in the table at room temperature, is a good indicator of the flow properties of the MBM and increases significantly with temperature (reaching 1.6 at 60 °C) [4]. According to Geldart et al. [13], granular materials with HR values in the ranges of 1.2–1.4 are classified as highly cohesive and difficult to flow and fluidize powders. This explains the difficulties and limitations of MBM studies thus far, due to severe feeding and operating issues.

Table 6-1: Meat and Bone Meal Specifications

Proximate analysis:		
Moisture	wt%	6.0
Ash	wt%	26.4
Volatiles	wt%	26.6
Fixed carbon	wt%	41.0
Ultimate elemental analysis:		
Carbon	wt%	42.6
Nitrogen	wt%	8.7
Hydrogen	wt%	6.3
Sulfur	wt%	0.0
Oxygen (by difference)	wt%	16.0
Main component analysis:		
Protein	wt%	55
Fat	wt%	12
Calcium	wt%	8
Phosphorus	wt%	4
Heating values:		
HHV	MJ/kg	17.8
HHV	MJ/m^3	8010
LHV	MJ/kg	16.4
Other properties:		
Sauter mean diameter	μm	40
Bulk density	kg/m^3	450
Hausner ratio	–	>1.3

6.2.2 ICFAR Laboratory-Scale Bubbling Fluidized Bed Pyrolysis Pilot Plant

The process flow diagram of the ICFAR bubbling fluidized bed pyrolysis pilot plant is shown in **Fig. 6-1**. The heart of the plant is an atmospheric fluid bed reactor, 0.078 m in diameter, with a 0.52 m long cylindrical section, equipped with an expanded section made up of a 0.065 m long truncated cone connecting to a second cylindrical section, 0.168 m in diameter and 0.124 m long. The fluidizing gas is injected at the base of the reactor through a perforated steel distributor plate with 33 holes, 0.5 mm in diameter, equally spaced over the cross section. The total reactor volume is $2.71 \times 10^{-3} m^3$, which

results in a vapor residence time of 2 s for all experiments. All experiments performed were 20 min in length with a minimum of 0.4 kg of MBM injected at an average feeding rate of 0.34 g/s.

A hot-filter capable of withstanding high temperatures is installed at the gas exit of the reactor. Each filter is made up of a perforated pipe connected to the gas exit wrapped with a perforated metal sheet with 100 μm holes. The resulting filter is, in all cases, 25 mm in diameter and 178 mm long. These hot filters have been designed to prevent the entrainment of solids (both sand and char). After every experiment, the mass of char and sand was weighed, to determine the mass of char produced. The char can then be separated from the sand for weighing and analysis via sieving or segregation.

The nominal operating conditions required the use of approximately 1 kg of sand with a Sauter mean diameter of 180 μm as the heat carrier and mixing medium in the reactor. The reaction was carried out at temperatures ranging from 450 to 600 °C. Nitrogen gas was used as the fluidizing and feeding system gas, and was metered using four Gas-Trak Sierra mass flowmeters.

The reactor is equipped with 18 thermo wells for temperature measurements and control, using type K thermocouples. Nitrogen-purged pressure taps were used to measure absolute and differential pressures throughout the unit. The reactor and process pressures are measured throughout the plant using either pressure gauges or a bank of Honeywell ST3000 pressure transmitters. All critical temperature, pressure and

flowrate measurements are gathered by a central data acquisition system and can be monitored and collected by a computer system programmed using LabView 2009.

The reactor body is fitted with 12 Watlow Mica electric band heaters, each of them with power ratings ranging from 335 to 1350 W, covering specific sections of the reactor body, and independently controlled using 12 Honeywell UDC200 Mini-Pro Digital controllers.

Once the feed is injected into the reactor and the reaction takes place, the produced vapors exit the top of the reactor through the hot filter section and flow into two cyclonic condensers in series. Both condensers employ an ice water bath as the cooling medium. The bio-oil vapors enter the condensers tangentially, forcing the vapors close to the cold steel condenser wall, rapidly quenching the bio-oil liquid, which is later collected in the bottom of the condenser. The cyclonic condensers are designed to have a very low pressure-drop and to prevent plugging or over-pressurization due to the viscous bio-oil or tars collecting within them. The condensers are also equipped with quick-connections on either end to facilitate oil collection after the experiment. Persistent aerosols are then separated in a cylindrical high-efficiency two-stage electrostatic precipitator demister and finally in a demister filter packed with fibreglass wool. Following this, the non-condensable gases are directed to an exhaust stack where they can be sampled, using a micro-GC gas bag. The condensers and the ESP are weighed before and after each experiment to accurately determine the mass of bio-oil produced.

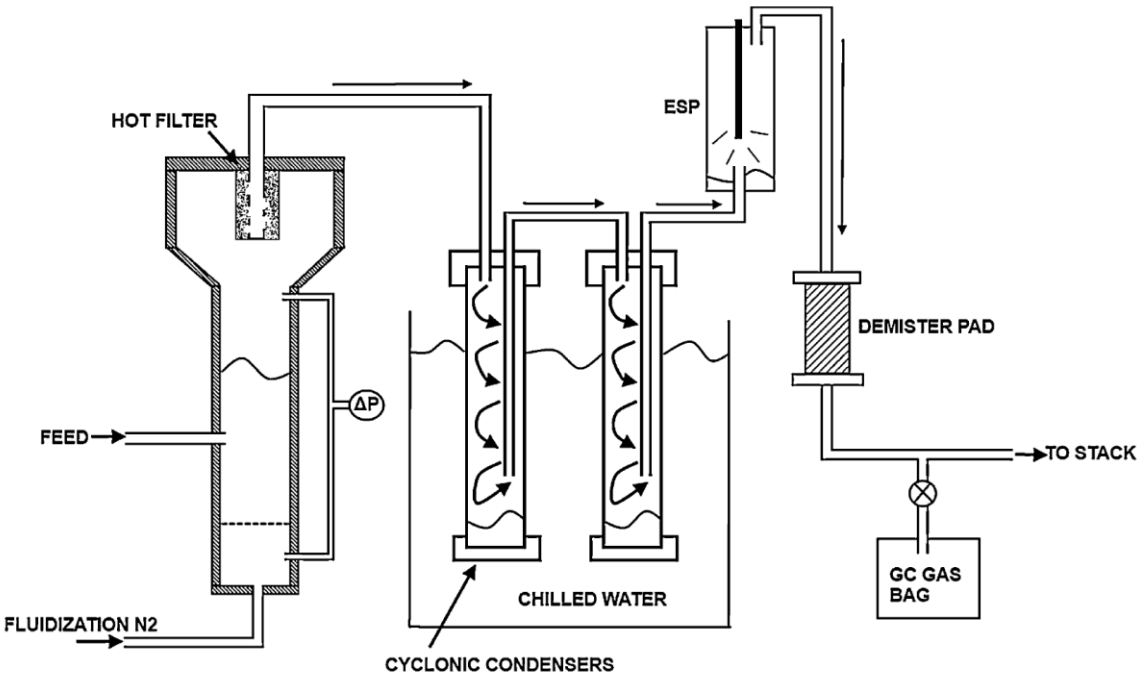

Figure 6-1: ICFAR Pilot Plant Process Flow Schematic

6.2.3 Analysis of Products

A Varian CP-4900 3-Column Micro Gas Chromatograph is used for the non-condensable gas analysis (with N_2 as the internal standard). The bio-oil liquid heating values were determined using an IKA C 200 bomb calorimeter, following the ASTM D4809-00 standard method, while the heating value of the product gas was calculated from the product gases composition determined with the GC and the lower combustion value of each gas constituent. The bio-oil moisture content was determined using a Mettler Toledo V20 Volume KF Titrator, and the bio-oil pH was determined using a Thermo Scientific Orion 2Stat pH Benchtop. The raw MBM and MBM bio-char ash analysis was performed using a PANalytical PW-2400 XRF Spectrometer. Finally, the Bio-oil volatile component analysis was performed using a Hewlett Packard HP 6890 Series GC-MS

System, using a DB-5 ms capillary column (30 m x 0.25 mm i.d., film thickness of 0.25 μm). Methanol was used as the solvent, and the bio-oil was dissolved in a ratio of 1 part bio-oil to 5 parts methanol. Phenanthrene was also dissolved in the sample in a ratio of 1 part phenanthrene to 20 parts bio-oil, as an internal standard. The GC–MS method was set to initialize at 47°C with a 2 min hold, then ramp-up at a rate of 5°C/min until 200°C, followed by an increased ramp-up at 20°C/min to 300°C, with a final 5 min hold to ensure that all products were detected through the column.

6.2.4 The ICFAR Intermittent Solid Slug Feeder Technology

Due to the highly cohesive and temperature-sensitive nature of MBM, a specially designed feeder was required for the experiments described in this work. Conventional feeders tend to consume too much energy for successful conveying (dilute-phase pneumatic transport lines) or experience rapid plugging (screw feeders and dilute-phase pneumatic transport), as the MBM becomes sticky in the feeding tube at temperatures above 50°C [4, 12]. Most industrial operators attempting to feed MBM are usually forced to feed above the bed, such as the case of Cascarosa et al. [11], which often results in poor mixing with the hot sand, as the MBM simply floats on top of the hot bed.

The ICFAR intermittent solid slug feeder technology [12] designed for this work and illustrated in **Fig. 6-2** has been used extensively at ICFAR for bubbling bed pyrolysis reactor experiments for long operation and has also been scaled up. The feeder for this work consisted of a slightly pressurized vertical solids storage silo (P1– roughly 2 psig or

115 kPa) leading to a 19 mm pneumatic pinch valve. The silo had a 4 L volume, with a cone angle of 70° from the horizontal. Within the silo, a specially designed rotating 'egg-beater' mixer prevented the bridging of solids. The instantaneous mass flow of gas flowing into the silo was determined by acquiring the Gas-Trak Sierra mass flowmeter signal responsible for delivering the nitrogen gas to the silo. The pinch valve was controlled by solenoid valves (SV 1A and 1B in Fig. 6.2) connected to a relay timer (IMO iSmart Relay, 10 I/O AC). Solids exiting the pinch valve flowed into a 12.7 mm, 0.6 m long horizontal feeding tube through a 90° angle connection. The volume within such connection, between the end point of the pinch valve and the horizontal feeding tube is called "slug chamber". For the purpose of the current study, a simple "T" fitting of constant diameter (12.7 mm) was utilized, with a vertical, 63.5 mm long section (measured from the base of the horizontal part of the "T"). A small continuous nitrogen gas flow (also measured and controlled using a Gas-Trak Sierra mass flowmeter) was fed into the feeding tube to prevent hot sand backflow into the feeding tube. Intermittent pulses of nitrogen were fed at a set pressure (P2 – roughly 30 psig or 308 kPa) to propel the MBM slugs, delivered from a control volume consisting of a 75 mL steel canister. The timing of the pulses was controlled by solenoid valves (SV 2 and SV 3 in Fig. 6.2) with the relay timer. When the pinch valve opens and closes, the MBM falls into the 'slug chamber' forming a plug, which is then propelled by the pulsating pressurized nitrogen gas volume contained in the canister into the reactor through the feeding tube. The solid mass flowrate was measured by calibrating the feeding system in open air before commencing the experiments. The total mass injected into the reactor was

measured by the difference between the mass of MBM loaded in the feeder prior to the experiment and that remaining after each experiment. Aside from the feeding tube connected to the reactor, which was made of stainless steel 316, the entire apparatus was manufactured using PVC, with several clear sections to allow for visual inspection of the feeder operation and for characterization of the solids flow.

Fig. 6-3 illustrates the ability of the ICFAR feeder to feed cohesive MBM at the constant average feeding rate of 0.34 g/s into open air (R_2 value of 0.9798). The data were generated by capturing the fed MBM in a cyclone with the solids outlet leading to a digital scale, which continuously outputs the instantaneous mass data to a computer.

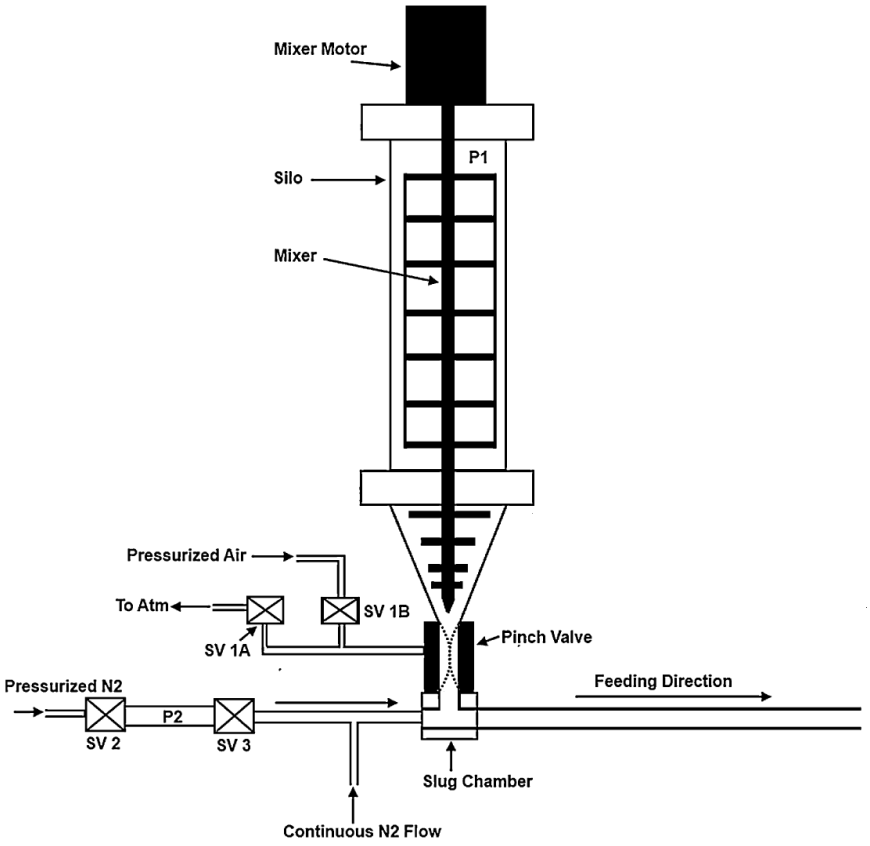

Figure 6-2: ICFAR Intermittent Solid Slug Feeder Schematic

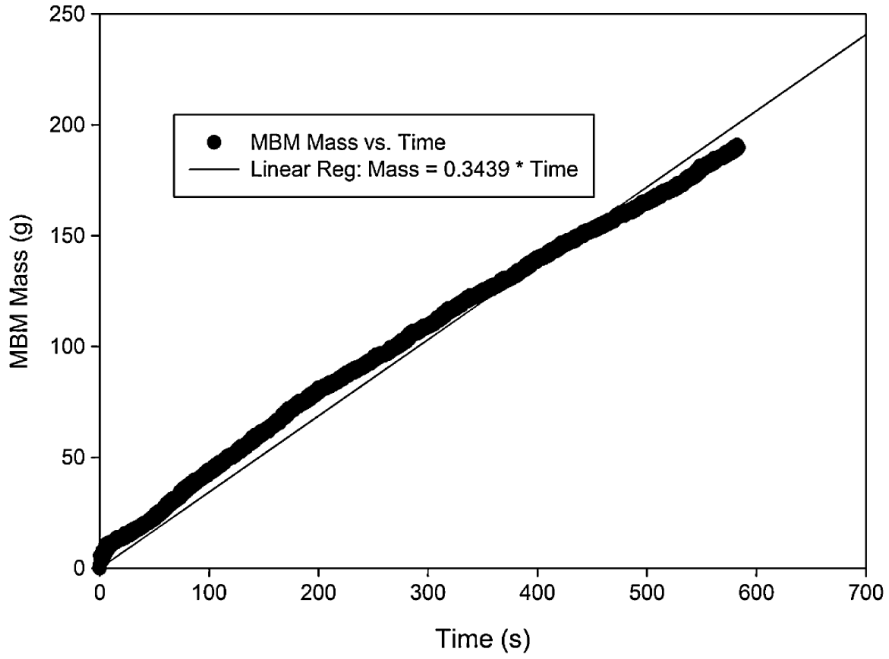

Figure 6-3: ICFAR Intermittent Solid Slug Feeder - Open Air MBM Feeding Rate

6.2.5 Heat of Pyrolysis Methodology and Equipment

For this study, a new technique was developed in order to quantify the heat required for the pyrolysis reaction (heat of pyrolysis), to later analyze the reaction sustainability using recycled product gases as a fuel source, and the overall energy consumption and yield of the process. The heat of pyrolysis is defined as the practical energy required to undergo the pyrolysis reaction, taking the MBM feed at room temperature and resulting in the products at reactor temperature. Since the reactor uses electrical heaters, the total power being consumed by the reactor heaters can be obtained from the constant 3-phase voltage of 208 V, which gives a root-mean-squared voltage (V_{RMS}) of 146.08 V, and the root-mean-squared current (I_{RMS}) being drawn by each heater, using CR Magentics Inc. Current Transformers (E235509), acquired by a computer using LabView 2009 software.

The average power consumption prior to the experiment could then be compared to the power consumed during the biomass feeding (considering any extra feeder gas injected), at the same bed temperature, to find the power being consumed by the reaction by difference. However this technique suffers from some serious inaccuracies due to a drastic change in heat losses between the two compared states: during biomass feeding and reaction, the electric heaters must provide more energy to the reactor, thus increasing the reactor wall temperature, which results in higher heat losses than in the absence of biomass feeding.

To eliminate this problem, the average power consumption and bed temperature must both be the same between regular feeding and calibration. The power consumption was therefore measured during an MBM experiment and subsequent experiments were carried out to determine the feedrate of reference feed, of known reaction/thermal properties, that would require the same power, at the same bed temperature. Distilled water was selected as the reference feed, since its specific heat capacity across various states and heat of vaporization are known. A high accuracy atomizing nozzle (**Fig. 6.4**), equipped with a water burette for flowrate measurement and a larger graduated cylinder for water storage, was used for the water injection. A Thermo Separation Products miniPump accurately injected the water. A fine spray, for good water distribution in the bed, was found to be critical to ensure an accurate calibration and avoid “slumping” and “bogging” of the fluidized bed.

The main variables in each experiment to be considered were the total nitrogen flows entering the reactor, the experimental operating temperature, and the mass flowrate of water injected, all of which were experimentally found to affect the total power consumption, with sufficient linearity for linear regression fitting, as shown in **Figs. 6-5** to **6-7**.

With this information, a complete water calibration of 17 experiments was performed on the reactor, ensuring that all power values observed during actual MBM experimentation would fall within the ranges calibrated for, to obtain the highest accuracy in the multi-variable linear regression. The multi-variable linear regression was performed using StatGraphics Centurion Data Analysis and Statistical software and resulted in Eq. (6.1) which has an R^2 value of 95.6 %.

$$POWER\,(W) = -372.613 + 6.20746\left(N_{2(SLM)}\right) + 31.6417\left(WaterFlow_{\,(g/\min)}\right) + 1.2666\left(Temp_{(^{\circ}C)}\right)$$

Equation 6.1

Using this equation, one can then measure the power consumption during an experiment with MBM, and solve for the equivalent water flow by inputting the known experimental variables of the total nitrogen flowrate used and the reactor temperature. Since the standard heat capacities of water in liquid and gas phase are known, as well as the heat of vaporization, the power consumed by the MBM pyrolysis reactions can then be accurately calculated. Dividing this value by the experimental MBM feedrate provides the effective heat of pyrolysis.

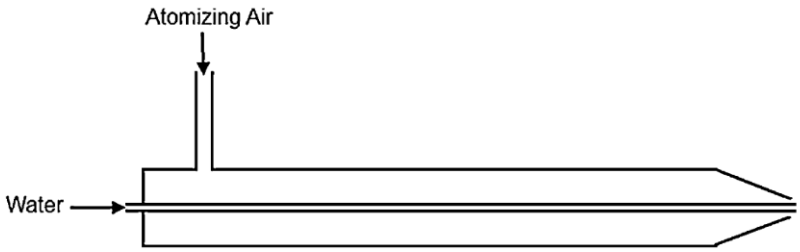

Figure 6-4: Atomizing Nozzle used for Water Calibration

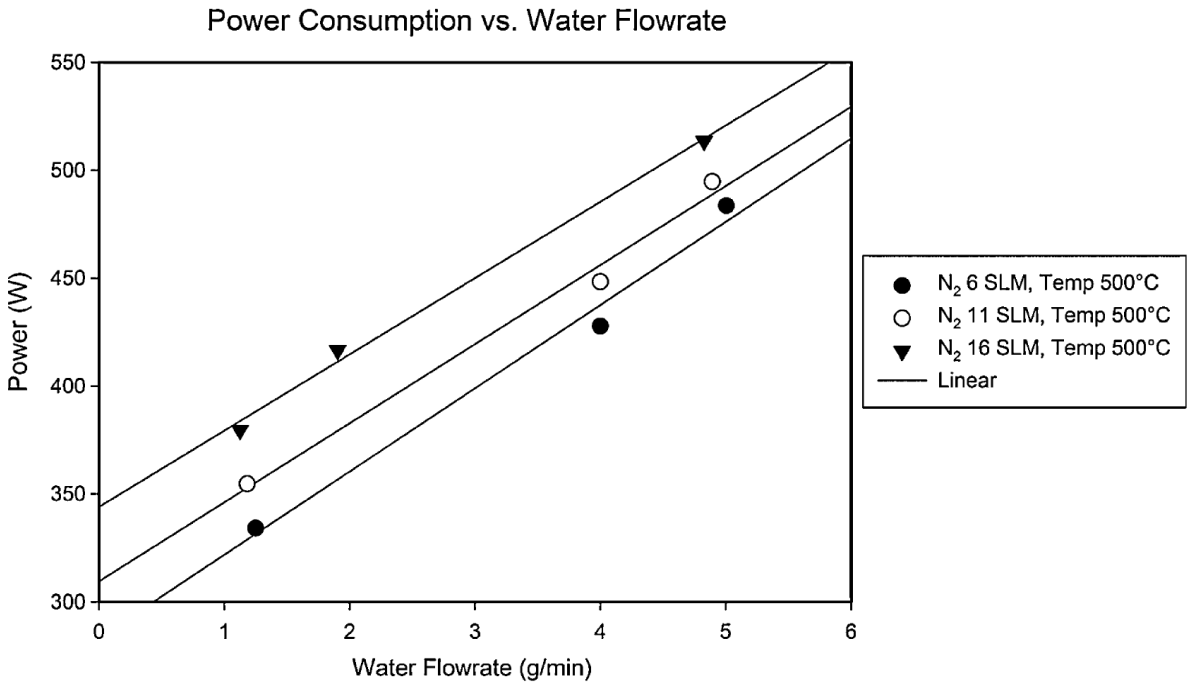

Figure 6-5: Power Consumption vs. Water Flowrate at Constant N_2 Flowrate and Temperature

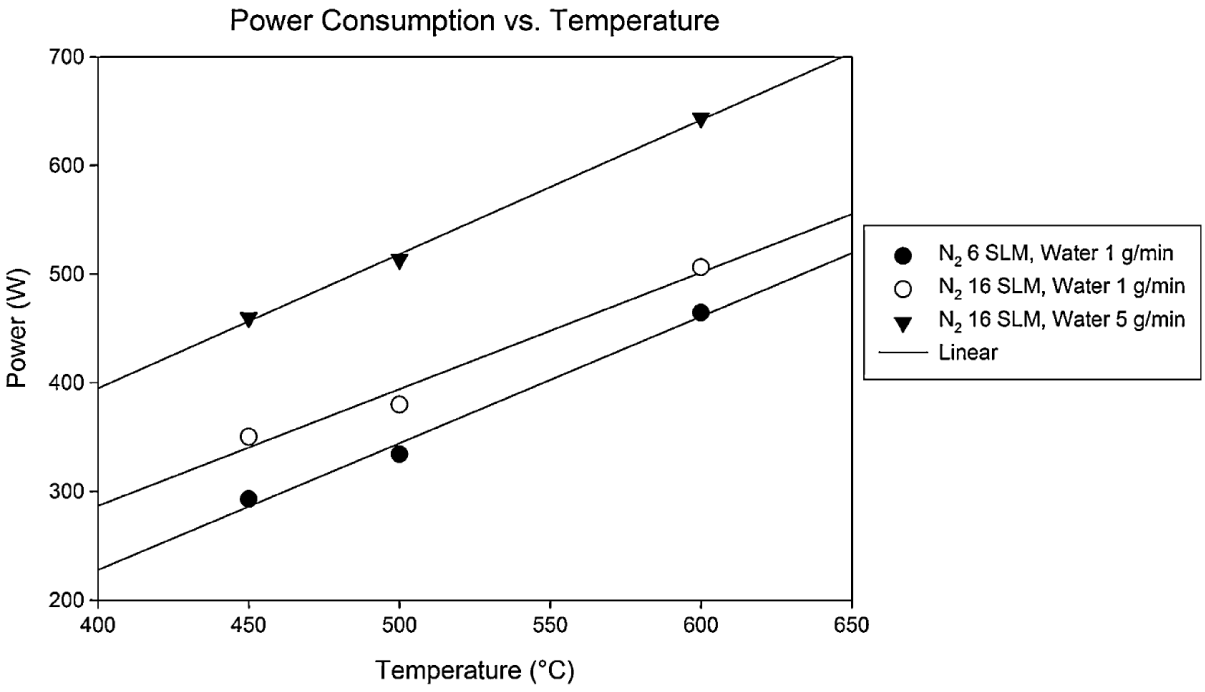

Figure 6-6: Power Consumption vs. Temperature at Constant N_2 Flowrate and Water Flowrate

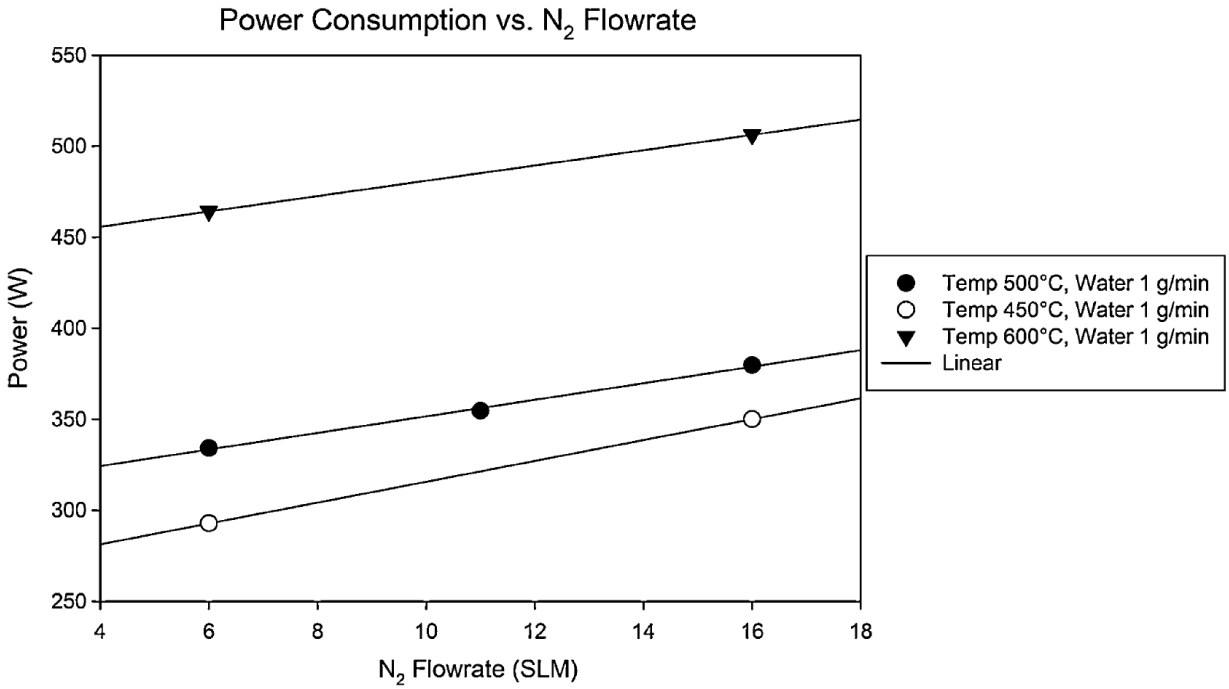

Figure 6-7: Power Consumption vs. N_2 Flowrate at Constant Temperature and Water Flowrate

6.3 Results and Discussion

6.3.1 Effect of Temperature on Product Yields

The effects of pyrolysis temperature on the average product distribution are shown in **Fig. 6-8**. The results were found to be very reproducible, as demonstrated by three replicate runs conducted for each condition. The gas yield was calculated by difference, but was confirmed with yield calculations from the Micro GC gas analysis, resulting in mass balance closures between 97.5 and 100.6% for all experiments. The room-temperature partial pressure of water saturating the gas stream and escaping the system, although very small, was calculated as a rough approximation and considered in the mass balance closure. As illustrated in the figure, the optimum temperature required to maximize the liquid yield is 550 °C, resulting in an average liquid yield of 43

wt%. As concluded by Conti et al. [14], if the operating temperature is higher than the temperature resulting in the maximum liquid yield, secondary cracking reactions in the gas phase are very fast, leading to more degradation of vapor products formed than formation of vapor products from further solid decomposition, and thus reducing the bio-oil and bio-char yields and correspondingly increasing the gas yield. Conversely, lower temperatures prevent the full decomposition of the biomass solids to vapors. In addition, the solid char yield always decreases with increasing pyrolysis temperature, while the non-condensable gas yield increases.

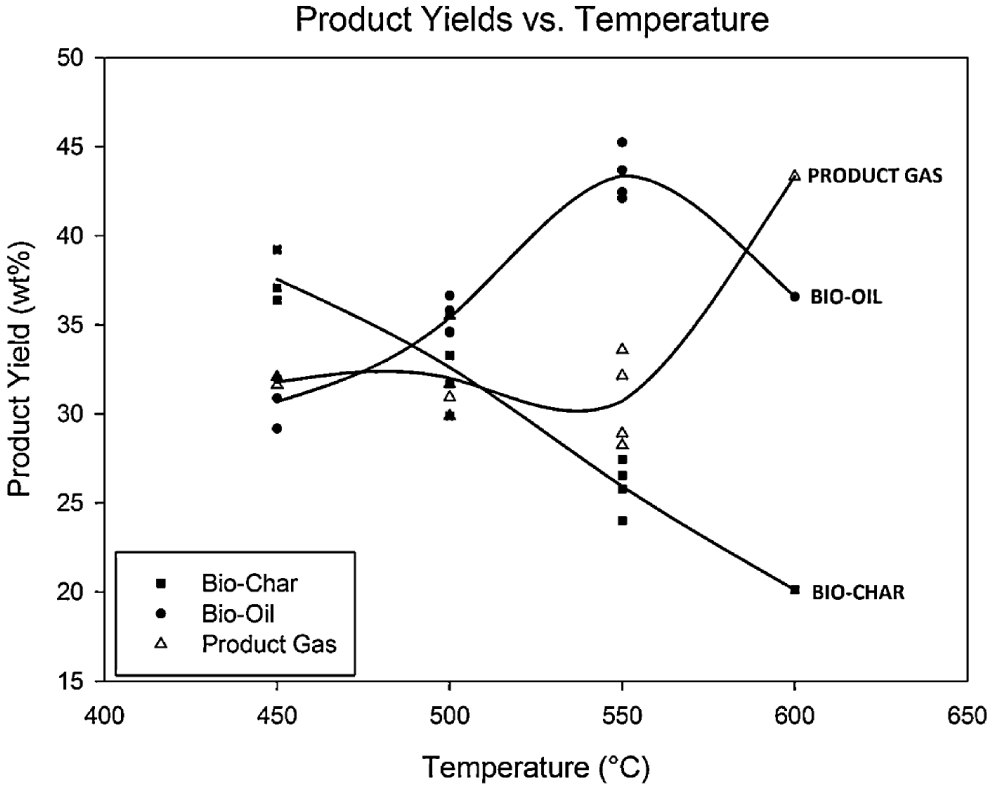

Figure 6-8: Product Yields vs. Temperature

6.3.2 Bio-oil Product Properties

Due to the centrifugal separation and cooling contributed by the cyclonic condensers, the bio-oil vapor is condensed and collected. The MBM bio-oil produced is homogenous and has a relatively low water content.

The main properties of the bio-oil, mixed from all condensation points forming a homogenous and single-phase product, from the MBM feedstock are presented in Table 6.2. The bio-oil has a much higher energy density than the raw MBM, and also contains negligible ash. The ash content was checked by muffle furnace combustion following the ASTM E872 standard method. This underlines the advantages of converting the raw MBM to liquid bio-oil, since the liquid product is more energy intensive, easier to transport, and better for combustion, due to the low ash content, thus leading to reduced equipment fouling and unnecessary continuous ash removal. To underline the transportation advantage of converting MBM to bio-oil, one can compare the HHV of the bio-oil compared to the HHV of the raw MBM in MJ/m_3, as the energy per unit volume for transportation is of critical economic importance (comparing **Table 6-1** and **Table 6-2**). In the case of MBM, the bio-oil has an HHV approximately five times higher than the raw biomass in MJ/m_3. The highest bio-oil heating value (HHV) was found at the highest yield condition of 550 °C. However, the highest water-free heating value was found at 500 °C. Interestingly, unlike most bio-oils which tend to be acidic, all the bio-oils produced with MBM were basic, having pH values in the range of 9–9.4, due to some basic nitrogen based compounds, such as nitriles and amides, produced in the bio-oil.

Further study would be required to determine whether the high nitrogen content of the bio-oil and the product gas would result in high NO_x emissions when they are combusted. It may be necessary to use scrubbers or catalytic converters specially designed to reduce NO_x emissions.

The chemical composition of the bio-oil at 550 °C was also analyzed by GC/MS (**Table 6-3**). The 42 compounds illustrated in the table had a NIST 98 library matching quality greater than 90%. The biooil contains many long-chain fatty acids and fatty nitriles/amides, which could be derived from the decomposition of the fats contained in the meat. The pure phenol mass percentage was calibrated in the GC/MS and calculated to be 1 wt% of the bio-oil.

The compounds were also further divided into the following chemical families, similar to Cascarosa et al. [11]: (1) aliphatic compounds with oxygen-containing functional groups, (2) aliphatic compounds with nitrogen-containing functional groups, (3) aromatic compounds with oxygen and/or nitrogen containing functional groups (mainly phenols and some benzyl/benzene compounds), (4) heterocyclic aromatic compounds, (5) aromatic hydrocarbons, and (6) aliphatic hydrocarbons. The abundancy trends followed the findings by Cascarosa [11] for MBM pyrolysis, with the greatest percentage of total area abundance of compounds being aliphatic compounds with oxygen-containing functional groups, followed by the aliphatic compounds with nitrogen-containing functional groups. No chlorine-containing compounds were detected.

Overall, the MBM bio-oil appears to be quite different than conventional bio-oils from woody biomass. For example, if compared to the wood pyrolysis bio-oil description in the critical review by Mohan et al. [15], it can be seen that the MBM bio-oil contains many more long-chain aliphatic compounds and acids, and fewer phenols and alcohols. By examining these compounds, it could be hypothesized that MBM bio-oil would therefore be much less polar than conventional bio-oils (and with a much more neutral pH), and may be more miscible with other fossil fuels, such as conventional diesel. Further work on the upgrading, miscibility and fuel quality of this bio-oil will be investigated in the near future.

Table 6-2: Average MBM Bio-oil Properties

Average MBM bio-oil properties				
Reaction temp (°C)	450	500	550	600
HHV (MJ/kg)	29.1	30.1	31.5	23.7
HHV (MJ/kg) – water free	34.6	36.7	32.8	31.2
HHV (MJ/m^3) – water free	41,520	44,040	39,360	37,440
Water content (wt)	16%	18%	10%	24%
pH	9.16	9.4	9.3	9.1
Elemental analysis:				
Nitrogen	8%	11%	11%	11%
Carbon	56%	60%	62%	57%
Hydrogen	5%	9%	9%	8%
Elemental analysis (water-free):				
Nitrogen	10%	13%	11%	15%
Carbon	66%	73%	65%	76%
Hydrogen	4%	8%	9%	7%

Table 6-3: Organic Compounds Detected in a Bio-oil Sample Produced at 550C and their Corresponding Chemical Families

Compound	RT (min)	Chemical family	Corr. area	% of total area
Acetic acid	4.34	1	11,785,786	1.07%
2-Furanmethanol	7.88	1	2,134,520	0.19%
Tetradecanoic acid	36.42	1	84,977,882	7.68%
14-Pentadecenoic acid	38.04	1	126,275,868	11.41%
Acetamide	6.92	2	6,018,281	0.54%
Dodecanamide	32.3	2	5,925,324	0.54%
Tetradecanamide	32.34	2	4,221,117	0.38%
Hexadecanenitrile	35.45	2	27,899,921	2.52%
Heptadecanenitrile	37.51	2	22,318,843	2.02%
Hexadecanamide	38.31	2	32,796,596	2.96%
Phenol	11.63	3	12,820,647	1.16%
Phenol, 2-methyl-	13.88	3	3,370,655	0.30%
Phenol, 4-methyl-	14.64	3	14,910,304	1.35%
Benzyl nitrile	16.56	3	9,168,294	0.83%
Phenol, 2,4-dimethyl-	16.91	3	3,000,884	0.27%
Benzenepropanenitrile	19.69	3	4,162,813	0.38%
Pyrrole	5.71	4	17,282,388	1.56%
Pyridine, 2-methyl-	7.1	4	4,094,085	0.37%
Pyridine, 3-methyl-	8.23	4	1,919,527	0.17%
Pyridine, 2,4-dimethyl-	10.14	4	1,715,153	0.16%
1H-Pyrrole-2-carbonitrile	17.28	4	6,771,781	0.61%
Indole	21.43	4	12,541,395	1.13%
1H-Indole, 3-methyl-	24.1	4	26,429,58	0.24%
Pyrrolo[1,2-a]piperazine-3,6-dione	34.44	4	2,078,724	0.19%
Cycloheptene	19.16	5	2,219,338	0.20%
Cyclotetradecane	37.13	5	5,529,552	0.50%
Cyclotetradecane	37.33	5	41,269,780	3.73%
1-Decene	11.73	6	2,090,788	0.19%
1-Undecene	14.94	6	3,494,996	0.32%
1-Dodecene	18.1	6	3,888,021	0.35%
1-Tridecene	21.14	6	3,004,465	0.27%
1-Tetradecene	24.03	6	7,576,357	0.68%
1-Pentadecene	26.75	6	4,520,078	0.41%
Pentadecane	26.95	6	4,938,019	0.45%
1,11-Dodecadiene	28.87	6	3,177,826	0.29%
1,13-Tetradecadiene	28.95	6	2,725,193	0.25%
1-Hexadecene	29.33	6	5,537,862	0.50%
1-Heptadecene	31.44	6	7,667,821	0.69%

6.3.3 Gas Product Properties

As shown in **Fig. 6-8**, the yield of pyrolysis non-condensable gases is quite flat across the temperature and then begins increasing dramatically at higher temperatures. This is largely because of the increase in the rate of secondary cracking reactions of the volatiles at the higher temperatures. **Table 6-4** illustrates the results from the Micro GC component gas analysis and underlines the trends with increasing temperature. It is important to note the trend of decreasing CO_2 and increasing CO with temperature. This is expected because the CO_2 is produced by carboxyls freed by pyrolysis at relatively low temperature and the secondary cracking reactions of volatiles produce mostly CO, H_2, and CH_4, rather than CO_2 [16]. This contributes highly to the increasing heating value of the gas obtained by pyrolysis at higher temperatures.

Table 6-4: Micro GC Analysis of Non-Condensable Gas Produced by Pyrolysis of MBM

	Comp. LHV (MJ/kg)	Average Composition (wt/wt)				Trend with temp
		450 °C	500 °C	550 °C	600 °C	
H_2	121.0	2.9%	2.5%	2.0%	0.9%	Decreasing
CH_4	50.0	2.3%	4.0%	4.6%	7.4%	Increasing
CO	10.1	6.7%	10.7%	13.5%	17.5%	Increasing
CO_2	0.0	77.9%	71.1%	61.4%	45.9%	Decreasing
Ethane	47.8	1.2%	2.0%	2.8%	4.1%	Increasing
Ethylene	47.2	1.0%	3.5%	3.4%	8.9%	Increasing
C3	46.4	1.7%	2.4%	5.8%	8.8%	Increasing
C4	45.8	1.0%	1.5%	3.6%	5.4%	Increasing
	GAS MIX LHV (MJ/kg):	7.7	10.6	13.4	19.3	

6.3.4 Bio-char Properties

Due to the high ash content (>70 wt%), the bio-char produced has quite a low heating value, decreasing further with temperature due to further cracking of its carbon-rich components. **Fig. 6-9** illustrates the heating value of the bio-char as a function of the reaction temperature. The ash analysis of raw MBM and of MBM bio-char is illustrated in **Table 6-5**. The bio-char ash contains over 50 wt% of calcium and some potassium, indicating that it could be a suitable catalyst for gasification [11]. The phosphorus content of nearly 40 wt% is also notable. Soil additive properties should be further investigated for the MBM bio-char product.

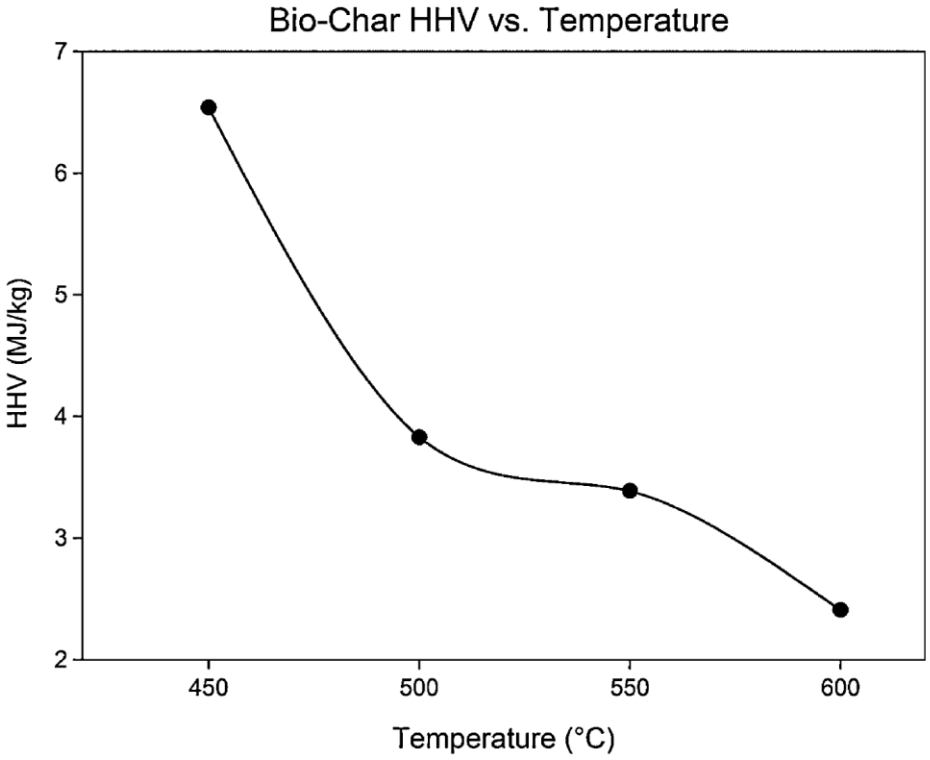

Figure 6-9: Effect of Temperature on Bio-char Heating Value (HHV)

Table 6-5: Raw MBM and MBM Bio-char Ash Analysis

Sample	SiO_2	TiO_2	Al_2O_3	Fe_2O_3	MnO	MgO	CaO	K_2O	Na_2O	P_2O_5	Cr_2O_3	Total	Ash (wt %)
Raw MBM	1.2	0.0	0.3	0.4	0.0	2.2	51.6	1.5	3.2	39.7	0.0	100	21.0
MBM bio-char at 550 °C	1.2	0.0	0.5	1.0	0.1	1.6	56.4	1.1	1.4	36.6	0.2	100	80.6

6.3.5 Heat of Pyrolysis

The overall pyrolysis process is endothermic and determining the heat required for the process and reaction is of great value for practical or industrial applications, for energy balances and energy requirements [17]. Using the accurate calibration technique described earlier, the average heat of pyrolysis for all experimental conditions tested was determined, as illustrated in **Fig. 6-10**.

As shown, more heat is required for pyrolysis at higher temperatures, due to the energy requirements for the more severe biomass decomposition and further endothermic thermal cracking of the formed products. Knowing the heat of pyrolysis will play a key role in being able to determine the optimal operating conditions for this process, since both the product quality/yield information and the energy balances have been determined.

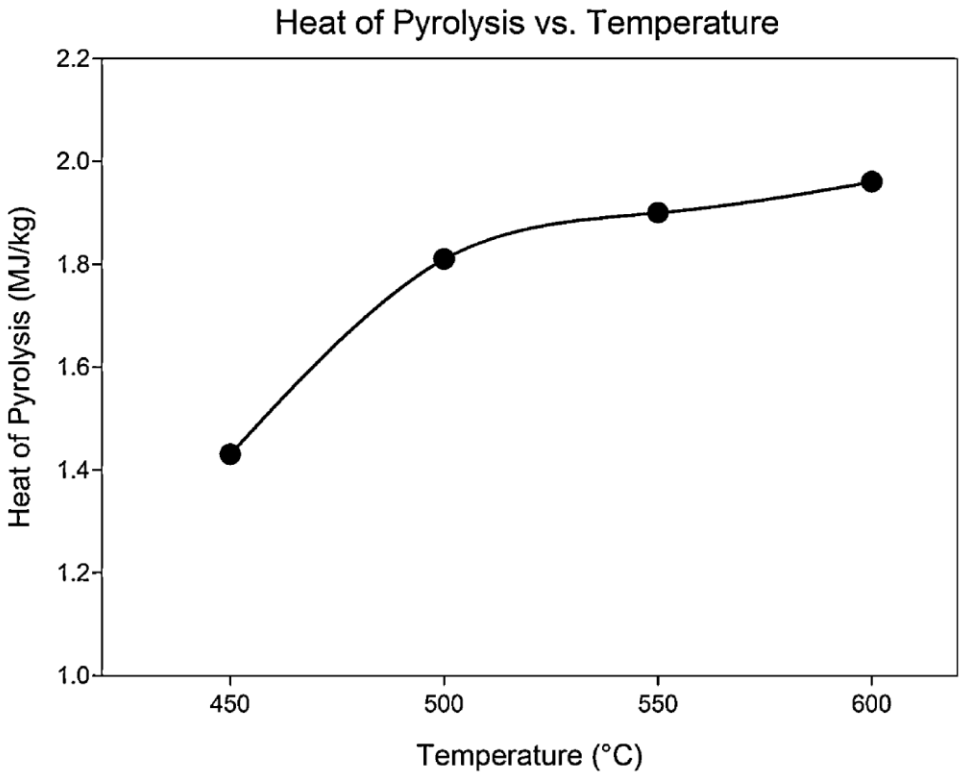

Figure 6-10: Heat of Pyrolysis vs. Temperature

6.3.6 Energy Balance and Process Thermal Sustainability

From an industrial standpoint or to design scaled-up applications, it is important to make the pyrolysis process self-sustaining, with respect to its energy requirement. Firstly, avoiding the use of fossil fuels to drive the process is advantageous from a sustainability perspective [17]. Secondly, it would in many cases be more economical to use many small decentralized plants, located near the biomass source, rather than a large centralized plant that would require expensive transportation of the low energy density biomass over long distances [18]. With a decentralized plant in particular, the pyrolysis non-condensable product gas itself would be an ideal source of fuel to drive the process and would, thus, be safely incinerated.

Fig. 6-11 illustrates the energy sustainability of the pyrolysis of MBM at different temperature conditions. The bar graph illustrates the low heating values (LHV) of the product gas, bio-oil and bio-char, from the bottom to the top of each bar, respectively. The white-dot symbol with dashed line represents the total practical energy required for the pyrolysis process, including both the heat of pyrolysis calculated and the energy required to heat all gas flows entering the reactor. From the graph it can be seen that, if the pyrolysis operating temperature is too high, there would be excess of gas produced, whereas, if it is too low, there may not be enough product gas to combust to sustain the process. From the schematic, it is shown that at all the pyrolysis conditions tested in this work, there is barely enough product gas energy to provide the heat required to the process, until 600 °C where there is a large excess. Therefore, the ideal pyrolysis temperature for MBM, with a safety margin, should be set to about 550 °C, which also corresponds to the conditions generating the maximum yield of liquid bio-oil (**Fig. 6-8**). Moreover, the bio-oil produced at 550 °C has the highest HHV, and the second highest water-free HHV (**Table 6-2**). However, to be safely sustainable (with a margin of safety), the operating temperature should be set at slightly higher than 550 °C. Quick tests should also be performed with any given MBM feedstock to capture any feedstock variation associated with different types of MBM produced in meat rendering plants.

Fig. 6-12 illustrates the comparison between the raw MBM energy and the total net captured product energy, which is the sum of the energy contained in the bio-oil, bio-char, and product gas, minus the practical energy that needs to be provided to the reactor for the pyrolysis reaction to take place, assuming zero heat losses. For each

condition, the process energy yield can be determined by dividing the net captured product energy by the raw MBM energy. At 550 °C, the pyrolysis process has a very high energy yield of 91%. The difference between the two lines characterizes the inefficiencies of the process and the relative energy lost in the heated gas stream leaving the reactor, as well as the energy not recovered from the vaporization and re-condensation of water and product vapors in the product gas stream. In a more efficient reactor system, designed for further high-quality heat recovery downstream of the reactor, the energy yield could be further increased.

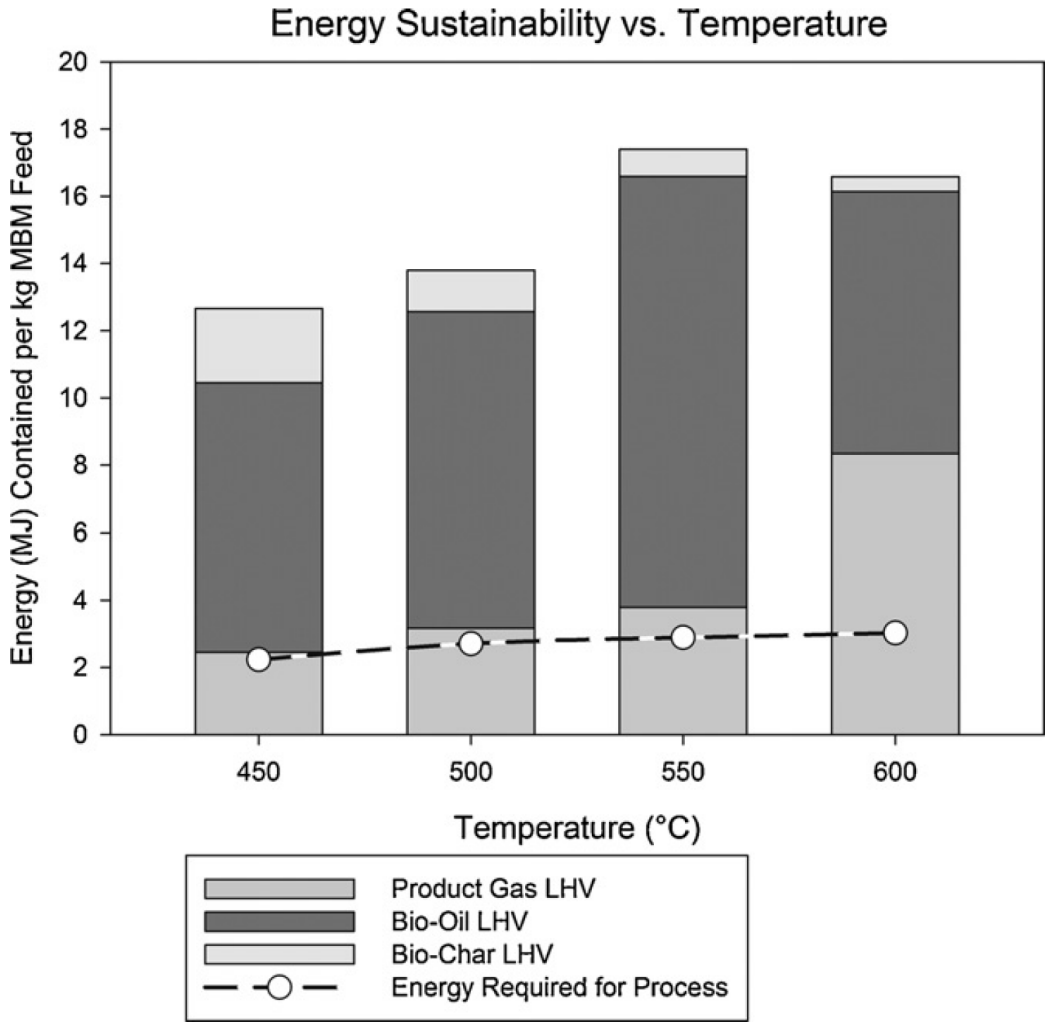

Figure 6-11: Energy Sustainability Schematic

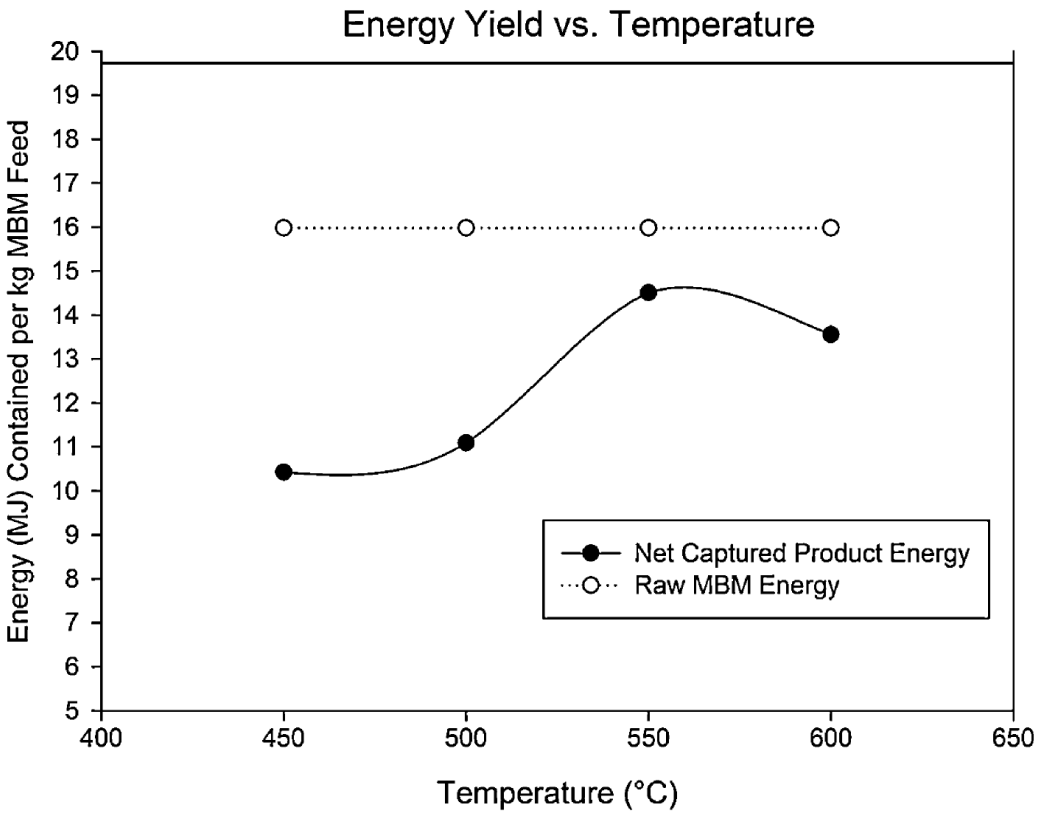

Figure 6-12: Comparison of Net Captured Product Energy and Raw MBM Energy vs. Temperature

6.4 Conclusions

The effects of processing temperature on the pyrolysis products generated using meat and bone meal (MBM) feedstock have been investigated in a continuous laboratory-scale bubbling fluidized bed reactor operating at a constant vapor residence time of 2 s. Feeding issues, due to the cohesive and temperature sensitive nature of MBM, encountered in previous studies, have been overcome by using the ICFAR Novel intermittent solid slug feeding technology.

The pyrolysis temperature greatly affects the product distribution. For a 2 s vapor residence time, 550 °C is the optimum pyrolysis temperature to maximize liquid bio-oil production from MBM.

The liquid bio-oil is homogenous and has low water content. The bio-oil is an attractive fuel with a significant high heating value (HHV) of 31.5 MJ/kg and an average liquid yield of 43 wt% at 550 °C. The highest water-free HHV (36.7 MJ/kg) was found at 500 °C, with a liquid yield of 35% at this temperature.

To achieve a sustainable process, the combustible non-condensable product gases need to be burned to generate the process heat requirements. The optimized pyrolysis temperature, at which the heat from the gas combustion can comfortably (with safety margin) provide the heat required for processing MBM, while maximizing the bio-oil liquid yield and process energy yield, is 550 °C. Under these conditions, the pyrolysis process practical energy yield is 91%.

The study also demonstrates a new technique to accurately determine the heat of pyrolysis reaction energy required by the process, using a non-invasive water calibration method.

6.5 Acknowledgements

The authors wish to express their gratitude to the Ontario Centres of Excellence (OCE), the Natural Sciences and Engineering Research Council of Canada (NSERC), the Vanier Canada Graduate Scholarship program, Agri-Therm Inc. and The University of Western Ontario for the financial support of this research program. Special thanks to Ester

Cascarosa, Dr. Jesús Arauzo, Dr. Fernando Bimbela, Dr. Jose-Luis Sanchez, and the rest of the Grupo de Procesos Termoquímicos in Zaragoza, Spain, for all the useful discussions and collaborations, and for their friendship.

6.6 References

[1] C.G. Soni, T. Pugsley, Steam gasification of meat and bone meal in a two-stage fixed bed reactor system, Asia-Pac. J. Chem. Eng. 6 (2011) 71–77.

[2] M. Ayllón, M. Aznar, J.L. Sanchez, G. Gea, J. Arauzo, Influence of temperature and heating rate on the fixed bed pyrolysis of meat and bone meal, Chem. Eng. J. 121 (2006) 85–96.

[3] C.G. Soni, Z. Wang, A.K. Dalai, T. Pugsley, T. Fonstad, Hydrogen production via gasification of meat and bone meal in two-stage fixed bed reactor system, Fuel 88 (2009) 920–925.

[4] R.A. García, R.A. Flores, C.E. Mazenko, Factors contributing to the poor bulk behavior of the meat and bone meal and methods for improving these behaviours, Bioresour. Technol. 98 (2007) 2852–2858.

[5] K. McDonnell, J. Desmond, J.J. Leahy, R. Howard-Hildige, S. Ward, Behaviour of meat and bonemeal/peat pellets in a bench scale fluidised bed combustor, Energy 26 (2001) 81–90.

[6] J. Beck, J. Brandenstein, S. Unterberger, K. Hein, Effects of sewage sludge and meat and bone meal co-combustion on SCR catalysts, Appl. Catal. B 50 (2004) 19–29.

[7] A. Chaala, C. Roy, Recycling of meat and bone meal animal feed by vacuum pyrolysis, Environ. Sci. Technol. 37 (2003) 4517–4522.

[8] M. Ayllón, G. Gea, M.B. Murillo, J.L. Sánchez, J. Arauzo, Kinetic study of meat and bone meal pyrolysis: an evaluation and comparison of different possible kinetic models, J. Anal. Appl. Pyrol. 74 (2005) 445–453.

[9] F.M. Berruti, K. Lenkiewicz, R. Xu, R.J. Bedmutha, S. Nova, F. Berruti, C. Briens, Novel fluid bed pilot plant for the production of bio-oil from biomass through fast pyrolysis. Récents progrès en génie des procédés, numéro, 94 (2007) ISBN 2-910239-68-3. SFGP, Paris, France.

[10] C. Hulet, C. Briens, F. Berruti, E.W. Chan, A review of short residence time cracking processes, Int. J. Chem. React. Eng. 3 (2005).

[11] E. Cascarosa, I. Fonts, J.M. Mesa, J.L. Sanchez, J. Arauzo, Characterization of the liquid and solid products obtained from the oxidative pyrolysis of meat and bone meal in a pilot-scale fluidised bed plant, Fuel Process. Technol. 92 (2011) 1954–1962.

[12] F.M. Berruti, L. Ferrante, F. Berruti, C. Briens, Optimization of an intermittent slug injection system for sawdust biomass pyrolysis, Int. J. Chem. React. Eng. 7 (2009) A84.

[13] D. Geldart, N. Harnby, A.C. Wong, Fluidization of cohesive solids, Powder Technol. 37 (1984) 25–37.

[14] L. Conti, G. Scano, J. Boufala, Bio-oils from arid land plants: flash pyrolysis of EUPHORBIA CHARACIAS bagasse, Biomass Bioenergy 7 (1994) 291–296.

[15] D. Mohan, C.U. Pitmman, P.H. Steele Jr., Pyrolysis of wood/biomass for bio-oil: a critical review, Energy Fuels 20 (2006) 848–889.

[16] Z. Luo, S. Wang, Y. Liao, J. Zhou, Y. Gu, K. Cen, Research on biomass fast pyrolysis for liquid fuel, Biomass Bioenergy 26 (2004) 455–462.

[17] R. Xu, L. Ferrante, C. Briens, F. Berruti, Flash pyrolysis of grape residues into biofuel in a bubbling fluid bed, J. Anal. Appl. Pyrol. 86 (2009) 58–65.

[18] P.C. Badger, P. Fransham, Use of mobile fast pyrolysis plants to densify biomass and reduce biomass handling costs – a preliminary assessment, Biomass Bioenergy 30 (2006) 321–325.

Chapter 7

7 Chapter 7: Conclusions and Recommendations

This chapter presents the main conclusions drawn from the work performed and reported in this thesis. Highlights of other applications and work performed as a result of the ICFAR feeding technology are also discussed. Recommendations for future research are then summarized.

7.1 Conclusions and Highlights

In a fluidized bed pyrolysis process, raw biomass material particles must be conveyed or injected into the reactor, using the least energy intensive and most practical feeding system. Currently there are two main types of feeders being used in industry: dilute phase pneumatic transport feeders and screw/auger feeders. However, these conventional feeding systems tend to encounter some operational problems.

Dilute-phase pneumatic transport feeders utilize a large amount of gas, which is typically recycled product gas, in order to suspend and convey particle materials in the feeding tube. This operation results in high energy consumption within the reactor and requires a more sophisticated condensation train due to extensive product vapour dilution.

Screw/Auger feeding systems are quite common with many pyrolysis reactor systems, given the advantage of having very low gas consumption (if any). Similarly to dense-phase pneumatic feeders, the solids in the screw feeder are forced down the feeding tube relatively slowly, resulting in potential reaction and chemical changes in the

feedstock prior to entering the reactor body. This may result in plugging and down-time, particularly with temperature-sensitive feedstocks such as meat and bone meal residues, Kraft lignin or dried distiller's grains. In addition, the screw/auger feeders are mechanical, with continuously moving parts, which results in a higher maintenance and downtime requirement over long-term operation.

In this thesis work, the novel ICFAR intermittent solid slug feeder was designed and constructed to mitigate feeding issues on fluidized bed pyrolysis reactors for pyrolysis. The feeder has been demonstrated to effectively convey various types of biomass, with sawdust, dried distillers' grains (DDG), meat and bone meal residues (MBM), *tucumã* seeds, and Kraft lignin as the focus of this text. No other technology has been able to feed meat and bone meal residues or unmodified Kraft lignin into fluidized bed pyrolysis reactors.

In order to study and optimize the feeder operation, the residue high-velocity slug flow fundamentals have been observed and characterized in the laboratory-scale feeder (<20 kg/h). In addition, a predictive model for the slug flow and velocity in the feeding tube was successfully developed by utilizing a sequential approach with validation from dedicated experimental data, using DDG, MBM and an 'ideal' nylon ball slug. The predictive model can be used as a design tool to develop an effective feeder for a given material and application, while being able to balance physical constraints with capital and energy costs. Based on this information and design fundamentals, a large-scale intermittent solid slug feeder was designed and constructed in order to apply the feeder

to larger industrially-relevant equipment. The previously developed predictive feeder model was validated with the scaled-up feeder. In addition, the application of the predictive model, led to an angled slug chamber design improvement that allows for improved slug size control, allowing a user to develop an effective feeder for any given material and application, while being able to balance physical constraints with capital and energy efficiencies.

The new large-scale feeder technology allows for the feeding of large biomass particles that traditional feeder technologies cannot handle. An issue with large particles is that they require relatively long drying, which must be optimized. A model was therefore developed for the feed preparation and drying required for large-scale feeding and pyrolysis utilizing carrot cylinders as the model feedstock. The effects of air temperature and air flowrate on the drying of blanched, peeled or unaltered carrot cylinder samples in a drying tunnel were successfully investigated and modelled. A new and simple model, based on the Crank computational model, has been proposed that effectively allows the shrinkage and internal and external mass transfer limitations to be considered in order to predict the diffusivity and mass transfer coefficient of biomass samples during drying. Overall it was found that the mass transfer coefficient increases with increasing air speed, and that diffusivity increases with temperature, as expected. The activation energy for moisture diffusion was found to be 31.76 kJ/ mol, which is comparable to values found in literature for the drying of various foods. The developed Crank computational model should be utilized further for the purpose of understanding the drying characteristics of several types of biomass, potentially leading to the

development of intense drying techniques for the biomass, which can then be employed upstream of pyrolysis reactors, using waste heat from the pyrolysis reactor and its condensation train.

The new feeder technology also made it possible to perform the first ever pyrolysis studies on pure meat and bone meal residue and unmodified and undiluted Kraft lignin in industrially-relevant equipment.

The implementation and application of the feeder for fast pyrolysis in laboratory-scale pyrolysis reaction for pure meat and bone meal residues, with in-depth analysis of the process and products, has been demonstrated. The effects of processing temperature on the pyrolysis products generated using meat and bone meal (MBM) feedstock have been investigated in a continuous laboratory-scale bubbling fluidized bed reactor operating at a constant vapor residence time of 2 s. Feeding issues, due to the cohesive and temperature sensitive nature of MBM, encountered in previous studies, have been overcome by using the ICFAR Novel intermittent solid slug feeding technology. The pyrolysis temperature greatly affects the product distribution. For a 2 s vapor residence time, 550 °C is the optimum pyrolysis temperature to maximize liquid bio-oil production from MBM.

The liquid bio-oil form MBM is homogenous and has low water content. The bio-oil is an attractive fuel with a significant high heating value (HHV) of 31.5 MJ/kg and an average liquid yield of 43 wt% at 550 °C. The highest water-free HHV (36.7 MJ/kg) was found at 500 °C, with a liquid yield of 35 wt% at this temperature.

To achieve a sustainable process, the combustible non-condensable product gases need to be burned to generate the process heat requirements. The optimized pyrolysis temperature, at which the heat from the gas combustion can comfortably (with safety margin) provide the heat required for processing MBM, while maximizing the bio-oil liquid yield and process energy yield, is 550 °C. Under these conditions, the pyrolysis process practical energy yield is 91%.

The study also demonstrates a new technique to accurately determine the heat of pyrolysis reaction energy required by the process, using a non-invasive water calibration method.

The results of pyrolysis studies utilizing the feeder with *tucumã* seeds and Kraft lignin as feedstocks are included in Appendix II and III, respectively.

7.2 Recommendations

The following points represent the recommendations for further work that would complement and extend the research described in this thesis:

1. The study of effects of the feeder on the stability of the fluidized bed reactor and its condensation train is recommended. As a result of this information, one would then be able to determine whether it is more attractive to utilize one large feeder at a given cycle time to meet the feeding rate requirement, or to utilize an array of smaller feeders. The feeder performance, expressed as the ratio of solids mass to pulse gas mass, has been shown to improve with feeder size, suggesting that one should utilize the largest feeder possible to meet the feeding rate requirement. However, from a mixing and reaction perspective, several feeders operating out of phase may be advantageous. Operating out of phase would moderate the reactor pressure fluctuations resulting from the formation of product gas and vapours from the feeder slug decomposition, which in turn could lead to improved fluidized bed stability and fewer vapour-loading related challenges in the condensation train.

2. A study to validate the feeder model with numerous other biomass feedstocks, especially with large particles, on the large-scale feeder is recommended. With a larger index of biomass feedstocks, a simplified relationship between the friction factor (λ_S) and the critical pressure to move the slug (ΔP_C) can be further validated. An emphasis should be placed on attempting to determine these

factors directly from particle characteristics that can be obtained from standard particulate laboratory measurements, such as from avalanching or dynamic shear cell measurements.

3. The effects of alternative feeding tube geometries should be investigated. For example, having a curved or inclined tube at the end of the feeding tube to feed above the fluidized bed but effectively penetrate the bed surface was demonstrated to work effectively for Kraft lignin (Appendix III). In addition, minor restrictions/throttles, or a screw-shaped winding feeding tube, could be utilized along the feeding tube to re-suspend the solids and maintain a unified slug, to avoid stragglers and gas leakage, while minimizing further the feeder gas consumption. The study and optimization of the feeding tube design is recommended.

4. In this work, the feeder has been primarily designed and optimized for use with fluidized beds for pyrolysis at high temperature and pressure slightly above atmospheric conditions. However, the feeder should be studied and utilized for various other processes for the conveying or injection of materials, such as the injection of catalyst or prepolymer in polyolefin fluidized bed reactors. At high pressure, the feeder should be pressure-balanced dynamically with a scuba-type diaphragm pressure mechanism that always ensures a slightly positive pressure in the feeder silo (using an inert gas blanket or product gas) relative to the reactor. Alternatively, the entire feeder and reactor assembly could be

contained within a vessel under pressurized conditions, meaning that the simple pressure balancing equipment and inexpensive feeder construction materials can be utilized.

5. The feeder should also be tested when applied to other high temperature processes such as gasification and combustion, to explore other potential applications for the feeder.

Appendix I

8 Appendix I: Green-Tech: Bio-Fuels High Growth Strategy (A Business Case Study and Teaching Note)[7]

8.1 Introduction

In mid-May 2011, Fernando Bruteque, the vice-president and one of the principal engineers of Green-Tech Inc. (Green-Tech), an entrepreneurial 'bio-fuel from wastes/residues' start-up company, was pondering the best growth strategies for the business. He faced the challenge of trying to position the company to attract and deal with potentially large customers down the line, such as the Royal Dutch Shell plc. (Shell), but also to serve small customers looking to better manage their residues or to convert their residues into higher-value products, all while maintaining positive cash flow in the short-term. Additionally, Green-Tech's main product technology was still in the final prototype stages, creating further challenges and uncertainties. Bruteque pondered what would be the appropriate growth strategy for Green-Tech, given its limited resources.

8.2 Green-Tech Inc.

In 2006, Green-Tech was founded and owned by private investors and a local research-intensive University. It had a pilot plant operation at a shared research facility in

[7] A version of this work has been published by Ivey Publishing:

Berruti, F.M., Liu, H. (2012). Green-Tech: Bio-Fuels High Growth Strategy (Case and Teaching Note). *Ivey Publishing*. 9B11M123/8B11M123.

Ontario, Canada. The University and well-known research facility allowed Green-Tech a huge competitive advantage due to its ability to collaborate with the research faculties to stay well ahead of competitors with its cutting-edge technology, as well as the ability to exploit many academic and industrial contacts and funding opportunities from the University. Green-Tech had been dedicated to developing, manufacturing and marketing mobile and stationary reactor process equipment for the production of bio-oil (a type of bio-fuel) and other products from biomass wastes and residues. In September 2009, Green-Tech became an official entrepreneurial start-up company, consisting of one chief executive officer (CEO), two vice-presidents, three part-time engineers and two technologists. There was increasing market demand to derive energy from renewable resources and Green-Tech seemed to offer a solution.

8.3 The Core Product & Technology: THE MPT1

Green-Tech developed a disruptive technology that could efficiently and cost-effectively convert low-value organic wastes and residues at the source (hence 'mobile') into high-value bio-outputs that could be used as alternative fuels, special chemicals and pharmaceuticals, food additives and soil-additives or fertilizers. The process, called 'fast pyrolysis,' could convert agricultural crops, waste and other biomass sources into bio-oil, bio-char and a product gas (that could be recycled and burned to create the energy required to run the process completely sustainably) (see Exhibit 1).

Green-Tech's core prototype product was the patented MPT1 (mobile pyrolysis technology), which had advantages of heat control, easy operation, easy maintenance,

single-person operation and low capital cost (see Exhibit 2). The MPT1 created many business opportunities and potential clients (with different residues to be processed) for Green-Tech (see Exhibit 3). Mobile pyrolysis could bring the pilot plant to the source (saving tremendously on bulky biomass transportation costs), convert bio-residues to bio-oil (which was effectively a concentrated output for easy storage or piping transport) and create additional valuable by-products (such as bio-char soil additives or fertilizers, if further refined). The MPT1 unit could process up to 10 tonnes per day (dry-basis) of biomass residue, producing roughly 60 per cent bio-oil, 20 per cent bio-char and 20 per cent product gas by weight. The product gas was combusted in the process to provide the energy to continue to drive the reaction. The product yields often differed depending on the feedstock being processed and the operating conditions. The bio-oil contained 60 to 80 per cent of the energy content of conventional oil (and therefore its price could be pegged to that of conventional oil based on its energy value), which was very attractive as a new source for oil companies, and also contained many useful chemicals and potentially pharmaceuticals that could be easily extracted from the liquid. In addition to these points, the advantages of the manufacturing and use of bio-oil could be summarized as follows:

- bio-oil was produced in a carbon dioxide (CO_2) neutral fashion (in fact, CO_2 was captured in the bio-char product, allowing clients to apply for carbon credits

where applicable); it contained no sulfur and produces less NO_X[8] than fossil fuels when combusted.

- bio-oil was directly combustible and could burn with a stable and sustained flame.
- bio-oil could be produced from wastes and residues, eliminating the negative impact on food supply and pricing of other marketed bio-fuels.
- bio-oil could be transported and refined using existing petroleum shipping and refinement infrastructure, with minor modifications.
- In the event of bio-oil spills or accidents, the product was completely biodegradable.
- The use of bio-oil reduced the negative environmental impact of burning biomass and agricultural wastes.
- The bio-oil production process destroyed pathogens that could be found in the residue being processed as feedstock.

---

[8] NO_X is the term used to describe nitric oxide (NO) and nitrogen dioxide (NO_2). These compounds are extremely harmful pollutants that create smog and acid rain, and destroy the ozone layer. They also can contribute negatively to lung diseases such as emphysema and bronchitis. NO_X is produced during combustion processes of conventional fuels at high temperatures, such as in car engines. As a result, the emissions of NO_X are highly regulated by the Environmental Protection Agency in the United States and by Environment Canada in Canada. Cleaning of emission gas streams by catalytic conversion or adjusting combustion conditions (adding water or additives in the fuel) to reduce NOX emissions can be costly.

- The manufacturing and use of bio-oil mitigated the negative impact of directing many wastes and residues to existing landfills — instead they could be utilized to create high-value products.

In 2009, Green-Tech had become one of the world leaders in mobile pyrolysis technology, being well ahead of competitors in proving and commercializing its technology. In addition to the mobile system, Green-Tech knew that its technology could be scaled-up easily for large stationary bio-oil production if certain clients had very high and continuous production of residues at one location.

8.4 New Market, Product Availability and Research & Development

Estimates show that Canada alone had more than 12 million bone-dry tonnes (bdt) of "accessible" forestry waste (mobile units were key to access many forestry areas economically and to process seasonal residues) and nearly 30 million bdt of agricultural waste available for bio-oil production[9]. Assuming the described yields from pyrolysis technologies, this bio-residue if converted to bio-oil could generate nearly 200 terawatt hours (TWh) of renewable electricity, which was enough to easily meet the near-term legislated renewable energy needs of both Europe and the United States, or an estimated bio-oil value of $US6.4 billion annually. If the bio-char product was added to the equation, an extra $US2.1 billion worth of energy would be generated annually. Translated into MPT units, the number needed to fill this market demand at its existing

[9] *D. Bradley (2006). European Market Study of BioOil (Pyrolysis Oil). Climate Change Solutions, IEA Bioenergy Task 40.*

capacity would exceed 2,200. These numbers were for Canada alone, ignoring the potential contribution of selling units directly to self-consuming markets such as China, India, Europe and Central and South America.

As a result of the large market and exciting technology, many clients from all over the world were interested in the prototype that Green-Tech was developing. Bruteque, who had a background in chemical engineering and business, was an original investor in Green-Tech and took the role of vice-president in 2009, taking control of the company's technical operations and design, as well as bridging the gap between the business and technical personnel and dealing with customers and manufacturers. Bruteque worked at Green-Tech part-time and did not take a salary, though he was invested in the company and had been compensated by "sweat equity" stock options after his first two years of work. In addition to Bruteque, Green-Tech had two other investors that acted as part-time design engineers for the company, but no full-time engineering staff were employed. These two investors were engineering academics, always pushing for more research and development (R&D) to perfect the technology but having no business commercialization experience. Two technologists were on staff to develop the products, draw new designs and generate manufacturing drawings and models and troubleshoot equipment prototypes. In addition, Green-Tech employed a part-time chief operating officer (COO) in charge of overall project and grant management. Green-Tech's CEO, with whom Bruteque and the Green-Tech COO worked closely to make business decisions and steer the organization, was employed by the University's technology

transfer division (which was responsible for the assistance and support of University spinoff companies).

Green-Tech had its principal prototype unit (MPT1), which was used for preliminary testing and for proving the technology, built in 2009. The company had learned a tremendous amount from the MPT1 and had already designed and drawn most of the changes for the next generation system which would be called MPT2. The company was constantly being contacted by clients interested in the technology, but as it was still new and developing, few clients were willing to risk an outright purchase of a unit. However, in 2011, an American University had contacted Bruteque and ordered an MPT2 that it could use for experimental testing while collaborating with Green-Tech by giving feedback on how the technology could be improved and helping to prove the technology by testing selected feedstock. Due to the partnership and the fact that the technology was still experimental, Green-Tech had agreed to sell the unit to the American University at a reduced cost of Cdn$650,000, relative to the official market price for the fully-commercial MPT that would be Cdn$900,000. The American University had agreed to pay Green-Tech almost entirely in full in 2011 (Cdn$500,000 up front), so that the costs of finishing the design and manufacturing drawings of the MPT2 in addition to ordering all the parts for production would be covered. In return, Green-Tech offered a full operators manual and three-week training on location for the delivered unit. The unit was to be delivered in early 2012.

Even though the technology was not yet perfected, the time had come to begin to enter the market more extensively with the MPT2. The options that Bruteque considered for this entrance included continuing to push for product sales (with the risk of liabilities and the need to include warranties or excessive customer service), attempting to further create some unit sales via research partnerships through University contacts, proving the technology around the world (but also potentially exposing the technology to 'reverse-engineering') or to investigate financing or leasing options of the units to clients, negotiating contracts based specifically on the client needs. Bruteque needed to quickly recommend to the company how to proceed to capture global markets early while generating cash flow. He also knew that once the company began entering the market, it was critical to grow quickly to capture a large market share rapidly and create barriers to entry for competitors or 'copycats,' while continuing with R&D to always remain a cutting-edge technology leader.

8.5 MPT Costing & Business Model

Green-Tech's business model was based on the concept of selling MPT mobile units to clients around the world that had a residue that they wanted to convert to high-value products (see Exhibit 4). The residue could be a by-product of a client's core business, such a sawdust for a wood-flooring business, or a problem for the client that required disposal, such as chicken litter or meat and bone meal residues (due to potential bacteriological or viral hazards). Green-tech was also open to alternative business arrangements with clients on a case-by-case basis, especially in this early high-growth phase while entering the market. Options could include leasing arrangements, deals

that negotiated ownership of the products or which party was in charge of operating the unit or simple bio-oil and bio-char product 'buy-back' discussions.

According to Green-Tech's estimates, it could fully manufacture the MPT units for roughly Cdn$380,000 (including materials, construction, testing, manuals and training). Once Green-Tech was fully commercial and producing many units, it was expected that the manufacturing could be streamlined and the materials/manufacturing costs would decrease.

8.6 Other Products & Business Opportunities

Based on the same pyrolysis technology as the MPT1, Green-Tech had already built, proven and established a smaller laboratory-scale bio-fuel production system called the LPT1 (little pyrolysis technology). This product was a one to 10 kilogram per hour fluidized bed fast-pyrolysis pilot plant designed to bridge the gap between lab-scale analysis and the fully-commercial bio-fuel production. Research facilities and Universities could easily and efficiently convert a wide variety of biomass feedstock into bio-oil, bio-char and bio-gas while carefully controlling critical reaction parameters such as temperature and reaction time. Many academic contacts had expressed interest in this technology by contacting Bruteque, as they knew that trying to design a unit from scratch would be much more costly than relying on the expertise at Green-Tech, but the company had not pursued extensive marketing of the LPT1 as of May 2011.

In order to feed the biomass residues into the reactor system, Green-Tech designed a special feeding system component of the reactor system called the SHOT-BETA. This

feeding technology was more energy efficient and resulted in much less plugging and downtime than commercially-available industrial alternatives, as well as being a much smaller capital investment. In 2011, this feeder technology was used on the MPT1 prototype, the LPT1, all reactors used at the University research facility and on the MPT2 design. The feeding technology was not patentable due to some technicalities and therefore was kept as a company trade-secret. The challenge regarding the feeder was that it could easily be replicated and built by competitors, but the real secret lay in how to properly operate the feeder.

In addition to the Green-Tech renewable biomass reactor applications, the company believed that its innovative feeder would be able to safely inject a large variety of solid materials into virtually any process. For example, the feeder could be used to inject many types of cohesive or free-flowing biomass, powders, granules, catalysts and particles such as polymers, rubber, coal and oil-shale into their respective processes.

Everywhere that Bruteque travelled there was huge interest in this feeder (due to many people having industrial feeder issues in various fields), and it appeared that there could be an impressive market for this technology as well. However, Green-Tech also had not pursued marketing this technology as of May 2011 due to the risks of getting involved in too many businesses and spreading its resources too thin.

8.7 Customer Selection

Prior to 2011, Green-Tech mainly had two types of potential customers. One type consisted of smaller potential clients who had their own farms or farm-cooperatives and

needed mobile units to convert their residues, such as grape skins and seeds, sugarcane bagasse, corn stover and meat and bone meal residues, into higher-value products. The bio-char produced by the process could be used directly in the fields as a soil additive to enrich the farmers' soil. The bio-oil produced could be burned by the farmers in boilers to produce energy to run their operations or could be bought back by Green-Tech or some other oil-refining company such as Shell, Exxon-Mobil, Total or Petrobras. The bio-oil could then be transformed into conventional (yet green and carbon neutral) fossil-fuel products such as gasoline, diesel or jet fuel. The other type of customers consisted of large oil companies worldwide that were interested in diversifying their energy portfolio to include alternative energy products such as bio-oil into their refining processes, but this market was still in the early stages of development. However, there was a large demand for bio-oil production as some companies were ready to begin refining bio-oil as part of their products and others required large quantities of bio-oil for testing purposes. Both types of customers were regarded as good business opportunities, but negotiating individual contracts and dealing with many types of customers could strain resources.

8.8 Competitors

In 2011, Green-Tech's mobile pyrolysis technology faced competition from two main types of competitors: large-scale fixed pyrolysis plants and pseudo-mobile small-scale competitors (no truly mobile technologies existed in the market).

A company called Ensyn based in Ottawa, Canada, used a large-scale patented process called Rapid Thermal Processing to transform 100 bdt per day of carbon-based feedstocks (mostly wood) into chemicals and food additives. The bio-product was then sold to a Texas-based seasoning and flavour company[10]. Press releases suggested that Ensyn was interested in developing several more fixed plants around the world with large capacities in the following years[11].

Another high-profile Canadian player in the bio-oil market was the publicly-held Dynamotive (OTCBB: DYTMF) that operated a 200 bdt per day plant in West Lorne, Ontario, and was in the process of constructing two more large-scale plants in Canada. Due to plant performance setbacks and the lack of a large, stable and continuous supply of feedstock to be shipped to its centralized facilities, Dynamotive's operations in Canada ceased[12]. Press releases appeared to indicate that operations were resuming for Dynamotive on some projects in Australia[13].

Several other players from around the world such as Three Seconds to Oil and BEST Pyrolysis appeared to be developing technologies for pyrolysis and advertising online, but the technologies were still under development.

---

[10] www.ensyn.com, accessed May 19, 2011.

[11] www.ensyn.com/2011/03/10/honeywells-envergent-technologies-selected-by-malaysian-company-for-renewable-energy-project, accessed May 19, 2011.

[12] Dynamotive Q3 2009 Quarterly Report. www.dynamotive.com/assets/resources/2009/Q3-2009.pdf, accessed May 19, 2011.

[13] www.dynamotive.com/2011/02/22/dynamotive-and-renewable-oil-corporation-agree-heads-of-terms-for-joint-venture-for-australia/, accessed May 19, 2011.

The only pseudo-mobile (modular parts on skids) technology was that of Advanced BioRefinery Inc. (ABRI), which consisted of a very different mechanical auger reactor design compared to Green-Tech's technology. Green-Tech's reactor was developed through extensive reactor design experience in the heavy oil industry, using a special design of the very well-known and established bubbling fluidized bed reactor. ABRI's technology could process one bdt per day and was not fully commercial in 2011. The company was seeking financing and partnerships to build several larger-scale auger pyrolysis units. Given the potential size of the market and the need for growth and development in the field, ABRI and Green-Tech were on very good terms and were considering ways of collaborating on future projects.

8.9 Future Challenges & Decisions

In 2011, Green-Tech employed a team of three management staff (including Bruteque who acted as the principal design engineer), two part-time academic inventor engineers and two full-time technologists, along with just enough cash on hand to internally finance the building of two MPT2s (see Exhibits 5 and 6). With these resources, Bruteque was thinking about the appropriate growth strategy in terms of employment and team organization, R&D strategies, new product-line introduction, business opportunities and customer selection. Given Green-Tech's desire to take the lead in the new and growing bio-fuel market and supply chain, the company needed to stay ahead of competition in technology development while rapidly beginning to enter the market, gain exposure and generate cash flow. The clock was ticking. How could Bruteque help position the start-up company for success?

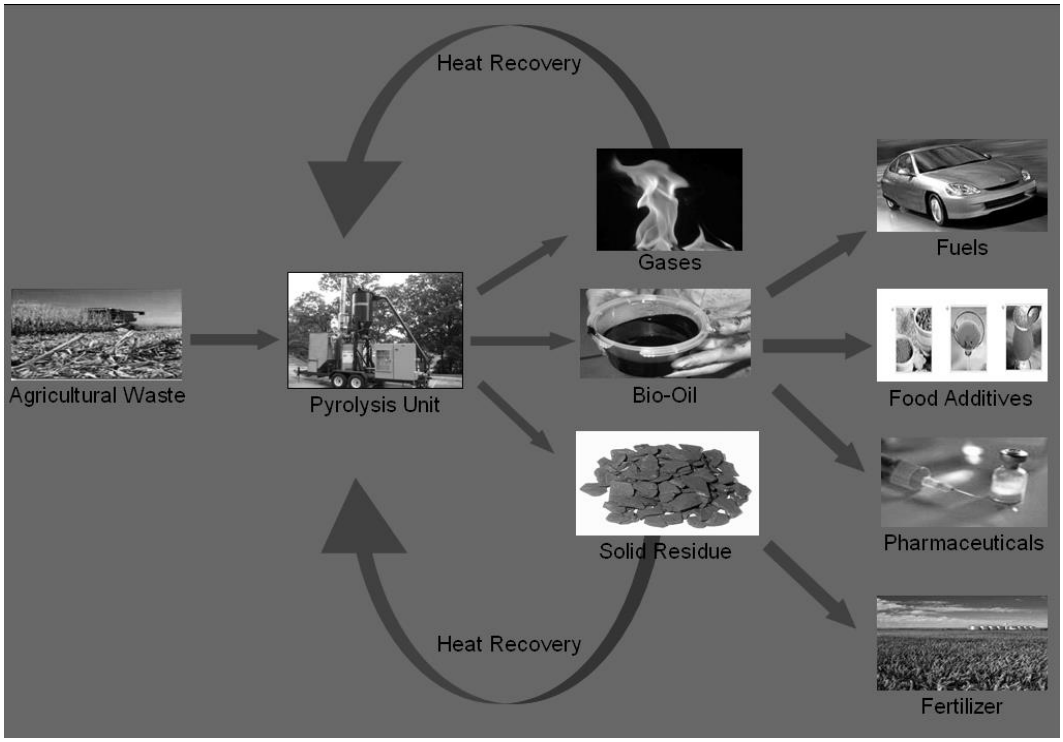

Figure 8-1: EXHBIT 1 - The Fast Pyrolysis Process[14]

[14] Source: F.M. Berruti (2007). Institute for Chemicals and Fuels from Alternative Resources (ICFAR), Western University

Figure 8-2: EXHIBIT 2 - Green-Tech's Mobile Pyrolysis System[15]

[15] Source: F.M. Berruti (2008). Institute for Chemicals and Fuels from Alternative Resources (ICFAR), Western University

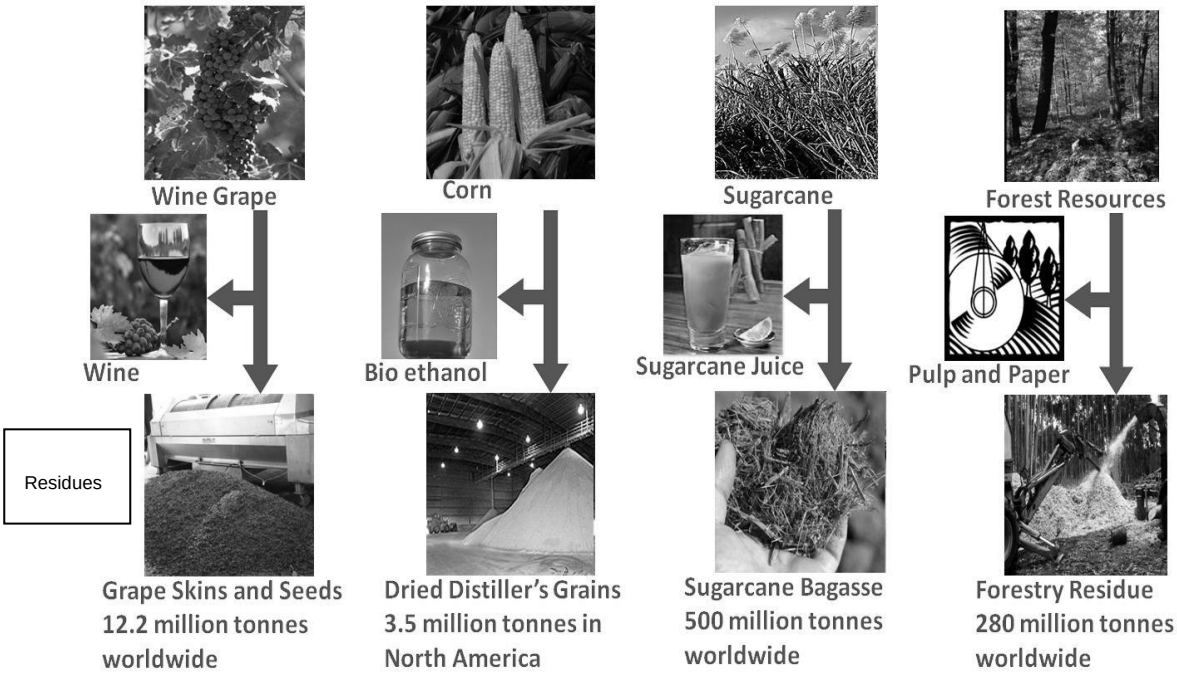

Figure 8-3: EXHIBIT 3 - Business Opportunities[16]

[16] Source: F.M. Berruti (2009). Institute for Chemicals and Fuels from Alternative Resources (ICFAR), Western University

1 metric ton of forestry residue (dry basis)	$	60
Produces:		
~600 kg Bio-oil (@ $0.25/kg[1])	$	150
~200kg Bio-char (@ $0.6/kg[2])	$	120
Carbon credits for bio-char (@ $0.07/kg[3])	$	14
TOTAL PRODUCT VALUE	$	284
NET PRODUCT VALUE	$	224
Operate 5 days/week, 10 tonnes/day, 20% down-time:		
Annual operating revenue	$	465,920
Estimated annual expenses and labour	$	170,000
Estimated after-tax income	$	210,103
For experimental unit:		
Capital expense	$	650,000
Simple payback (years)		3.1
For fully commercial unit:		
Capital expense	$	900,000
Simple payback (years)		4.3

1 Green-Tech forward contract for bio-oil purchase from an American oil refining broker

2 Horticultural Char TIME (Dec. 2008)

3 EU Carbon Trading (www.pointcarbon.com)

Figure 8-4: EXHIBIT 4 - MPT Economic Considerations for Green-Tech Clients[17]

[17] Source: F.M. Berruti (2011). Institute for Chemicals and Fuels from Alternative Resources (ICFAR), Western University

REVENUE		
Sales revenue		
Sales (MPT2)	$	650,000
Net sales	$	650,000
TOTAL REVENUE	$	650,000
EXPENSES		
Cost of goods sold		
Purchases (MPT2 materials)	$	206,000
Total cost of goods sold	$	206,000
General & admnistrative expenses		
Manufacturing & electrical	$	112,800
Accounting & legal	$	2,250
Contract engineering	$	65,000
Contract engineering recovery (grant)	-$	30,424
Research & development expense and equipment	$	25,000
Research & development recovery (grant)	-$	10,000
Professional & directorship salary (COO)	$	70,000
Technician salaries	$	95,450
Internship support (engineering student researcher for 6 months)	$	10,000
Consulting fees - national research grant payment	$	9,345
Interest & bank charges	$	119
Office supplies	$	1,009
Computer purchases	$	2,301
Software license	$	800
Travel, meals & entertainment	$	443
Equipment and engineering insurance	$	7,506
Advertising & promotion	$	2,525
Subcontractor expenses	$	389
Telephones	$	900
IT support	$	450
Office space (rent)	$	12,000
Total general & admin. expenses	$	377,863
TOTAL EXPENSES	$	583,863
Earnings before interest and taxes (EBIT)	$	66,137
Income tax	$	19,180
NET INCOME	$	46,957

Figure 8-5: EXHIBIT 5 - Income Statement - Year Ending April 30, 2011 (CDN$)[18]

[18] Source: Adapted from company files.

ASSETS		
Current assets		
Cash (chequing)	$	132,000
Account receivable	$	150,000
Equipment	$	140,942
Total current assets	$	422,942
TOTAL ASSET	$	422,942
LIABILITY		
Current liabilities		
Accounts payable	$	117,998
Customer deposits	$	72,500
GST collected	$	2,753
GST/HST paid/recovered on purchases	-$	10,432
Accruals	$	22,555
Total current liabilities	$	205,374
Liabilities		
Note payable (to university)	$	51,042
Due to grant organization	$	25,000
Total liabilities	$	76,042
TOTAL LIABILITY	$	281,417
EQUITY		
Share capital		
Common shares	$	94,568
Total share capital	$	94,568
Retained earnings		
Retained earnings	$	46,957
Total retained earnings	$	46,957
TOTAL EQUITY	$	141,525
LIABILITIES AND EQUITY	$	422,942

Figure 8-6: EXHIBIT 6 - Balance Sheet - Year Ending April 30, 2011 (CDN$)[19]

[19] Source: Adapted from company files.

8.10 TEACHING NOTE

> *"The skills needed to bring something to market are different from the skills needed to come up with great ideas."* – Joe Compeau, Professor at the Richard Ivey School of Business[20]

8.11 Case Synopsis

Green-Tech Inc. (Green-Tech), a Canadian company founded in 2006, was dedicated to developing, manufacturing and marketing portable and stationary systems for the production of bio-oils and bio-char from biomass residues and wastes. Green-Tech is a recent spinoff company from a large university research centre with a very good reputation in providing bio-energy solutions. Although quite well-positioned and focused, Green-Tech has to deal with relationships with large companies such as Shell that in effect control a large and complete supply chain of oil-related business, as well as small firms and clients that are unable to manage their waste effectively. Large firms may provide plenty of business opportunities for Green-Tech, but they may also jeopardize the company's autonomy. Small customers on their own may not bring in enough cash flow but may provide Green-Tech with sufficient freedom to pursue its own strategic goals. Both relationships seem to lead to a promising future for this entrepreneurial start-up company but also create serious risks and consequences.

At the time of this case, Fernando Bruteque, vice-president and one of the principal engineers of Green-Tech, is seeking the appropriate growth approach for Green-Tech. Being in charge of business operations, Bruteque, who has an extensive background in

---

[20] ***Madhavi Acharya-Tom Yew***, *Armed with a Patent War Chest, Kodak Mulls its Options*, *Thestar.com, July 20, 2011*, *www.thestar.com/business/companies/rim/article/1027968--armed-with-a-patent-war-chest-kodak-mulls-its-options*, *accessed January 18, 2012.*

chemical engineering, also has to maintain a balance between research and development (R&D), investor and client concerns and business opportunities. What would be the appropriate growth strategies and business operation strategies for a resource-constrained firm such as Green-Tech? Why? How should they proceed?

8.12 Key Words

High-growth, Organizational planning, Goal-setting, Cash flow, Financing, Product lines, Product distribution, Customer management, Intellectual property, Research and development.

8.13 Potential Audience and Instructor's Material

This case was developed for use in entrepreneurship, international business and strategic management courses. It is suitable for MBA, EMBA and advanced HBA programs. At the beginning of case discussion the instructor may find that students are very optimistic about the future of new technologies and believe that implementing new and improved processes is easy. Thus, it is essential for the instructor to bring up the hidden issues that inventors, developers and entrepreneurs usually face in reality. In particular, this case makes inexperienced students aware of the difficulties and challenges that entrepreneurs may deal with while acknowledging the tremendous opportunities that innovative technology may bring. As for EMBA students, the instructor may start by asking students to lay out the potential issues as well as business opportunities. Before tackling these identified issues, however, the instructor should

focus students' attention on the positioning of Green-Tech, from which one can delineate the scope of business and strategy alternatives.

8.14 Teaching Objectives

The case is structured to teach the following learning objectives:

1. The nature of an R&D centred, entrepreneurial start-up company;
2. New technology and new market drivers and competition;
3. The dilemmas that small start-up firms usually face;
4. Corporate growth strategy;
5. "The learning-by-doing process";
6. The challenges and importance of start-up cash flow and acquiring quality resources.

8.15 Suggested Assignment Questions

1. Describe Green-Tech's related industry and market. What are the trends? How do government policies affect these markets?
2. Describe and analyze Green-Tech as a corporation. What is the company structure? Is the company financially healthy?
3. Describe the dilemma that Green-Tech faces regarding R&D improvement versus product availability (R&D strategy versus new product introduction).
4. Describe the decisions that Green-Tech faces regarding which products to focus on and market and the business opportunities therein. Are the business opportunities and market size significant? What are the pros and cons of a focused versus diversified growth strategy?

5. Describe the decisions that Green-Tech faces regarding customer selection. What are the advantages of working with either with big market customers or small customers? How could these decisions affect Green-Tech's autonomy and sustainability as a corporation?

8.16 Analysis

1. **Describe Green-Tech's related industry and market. What are the trends? How do government policies affect these markets?**

There is an increasing need to derive energy from renewable resources, and the instructor may start by identifying the industry trends (see Exhibit TN-1). Economic downturns, government incentives and certain industry promotions highly affect the growing bio-oil market — there is a large and important political element with buzzwords such as 'environmental,' 'green,' 'renewable,' 'sustainability' and 'dependency on foreign oil.'

2. **Describe and analyze Green-Tech as a corporation. What is the company structure? Is the company financially healthy?**

Green-Tech is a spinoff with a somewhat messy corporate structure. There are some full-time and some part-time employees, of whom some are paid and some receive sweat equity. In start-up companies, especially when cash flow is a challenge (as in this case), creative corporate structures and deals tend to occur more often. As Green-Tech grows and gains cash flow it will be very important to create a clear and solid corporate structure with accountable and responsible roles for employed individuals, while some of the shareholders who are technically involved can play managerial, board or overseeing/consulting roles.

Students should analyze the financial details of the company. The company health appears relatively strong as long as good cash flows, such as the unit sale to the American university, continue to be generated on a consistent basis. Otherwise, if there is a slowdown in generated cash flows, the company's burn rate will begin being a serious issue. Currently the cash situation is positive, allowing for some short-term flexibility, and the debt-to-equity ratio is about two, which is reasonable. Instructors and students can discuss various financing options that would be available to Green-Tech at the moment to allow it to more rapidly pursue its goals, such as loans (which could be acquired considering the relatively strong financial statements), mezzanine financing/venture capital (quite risky, since venture capitalists tend to try to mitigate their own investment risks as much as possible while still seeking a return that is only reasonable if a lot of risk is taken) or diluting the company further with new investors (a committed and involved angel investor could be useful).

3. **Describe the dilemma that Green-Tech faces regarding R&D improvement versus product availability (R&D strategy versus new product introduction).**

After a series of road shows for experimental units in 2009, many customers seemed very interested in the units that Green-Tech had developed. Though the R&D team believed that these experimental units still required further improvement, Bruteque saw the current opportunities and knew that the units could continue to improve through generations (see Exhibit TN-2). He recommended that experimental units were ready to go and helped to generate the cash flow that Green-Tech needed. Students should understand the challenges and mindsets of inventors/entrepreneurs who want

to continually improve their products (more and more R&D because the product is never perfect), whereas there is a certain point at which improvements need to stop and products need to be commercialized (even in a discounted experimental state) to generate cash flow and truly understand the market needs and what improvements would be demanded by the user and market.

4. **Describe the decisions that Green-Tech faces regarding which products to focus on and market and the business opportunities therein. Are the business opportunities and market size significant? What are the pros and cons of a focused versus diversified growth strategy?**

Huge business opportunities are available for Green-Tech in many areas and the company has to decide which projects to undertake. This is a serious dilemma for many start-ups, as they must decide whether to stay focused (all eggs in one basket, risky cash flow) or go for diversification (spread risks, smaller cash flows from many sources, become diluted) (see Exhibits TN-3 and TN-4).

5. **Describe the decisions that Green-Tech faces regarding customer selection. What are the advantages of working with either with big market customers or small customers? How could these decisions affect Green-Tech's autonomy and sustainability as a corporation?**

Though big customers may offer the local firm many benefits, they may exert huge pressure on the company as well, potentially leading to a lack of autonomy and difficulty in negotiating fair partnerships. Likewise, small customers may have different advantages and limitations (see Exhibit TN-5). In bringing up this issue the instructor

should make students more aware of the potential implications of the customer selection on the business, as there is no clear cut answer to the question.

8.17 Additional Possible Discussion Questions

6. **Perform a SWOT Analyis for Green-Tech. Do you think the company has positive prospects for the future?**

If most students in the class are advanced undergraduate students (such as HBA), the instructor could start the discussion by asking this question. Students will tend to use a strengths, weaknesses, opportunities and threats (SWOT) analysis to assess the future prospects of Green-Tech (see Exhibit TN-6). The SWOT analysis indicates very attractive growth opportunities in the renewable energy market with Green-Tech's strong value proposition, as long as it can address the threats and weaknesses effectively.

7. **With limited resources on hand for short-term operating capital, what are Green-Tech's options to fund its growth? What steps should Green-Tech take to gain the financing that it requires?**

Green-Tech should seek investors/partners/financing.

Green-Tech may seek outside partners or investors to help out with limited capital. Investors will dilute the current stock, but if properly selected with good connections, an angel investor could be very beneficial. Venture capital and private equity funds could be a solution, but they might also engender a very high level of risk because the company may lose autonomy. Alternatively, Green-Tech can also collaborate with potentially large customers such as large oil companies and also apply for government grants.

In order to attract financing, Green-Tech should do the following:

1. **Prove and demonstrate technology**

Green-Tech needs to show its proven technology to produce bio-fuels. This may interest potential investors who are looking for business investment opportunities in future technology.

2. **Create and present a feasible and focused business plan**

Green-Tech needs to come up with a viable business plan that demonstrates a convincing forecast of the new technology. Thus, a detailed cost-benefit and economic analysis is needed to persuade new investors. The business plan should address the following items:

Scope of Business Plan (Market Analysis)

New product launch

Pros and cons of Green-Tech launching its current products (see Exhibit TN-2). This is a debate between R&D and sales. Green-Tech has to make a decision on when it is ready to launch its new product.

Product Strategy

This is a decision of whether or not the company should diversify (see Exhibits TN-3 and TN-4). The focus strategy may only enable a few game-changing products that are easy to control and monitor, but result in slower entry. On the other hand, diversification will

help to release various products at the same time, which helps increase brand exposure but may result in losing focus.

Customer selection

Choosing large customers or small ones will have different impacts on Green-Tech's future (see Exhibit TN-5). It is important to make students aware that everything comes at a price.

Business model

Green-Tech has to decide on its market positioning and commit to a well-researched and refined business model for how it will unfold into the market. In doing so, Green-Tech will learn who to collaborate with and who to compete with, thus mitigating its business risks. For example, Green-Tech needs to decide if it is going to sell or rent the MPT product (as well as any other products that it decides to commercialize fully). If Green-Tech were to rent the MPT units, it could collect rental and service fees, purchase the chemical products produced and sell the products with previously-obtained forward contracts to oil companies (in this case Green-Tech would have to ensure that the products are made properly and to oil company specifications). If Green-Tech were to sell the units, it could still make an arrangement to act as a broker and obtain forward contracts to sell the buyers' pyrolysis oil and char (as long as it is made to specifications). A third option is that Green-Tech both sells and rents the units and finds a partner who will act as the products broker for the clients (there are currently some interested brokers of this type in the market for pyrolysis bio-oil). All these business

models need to be researched, analyzed and modelled by Green-Tech before one model can be selected.

Summary of Example Suggestions for Green-Tech

- Needs a convincing business model for potential investors;
- Enhance product adoption through providing cost-benefit analysis for the potential customers;
- Be aware that the current global economic environment (especially concerning European government debts and the U.S. economic downturn) may not be in favour of bio-oil industry development;
- Committed human resources including a strong management team and engineers are needed to ensure the choice of appropriate strategies and operation effectiveness. Currently only R&D is ready for growth.

8.18 Other Key Points of Discussion

- Academics, design engineers and other inventors will endlessly continue to push R&D and improve prototypes — even if the technology is not perfect, one can enter the market to generate cash flow while continuing R&D. The key is balancing the team properly.

- The Green-Tech team had several part-time engineers and managers, resulting in some bottlenecks in efficiency. A central full-time senior engineering figure should be hired (to balance the technologists and part-time engineers) so that Bruteque and the other investors can still be involved as engineers but on a supervisory level depending on their availability.

- There are many government grants available for start-ups to cover some operating costs or salaries for technologists/engineers. There are also many low-interest loans if grants are unavailable. Green-Tech should focus on applying to these types of grants in the short-term so that it can focus on internally financing products.

- It could be beneficial for Green-Tech to begin selling the commercially-ready and tested LPT1 to universities and research facilities around the world. The key is managing the contracts so that payment terms are received to comfortably internally finance the production (which can be outsourced and then assembled in-house). Even though there are no patents mentioned on the LTP1, the cash flow from many clients is on the table now and should be exploited rather than fearing reverse-engineering. Since Green-Tech has a main competitive advantage of rapid R&D (being affiliated with the University and Research Institute), Green-Tech can always be ahead of any technology that it markets. The same argument can be made for the feeding technology. The cash is on the table and older feeder generations can be sold while keeping the most cutting-edge feeder technology as an in-house trade secret. As these side-products are already developed and commercially ready, they can generate significant extra cash flow for Green-Tech without distracting from the MPT development and commercialization. Green-Tech should be careful with sales of these units to underline that they are experimental units and to minimize warranties/liabilities/customer service — otherwise, this could begin taking up

many resources down the road. The key is selling to universities and research facilities worldwide with secure payment terms and safe contracts.

- Patenting is not always the solution, given the different intellectual property (IP) protection laws around the world. It can be expensive and ineffective.

In the short-term, Green-Tech should build the next generation of MPT units (perhaps two in the short-term and then unfold 10 more in the next couple years), some being sold to partner-clients (a special type of relationship) and some being leased or financed through universities or research centres. This will allow Green-Tech to continue to tour and prove the technology while also learning from partner-clients to develop the third generation technology down the road. After a few iterations, the technology R&D will begin to stabilize and be completely commercially ready in perfect time for the bio-oil market to be peaking.

8.19 What Bruteque Actually Recommended

- To halt design and experimentation temporarily to focus resources on designing two MPT units — one that was sold to the American university partner/client and one that would be kept by Green-Tech for further testing and technology proving (for investment purposes). Once tested, Bruteque recommended that the company obtain financing/contracts (through private investors, partner-clients or university/research partners) to build 10 more units in the next two years to gain visibility and further tour the product. Once production was under

way and financing was secured, resources would again be dedicated to R&D extensively to stay on the cutting edge.

- To hire and train a senior engineer to balance the part-time engineers, management and technologists. This individual would be the core for design, with a lot of assistance and input from the other part-time engineers and investors (Bruteque included), while managing the technologists. This individual (long-term) would balance Green-Tech and would be able to connect all the designs into 'working packages' that would add value to Green-Tech's company and offering.

- To work with the other vice-president to apply to as many governmental grants and interest-free loans for 'green' start-ups in order to alleviate short-term cash flow issues and promote internally financing production.

- To market and begin selling both the feeder technology and LPT1 units, while also directing potential clients to its partnered research facility for consulting and feasibility studies for their potential residues, to grow a potential client base and generate cash flow. The 'reverse-engineering' risk was to be mitigated by continuous R&D to stay ahead of the products that Green-Tech would actually sell.

- To begin establishing a relationship with oil refineries for bio-oil upgrading and to begin R&D projects internally on bio-oil upgrading with the university (the last technological key to establish the market).

- To begin approaching investors and partners, particularly with petrochemical and manufacturing experience, to plan for large-scale production down the road. Bruteque underlined the idea that Green-Tech was truly not positioned to be a large-scale manufacturer in the future but would always be the design and R&D centre, and therefore key investors and partners with appropriate financing and skills would be necessary down the road to scale up production. Discussions with pyrolysis bio-oil brokers would also be entertained to gain more understanding in the supply chain, including how the industry works for product moving and what the associated costs are.

8.20 Conclusion

This is a good case to delineate why and how a start-up new technology firm's growth options are constrained and yet very challenging from a decision-making point of view. Even though new technologies may at times seem to be proven and ready, the level of challenge to bring them to market can still be very high. As this case reveals, management has to deal with almost every issue, ranging from strategy, marketing, R&D, finance, human resources and organization. The corporate growth of these businesses truly entails a 'learning-by-doing' process.

Exhibit TN-1

INDUSTRY TREND MARKET DRIVERS

- Increased need to derive energy from domestic sources
- Increased need to maintain industrial competitiveness
- Increased need to mitigate negative environmental impacts from fossils

fuels and sequester carbon

- Increased need to secure energy independence
- Increased desire to reduce landfill impacts
- Increased desire for green products/jobs

Source: D. Bradley (2006), European Market Study of BioOil (Pyrolysis Oil), Climate Change Solutions, IEA Bioenergy Task 40.

Exhibit TN-2

R&D IMPROVEMENT VERSUS PRODUCT AVAILABILITY

Early experimental products	
Pros	**Cons**
Early capture of the markets	Lower customer satisfaction
Generate cash flow	Better substitute product may come up soon
Provide learning opportunities	Maintenance fee is too high
Better customer loyalty	Customer benefit is low

Source: Created by authors.

Exhibit TN-3

FOCUSED STRATEGY

Pros	Cons
Technology leader	Slow to skim the market opportunities
Clear company position	Risky bet
High customer perceived value	Strong substitutes may come up
High customer loyalty	May face technology bottleneck
Healthy finance	Which one to focus on?
Good learning/experience curve	Opportunity cost

Source: Created by authors.

Exhibit TN-4

DIVERSIFIED STRATEGY

Pros	Cons
Capture high-growing market opportunities	Unclear corporate strategy
Less risk of wrong product introduction	Unclear R&D strategy
Gain market visibility	High financial burden
Demonstrate technology development competence	Complex management issues
Gain R&D options	Complex production issues
Preserve full-scale opportunities	Difficult budget control

Source: Created by authors.

Exhibit TN-5

REASONS FOR CUSTOMER SELECTION

Big customers	Small customers
Good reputation	High profit margin
Steady cash flow	High flexibility
Existing channels	High autonomy
Management support	High bargaining power
Sustainability	High future gains

Source: Created by authors.

Exhibit TN-6

GREEN-TECH SWOT ANALYSIS

Internal strength and weakness

Green-Tech's strengths

1. Advanced technology
Green-Tech's strength is advanced technology that is far ahead of competitors.
2. R&D team
Green-Tech's competitive advantage builds upon its strong R&D team that constantly provides innovative products.
3. Reputation
Green-Tech comes from a well-known University that not only gives it tremendous resources but also helps to broaden its social network.

Green-Tech's weakness

1. Financial resources
Green-Tech still seems to struggle with insufficient financial resources that will constrain its operation in the short term and hurt its autonomy in the long term.
2. Not easy to patent
Green-Tech largely cannot patent its innovative products, which can be easily imitated by competitors. Thus, Green-Tech needs to find a solution for patents in the feeding system, since it is installed in both the MPT and LPT series.
3. Human resources
Green-Tech seems to lack enough professionals to fulfill its future tasks including full-time R&D, marketing, sales, etc. This will constrain its future expansion of a larger portfolio of new products on hand and multiple business investment opportunities in the world.

External opportunities and threats

The instructor may guide the students to lay out a list of market drivers (see Exhibit TN-1). To better understand the possible market opportunities, the instructor may also like to balance the discussion by reminding the students of the accompanied risks as well. Thus, discussion may focus on the market opportunities and market threats.

Exhibit TN-5 (continued)

Green-Tech's opportunities

1. Environment concern
People are increasingly aware of the environmental issues such as the fuel shortage and pollution that oil usage may cause. These issues draw the attention of governments and oil companies, which will be interested in the new technology that Green-Tech can offer.
2. The need for a substitutive energy solution
The need for a clean energy solution is a business opportunity for Green-Tech. In particular, Green-Tech is one of the leading companies that effectively converts bio-wastes and residues into bio-fuel. In the meantime, this new technology can help farmers not only get rid of bio-waste but also generate more income.

Green-Tech's threats

1. Imitation

Replication is easy, so Green-Tech should investigate patents to protect its technology. If patents are not possible, Green-Tech should treat many aspects of its technology as trade-secrets. Green-Tech has to constantly stay ahead of marketed products being sold to protect its latest technology from imitation.

2. European government debts

Because of huge government debts, European countries may increase corporate tax as well as cut government expenditure, which will jeopardize the future of innovative products on which Green-Tech relies.

3. Oil company upgrading willingness/readiness

Although the bio-oil and bio-char that Green-Tech produces are interesting products (high energy content with many potential applications) and could be burned directly in specialty engines (for remote community energy, for example), they do require upgrading/cleaning to be converted into conventional oil products that could be used in all existing petrochemical infrastructure. Ensuring that oil companies will be interested and willing to invest to perfect and implement these upgrading technologies is a risk for Green-Tech. However, the market does appear to be moving in this direction and competition pressures between the oil companies may force some of them to break through into upgrading pyrolysis bio-oils. In addition, pyrolysis bio-oil is the only renewable bio-fuel type that can be upgraded to jet fuel quality at this time.

4. Other clean energy solutions

Some other clean energy solutions such as solar cells and wind turbines will also affect the potential prospects of Green-Tech.

Source: Created by authors.

Appendix II

9 Appendix II: Fast Pyrolysis of Amazon Tucumã (Astrocaryum aculeatum) Seeds in a Bubbling Fluidized Bed Reactor[21]

9.1 Introduction

Brazil is known as a pioneer in the production of renewable fuels. The use of biomass and its products in Brazil has gradually increased during the last 20 years, showing the high potential for the development of bio-fuels and bio-chemicals as viable alternatives to products derived from fossil fuels. However, there are still numerous challenges that need to be overcome to make such developments fully sustainable.

The Amazon rainforest, located in the North of Brazil, is the largest tropical rainforest on Earth, and is known for its rich biodiversity. The state of Amazon, completely covered by the Amazon rainforest area, is quite different from its neighboring regions in Brazil. For example, the low and disperse population density, the long distances between local production and consumption of energy, dense forests and transportation difficulties, all create a geographical context in which the energy problems of small local communities become complex. The dense Amazon rainforests and long rivers have made such communities very isolated and inaccessible. As a result, energy supply models that have

[21] A version of this work has been published in the Journal of Analytical and Applied Pyrolysis:

Lira, C.S., **Berruti, F.M.**, Palmisano, P., Berruti, F., Briens, C. (2013). Fast Pyrolysis of Amazon Tucumã (Astrocaryum aculeatum) Seeds in a Bubbling Fluidized Bed Reactor. *Journal of Analytical and Applied Pyrolysis* 99, 23-31, http://dx.doi.org/10.1016/j.jaap.2012.11.005.

been developed and successfully implemented in other areas cannot be recommended as a pre-determined solution to improve the existing energy supply [1].

In practice, solutions should involve the sustainable use of under-exploited forest products or residues to create value-added chemicals and fuels, while ensuring the continued conservation and reproduction of forest species. In addition, electricity generation from natural resources and distribution to isolated communities in the Amazon should be implemented with the training and input of local inhabitants. By working with the local communities, a more complete understanding of the cultural implications of the energy processes would be obtained, making the development of a truly sustainable and successful long-term process for the communities much more likely [2].

Attempts to find a reliable, highly accessible biomass, with reasonable properties for fuel production, have led to the consideration of the *tucumã* seed (*Astrocaryum aculeatum*) as a viable candidate for bio-fuel production, which is the core and inedible portion of an Amazon native fruit. This cheap material, with no other current use, could be ground and pyrolyzed to obtain bio-oil which is easy to store and transport, and much safer than gaseous products. Currently, there are no studies about *tucumã* seeds and their potential for bio-oil production, nor studies concerning characterization of feedstock, analysis of final products from thermal processes, or any economic considerations for the implementation of pyrolysis as a means to create value from this residue.

The *tucumã* tree is solitary, spiny and monoecious, and usually 10-25 m tall with 30 cm diameter spikes in internodes. The plant is exceptionally tolerant of poor, degraded soils and can withstand periods of drought for several months in areas receiving over 1600 mm rain each year. The *tucumã* tree is usually found in secondary forests, but it will also invade savanna and pasture land, where it appears to be quite fire-resistant. It grows at densities of up to 50 trees per hectare.

The fruits are produced throughout the year, but peak production occurs from January to June. On average, the trees produce 2 to 3 bunches per year, but can produce more than five. Each bunch weighs between 10 and 30 kg contains 200 to 400 fruits. A typical palm tree produces about 50 kg fruit per year, even in poor soil. Fruit yields could likely be improved tremendously by using modern growth management, fertilizer and selection techniques [3].

In general, *tucumã* fruits are traded in markets in Manaus, the capital of Amazon state. The fruits arrive mainly from small cities in the same state, such as Autaz Mirim, Autazes, Barreirinha, Cacau Pireira, Coari, Fonte Boa, Iranduba, Itacoatiara, Lago do Limão (Iranduba), Manacapuru, Manicoré, Novo Remanso (Itacoatiara), Paraná da Eva, Parintins, Presidente Figueiredo, Rio Madeira, Rio Preto da Eva, Tefé, Terra Preta and Urucará. Average consumers usually buy 5 to 30 bags per week, containing roughly 900 *tucumã* fruits. The price per bag is in the range from R$ 30 to R$ 70 each (or USD$ 20 to USD$ 45). About 50% of the *tucumã* fruits sold at markets are provided by farmers [4].

In the Amazon, the pulp is consumed while the fruit is fresh, but it can also be used as a filling for sandwiches and pastries, or in the preparation of creams and ice-creams. The *tucumã* seed, after obtaining the pulp, is discarded as waste in garbage containers. The raw shell of the seed (37.8% of the weight of the seed semi-dried) can be used as bio-coal. The *tucumã* almond (61% weight the core semi-dried) can be extracted with hexane to produce an oil (with a yield of 40-50 wt%) whose fatty acids are primarily composed of triglycerides (90%), and the remainder being short and medium saturated carbon chains (C8-14). These oil molecular characteristics, the high product yield, and the continuous high consumption of pulp, and, therefore, the continuous availability of the discarded *tucumã* seed raw material, has resulted in *tucumã* being extensively studied for the production of biodiesel [3]. However, the cost of production, when compared to fossil-based diesel, has been the main obstacle for the production and marketing of this biodiesel. The most significant factor contributing to the price of the biodiesel being much higher than conventional diesel is the actual biodiesel production process and the refining of the raw plant oils [5].

Another argument in favor of biodiesel production is the potential benefit to the natural environment. The main argument behind the policies in favor of biofuels is based on the idea that biofuels do not increase the concentration of greenhouse gases in the atmosphere. In fact, the amount of CO_2 emitted by biodiesel in the combustion phase is the same as that absorbed by the plant during its growth through photosynthesis, resulting in a neutral carbon budget. However, a more careful analysis of the biofuel life cycle reveals that fossil fuels are used in the trans-esterification processing step and for

transporting the raw materials from the field to the centralized processing plants and from there to the final users. If the biodiesel obtained as output of the process were reinvested in the process, the yield would be significantly lower than reported and the land requirements significantly higher [6].

Finally, biodiesel production creates a tremendous amount of waste and glycerin (1.3 metric tons created for every metric ton of biodiesel produced [7]), making the large-scale production of biodiesel difficult as there is limited demand for the by-products. As a result, these by-products would become considered wastes requiring proper disposal, with additional related economic and energetic costs [8].

Due to these serious limitations of biodiesel production, it is also important to study and develop other alternative process for biofuel production in order to address the energy issues of communities in the Amazon in a sustainable and economically viable manner. One such process alternative that has been receiving significant attention is pyrolysis.

Pyrolysis, which consists of thermal decomposition of organic materials in the absence of oxygen, converts biomass into a solid biochar product, a liquid bio-oil and a combustible gas by-product. The biochar product, composed primarily of fixed and volatile carbon and ash, can be used as a soil amendment or, alternatively, it can be refined to activated carbon [9-12]. In addition, due to the biochar's high stability and carbon content, the process results in carbon sequestration, actually removing carbon from the atmosphere, which makes the process carbon negative and potentially eligible for carbon credits [13]. Furthermore, due to its low sulphur and phosphorus content, as

well as its structural and reactivity properties, the solid biochar product can be used in the chemical, pharmaceutical and food industries [14]. The liquid bio-oil product has the potential to be used as a source for specialty chemicals and pharmaceuticals, flavoring agents, fuel for combustion in turbines to generate electricity or an intermediate for subsequent conversion to synthesis gas, from which clean fuels and chemicals can be produced [15-17]. The by-product gases have high energy content and can be combusted within the pyrolysis plant to thermally sustain the endothermic pyrolysis process [18].

The pyrolysis of biomass residues for biofuel production have been illustrated in many studies [19-21], which demonstrate that pyrolysis is one of the most suitable process for conversion of local biomass into bio-fuel in the Amazon state.

The objective of this study is to demonstrate the feasibility of using fast pyrolysis to convert the *tucumã* seed into value-added products and biofuels. The effect of temperature and operating conditions on the bio-oil and biochar yields and properties have been experimentally studied in a laboratory scale fluidized bed at the Institute for Chemicals and Fuels from Alternative Resources (ICFAR) at Western University in Canada. The excellent heat transfer and mixing capabilities, scalability, simplicity, relatively low capital, operating and energy expense, and relatively low temperature and gas/solid ratio, make the pyrolysis in the fluidized bed reactor technology one of the most practical reactor options [22]. The liquid biofuel (pyrolysis bio-oil) has the potential to be used as a source to produce upgraded fuels and specialty chemicals, and can be

stored and transported easily [23]. In addition, the pyrolysis process energy yield will also be examined as an indicator for the feasibility of implementing a pyrolysis reactor unit (preferably mobile, in order to significantly reduce biomass transportation costs and to deal with the geographically dispersed and fluctuating supply of *tucumã* seed) in Amazon State for *tucumã* seed conversion.

9.2 Experimental Set-Up, Materials and Methodology

9.2.1 The ICFAR Laboratory-Scale Bubbling Fluidized Bed Pyrolysis Pilot Plant

The reactor used in the experiments was a fast pyrolysis pilot plant designed by the Institute for Chemical and Fuel from Alternative Resources (ICFAR) at Western University. A schematic diagram of the reactor is shown in **Fig. 9-1**. The main part of the plant is a fluidized bed reactor operating at atmospheric pressure, 0.076 m in diameter, and with a 0.58 m long cylindrical section. A packed hot filter made of ceramic wool and fine metal mesh, 0.15 m long and 0.05 m in diameter, was utilized to prevent all solids from escaping the reactor.

Silica sand (1.5 kg, resulting in a 0.2 m defluidized bed height) was used as inert heat transfer material. The reactor was heated by four radiative electric heaters, which covered the dense sand bed and the freeboard sections. Each heater was controlled by a type K thermocouple, located within the bed at the same height as the heater, using a Watlow PID Digital controller. In this set of experiments, the temperature was kept constant over the whole height of the reactor.

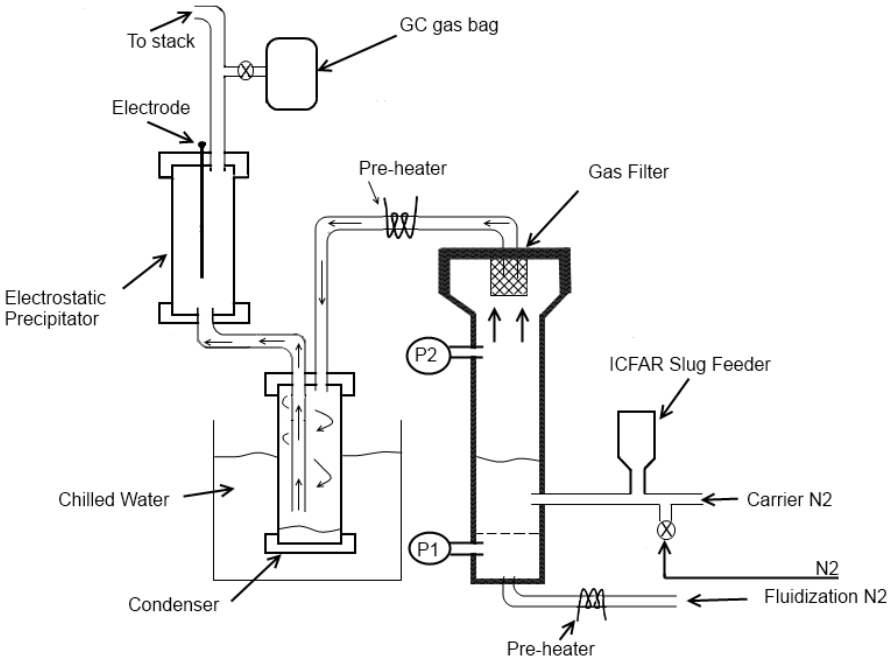

Figure 9-1: Process Flow Diagram of ICFAR Fluidized Bed Pyrolysis Pilot Plant

The biomass was fed into the reactor using an intermittent solid slug feeder system, located 0.12 m above the sparger gas distributor. The feeding system is shown in **Fig. 9-2**. A hopper filled with biomass discharges through a pneumatically activated valve. The valve opens periodically every 4 s, for short periods of time (0.5 s), allowing small amounts of biomass to fall into a horizontal *slug chamber*. During each cycle, the biomass forms a slug that is conveyed into the reactor at high velocity by a small pulse of nitrogen gas contained in a 75 mL capacitance volume at 40 psig. In addition, to prevent any backflow of hot solids into the feeding tube, a continuous stream of nitrogen carrier gas was sent to the reactor [22].

The fluidizing and the continuous carrier gas flows were metered using two Gas-Trak Sierra mass flowmeters, and were set to 2.87×10^{-4} Nm^3/s for carrier gas flow and 1.43×10^{-4} Nm^3/s for fluidization gas flow (these flows were adjusted for temperature to maintain a constant gas residence time in the reactor). Once the feed is injected, the produced vapors exit the top of the reactor through the hot filter section. The filter retains all the solids inside the reactor, to avoid any loss of sand and coke particles from the bed. The product gases and vapors, and the carrier gas flow into the condensing system where the bio-oil vapors are rapidly quenched. Persistent aerosols are then separated in a special designed electrostatic precipitator, while the non-condensable gases are directed to a gas-sampling bag, for future analysis, or vented.

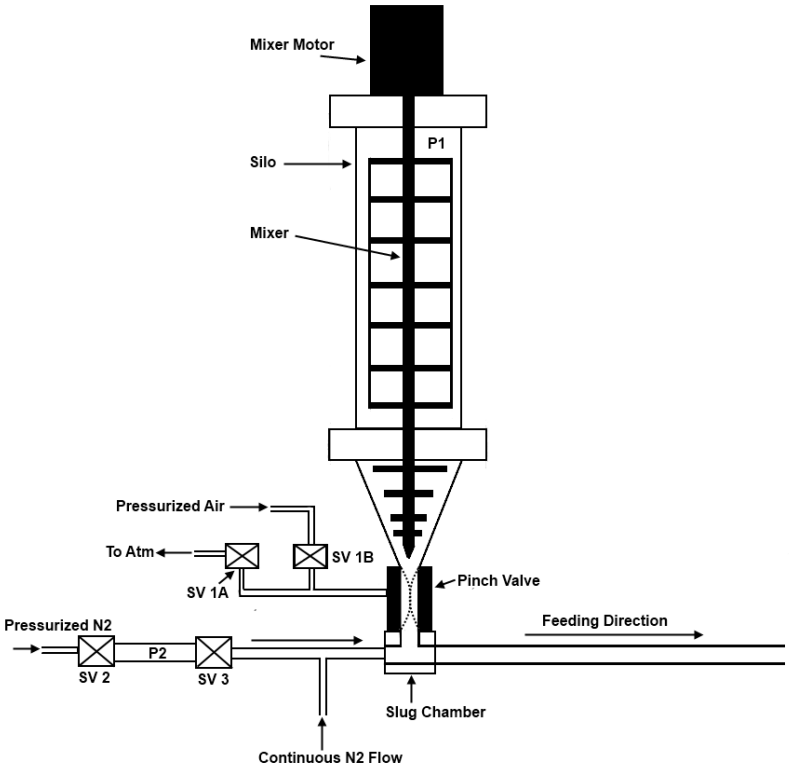

Figure 9-2: The ICFAR Intermittent Solid Slug Feeder

9.2.2 The Feedstock and Materials

In this experimental work, the biomass feedstock was *tucumã* (*Astrocaryum aculeatum*) seed that was obtained in market fairs in Manaus, the capital of Amazon State (Brazil). All the feedstock was air-dried and ground to particle sizes less than 2mm. **Table 9-1** shows the main characteristics of the *tucumã* seed.

Table 9-1: Physical and Chemical Properties of Tucumã Seeds

Property	Value
Density (kg/m^3)	1298.8 ± 0.8
Higher heating value (MJ/kg)	21.08 ± 0.95
Lower heating value (MJ/kg)	19.47 ± 0.31
Proximate analysis (%wet basis)	
Fixed carbon	18.67 ± 0.24
Volatile	69.35 ± 0.17

Ash	2.78 ± 0.21
Moisture	9.2 ± 0.1
Ultimate analysis (% dry and ash free basis)	
C	54.87
H	7.68
N	1.09
O	33.31

A mass of 1.5 kg of silica sand (128 µm Sauter mean diameter and 2650 kg/m^3 density) was introduced into the reactor as the bed inert material.

Nitrogen was used for the fluidizing and feed carrier gases and for the gas pulses. It also served as internal standard for the gas analysis. It is therefore essential to exactly control the nitrogen flowrate and to maintain it at a constant value.

9.2.3 Methodology

At least two experimental pyrolysis runs were carried out for each experimental condition, followed by the complete cleaning of the entire reactor before subsequent runs, to mitigate residue accumulation and the influential effects of previous experiments. The total amount of biomass injected for each run was 0.2 kg. Before each experiment, the controllers and the flowmeters were set according to **Table 9-2** to achieve a hot vapor residence time inside the reactor of 1.4 seconds.

Table 9-2: Gas Flowrate for the Fluidized Bed Reactor

T (°C)	400	450	500	550	600
N_2 (Carrier gas flow) (x10^{-5} Nm^3/s)	3.27	3.04	2.84	2.70	2.52
N_2 (Fluidization gas flow) (x10^{-5} Nm^3/s)	8.17	7.60	7.11	6.70	6.30
Theoretical hot vapor residence time (s)	1.44	1.43	1.42	1.42	1.41

The bio-oil production was determined by weighing the condenser and the electrostatic precipitator before and after each run. The non-condensable gas was sampled in a GC gas-sampling bag from a valve located after the electrostatic precipitator, to calculate the gas yield and determine the gas composition. The product gases, mainly composed of H_2, CO, CO_2, CH_4 and some low molecular weight hydrocarbons were detected in a HEWLETT PACKARD 6890 Series II GC gas chromatograph equipped with a thermal conductivity detector and a Restek Shincarbon Micropacked column (1 mm internal diameter and 2 m long). Nitrogen was used as internal standard, to provide accurate gas yields.

Since all solids were retained inside the bed by the hot filter, the product solid char (composed of char and ash) yield was determined from the change in mass of the fluidized bed contents after each run.

The elemental composition of the biomass feedstock was analyzed using a Flash EA 1112 Series CHNS-O analyzer. The volatile matter of the biomass feedstock was carried out following the ASTM E872 standard method and the fixed carbon was calculated by difference (considering the moisture, ash, and volatile matter).

The moisture content of both the organic and aqueous phases of the bio-oil was determined by using a Karl Fisher titrator V20.

The bio-oil produced by pyrolysis at 550°C (optimum condition regarding the bio-oil heating value) was collected from the condensers and demister and mixed homogeneously. A representative sample of the bio-oil was then diluted to 1.0 mg/mL

in methanol and characterized using an HP6890 GC-MS (Agilent) coupled with a Waters Quattro Micro MS with MS library. A DB-5ms column (30m x 0.25mm x 0.25µm) equipped with a guard column (5m x 0.25mm x 0.25 µm) and an autosampling splitless injector were used. The electron energy was set to 70 *e*V with a source temperature set at 250°C and the GC interface temperature of 250°C. The scan was performed from 50.00 to 650.00u in the EI+ mode. The temperature program used had a starting temperature of 40°C with a hold of five minutes. The temperature was then increased by 5°C/min until 280°C, with a final hold of 10 minutes. The total run time was 68 minutes. Only peak matches in the MS library greater than 90% were considered.

The heating values of the raw biomass, of the organic phase of the liquid bio-oil, and of the biochar were determined using an IKA C200 Oxygen Bomb Calorimeter following the ASTM D4809-00 standard method, while the heating value of the product gas was calculated by the product gases composition and the lower combustion value of each gas constituent.

The acidity (pH) of the bio-oil was measured by an Orion 2 Star pH benchtop and the moisture content of the raw biomass used for the experiments was measured with a Metler Toledo HB43-S Halogen Moisture Analyzer. Regarding the inorganic compounds analysis, the ash was obtained using a Thermolyne Benchtop Murffle Furnace and the raw *tucumã* and *tucumã* biochar ash analysis were performed using a PANalytical PW-2400 XRF Spectrometer. The samples were ashed at 450 and 1000°C and then 0.5 g of the ash was fused at 1000°C for 20 minutes with 6.50 g borate flux to form a casted

glass bead which could then be analyzed. The reported detection limit of this procedure is 0.01 wt%.

9.3 Results and Discussion

9.3.1 Effect of Temperature on Product Yields

Fig. 9-3 illustrates the effect of the reactor temperature on the production of bio-oil, biochar and permanent gases. The gas yield was calculated by difference (since the yield of bio-oil and biochar is physically measured), and was confirmed with the yield calculations from the GC gas analysis, resulting in a variation between 0.5 and 4.0% for the mass balance closure.

The results were repeatable as demonstrated by replicating runs. Fig. 3 shows that the optimum temperature to maximize the liquid yield is around 500°C. Conti [25] and Zanzi [26] concluded that secondary cracking reactions in the gas phase are very fast when the temperature is higher than the maximum liquid yield temperature, which is evident in this data as the higher operating temperatures resulted in a decreasing solid char and liquid bio-oil yields, while the gas yield steadily increased.

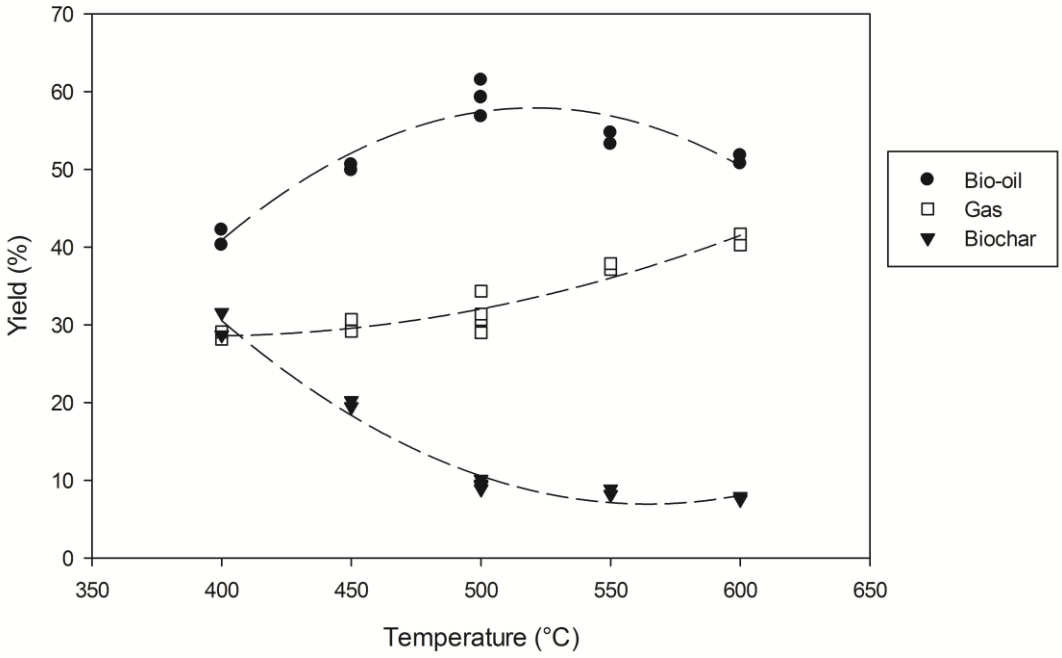

Figure 9-3: Pyrolysis Product Yields vs. Temperature

9.3.2 Effect of Temperature on Bio-oil Properties

The bio-oil collected showed to be stable and oily, with a dark-brown and homogeneous color. Another point is its smoky and relatively pleasant smell, which can be attributed to the low nitrogen contaminants in the biomass fed [29]. Further work should be conducted on the *tucumã* seed bio-oil to evaluate its viability as a food additive or flavoring agent.

Fig. 9-4 shows the effect of the temperature in the water content of the bio-oil. The result shows that between 450 and 550°C the water content reduces slightly, and much higher water content can be achieved at the 400 and 600°C operating conditions. The water in the bio-oil can be originated by both the original moisture in the biomass feed and the pyrolysis reaction (pyrolytic water), which affects the viscosity and stability of

the product. High water content decreases the heating value and density of the bio-oil, and can result in destabilization and phase-separation of the bio-oil [29]; however, it also reduces the viscosity and enhances the fuel fluidity, which is good for bio-oil combustion in engines [30].

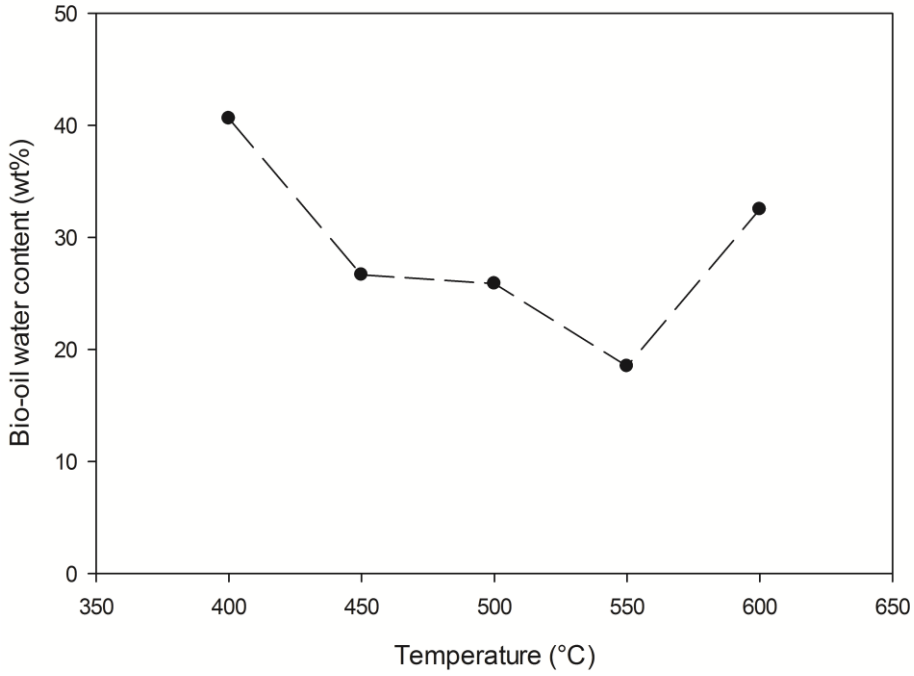

Figure 9-4: Effect of Temperature on Bio-oil Water Content

Fig. 9-5 shows the higher heating value of the organic phase of the liquid fraction obtained from the *tucumã* pyrolysis process. The lowest moisture content and the highest HHV of the oil fraction were obtained at the 550^{o}C operating temperature in the reactor. Therefore, the best temperature for high bio-oil yields was not the same as the best temperature regarding bio-oil higher heating value. This result shows the importance of bio-oil properties on the determination of the best operational temperature.

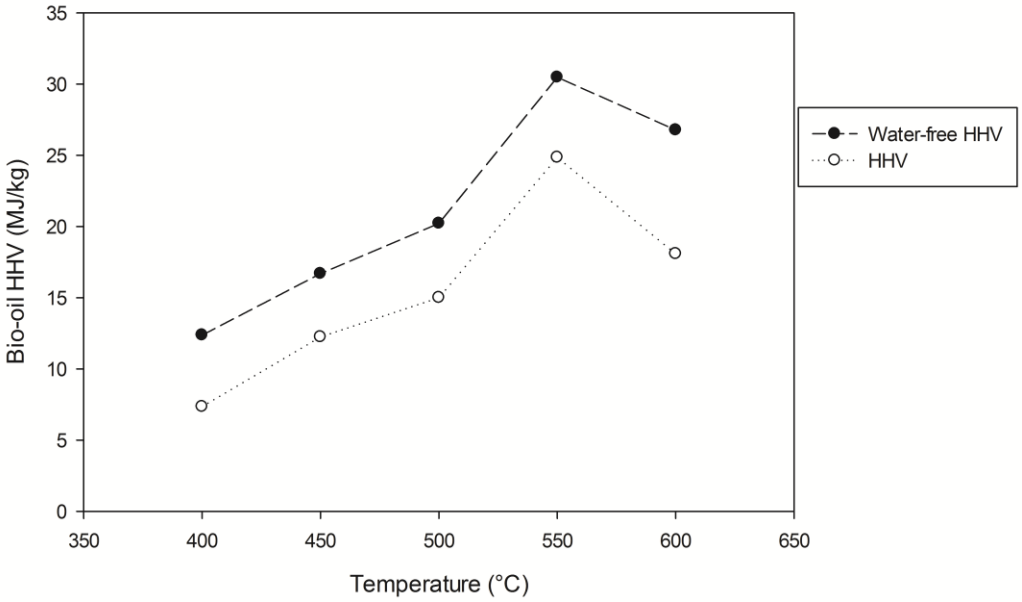

Figure 9-5: Effect of Temperature on Bio-oil HHV

Results of the ultimate analysis of *tucumã* bio-oil are shown in **Fig. 9-6**, where we can notice the highest carbon content in the range between 500 and 550^{o}C.

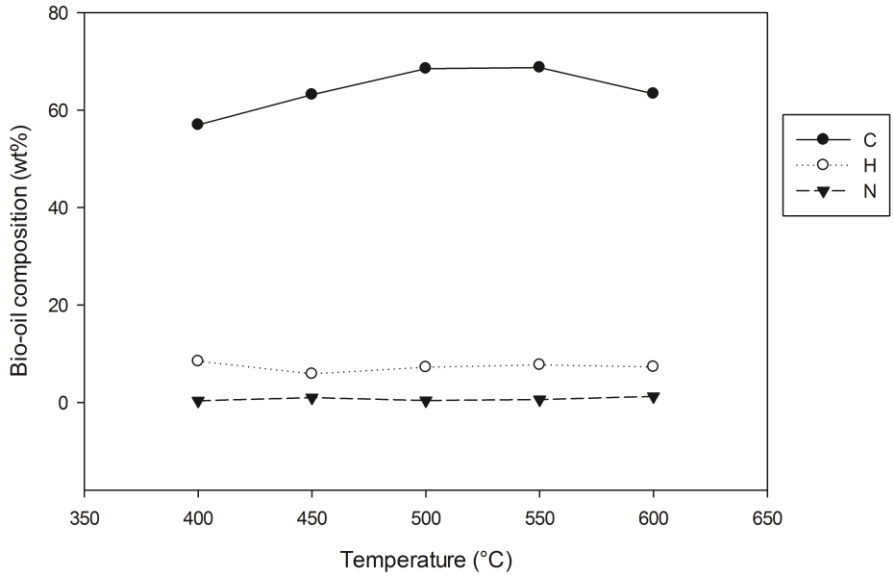

Figure 9-6: Bio-oil Ultimate Analysis vs. Temperature

The proximate analysis of bio-oil demonstrated that this material presents negligible ash content. The complete characteristics of the bio-oil are shown in **Table 9-3**. Pyrolysis product yields show the advantage of converting *tucumã* seeds into bio-oil due to its higher energy content and ease of transportation, which is a very important factor in the Amazon forest, due to its geographical challenges. Furthermore, the low ash content of the bio-oil also leads to reduced equipment fouling and ash removal.

Table 9-3: Bio-oil Proximate Analysis

Proximate Analysis	Composition (% dry basis)
Volatiles	96.95
Fixed Carbon	3.05
Ash	n.d.

n.d. = not detectable

Table 9-4 shows the average measured pH of the bio-oil produced at each tested reactor temperature condition, which was in the range from 2.4 to 2.9. The most acidic bio-oil was produced at 500^{o}C.

Table 9-4: Bio-oil's pH Variation with Production Temperature

T (°C)	400	450	500	550	600	*Average*
pH	2.65	2.65	2.43	2.69	2.87	***2.66***

The acidic characteristic of the bio-oil is associated with the notable absence of nitrogen-containing compounds [28] and with the organic acids from biopolymer

degradation. The main problems related to the acidity of the bio-oil are the corrosion of vessels and pipework [29].

The chromatogram from the GC-MS of the *tucumã* bio-oil produced at 550°C (optimal condition from an energy standpoint) can be seen in **Fig. 9-7**, while the results are summarized in **Table 9-5.** Bolded compounds in **Table 9-5** have been confirmed by spiking with pure standards. As the table illustrates, typical pyrolysis products are present in the *tucumã* bio-oil, including furans, phenols, levoglucosan and some short-chain acidic compounds (acetic acid, propanoic acid), which cause the low pH of the *tucumã* bio-oil [29].

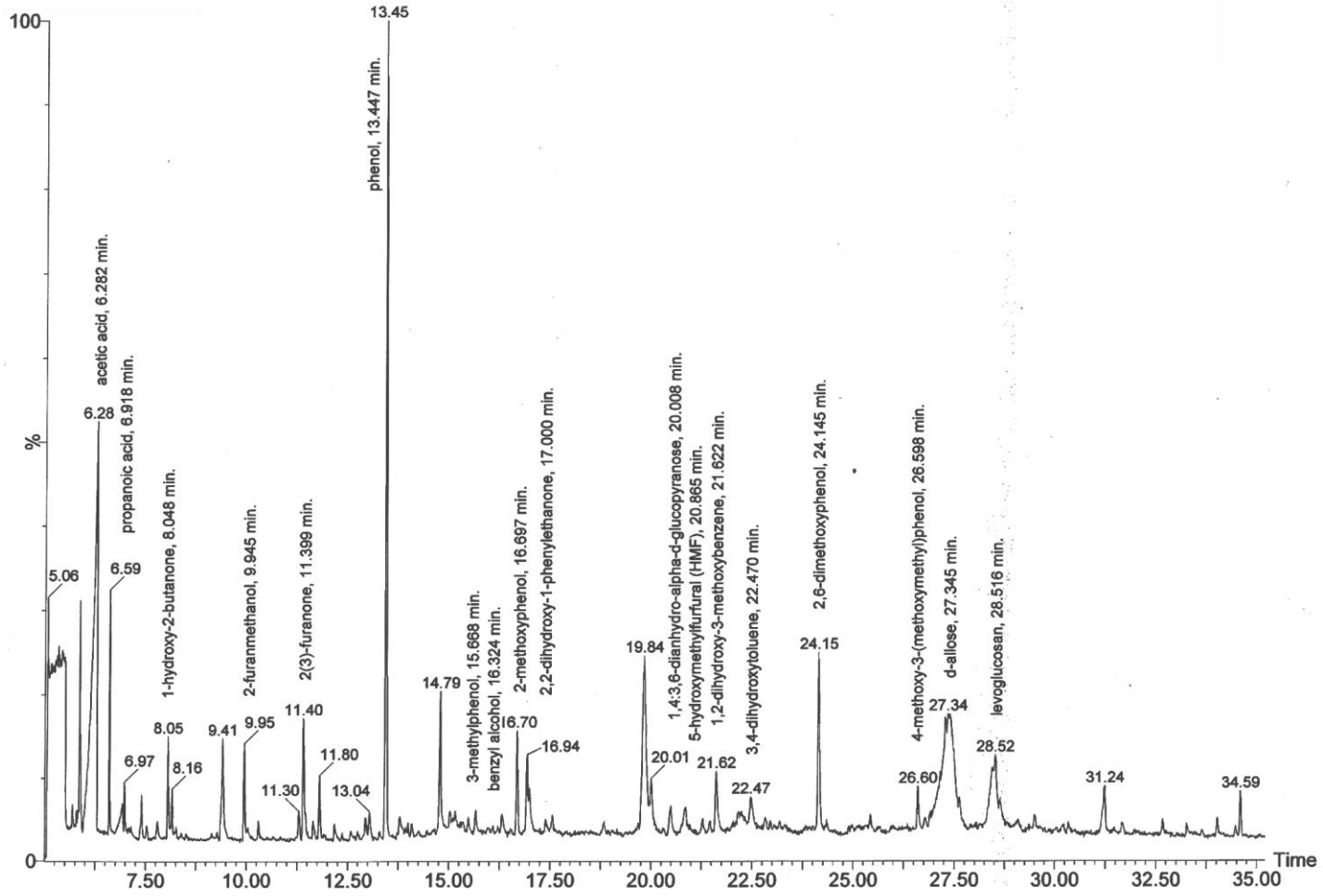

Figure 9-7: Chromatogram of Bio-oil at 550°C

Table 9-5: Main Peak Compounds in Bio-oil from GC-MS Analysis

Peak	Retention Time (min)	Area (%)	Compound Name
1	5.858	1.84	glycerol
2	6.282	14.64	acetic acid
3	6.918	--	propanoic acid
4	6.968	--	methyl glycolate
5	8.048	1.02	1-hydroxy-2-butanone
6	9.945	1.02	2-furanmethanol
7	10.298	--	3-butyldihydro-2(3H)-furanone
8	11.399	1.88	2(3H)-furanone
9	**13.447**	**9.35**	**phenol**
10	15.668	--	3-methylphenol
11	16.324	0.41	benzyl alcohol
12	**16.697**	**1.32**	**2-methoxyphenol (Guaiacol)**
13	17.000	0.81	2,2-dihydroxy-1-phenyl ethanone
14	20.008	1.15	1,4:3,6-dianhydro-alpha-D-glucopyranose
15	**20.865**	**0.43**	**5-hydroxymethylfurfural (HMF)**
16	21.289	--	2,3-anhydro-D-mannosan
17	21.622	1.25	1,2-dihydroxy-3-methoxybenzene
18	22.47	0.66	3,4-dihydroxytoluene
19	24.145	2.4	2,6-dimethoxyphenol
20	25.427	--	vanillin
21	26.598	0.67	4-methoxy-3-(methoxymethyl)phenol
22	**27.345**	**3.12**	**Saccharide Derivative**
23	**28.516**	**3.79**	**levoglucosan**
24	31.664	1.04	3,4-dimethoxy-5-hydroxybenzaldehyde
25	32.663	--	4-allyl-2,6-dimethoxyphenol
26	**33.259**	**--**	**3,5-dimethoxy-4-hydroxyacetophenone**
27	34.016	0.63	3,5-dimethoxy-4-hydroxybenzyl alcohol

Usually the acidic compounds present in pyrolysis bio-oils derived from lignocellulosic biomasses (especially from forestry residues) have lower molecular weights (having carbon chains with fewer than 7 carbons) and a discrete amount of one or more sugars, such as levoglucosan [35, 36]. Levoglucosan presence in the bio-oil is due to thermal cracking of carbohydrates (cellulose and starch present in the initial biomass [37]).

Another compound of interest within the bio-oil is guaiacol, which is commonly used as a pesticide or as a precursor for synthesizing flavoring agents [38].

In addition, a saccharide derivative was detected in this bio-oil at 27.345 minutes, with a high library match (99%) indicating D-allose. This sugar would be of particular interest as it is one of the rarest sugars found in nature and is currently being used in the pharmaceutical industry for various applications, including being used as promising anti-oxidant, anti-tumoural agent, and ischemic injury inhibitor [39, 40]. D-allose has a current market price ranging from $120-$755/g (Omicron Biochemicals Inc. and Sigma Aldrich). D-allose could not be detected in the raw *tucumã* by water extraction at various temperatures, and could therefore potentially be produced by the pyrolysis reaction or could represent a mis-match in the GC-MS analysis. Further work on the confirmation, extraction and purification of D-allose and other compounds of interest from these bio-oils will be performed.

The most economic usage of bio-oil produced from *tucumã* residues would likely involve the extraction of higher-value chemicals, such as guaiacol, with the remainder of the bio-oil being used as a fuel source or additive, due to its significant yield and higher heating value.

9.3.3 Effect of Temperature on Gas Properties

Fig. 9-8 shows that high temperatures led to an increased production of all non-condensable gases, with the exception of CO_2. This is largely because of the increase in the rate of secondary cracking reactions of the volatiles at higher temperatures.

Although the CO yield is increasing, the proportion of CO_2 in the product gases decreases with increasing temperature because the CO_2 is produced by carboxyls released at relatively low temperature, and the secondary reactions of volatiles produce mostly CO, H_2 and CH_4 rather than CO_2 [27]. This demonstrates that at higher temperature, a higher heating value gas could be obtained by the pyrolysis of biomass [19].

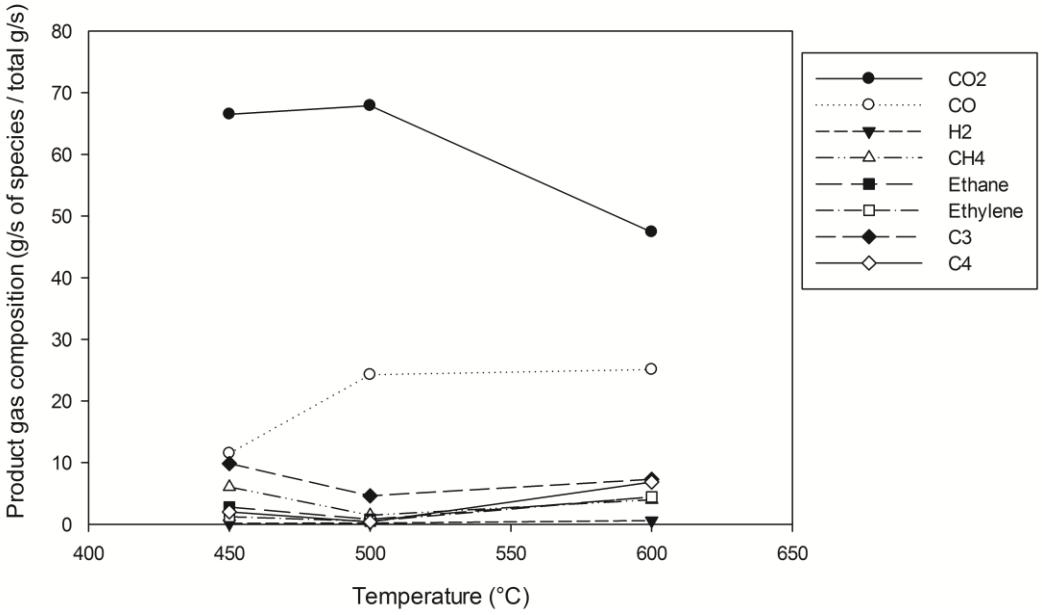

Figure 9-8: Product Gas Composition vs. Temperature

9.3.4 Effect of Temperature on Biochar Properties

Fig. 9.9 shows that the heating value of the biochar decreases with the temperature increment, which is in agreement with **Fig. 9-10**, which illustrates the decreasing carbon content in the biochar with increasing temperature.

The ash analysis of raw biomass and the biochar from the 500°C operational condition is shown in **Table 9-6**. The biochar ash contains 5 wt% Calcium, indicating that it would not be a suitable catalyst for other thermal processes such as gasification [28]. However, the biochar could be used in the Amazon to improve soil fertility. Magnesium oxide appears in high concentration in the biochar and it is a good nutrient source for plant growth [31]. Potassium and phosphorous are also supplied to plants as fertilizers in many products [32]. Silicon is also an important compound to prevent the drying up of plant leaves and to promote pollen fertility [33]. Furthermore, proper silicon management appears to be necessary in temperate as well in tropical countries to optimize agricultural yields and for plant disease control [34]. The concentration of these compounds (Mg, K, P, Si) found in tucumã biochar total 85 wt%, showing good potential for the biochar as a natural soil amendment and fertilizer additive.

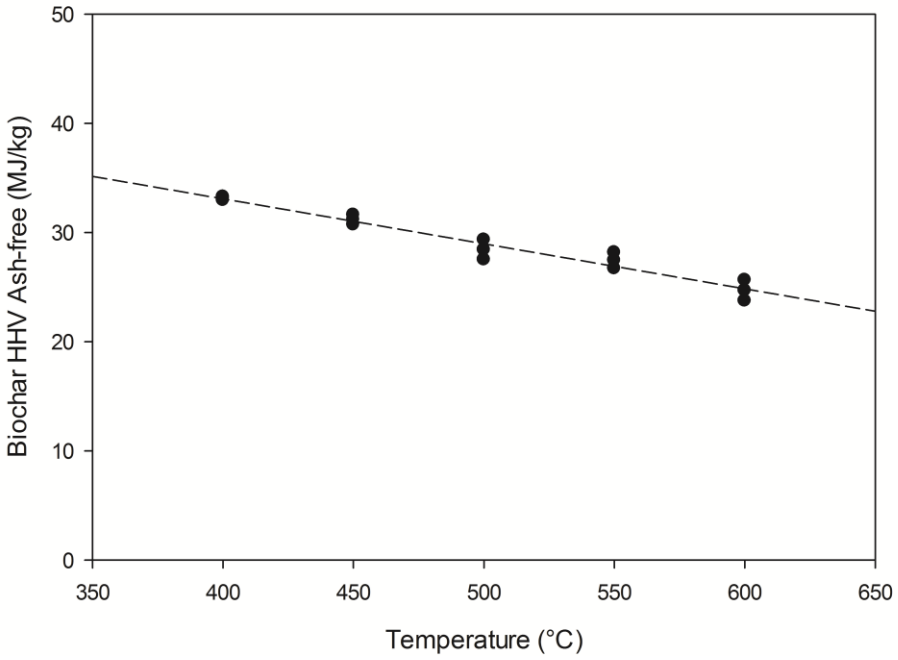

Figure 9-9: Effect of Temperature on Biochar HHV

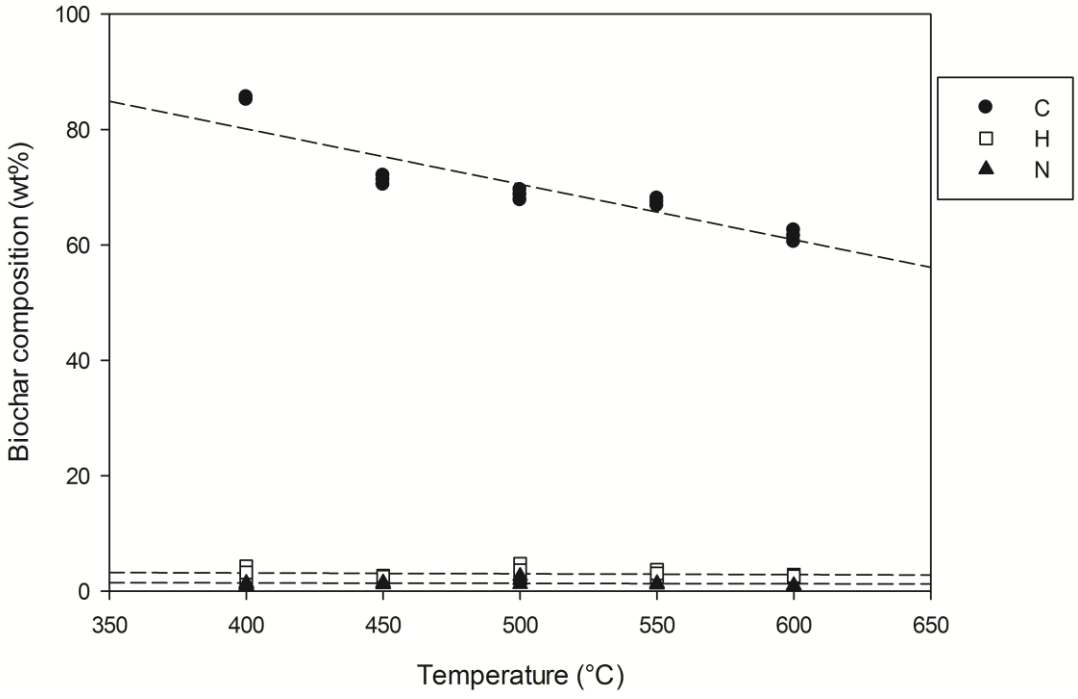

Figure 9-10: Ultimate Analysis of Biochar vs. Temperature

Table 9-6: Raw Tucumã and Tucumã Biochar Ash Analysis

Sample	SiO_2	TiO_2	Al_2O_3	Fe_2O_3	MnO	MgO	CaO	K_2O	Na_2O	P_2O_5	Cr_2O_3	Total	Ash (wt%)
Raw *tucumã*	33.48	0.16	0.66	8.39	0.33	11.40	6.65	24.25	3.02	11.48	0.01	99.88	1.93
Tucumã Biochar at 500°C	33.48	0.18	0.18	3.53	0.35	15.1	5.82	25.76	5.29	10.58	0.18	100.52	19.30

9.3.5 Energy Balance

Pyrolysis is an endothermic process so the determination of the practical process energy yield and the energy requirements to maintain the reactor temperature is of great importance for practical and/or industrial application of this process. The heat of pyrolysis for this study is defined as the practical energy required to carry out the pyrolysis reaction, taking the injected raw materials from room temperature and resulting in the products at reactor temperature [24]. The reactor used for the

experiments was not calibrated for accurate heat of pyrolysis calculation, so the heat of pyrolysis was estimated from the difference between the enthalpy of all the products and the enthalpy of the feed, including an energy credit for the heat recovery in the condensation train.

Fig. 9-11 illustrates the practical energy yield of the pyrolysis reaction (not including milling, grinding or drying, but starting with biomass of realistic moisture content). The bar graph represents the total energy contained in the products while the line above the bar graphs represents the total practical energy input that needs to be provided to the reactor to carry out the pyrolysis reaction. The difference between the bar and the line represents energy losses and the fact that the energy from cooling and condensing all the products was not recovered in the laboratory experiments. The highest energy yield (and also the best condition from bio-oil yield and heating value quality) is achieved by operating the reactor at 550°C, resulting in a practical energy yield of 90% in our case. The dashed line with white dot on the graph illustrates the practical reaction energy required by the process (heat of pyrolysis and inlet gas heating), which ranges from 0.8 to 4.9 MJ per kg of biomass feed. Since the energy contained in the product gas is higher than these values (ranging from 2.26 to 6.67 MJ) at all operating conditions, the pyrolysis of the *tucumã* seeds could be self-sustaining at all operating conditions (with more safety margin at higher temperatures), if the product gas is combusted to provide the energy for the process. In conclusion, a pyrolysis gas containing a significant amount of carbon monoxide along with methane, hydrogen, and other combustibles, might be used as a fuel [30].

The process energy self-sustainability is very important in order to eliminate the need of additional fuels to carry out the process, and makes the implementation of independent mobile pyrolysis units easier [19]. Mobile pyrolysis reactors would be ideal for use in the Amazon to avoid the complications and expensive economics of accumulating the biomass in one location (which is originally widely dispersed in the forest), then shipping the bulky biomass to a centralized location for processing [23]. As a result of utilizing mobile units, balancing the energy needs with the energy production of the process becomes more important since the process cannot be integrated into an industrial complex. In addition, the flexibility of having a mobile unit addresses the issues of fluctuation in supply of *tucumã* in one location (due to dispersion and erratic production).

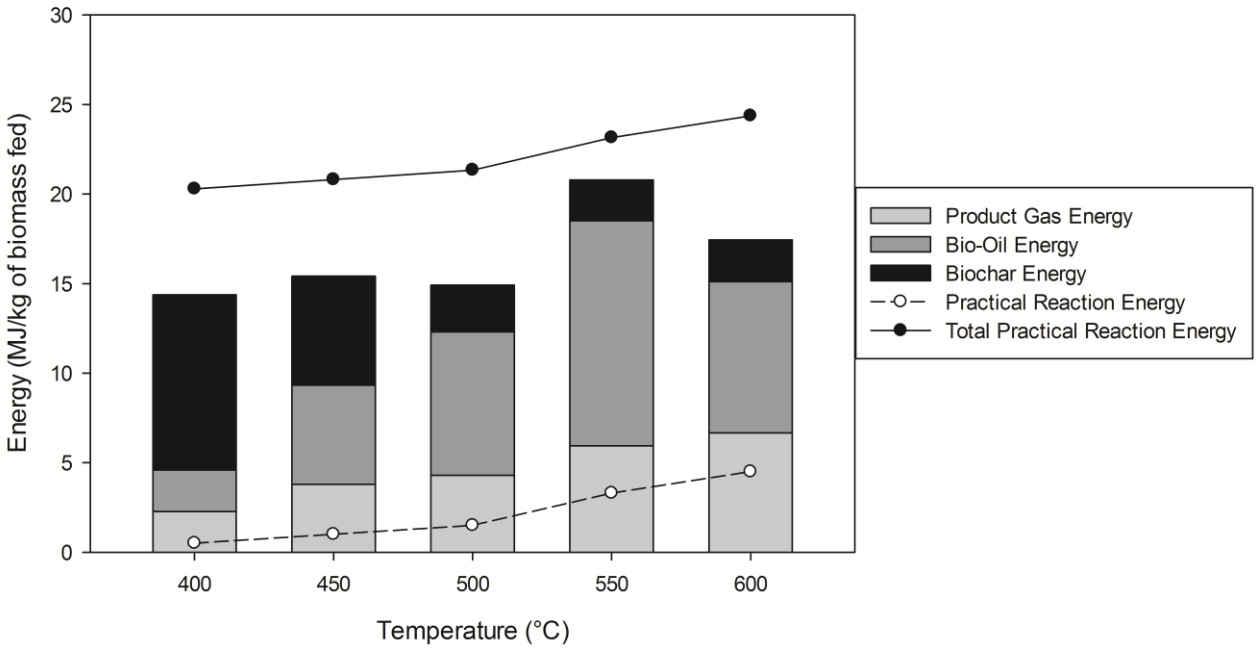

Figure 9-11: Energy Balance and Thermal Sustainability

9.4 Conclusions

The utilization of *tucumã* seeds to produce bio-oil has been shown to have positive fuel properties that could lead it to be potentially used as an alternative to replace fossil fuels, which are widely used to create electricity in isolated communities in the state of Amazon in Brazil. Due to the high water-free calorific value, which can reach values of roughly 30.5 MJ/kg, the low moisture content below 20 wt%, and the relatively high liquid yield (approximately 55 wt%), the bio-oil produced from *tucumã* pyrolysis could be an attractive alternative for power generation. The pyrolysis process at 550 °C appeared to be optimal for converting *tucumã* seeds into valuable products. Moreover, the *tucumã* bio-oil includes several compounds of interest for the chemical and pharmaceutical industry, such as guaiacol. Regarding the other pyrolysis products, the biochar could potentially be used as a soil amendment agent, and the product gases could be used to provide the energy required for the process. Further work on the technical and economic feasibility is being conducted to understand the limitations of the process and verify the implementation potential of the process in the Amazon region. Further work on the confirmation, extraction and purification of guaiacol and other compounds of interest from these bio-oils will be performed.

9.5 Acknowledgements

The authors thank the financial support provided by National Council of Technological and Scientific Development (CNPq) along with the Natural Sciences and Engineering Research Council of Canada (NSERC) and the MITACS Program for the scholarships for the students involved in this research. The authors would also like to acknowledge Dr.

Mamdouh Abou-Zaid and his colleagues at Natural Resources Canada for their knowledge and the helpful contribution of the verification and improvement of the GC-MS analysis of the bio-oil.

9.6 References

[1] E.J.F Barreto, Preface, in: E.J.F. Barreto, G. Rendeiro, M. Nogueira (Eds.), Combustion and Gaseification of Solid Biomass (in Portuguese) Combustão e Gaseificação de Biomassa Sólida, Brazilian Ministry of Mines and Energy, Brasília, 2008, pp. 13-17.

[2] J.C.Correia, The energy supply to isolated communities (in portuguese) Atendimento energético para pequenas comunidades isoladas: barreiras e possibilidades, T&C Amazônia 3:6, 2005, pp. 30-35.

[3] F.A.O., Food and fruit-bearing forest species – 3: Examples from Latin America, 1986, pp. 40-42.

[4] A.L. Viana, C.S.C.R. Souza, I.N.L. Santos, J.G. Souza, A.P. Castro, General aspects of trade of *tucumã* in open markets (in portuguese), Aspectos Gerais da Comercialização do *Tucumã* do Amazonas nas Feiras da Cidade de Manaus, Amazonas. Proceedings: 1st International Seminar of Environment Sciences and Sustainability in the Amazon, Federal University of the Amazon – UFAM, Manaus, Amazon, 2010, pp. 2-8.

[5] H. Fukuda, A. Kondo, H. Noda, Biodiesel Fuel Production by Transesterification of Oils: review. J. Biosci. Bioeng. 92 (2001) 405-416.

[6] D. Russi, An integrated assessment of a large-scale biodiesel production in Italy, Energ. Policy 36 (2008) 1169-1180.

[7] S. Bernesson, D. Nilsson, P.A. Hansson, A limited LCA comparing large- and small scale production of rape methylester (RME) under Swedish conditions, Biomass Bioenerg. 26 (2004) 545–559.

[8] S. Ulgiati, A comprehensive energy and economic assessment of biofuels: when ‘‘green’’ is not enough. Crc. Cr. Rev. Plant. Sci. 20:1 (2001) 71–106.

[9] A.A. Boateng, P.H. Cooke, K.B. Hicks, Microstructure development of chars derived from high-temperature pyrolysis of barley huls, Fuel 86 (2007) 735-742.

[10] J.W. Gaskin, C. Steiner, K. Harris, K.C. Das, B. Bibens, T. ASABE 51 (2008) 2061-2069.

[11] K.Y. Chan, L. Van Zwieten, I. Meszaros, A. Downie, S. Joseph, Aust. J. Soil Res. 45 (8) (2007) 629-634.

[12] M. Rondon, J. Lehmann, J. Ramírez, M. Hurtado, Biological nitrogen fixation by common beans increases with biochar additions, Biol. Fert. Soils. 43 (2007) 699-708.

[13] D.A. Laird, R.C. Brown, J.E. Amonette, J. Lehmann, Review of the pyrolysis platform for coproducing bio-oil and biochar, Biofuel Bioprod. Bior. 3 (2009) 547-562.

[14] J.M. Encinar, F.J. Beltran, J.F. Gonzalez, M.J. Moreno, Pyrolysis of maize, sunflower, grape and Tobacco Residues, J. Chem. Technol. Biot. 70 (1997) 400-410.

[15] S. Gust, in: A.V. Bridgwater, D.G.B Boocok (Eds.), Developments in Thermochemical Biomass Conversion, Blackie Academic, London, 1997, pp. 481-488.

[16] K. Oehr, Acid Emission reduction, US Patent 5,458,803, 1995.

[17] B. Freel, R.G. Grahan, Bio-oil preservatives, US Patent, 6,485, 841, 2002.

[18] L.K.Mok, M.A. Bergougnou, H.J. de Lasa, Fast Pyrolysis of biomass for the production of chemicals and fuels from wood. 4th Bioenergy R and D Seminar, Winnipeg, March 1980.

[19] R. Xu, L. Ferrante, C. Briens, F. Berruti, Flash pyrolysis of grape residues into biofuel in a bubling fluid bed, J. Anal. Appl. Pyrol. 86 (2009) 58-65.

[20] R. Xu, L. Ferrante, K. Hall, C. Briens, F. Berruti, Thermal self sustainability of biochar production by pyrolysis, J. Anal. Appl. Pyrol. 91 (2011) 55-66.

[21] P.R.Bonelli, P.A. Della Rocca, E.G. Cerrella, A.L. Cukierman, Effect of pyrolysis temperature on composition, surface properties and thermal degradation rates of Brazil Nut shells, Bioresource Technol. 76 (2001) 15-22.

[22] F.M. Berruti, K. Lenkiewicz, R. Xu, R.J. Bedmutha, S. Nova, F. Berruti, C. Briens, (2007) "Novel fluid bed pilot plant for the production of bio-oil from biomass through fast pyrolysis," Récents progrès en génie des procédés, numéro 94. ISBN 2–910239-68–3. Ed. SFGP, Paris, France.

[23] P.C. Badger, P. Fransham, Use of mobile fast pyrolysis pplants to densify biomass and reduce biomass handling costs – A preliminary assessment, Biomass Bioenerg. 30 (2006) 321-325.

[24] F.M. Berruti, L. Ferrante, C.L. Briens, F. Berruti, Pyrolysis of cohesive meat and bone meal in a bubbling fluidized bed with an intermittent solid slug feeder, J. Anal. Appl. Pyrol. 94 (2012) 153-162

[25] L. Conti, G. Scano, J. Boufala, Bio-oils from arid land plants: flash pyrolysis of EUPHORBIA CHARACIAS bagasse, Biomass Bioenerg. 7 (1994) 291-296.

[26] R. Zanzi, K. Sjostrom, E. Bjornborm, Rapid pyrolysis of agriculture residues at high temperature, Biomass Bioenerg. 23 (2002) 357-366.

[27] Z. Luo, S. Wang, Y. Liao, J. Zhou, Y. Gu, K. Cen, Research on biomass fast pyrolysis for liquid fuel, Biomass Bioenerg. 26 (2004) 455-462.

[28] E. Cascarosa, I. Fonts, J.M. Mesa, J.L. Sánchez, J. Arauzo, Characterization of the liquid and solid products obtained from the oxidative pyrolysis of meat and bone meal in a pilot-scale fluidised bed plant, Fuel Process. Technol. 92 (2011), 1954-1962

[29] A.V. Bridgwater, A review of fast pyrolysis of biomass and product upgrading, Biomass Bioenerg. 38 (2012) 68-94

[30] D. Vamvuka, Bio-oil, solid and gaseous biofuels from biomass pyrolysis processes – An overview, Int. J. Energ. Res. 35 (2011) 835-882

[31] R. Mikkelsen, Soil and fertilizer magnesium, Better Crops 94 (2010) 26-38

[32] S.C. Hodges, Soil fertility basics, Chapter 1, Soil Science Extension, North Carolina State University

[33] Y. Miyake, E. Takahashi, Effect of silicon on the plant growth of solution cultured cucumber plants, Soil Sci. Plant. Nutr. 29 (1983) 71-84

[34] G.H. Korndörfer, I. Lepsch, Effect of silicon on plant growth and crop yield, Stud. Plan. S. 8 (2001) 133-147

[35] A. Oasmaa, E. Kuoppala, A. Ardiyanti, R. H. Venderbosch,§and H. J. Heeres, Characterization of Hydrotreated Fast Pyrolysis Liquids, Energy Fuels 24 (2010) 5264–5272

[36] A. M. Azeez, D. Meier, J. Odermatt, and T. Willner, Fast Pyrolysis of African and European Lignocellulosic Biomasses Using Py-GC/MS and Fluidized Bed Reactor. Energy Fuels 24 (2010) 2078–2085

[37] C.M. Lakashmanan and H.E. Hoelscher, Production of levoglucosan by pyrolysis of carbohydrates, Ind. Eng. Chem. Res. 9 (1970) 55-59

[38] R.Simon, B.De La Calle, S.Palme, D.Meier, E. Anklam. Composition and analysis of liquid smoke flavouring primary products, J. Sep. Sci. 28 (2005) 871-882.

[39] Y. Ishihara, K. Katayama, M. Sakabe, M. Kitamura, M. Aizawa, M. Takara, and K. Itoh, Antioxidant properties of rare sugar D-allose: Effects on mitochondrial reactive oxygen species production in Neuro2A cells, J. of Biosci. and Biotech. 112 (2011) 638-642.

[40] M. Mizote, K. Hirooka, K. Fukuda, T. Nakamura, T. Itano, F. Shiraga. D-Allose as ischemic retina injury inhibitor during rabbit vitrectomy, Jpn. J. Ophthalmol. 55 (2011) 294-300.

Appendix III

10 Appendix III: Kraft Lignin Pyrolysis in a Fluidized Bed Reactor

This appendix section is a published presentation from the International Conference on Thermochemical Conversion Science (tcbiomass 2011) in Chicago, Illinois, USA. The presentation was authors were Pietro Palmisano, **Federico M. Berruti**, Valentina Lago, Franco Berruti, and Cedric Briens. The presentation showcases that the novel feeding technology was able to successfully feed Kraft lignin, which is a very challenging and temperature-sensitive feedstock, which resulted in the very first study of Kraft lignin pyrolysis in industrially relevant equipment.

The presentation can be found at the following link:

http://www.gastechnology.org/tcbiomass2013/tcb2011/06_tcb2011_Pyrolysis_II.pdf

Scroll down on the website until the title slide of the presentation (found on the following page of this thesis) is displayed.

KRAFT Lignin Pyrolysis in a Fluidized Bed Reactor

Pietro Palmisano, Federico Berruti,
Valentina Lago, Franco Berruti,
Cedric Briens

Institute for Chemicals and Fuels from Alternative Resources
The University of Western Ontario

Name:	Federico M. Berruti, P.Eng.
Post-secondary	Western University
Education and Degrees:	London, Ontario, Canada 2004-2009 BESc
	The Richard Ivey School of Business Western University London, Ontario, Canada 2006-2009 HBA
	Western University London, Ontario, Canada 2009-2013 Ph.D.
Selected Honours & Awards:	NSERC Vanier Canada Graduate Scholarship (VCGS3) Doctoral Scholarship 2010-2013
	NSERC Michael Smith Foreign Study Supplement Scholarship Doctoral Research Fellowship 2010
	NSERC Alexander Graham Bell Canada Graduate Scholarship (CGS-M) First Year Graduate Scholarship 2009
	James M. Hay Gold Medal in Chemical & Biochemical Engineering Graduating Award 2009
	G.E. Hall President's National Scholarship Undergraduate Full National Scholarship 2004-2008
Related Work Experience	Ph.D. Student Researcher ICFAR, Western University 2009-2013
	Vice-President Agri-Therm Inc. 2009-Present

Course Instructor
Faculdade de Enhenharia Mecânica (FEM)
Universidade Estadual de Campinas (UNICAMP)
2011

Consultant/Researcher
Grupo de Procesos Termoquímicos (GPT)
Universidad de Zaragoza, Spain
2010

Teaching Assistant
Western University
2009

Selected Publications:

Berruti, F.M. (2013). Novel intermittent solid slug feeder for fast pyrolysis reactors: Fundamentals and modeling. *Powder Technology*, 247, 95-105, http://dx.doi.org/10.1016/j.powtec.2013.07.008.

Berruti, F.M. (2013). Biomass Residue Fast Pyrolysis: the Future Outlook. Canadian Biomass, February 12, 2013: http://www.canadianbiomassmagazine.ca/content/view/3954/133/

Lira, C.S., **Berruti, F.M.**, Palmisano, P., Berruti, F., Briens, C. (2013). Fast Pyrolysis of Amazon Tucumã (Astrocaryum aculeatum) Seeds in a Bubbling Fluidized Bed Reactor. *Journal of Analytical and Applied Pyrolysis*, 99, 23-31.

Berruti, F.M., Liu, H. (2012). Green-Tech: Bio-Fuels High Growth Strategy (Case and Teaching Note). *Ivey Publishing*. 9B11M123/8B11M123. Case featured by The Aspen Institute Center for Business Education (www.caseplace.org). 322 case purchases by November 21, 2012 (Ivey usage statistics).

Berruti, F.M., Ferrante, L., Briens, C., Berruti, F. (2012). Pyrolysis of Cohesive Meat and Bone Meal in a Bubbling Fluidized Bed with an Intermittent Solid Slug Feeder. *Journal of Analytical and Applied Pyrolysis* 94, 153-162, doi:10.1016/j.jaap.2011.12.003.

Berruti, F.M., Ferrante, L., Briens, C., Berruti, F. (2009). Optimization of an Intermittent Solid Slug Injection System for Sawdust Biomass Pyrolysis. *International Journal of Chemical Reactor Engineering (IJCRE)*: Vol. 7: 1.

Berruti, F.M., Ferrante, L., Briens, C., Berruti, F. (2009). Optimization of an Intermittent Solid Slug Injection System for Sawdust Biomass Pyrolysis. *The 2nd International Congress on Green Process Engineering (GPE 2009)*, July 14, 2009 for conference proceeding.

Berruti, F.M. (2009). Fast Pyrolysis: An Old and New Engineering Solution. *CFES Project Magazine, CFES,* November Issue, 2008, P. 12-15.

Berruti, F.M. Klaas, M., Briens, C., Berruti, F. (2009). Model for convective drying of carrots for pyrolysis, *Journal of Food Engineering* 92, 196-201, doi:10.1016/j.jfoodeng.2008.10.036

Berruti, F.M., Lenkiewicz, K., et al. (2007). Novel Fluid Bed Pilot Plant for the Production of Bio-oil from Biomass through Fast Pyrolysis. *Récents Progrès en Génie des Procédés, Numéro 94*. ISBN 2-910239-68-3, Ed. SFGP, Paris, France.